

**UNIVERSITY OF FOGGIA**



HR EXCELLENCE IN RESEARCH

---

**PhD course in**  
**“Translational medicine and foods: Innovation, safety and Management”**  
**(XXXIII Cycle)**

Coordinator: PROF. MATTEO ALESSANDRO DEL NOBILE

PhD Thesis

**“EFFECTS OF FERMENTED WHEAT GERM EXTRACT ON ORAL  
CANCER CELLS AND RESEARCH OF BIOMARKERS FOR  
DIAGNOSIS AND PROGNOSIS OF ORAL CANCER.”**

PhD candidate: Khrystyna Zhurakivska  
Tutor: prof. Lorenzo Lo Muzio

---

Academic year: 2019/2020

## SUMMARY

<b>Abstract.....</b>	<b>3</b>
<b>1. Introduction.....</b>	<b>5</b>
<b>1.1 Oral cancer.....</b>	<b>5</b>
<b>1.2 Nutraceuticals .....</b>	<b>6</b>
<b>2. The effects of adjuvant fermented wheat germ extract on cancer cell lines. 8</b>	
<b>2.1 Background .....</b>	<b>8</b>
<b>2.2 Systematic review of scientific literature concerning the in vitro activity of FWGE on malignant cells.....</b>	<b>8</b>
<b>2.3 Results.....</b>	<b>14</b>
<b>2.4 Discussion.....</b>	<b>17</b>
<b>2.5 Conclusions .....</b>	<b>20</b>
<b>3. Effects of fermented wheat germ extract on oral cancer cells.....</b>	<b>21</b>
<b>3.1 Materials and methods.....</b>	<b>21</b>
<b>3.3 Results.....</b>	<b>25</b>
<b>3.3 Discussion.....</b>	<b>32</b>
<b>4. Immunohistochemical Analysis of Musashi-2 and Cyclin-D1 Expression in Patients with Oral Squamous Cells Carcinoma.....</b>	<b>36</b>
<b>4.1 Introduction .....</b>	<b>36</b>
<b>4.2 Materials and Methods .....</b>	<b>37</b>
<b>4.3 Results .....</b>	<b>39</b>
<b>4.4 Discussion.....</b>	<b>46</b>
<b>5. Meta-analysis of PD-L1 expression in tumour cells and its correlation with prognosis of patients suffering for oral squamous cells carcinoma.....</b>	<b>49</b>
<b>5.1 Introduction.....</b>	<b>49</b>
<b>5.2 Materials and methods.....</b>	<b>50</b>

5.3 Results .....	52
5.4 Discussion.....	63
<b>6. Computational analysis of TP53 mutational landscape unveils key prognostic signatures and distinct pathobiological pathways in head and neck squamous cell cancer.....</b>	<b>70</b>
6.1 Introduction.....	70
6.2 Materials and methods.....	72
6.3 Results.....	115
6.4 Discussion.....	173
<b>7. Conclusions.....</b>	<b>179</b>
<b>References .....</b>	<b>181</b>
<b>Appendix 1: Journal publications .....</b>	<b>196</b>
<b>Appendix 2: Abstracts and Conference Proceedings.....</b>	<b>199</b>
<b>Appendix 3: Oral Presentations .....</b>	<b>201</b>
<b>Appendix 4: Honors and Awards.....</b>	<b>202</b>

## **ABSTRACT**

Oral squamous cell carcinoma (OSCC) represents one of the most aggressive types of cancer. The disease occurs when the accumulation of multiple genetic mutations in the oral epithelial cells leads to an irreversible damage of DNA and the cells lose their normal life cycle. The prognosis correlates to several factors and an early diagnosis, certainly, improves the outcome. The treatment strategy for OSCC incorporates both the surgical and oncologic approaches. There are two main challenges of the current research in cancer treatment: the first one is the development of more personalized and effective therapies, since not all tumors of the same stage respond to the therapy in the same way, and the second one is the setup of a more targeted therapy, that can affect only the cancer cells, without destroying healthy ones. Many efforts are made to find compounds that can support and improve the cancer therapy, and great attention is focused on some of natural products, known to have beneficial properties on the human organism.

The aim of this thesis is to present results deriving from a research directed to investigate a possible use of a natural compound, Fermented Wheat Germ Extract (FWGE), for the treatment of Oral squamous cell carcinoma (OSCC).

In order to summarize the scientific evidence of the use of FWGE for treatment of cancer cells, a systematic review of the literature was performed. Sixteen articles were included in the final qualitative analysis. Various types of cancer cells treated with FWGE have been analyzed, showing mainly cytotoxic effects, alteration of the cell cycle, antiproliferative effects, and induction of apoptosis.

After that, a series of in vitro experiments, including MTT assay, invasion and migration assays were performed to investigate the effects of the treatment of OSCC cells (HSC-3, SAS and SCC-25) with different concentrations of FWGE. The inhibitory effect on viability

of OSCC cells, exerted by chemotherapeutic drugs (cisplatin and 5-fluorouracil) and the combination of these with FWGE, was also evaluated. The results showed a significant reduction of cells viability after treatment with FWGE. Regarding migration and invasion capacity, the HSC-3 cells resulted to be the most sensitive to the treatment with FWGE. The combination of chemotherapeutic drugs and FWGE at 10mg/ml led to a significantly higher decrease in cell viability.

A secondary purpose of this thesis regarded the investigation of prognostic meaning of certain mutations and expression of proteins characterizing OSCC.

Firstly, a histologic and bioinformatic analysis of Musashi 2 (MSI2) expression was performed and its correlation with clinic-pathologic and prognostic features of OSCC evaluated. Musashi-2 is an RNA-binding protein, playing a fundamental role in the oncogenesis of several cancers. A bioinformatic analysis was performed on data downloaded from The Cancer Genome Atlas (TCGA) database. The MSI2 expression data were analysed for their correlation with clinic-pathological and prognostic features. In addition, an immunohistochemical evaluation of MSI2 expression on 108 OSCC samples included in a tissue microarray and 13 healthy mucosae samples was performed. 241 patients' data from TCGA were included in the final analysis. No DNA mutations were detected for the MSI2 gene, but a hyper methylated condition of the gene emerged. MSI2 mRNA expression correlated with Grading ( $p = 0.009$ ) and overall survival ( $p = 0.045$ ), but not with disease free survival ( $p = 0.549$ ). Males presented a higher MSI2 mRNA expression than females. The immunohistochemical evaluation revealed a weak expression of MSI2 in both OSCC samples and in healthy oral mucosae. In addition, MSI2 expression directly correlated with Cyclin-D1 expression ( $p = 0.022$ ). However, no correlation has been detected with prognostic outcomes (overall and disease free survival). The role of MSI2 expression in OSCC seems to be not so closely correlated with prognosis, as in other human neoplasms.

The correlation with Cyclin-D1 expression suggests an indirect role that MSI2 might have in the proliferation of OSCC cells, but further studies are needed to confirm such results.

Secondly, the role of programmed death ligand 1 (PD-L1) in the tumour immunity and its potential function as a marker for OSCC prognosis were investigated through a meta-analysis. The studies were identified by searching PubMed, SCOPUS, Web of Science and were assessed by two of the authors. After the selection process, 11 articles met eligibility criteria and were included in the meta-analysis. Quality assessment of studies was performed according to the REMARK guidelines, and the risk of biases across studies was investigated through Q and I<sup>2</sup> tests. Meta-analysis was performed to investigate the association between the PD-L1 expression either overall survival (OS), disease-free survival (DFS), disease-specific survival (DSS), gender and lymph node metastasis. A total of 1060 patients were analysed in the 11 studies included in the meta-analysis. Pooled analysis revealed that the expression of PD-L1 did not correlate with poor OS (HR, 0.60; 95% CI: [0.33, 1.10]; P = 0.10), DFS (HR, 0.62; 95% CI: [0.21, 1.88]; P = 0.40), DSS (HR, 2.05; 95% CI: [0.53, 7.86]; P = 0.29) and lymph node metastasis (HR, 1.15; 95% CI: [0.74, 1.81]; P = 0.53). Furthermore, results of the meta-analysis showed that high expression of PD-L1 is two times more frequent in female patients (OR, 0.5; 95% CI: [0.36, 0.69]; P < 0.0001) compared to males. For all the three outcomes analysed, a high rate of heterogeneity was detected (I<sup>2</sup> > 50%). High PD-L1 expression did not correlate with poor prognosis of patients suffering for oral squamous cell carcinoma. Studies published on the topic showed a significant variation in results, limiting the use of PD-L1 expression by immunohistochemistry as prognostic biomarker in clinical practice.

Lastly, the role of the tumour-suppressor gene TP53 was evaluated in different head and neck squamous cell carcinoma (HNSCC). A systematic bioinformatics appraisal of TP53 mutations was performed on 415 HNSCC cases available on The Cancer Genome Atlas (TCGA). The following features were analysed and correlated with known

clinicopathological variables: mutational profile of TP53, location (within secondary structure and predicted domains of p53 protein) and well-known hotspot mutations. Interactome–genome–transcriptome network analysis highlighted different gene networks. An algorithm was generated to develop a new prognostic classification system based on patients' overall survival. TP53 mutations in HNSCCs exhibited distinct differences in different anatomical sites. The mutational profile of TP53 was an independent prognostic factor in HNSCC. High risk of death mutations, identified by our novel classification algorithm, was an independent prognostic factor in TCGA HNSCC database. Finally, network analysis suggested that distinct p53 molecular pathways exist in a site- and mutation-specific manner. The mutational profile of TP53 may serve as an independent prognostic factor in HNSCC patients, and is associated with distinctive site-specific biological networks.

## 1. INTRODUCTION

### 1.1 Oral cancer

Oral squamous cell carcinoma (OSCC) represents one of the most aggressive types of cancer, with more than 400,000 new cases and 146,000 deaths in 2015 worldwide.[1-4] The incidence of OSCC is increasing and the average age of the affected patients decreases.[5] Highest incident for oral cavity cancer was reported in south-central Asia (40.9% of all incident cases).[2] The incidence of oral cavity cancer was consistently greater among men than women, with an M/F rate ratio of 2.1, ranging from 5.2 for Central and Eastern Europe to 1.4 for Northern Africa, Western Asia and Oceania.[2] The disease occurs when the accumulation of multiple genetic mutations in the oral epithelial cells leads to an irreversible damage of DNA and the cells lose their normal life cycle. The factors universally accepted to be carcinogenic include tobacco, alcohol consumption, betel quid or a combination of them. The prognosis correlates to several factors and an early diagnosis, certainly, improves the outcome.[5-9] In fact, patients diagnosed in early stages have a longer life expectancy compared to patients who get the diagnosis in advanced stages.[10]

Recently the 8th edition of the American Joint Committee on Cancer (AJCC) introduced in the staging system of the OSCC the depth of invasion (DOI) as a variable for the T category.[11] The new staging manual highlights the importance to distinguish between tumors with different DOI and the need to use the latter for staging purposes. However, although tumor-node-metastasis (TNM) staging is routinely used to predict tumor behavior and, hence, to inform the choice of treatment strategies for OSCC, patients with same TNM stages may result in dramatically different survival time.[12]

The treatment strategy for OSCC incorporates both the surgical and oncologic approaches. With regards to the advanced OSCC, guidelines from the National Comprehensive Cancer

Network still today recommend surgical excision followed by concurrent single-agent cisplatin chemo-radiotherapy in T3 or T4 lesions demonstrating adverse features of extracapsular spread and/or positive margins.[13] The oncological management consists of radiotherapy, chemotherapy and biologic therapy and is fundamental for patients with advanced or recurrent disease. The advent of new treatment modalities that demonstrated benefits for other types of malignancies, failed to improve survival for OSCC patients, remaining the 5-years survival rate under 60%.[13, 14]

There are two main challenges of the current research in cancer treatment: the first one is the development of more personalized and effective therapies, since not all tumors of the same stage respond to the therapy in the same way, and the second one is the setup of a more targeted therapy, that can affect only the cancer cells, without destroying healthy ones.[15] This last point arises because of the toxicity that the current chemotherapy drugs have on the human body and that leads the patient to develop a series of side effects, that significantly worsen the patients' quality of life and, many times, require the interruption of therapy.[16] Many efforts are made to find compounds that can support and improve the cancer therapy, and great attention is focused on some of natural products, known to have beneficial properties on the human organism.

## **1.2 Nutraceuticals**

'Nutraceutical' term (a combination of the words "nutrition" and "pharmaceutical") refers to any substance considered to be a food or a food ingredient that provides medical and health benefits.[17]

Recently, more and more attention has been placed on the use of nutraceuticals as therapeutic agents for cancer prevention, as well as supplements to conventional therapy because of their promising effects and a low rate of toxicity. [18-20] A number of natural compounds have

been found to inhibit one or more pathways that contribute to proliferation of cancer cells and metastatic processes.[21]

Fermented wheat germ extract (FWGE; trade name AVEMAR™) is a product of industrial fermentation of wheat germ. Its production process is patented and is derived from the extraction of wheat germ and fermentation by *Saccharomyces cerevisiae*, followed by separation of the fermentation liquid, drying, and then granulation. As with other nutraceuticals, FWGE contains various molecules, but recent studies assume that the two quinones, 2-methoxy benzoquinone and 2, 6-dimethoxy benzoquinone, which are present in wheat germ as glucosides, are likely to be responsible for some of the biological properties of FWGE.[22]

Quinones are cyclic organic compounds containing two carbonyl groups (C=O) linked to the cyclic structure of a conjugated system. Several anticancer compounds, e.g., Mitomycin C, Mitotraxan, Doxorubicin, and Daunorubicin, are quinone derivatives.[23, 24] The anticancer characteristics of AVEMAR have been deeply investigated, and results have suggested its metabolic, antiproliferative, and antimetastatic effects.[25-27]

Few clinical studies were also conducted in order to test the effects of FWGE supplement on patients undergoing conventional chemotherapy for melanoma[28] and colorectal cancer.[29] The results revealed significantly better data on disease progression and survival in the groups supplemented with FWGE compared to the control groups treated with the conventional drugs only.

Despite the anti-tumor activity of FWGE has been reported for many cancer cell types, its action on oral squamous cell carcinoma cells has been poorly investigated.[30]

The main aim of the thesis was to evaluate the effects of FWGE on oral squamous cell carcinoma. Simultaneously, a research on some molecular aspects of OSCC, as well as

investigation on prognostic factors, were also performed and results briefly reported hereunder.

## **2. THE EFFECTS OF ADJUVANT FERMENTED WHEAT GERM EXTRACT ON CANCER CELL LINES**

### **2.1 Background**

Fermented wheat germ extract (FWGE; trade name AVEMAR) is a nutraceutical compound obtained from a fermentation process of wheat germ by *Saccharomyces cerevisiae*, followed by some patented steps which lead to obtaining a grainy compound. Several studies have been conducted in order to investigate its biological activity. In particular, a great interest raised for its potential anticancer properties, proposed by some authors.

The antimetabolic effects of FWGE on cancer cells seems to be due to a hypermetabolic state of the cancer cells and their upregulated utilization of glucose[31, 32]. The antimetastatic effect of FWGE, besides the immune-reconstitution, may also be due to its cell adhesion inhibitory, cell proliferation inhibitory, apoptosis enhancing, and antioxidant characteristics, which have also been observed in some in vitro experiments.[33] The antiproliferative action has been investigated in in vitro and in vivo studies performed on various human cancer cell lines and animal models, and results have shown a reduction of tumor growth in a dose-dependent manner.[34, 35]

The antimetastatic effect of FWGE investigated in vitro and in vivo by several studies appears to be promising for FWGE to be used alone or in association with traditional anticancer agents.[33, 36]

### **2.2 Systematic review of scientific literature concerning the in vitro activity of FWGE on malignant cells.**

The aim of this systematic review was to summarize the data available in the scientific literature concerning the in vitro activity of FWGE on malignant cells.

The systematic review was performed according to the Preferred Reporting Items for Systematic Reviews and Meta-Analyses (PRISMA).[37] A systematic review of English articles in electronic databases (PubMed, Scopus, and Web of Science) was performed using search terms: (AVEMAR OR “wheat germ extract”) AND (cancer OR antitumoral OR anticancer). No restrictions were imposed on the study designs.

The criterion for inclusion in this systematic review was in vitro original studies on human tumor cell lines where the effects of FWGE have been evaluated. No restriction on publication dates was applied. No restriction of materials and methods was applied.

The exclusion criteria were letters to the editor, in vivo studies, and reviews. Articles and abstracts written in languages other than English were excluded.

A first selection was performed by reading the titles and the abstracts of the search results. After this round, duplicates resulting from the use of different databases were removed. The abstracts that seemed to meet the inclusion criteria were selected and the full texts were read. Once the full-text evaluation was performed, only studies meeting all inclusion criteria and considered eligible by both authors were included in the review. Disagreements between the authors were resolved through discussion.

Furthermore, the bibliographies of the included articles were examined in order to find other studies to include in this review.

The data concerning the type of the cells and the main evaluations performed on them were collected and the results are summarized in Table 1. No differentiation between methods was applied, and only the final results were considered.

The primary outcomes of the review regarded types of cancer cell lines subjected to the investigation and the main results concerning the cell viability, proliferation, and apoptosis observed in the studies. No quantification was made, but only significant results were considered and reported in the present review.

The secondary outcomes regarded other types of interventions and evaluations performed on the cells, their results in term of cellular metabolism, and enzymatic activity.

Table 1: Main data of the included studies, reporting the first author, the year of publication, the title, the types of the cells subjected to the treatment, the investigation procedures performed, and the main results of the experiments.

Author	Year	Title	Cell Type	Investigations	Main Results	Secondary Outcomes
<b>Comin - Andui x et al.[35]</b>	2002	Fermented Wheat Germ Extract Inhibits Glycolysis/Pentose Cycle Enzymes and Induces Apoptosis through Poly (ADP-ribose) Polymerase Activation in Jurkat T-cell Leukemia Tumor Cells.	Jurkat T-cell Leukemia Tumor Cells.	Cell cycle analysis, cell viability assay, assessment of apoptosis.	Cytotoxic effects, alteration of the cell cycle, induction of apoptosis.	Cleavage of PARP, Transketolase, G6P DH, HK, LDH inhibition.
<b>Fajkaboja et al. [38]</b>	2002	Fermented wheat germ extract induces apoptosis and downregulation of major histocompatibility complex class I proteins in tumor T and B cell lines.	Jurkat leukemic T cells, Burkitt lymphoma B cell lines, myelomonocytic cell line.	Detection of apoptotic cells, measurement of cell proliferation	Induction of apoptosis, antiproliferative effect.	Elevation of intracellular Ca <sup>2+</sup> concentration.
<b>Imir et al. [39]</b>	2018	Mechanism of the anti-angiogenic effect of AVEMAR on tumor cells.	NCI-N87 (gastric tubular adenocarcinoma), PC3 (prostate carcinoma), HeLa (adenocarcinoma) and A549 (lung adenocarcinoma)	Investigation of anti-angiogenic effects.	Inhibition of induced VEGF levels.	Inhibition of Cox-2 levels.

<b>Judson et al. [40]</b>	2012	Characterizing the efficacy of fermented wheat germ extract against ovarian cancer and defining the genomic basis of its activity.	Ovarian cancer cell lines.	Cell viability assays.	Cytotoxic effects, increase of cisplatin sensitivity.
<b>Marcsek et al. [41]</b>	2004	The Efficacy of Tamoxifen in Estrogen Receptor-Positive Breast Cancer Cells Is Enhanced by a Medical Nutrient.	MCF-7 breast cancer cells.	Cytotoxic effects evaluation, detection of apoptosis and mitosis, evaluation of tamoxifen-combined treatment.	Cytotoxicity, induction of apoptosis.
<b>Mueller et al. [42]</b>	2011	Promising cytotoxic activity profile of fermented wheat germ extract (Avemar®) in human cancer cell lines.	testicular cancer (H12.1, 2102EP, 1411HP, 1777NRpmet), colon cancer (HCT-8, HCT-15, HCT-116, HT-29, DLD-1, SW480, COLO205, COLO320DM), NSCLC (A549, A427, H322, H358), head and neck cancer (FADU, A253), cervical epidermoid carcinoma (A431), mammary adenocarcinoma (MCF-7, BT474), ovarian adenocarcinoma (A2780), gastric Cancer (M2), anaplastic thyroid cancer (8505C, SW1736), papillary thyroid cancer (BCPAP), follicular thyroid cancer (FTC133),	Growth inhibition experiments, apoptosis evaluation.	Antiproliferative activity.

			melanoma, hepatoma (HepG2), glioblastoma (U87MG), neuroblastoma (SHSY5Y, SIMA).			
<b>Otto et al. [43]</b>	2016	Antiproliferative and antimetabolic effects behind the anticancer property of fermented wheat germ extract.	Adenocarcinoma of the breast (MDA-MB-468) and (MDA-MB-231) and (BT-20), adenocarcinoma of the pancreas (ASPC-1) and (BxPC-3), adenocarcinoma of the stomach (23132/87), adenocarcinoma of the colon (HT-29) and (HRT-18), invasive breast ductal carcinoma (MCF-7).	Effects on cell growth, Cell cycle analysis.	Cytotoxic, antiproliferative and growth delay effects.	Depletion in cellular ATP and decrease in the NADH/NAD <sup>+</sup> ratio.  Impaired glucose consumption and significantly reduced production of lactic acid.  Induction of autophagy in HRT-18 cells.
<b>Saiko et al. [44]</b>	2007	Avemar, a nontoxic fermented wheat germ extract, induces apoptosis and inhibits ribonucleotide reductase in human HL-60 promyelocytic leukemia cells.	Human HL-60 promyelocytic leukemia cells.	Apoptosis evaluation, cell cycle distribution analysis.	Induction of apoptosis, cell growth inhibition.	Decreasing of dNTPs, direct enzyme attenuation (ribonucleotide reductase; RR).
<b>Saiko et al. [34]</b>	2009	Avemar, a nontoxic fermented wheat germ extract, attenuates the growth of sensitive and 5-FdUrd/Ara-C cross-resistant H9 human lymphoma cells through induction of apoptosis.	Human lymphoma cells H9, 5-FdUrd/Ara-C cross-resistant H9 human lymphoma cell line.	Growth inhibition assay, apoptosis evaluation.	Growth inhibition, induction of apoptosis.	
<b>Tai et al. [45]</b>	2013	Fermented Wheat Germ Extract Induced Cell Death and Enhanced Cytotoxicity of Cisplatin and 5-Fluorouracil on Human Hepatocellular Carcinoma Cells.	Hepatocellular carcinoma (HCC) HepG2, Hep3B, and HepJ5 cells.	Cell viability Assay, evaluation of cisplatin and 5-fluorouracil	Antiproliferative activity, enhanced cytotoxicity of chemotherapeutic.	

				combined treatment.	
<b>Wang et al. [46]</b>	2015	Preclinical Evaluation on the Tumor Suppression Efficiency and Combination Drug Effects of Fermented Wheat Germ Extract in Human Ovarian Carcinoma Cells.	SKOV-3 and ES-2 human ovarian carcinoma cells.	Cell viability evaluation, cell death markers analysis, evaluation of cisplatin- or docetaxel-combined treatment.	Suppression of cell proliferation, caspase-related apoptosis activation, increased cytotoxicity of cisplatin and docetaxel.
<b>Yang et al. [30]</b>	2016	Inhibitory Effects of AVEMAR on Proliferation and Metastasis of Oral Cancer Cells.	Human oral squamous carcinoma SCC-4 cells.	Cell viability evaluation, cell apoptosis assay wound-healing migration assay, cell invasion assay.	Inhibition of cell viability, induction of cell apoptosis, suppression of migration and invasion capacity.
<b>Zhang et al. [47]</b>	2015	Effect of Fermented Wheat Germ Extract with Lactobacillus plantarum dy-1 on HT-29 Cell Proliferation and Apoptosis.	Human HT-29 colon cancer cells.	Growth inhibition assay, assessment of apoptosis.	High antiproliferative effects, induction of cell apoptosis.
<b>Barisone et al. [48]</b>	2017	A purified, fermented, extract of Triticum aestivum has lymphomacidal activity mediated via natural killer cell activation.	Lymphoma cells, T-cell leukemia (Jurkat), lung (H1650), breast (MCF-7) and hepatic (HepG2) cancer cell lines.	Cytotoxic activity assay, apoptosis and cell cycle.	Cytotoxic activity, apoptotic activity.
<b>Szende et al. [49]</b>	2004	Effect of Simultaneous Administration of Avemar® and Cytostatic Drugs on Viability of Cell Cultures, Growth of Experimental Tumors, and Survival of Tumor-Bearing Mice.	Human breast adenocarcinoma cell line (MCF-7), hepatocyte carcinoma (HepG2).	Cytotoxicity testing of Avemar associated with various cytostatic drugs (5 FU, Dacarbazine, Adriblastina).	Did not increase nor decrease cell viability.

---

<b>Boros et al. [50]</b>	200	Wheat Germ Extract Decreases Glucose Uptake and RNA	MIA pancreatic adenocarcino ma cells.	Evaluation of glucose utilization rates and lactate production.	Regulation of tumor cell proliferation.	Inhibitory effect on glucose consumption, little effect on lactate production.
	1	Ribose Formation but Increases Fatty Acid Synthesis in MIA  Pancreatic Adenocarcinoma Cells.				

---

PARP: poly ADP ribose polymerase, ATP: Adenosine triphosphate, G6PDH: Glucose-6-phosphate dehydrogenase, LDH: Lactate dehydrogenase, NADH: reduced Nicotinamide adenine dinucleotide; NAD<sup>+</sup>: oxidized nicotinamide adenine dinucleotide; HK: Hexokinase, 5-FdUrd/ara-C: 5-fluorodeoxyuridine/cytosine arabinoside; HeLa: human cervical carcinoma, RT-qPCR: Total RNA isolation and reverse transcription-quantitative polymerase chain reaction, dNTPs: deoxyribonucleoside triphosphates; Cox-2: cyclooxygenase-2; VEGF: vascular endothelial growth factor; dNTPS: deoxyribonucleoside triphosphates.

### 2.3 Results

A total of 56 titles and articles from PubMed, 53 from Scopus, and 52 from Web of Science were screened in the first round of the selection process. After duplicates were removed, 20 studies were identified as acceptable for full-text evaluation and their full texts were read. At the end of the selection process, 16 articles [27, 30, 34, 35, 38-42, 44-48, 51] were included in qualitative analysis, while four [22, 36, 52, 53] were excluded for not complying with inclusion criteria.

The flowchart in Figure 1 represents the selection process for the inclusion of studies.

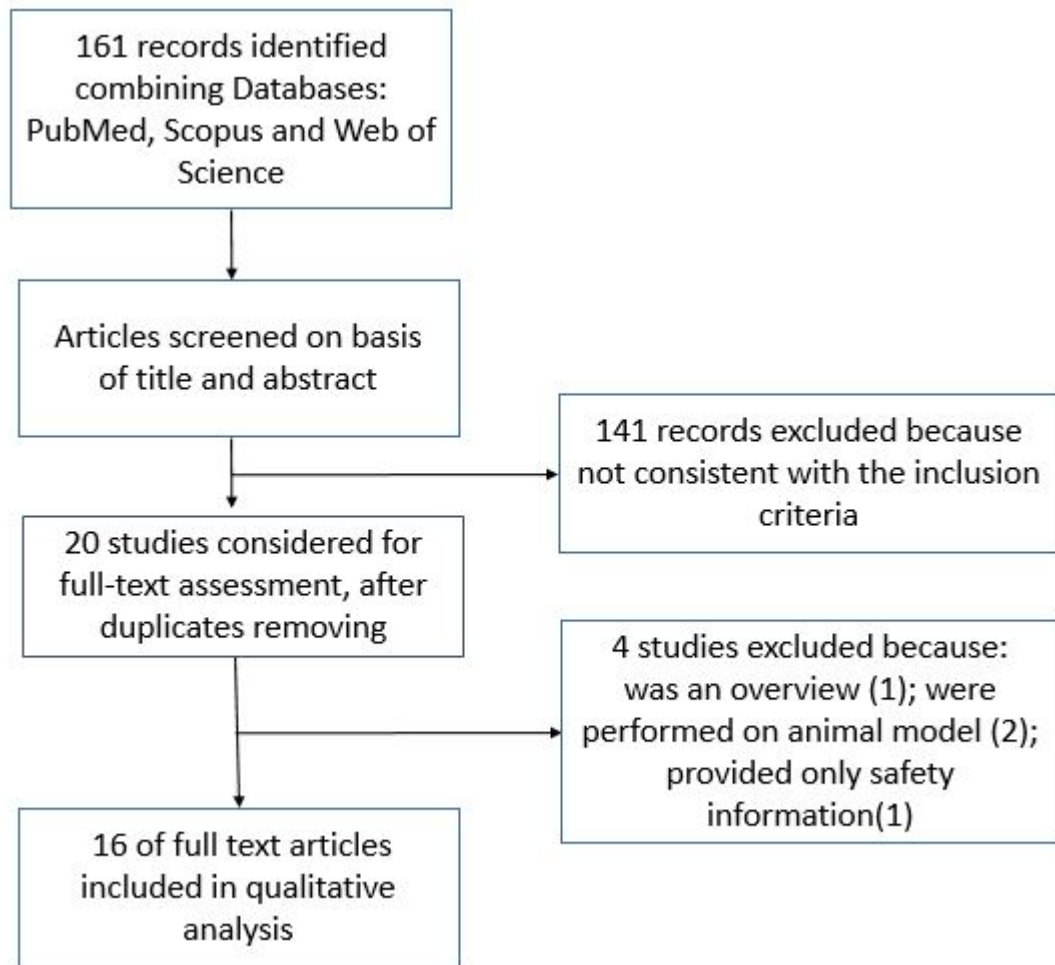


Figure 1. Flowchart of the selection process for the studies inclusion.

### *Characteristics of Included Studies and Primary Outcomes*

All sixteen studies selected for the review were in-vitro studies published in English. The effects of FWGE were investigated on the following cell lines:

(1) Jurkat leukemic T cells were studied by three studies [35, 38, 48] and the treatment resulted in cytotoxic effects, alteration of the cell cycle, antiproliferative effects, and induction of apoptosis;

(2) Lymphoma cells were subjected to the treatment and the effects investigated by three studies [34, 38, 49] showed growth inhibition, induction of apoptosis, antiproliferation,

and cytotoxic effects;

(3) Gastric cancer cell line experiments reported in three papers [39, 42, 43] found antiproliferative, cytotoxic, cytostatic, and growth-delay effects;

(4) Ovarian cancer cell lines, when subjected to treatment with AVEMAR, showed cytotoxic effects [40], antiproliferative activity [42], and suppression of cell proliferation[46];

(5) Breast cancer cell lines appeared to undergo cytotoxicity and apoptosis [41-43], while, in one study [51] investigating the combined administration of AVEMAR and cytostatics, the treatment with AVEMAR resulted in no increase or decrease of cell viability compared to untreated cells;

(6) When applied to colon cancer cell lines, FWGE showed antiproliferative activity [42], cytotoxicity, cytostasis, and induction of cell apoptosis [47];

(7) The treatment of hepatic cancer cells appeared to cause cytotoxicity, apoptosis [48], and an inhibition of proliferation [42, 45];

(8) Other types of cell lines investigated in the included studies were prostate cancer cells, endocervical adenocarcinoma [39], cervical epidermoid carcinoma cells [42], testicular cancer cell lines [42], head and neck cancer [42], thyroid and pancreatic cancer cells [50], melanoma, hepatoma, glioblastoma, neuroblastoma [39], and oral squamous carcinoma cells [30]. In all cases, the effects of AVEMAR treatment provided results similar to those previously mentioned.

### *Secondary Outcomes*

Additional results that emerged from the experiments include:

(1) Enzyme activities evaluation. In particular, FWGE was found to inhibit Glucose-6-phosphate dehydrogenase (G6PDH), Lactate dehydrogenase (LDH) and Hexokinase (HK) activity in Jurkat T-progeny leukemia cells [35]. The inhibition of ribonucleotide reductase (RR) activity in promyelocytic leukemia cells was established by Saiko et al. [44]. A suppression of the expression of matrix metalloproteinase-2 (MMP-2) and urokinase plasminogen activator (u-PA) was revealed in oral cancer cells (SCC-4) treated with Avemar [47];

(2) Presumable anti-angiogenic effects of FWGE on human cervical carcinoma (HeLa) and human lung adenocarcinoma (A549) cells through the inhibition of vascular endothelial growth factor (VEGF) and cyclooxygenase-2 (Cox-2) levels [39];

(3) Impaired glucose consumption and reduced production of lactic acid in some adenocarcinoma cell lines [43, 50].

## **2.4 Discussion**

Nutraceuticals are gaining importance in the prevention and treatment of different diseases.

In particular, cancer treatment is a challenge that is still ongoing because of the difficulties presented by conventional drugs, which are often accompanied by serious side effects and unsatisfactory results. FWGE is a nutraceutical that has been reported to possess unique “cancer-fighting” characteristics [54]. Its antiproliferative and cytotoxic activity, as well as its induction of apoptosis in human cancer cells, have been affirmed by several studies [35, 38, 41]. Some studies [27, 35, 43] investigated the metabolic changes in tumor cells in response to the treatment with FWGE and revealed important alterations in enzymes involved in direct glucose oxidation (G6PDH), non-oxidative glucose utilization

(transketolase) toward nucleic acid synthesis, glycolysis (LDH), and glucose activation (HK). The inhibition of the key pathways of sugar metabolism and DNA-synthesis seems to contribute to the proliferation inhibiting capacity of FWGE. Saiko et al. [44] found that treatment with AVEMAR carried a direct enzyme attenuation of ribonucleotide reductase, which was demonstrated to be significantly up-regulated in tumor cells. In another study [38], some early biochemical events, such as tyrosine phosphorylation and the increase of intracellular Ca<sup>2+</sup> concentration, occurred in response to the treatment and was associated with increased apoptosis of the tumor cells. Judson et al.[40] have also identified genes and molecular signaling pathways associated with FWGE activity on investigated cells and these pathways include hedgehog signaling, activin A signaling regulation, and regulation of GAP 1/Synthesis (G1/S) phases transition. Moreover, some of the studies included in this review suggested that AVEMAR could potentially inhibit cancer cell migration and invasive capacities [30]. Such actions can be important especially for some types of tumors, such as the oral squamous cell carcinoma [55, 56], for which the highest mortality is due to the ability of lymph node metastasis or metastasis to distant organs. Imir et al. [39] investigated the ability of FWGE to inhibit angiogenesis and obtained very encouraging results stating that AVEMAR exerts anti-angiogenic effects by inhibiting VEGF and Cox-2 gene expression. This mechanism of action has already been proposed for the anti-angiogenic activity of polyphenols and polyphenol-rich foods in “in vitro” and “in vivo” models of angiogenesis[57]. Another important finding was that the treatment with AVEMAR results in widespread apoptosis in lymphoid tumor cells, but it does not induce apoptosis of healthy resting mononuclear cells [38].

In some studies, the association of FWGE with conventional anticancer drugs has also been investigated in order to search for possible solutions to overcome the drug resistance that frequently occurs during anticancer chemotherapy and limit the side effects that traditional treatments entail. The results are promising for the addition of this natural compound to

cisplatin chemotherapy of epithelial ovarian cancer cell lines [40, 46] and hepatocellular carcinoma cells [45], to tamoxifen in the treatment of breast cancer cells [41], to docetaxel in ovarian carcinoma cells [46], to 5-Fluorouracil (5-FU) in colon cancer cells [42], and to the treatment of hepatocellular carcinoma cells [45]. Only one study [51] reported poor results for simultaneous use of AVEMAR and Dacarbazine, 5-fluorouracyl, or Adriblastina, where the addition of the nutraceutical did not increase nor decrease the viability of any of the cell cultures. However, the authors concluded that, based on the findings in the literature that have stated immunomodulatory and antimetastatic effects of AVEMAR [29, 33, 36, 38], the latter may be administered with cytostatic drugs without increasing toxicity or decreasing the antiproliferative effect of the cytostatics. Concordant conclusions were reached by Yeend et al. [58] in their systematic review that considered clinical studies evaluating the adjunction of AVEMAR to conventional cancer treatments when compared to conventional cancer treatment alone.

It should be noted that, in some of the included studies [47, 48], the nutraceutical was not purchased from the manufacturing company, but instead produced in the laboratory through the use of *Lactobacillus plantarum* dy-1 on fresh wheat germ. Barisone et al. [48] described a different way of obtaining the fermented wheat germ extract by using *Saccharomyces cerevisiae*. They also compared the in vitro activity of FWGE with that of AVEMAR and concluded that the killing activity was equivalent [48].

An important aspect to consider when experimenting with new principles is their safety. Although wheat germ is a commonly consumed food with no known adverse effects, the toxicity of AVEMAR has been investigated in various studies as summarized by Heimbach et al. [52]. Though this study reported that the use of AVEMAR pulvis would not be expected to cause adverse effects, the scientific literature on this is sparse. Further in vitro and in vivo studies are needed to assure its product safety as an ingredient in dietary supplements or as ~~an~~ anticancer drug.

## **2.5 Conclusions**

The available data suggest that FWGE can be a promising compound that can be integrated into or improve the current treatment of cancer. However, further in vitro and in vivo studies are necessary to prove its effectiveness and safety in humans.

### **3. EFFECTS OF FERMENTED WHEAT GERM EXTRACT ON ORAL CANCER CELLS.**

In order to evaluate the effects of FWGE on oral cancer cells, a series of in vitro experiments were conducted.

#### **3.1 Materials and Methods**

##### *Cell lines*

Human OTSCC cell lines HSC-3, SAS and SCC-25 were kindly gifted by Dr. Yasusei Kudo, Department of Oral Molecular Pathology, Institute of Health Biosciences, The University of Tokushima Graduate School, Tokushima Japan or were obtained from Japanese Collection of Research Bioresources (JCRB) Cell Bank, JCRB0623 (HSC-3), ATCC, Wesel, Germany, CRL-1628 (SCC-25) and JCRB Cell Bank, JCRB0260 (SAS). Cell lines were routinely cultured in 1:1 Dulbecco's Modified Eagle Medium (DMEM):Ham's Nutrient Mixture F-12 (Gibco, Carlsbad, CA, USA), supplemented with 10% heat-inactivated FBS (Gibco), 100U/ml penicillin, 100µg/ml streptomycin, 50µg/ml ascorbic acid, 250ng/ml amphotericin B and 0.4ng/ml hydrocortisone (all from Sigma Aldrich, St Louis, MO, USA).

All cell lines were cultured at 37 °C in a humidified atmosphere of 95% air and 5% CO<sub>2</sub> and passaged routinely using trypsin-EDTA (Sigma- Aldrich).

##### *Drugs and chemicals*

FWGE was donated by American BioScience Inc. under form of Fermented Wheat Germ Extract – Super concentrate (FWGE-SC<sup>®</sup>), with the trademark of Metatrol<sup>®</sup>. The solution was prepared, considering the proportion indicated by the manufacturer (41mg of FWGE-SC<sup>®</sup>= 5500mg of FWGE). For each experiment, a fresh stock solution containing 100mg/ml

FWGE was prepared to serum-free DMEM/F-12 media with 0.5% lactalbumin (Sigma-Aldrich), vortexed, centrifuged and passed through a 0.22 $\mu$ m filter.

#### *Cell Viability Assay*

HSC-3, SAS and SCC-25 cell lines were seeded into 96-well flat-bottom tissue plates, each in its own media, with density of  $5 \times 10^3$  cells per well. SAS cells were seeded with density of  $2 \times 10^3$  cells per well. After 24h of incubation at 37°C and 5% CO<sub>2</sub>, the cells were treated with different concentrations of FWGE (2, 5 and 10mg/ml) and control cells were treated with normal media mixed with Lactalbumin medium (9:1). Cell growth was determined by the MTT (3-(4,5-dimethylthiazol-2-yl)-2, 5-diphenyltetrazolium bromide) assay (Sigma-Aldrich)[59] according to the manufacturer's protocol at 24, 48 and 72h of incubation. Absorbance was measured at the wavelength of 550nm with Victor 3V multilabel reader (Perkin Elmer).

#### *Transwell invasion and migration assays*

Transwell migration and invasion assays were performed in 6.5mm inserts with an 8 $\mu$ m pore size (Corning, Corning, NY, USA). For invasion assays, membranes were coated with 50 $\mu$ l of MyoGel[60, 61] (2.4mg/ml), an extracellular matrix developed in laboratory of University of Oulu solidified with 0.8mg/ml type I collagen from rat tail (Corning) in serum free medium. The HSC-3 and SAS cells were seeded into the upper chamber with a density of 70,000 cells, diluted in 100 $\mu$ l medium containing 0.5% of lactalbumin instead of FBS. Then, 100 $\mu$ l of medium containing indicated amounts of FWGE suspended in lactalbumin was added on top of the cells. As a chemoattractant, 500 $\mu$ l of medium supplemented with 10% FBS was used in the lower chamber.

The transwell plates were incubated at 37°C for 24 and 48h for migration assay and for 72h for invasion assay. Then, the cells were fixed in 4% neutral buffered formaldehyde for 1h

and washed once with PBS. Cells were stained with 1% Toluidine Blue and 1% Borax for 10 min at room temperature and washed several times with deionized water. Then, non-invaded cells on the upper surface of the filter were carefully removed with a wet cotton swab. Toluidine blue stain was eluted with 1% SDS and absorbance was measured at 650nm using a Victor2 Microplate Reader (Perkin Elmer Wallac).[60] All the experiments have been performed in triplicate and repeated from three to five times. The average of the results is reported.

### *3D tumor spheroid invasion assay*

Spheroids were generated for three cell lines (HSC-3, SAS, SCC-25) following the protocol described by Naakka et al.[62] Briefly, the cells were seeded in a complete growth medium at a cell density of  $1 \times 10^3$  cells/well into ultra-low attachment (ULA) 96-well round bottom plates (Corning, NYC, NY, USA) and incubated at 37°C for 4 days. After visual confirmation, spheroids were embedded in 50µl gel containing 0.5mg/ml Myogel[60], 0.5mg/ml of Fibrinogen (Merck), 0.3U/ml Thrombin (Sigma-Aldrich) and 33.3µg/ml of Aprotinin (Sigma-Aldrich). The plate was then transferred to the incubator at 37°C for 30 min in order to allow gel to solidify. 100µl of complete culture medium containing different concentrations (2, 5 and 10mg/ml) of FWGE were gently added on top of gel. Control wells were added with normal medium combined with lactalbumin (9:1). Spheroids were imaged at 0h and, after 2, 3, 4, 7, 9 and 11 days of incubation, using a Nikon Eclipse TS100 inverted light microscope, with 4x objective magnification, connected to a Canon PowerShot S50 camera.(Fig.1) Fiji software[63] was used for measuring the area covered by spheroids. The change in spheroid area at each time point compared with the area at 0h was calculated. Each experiment has been performed in triplicate and repeated three times.

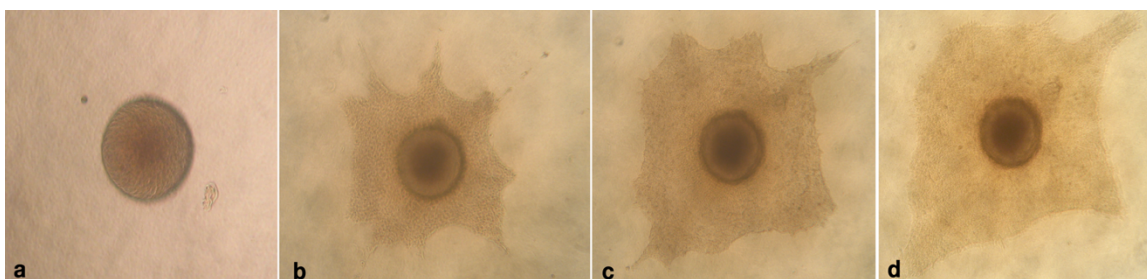


**Figure 1:** Spheroids of SAS imaged at 0h (a), after 2 (b), 3 (c) and 4 (d) days of incubation, using a Nikon Eclipse TS100 inverted light microscope, with 4x objective magnification, connected to a Canon PowerShot S50 camera.

*Treatment with chemotherapeutic drugs alone and in association with FWGE*

The inhibitory effect on viability of HSC-3 and SAS cells, exerted by chemotherapeutic drugs (cisplatin and 5-fluorouracil) and by the combination of these with FWGE, was evaluated by MTT assay[59], as described above. For FWGE and cisplatin (Cis), powder was dissolved in culture medium, while DMSO was used to dissolve 5-fluorouracil (5-FU). Stock solutions were then diluted in culture medium to reach fixed final concentration values for each compound. In particular, FWGE was assayed at 5 and 10mg/ml in combination with Cis or 5-FU at 0.5 $\mu$ g/ml. Combined chemotherapeutic treatment was carried out by mixing Cis and 5-FU at 0.1 $\mu$ g/ml and 0.25 $\mu$ g/ml final concentration, respectively. Moreover, the effect on cell viability was also evaluated after combined treatment with both FWGE and chemotherapeutic drugs. DMSO was kept at 0.1% constant final concentration. The concentration of chemotherapeutics was chosen based on previous experiments testing a range of concentrations from 0,1  $\mu$ g/mL to 20 $\mu$ g/mL, for both single drugs and combinations of them (data not shown).

The day before starting treatment, cells were seeded in 96-well plates, at a density of  $2 \times 10^3$  cells/well. Cells were allowed to attach overnight and then incubated with compounds, or with DMSO only, for 24, 48 and 72 hours. All experiments were performed in triplicate and repeated three times.

### *Statistical analysis*

Analysis of data were performed using IBM SPSS Statistics Version 25 (SPSS, Inc.) and GraphPad Prism Version 6.01 (GraphPad Software, Inc.). Data distribution was evaluated using Kolmogorov-Smirnov and Shapiro-Wilk tests. ANOVA and Kruskal-Wallis tests were applied for multiple comparisons, while Dunn and Tukey tests were used for post-hoc analysis.

## **3.2 Results**

### *Dose-dependent efficacy of FWGE in reducing cell viability*

To assess the effects of FWGE on cell viability of OTSCC cell lines, cells were treated with different concentrations of the compound and MTT assay was performed.

The concentration values of FWGE were decided considering what reported in the previous studies.[30, 42, 45, 47] An initial experiment of cell viability was carried out by testing three concentrations (0.1, 1 and 10mg/ml). Subsequently, two additional concentrations within this range (2 and 5mg/mg) were explored. Based on cellular response, the concentrations of 2, 5 and 10mg/ml were chosen for further experiments.

HSC-3 and SCC-25 cells showed a significant ( $p < 0.01$ ) reduction in their viability when treated with FWGE at 5 and 10mg/ml compared to untreated cells.(Fig.1a, 1b) Concerning SAS, a significant cytotoxicity was detected upon treatment with the highest concentration (10mg/ml) only.(Fig. 1c)

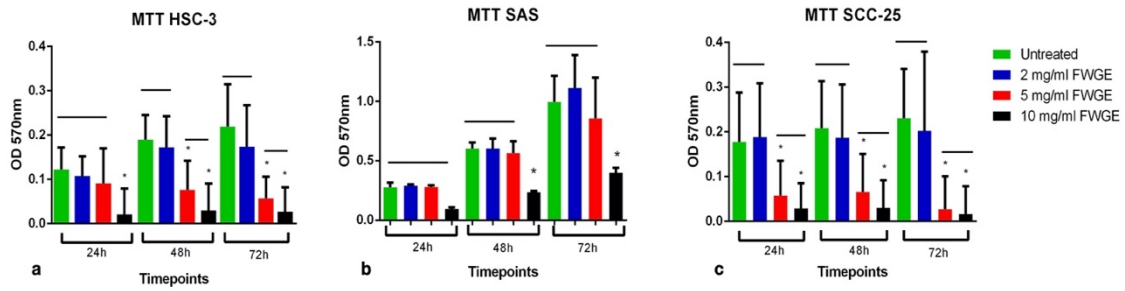


**Figure 1:** Effects of FWGE treatments (2, 5 and 10mg/ml) on HSC-3 (a), SAS (b), SCC-25 (c) cell viability assessed by MTT assay. The Optical density (OD) was measured at 570 nm. Timepoints of measurements were established at 24 hours, 48 hours and 72 hours after cell treatment. Columns and bars represent means and standard deviations (SD). \*  $p < 0.05$  compared to controls (untreated). Line over bars indicates no significant difference. Line over bars with \* indicates a significant difference between groups.

Table 2 summarizes the results of multiple comparisons, resulting from MTT assay.

	HSC-3			SAS			SCC-25		
	24h	48h	72h	24h	48h	72h	24h	48h	72h
<b>Untreated vs 2mg/ml</b>	.8385	.8534	> .9999	>.9999	>.9999	>.9999	>.9999	> .9999	> .9999
<b>Untreated vs 5mg/ml</b>	.3722	***	***	>.9999	>.9999	>.9999	**	***	***
<b>Untreated vs 10mg/ml</b>	***	***	***	>.9999	***	**	***	***	***
<b>2mg/ml vs 5mg/ml</b>	.7960	***	*	>.9999	>.9999	>.9999	**	*	**
<b>2mg/ml vs 10mg/ml</b>	***	***	***	>.9999	***	*	***	***	***
<b>5mg/ml vs 10mg/ml</b>	**	.1305	> .9999	>.9999	**	0.4503	> .9999	> .9999	> .9999

Table 2: Effects of FWGE treatment on cell viability assessed by MTT assay.

p-values of multiple comparisons; significant results in bold.

\*  $p < 0.05$ ; \*\*  $p < 0.01$ ; \*\*\*  $p < 0.001$ .

## *Invasion and migration capacity of cancer cells is differentially influenced by treatment with FWGE*

### Tranwells invasion and migration assay

Tranwells method was used to evaluate whether treatment with FWGE could affect the ability of cancer cells to migrate through a semipermeable membrane and invade extracellular matrix.

HSC-3 cells treated with 5 and 10mg/ml FWGE significantly ( $p < 0.01$ ) reduced their migration and invasion capacity. (Fig. 2a) Concerning SAS, the highest concentration of FWGE (10mg/ml) was necessary to significantly ( $p < 0.01$ ) inhibit their migration and invasion ability. (Fig. 2b) On the contrary, no significant effect was observed on this cell line for the treatment with 2 and 5mg/ml. The results are summarized in Table 3.

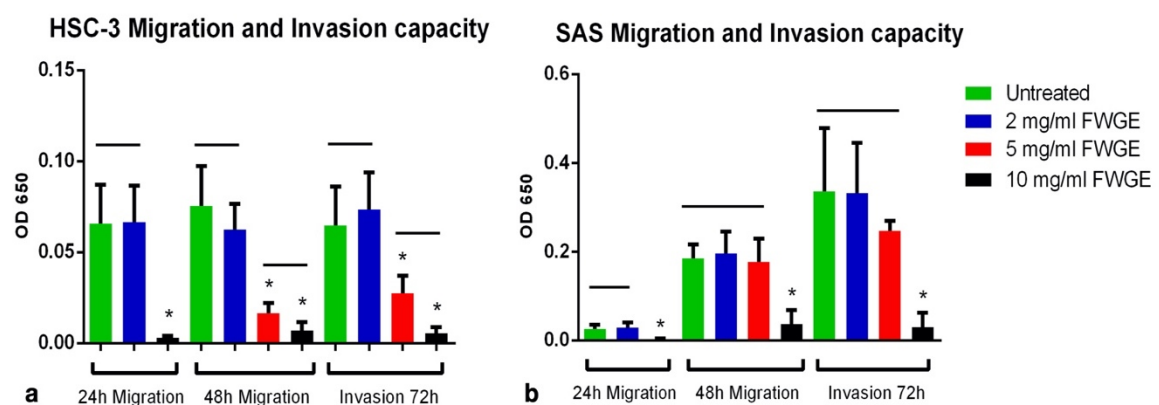


**Figure 2:** Transwell migration and invasion assay of HSC-3 (a) and SAS (b) cells treated with FWGE at concentration of 2, 5 and 10 mg/ml. The optical density (OD) was measured at 650 nm. Timepoints of the measurements were established at 24 and 48 hours for migration assay and 72 hours for invasion assay. Columns and bars represent the average  $\pm$  SD. Line over bars indicates no significant difference. \*  $p < 0.05$

	HSC-3			SAS		
	<i>Migration 24h</i>	<i>Migration 48h</i>	<i>Invasion 72h</i>	<i>Migration 24h</i>	<i>Migration 48h</i>	<i>Invasion 72h</i>
<b>Untreated vs 2mg/ml</b>	>.9999	0,8273	>.9999	>.9999	>.9999	>.9999
<b>Untreated vs 5mg/ml</b>		***	**		>.9999	>.9999
<b>Untreated vs 10mg/ml</b>	***	***	***	***	***	***
<b>2mg/ml vs 5mg/ml</b>		**	**		>.9999	>.9999
<b>2mg/ml vs 10mg/ml</b>	***	***	***	***	***	***
<b>5mg/ml vs 10mg/ml</b>		0,5395	.1614		***	***

Table 3: Effects of FWGE treatments on Migration and Invasion ability of OSCC cells evaluated with Transwells method.

p-values of multiple comparisons among treatments;

The results indicate the differences between treatments with various concentrations of FWGE at different timepoints (24-48-72 hours); significant results in bold. \* p< 0.05; \*\* p< 0.01; \*\*\*p< 0.001;

### 3D tumor spheroid invasion assay

The area of the spheroids formed by the OTSCC cells (HSC-3, SAS, SCC-25) was analyzed and compared in controls (untreated cells) and cells treated with 2, 5 and 10mg/ml FWGE, at the different time points. The results showed a significant reduction in the invasive capacity of HSC-3 cells when treated with 5 and 10mg/ml FWGE on day 2 and 4. On day, this effect was confirmed only for the concentration of 10mg/ml FWGE.(Fig.3a) Concerning SCC-25 cells, treatment with 5 and 10mg/ml FWGE induced a significant reduction of cell

invasion on day 7, 9 and 11.(Fig.3b) Regarding SAS, a significant effect occurred with treatment at the highest concentration of FWGE (10mg/ml) on day 2, 3 and 4. (Fig.3c)

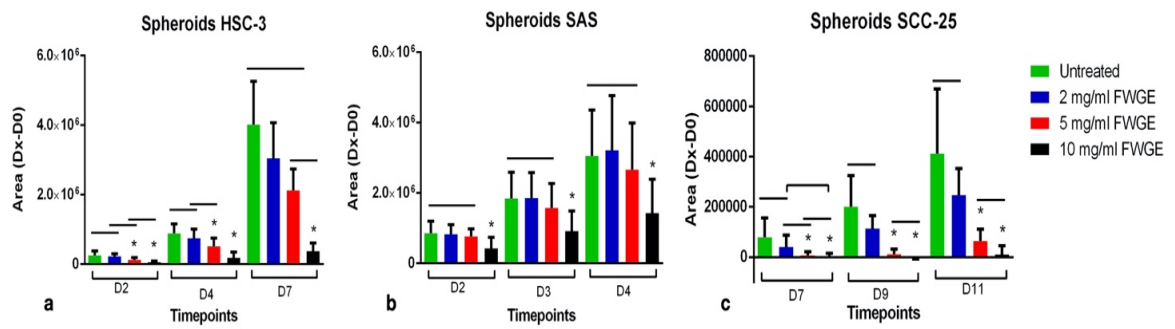


**Figure 4:** Spheroid invasion assay of HSC-3 (a), SAS (b) and SCC-25 (c) cells. The columns represent the difference in the spheroids area between a specific timepoint (day 2, 3, 4, 7, 9 and 11) and the beginning of the analysis (day 0). The columns and bars represent the average  $\pm$  SD. Line over bars indicates no significant difference. \*  $p < 0.05$

The results of multiple comparisons at different timepoints are presented in Table 4.

	HSC-3			SAS			SCC-25		
	D2	D4	D7	D2	D3	D4	D7	D9	D11
<b>Untreated vs 2mg/ml</b>	>.9999	>.9999	>.9999	>.9999	>.9999	>.9999	.3066	>.9999	>.9999
<b>Untreated vs 5mg/ml</b>	**	*	.1652	>.9999	>.9999	>.9999	***	***	**
<b>Untreated vs 10mg/ml</b>	***	***	***	**	***	***	***	***	***
<b>2mg/ml vs 5mg/ml</b>	.0554	.2445	>.9999	>.9999	>.9999	>.9999	.3066	*	*
<b>2mg/ml vs 10mg/ml</b>	***	***	*	**	***	***	.1821	***	***
<b>5mg/ml vs 10mg/ml</b>	.0780	*	.4351	*	*	*	>.9999	>.9999	.8937

Table 4: Effects of FWGE treatments on Invasion ability of OSCC cells evaluated with Spheroids method.

p-values of multiple comparisons among treatments; The results indicate the differences among groups in term of invasion area at different timepoints (D=day).

\* p< 0.05; \*\* p< 0.01; \*\*\*p< 0.001.

*Combination of Chemotherapeutic drugs with highly concentrated FWGE enhanced their activity against cancer cells*

Prior to start treatment with 5-fluorouracil, used alone or in combination with cisplatin, HSC-3 and SAS cells were incubated with DMSO only, in order to test its ability to inhibit cell viability, as well as to identify the best solvent concentration to be used in MTT assay. To accomplish these tasks, cells were grown in culture medium containing different DMSO concentrations ranging between 1.25% and 0.05%. Results obtained demonstrated that DMSO exerts no significant inhibitory effect on viability when used at a final concentration  $\leq 0.1\%$  ( $p>0.05$  when compared with DMEM).

Regarding the comparison among chemotherapeutic drugs, treatment with Cisplatin (0.5 $\mu$ g/mL) was able to induce a higher inhibitory effect ( $p<0.05$ ) on HSC-3 cell viability

than those exerted by 5-fluoruracil (0.5µg/mL) alone or by combined drugs (cis 0.1µg/ml + 5-FU 0.25µg/mL). When cisplatin, 5-fluorouracil or both were used in combination with FWGE at high concentration (10mg/ml), cell viability of HSC-3 and SAS cells was further reduced compared to that of cells treated with chemotherapeutic drugs alone. These results were confirmed for all timepoints except that of 5-Fluorouracil at 48h. A summary of obtained results is presented in Table 5. The most significant results were obtained 72 hours after treatment (Fig. 4a, 4b)

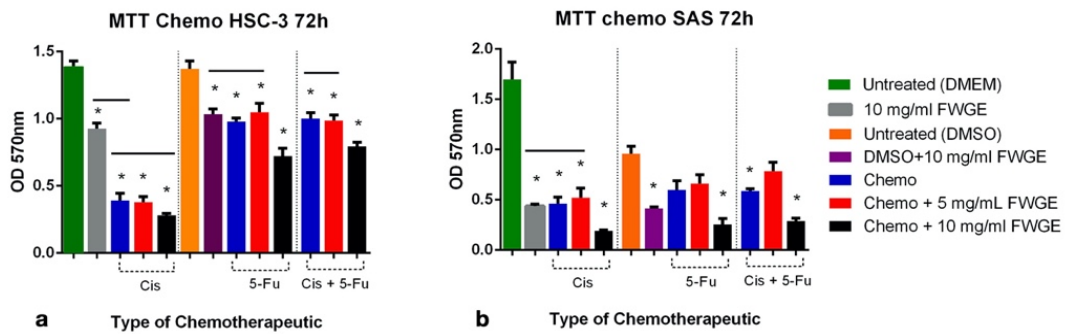


**Figure 4:** Effect of chemotherapeutic drugs and FWGE, used alone or in combination, on HSC-3 (a) and SAS (b) cell viability assessed by MTT assay at 72 hours after cell treatment. The optical density (OD) was measured at 570 nm. Columns and bars represent means and Standard Deviations (SD). \*: p<0.05. Line over bars indicates no significant difference. Line over bars with \* indicate a significant difference between groups. Cis: Cisplatin; 5-Fu: 5-Fluorouracil; FWGE: Fermented Wheat Germ Extract.

	HSC-3			SAS		
	24h	48h	72h	24h	48h	72h
<b>Untreated vs Cis</b>	>.999	***	***	>.999	***	***
<b>Untreated vs Cis+5mg/mL FWGE</b>	>.999	***	***	>.999	***	***
<b>Untreated vs Cis+10mg/mL FWGE</b>	***	***	***	***	***	***

<b>Untreated vs 5-FU</b>	>.999	>.999	***	>.999	>.999	>.999
<b>Untreated vs 5-FU+5mg/mL FWGE</b>	>.999	>.999	**	>.999	.199	>.999
<b>Untreated vs 5-FU + 10mg/ml FWGE</b>	***	>.999	***	***	***	***
<b>Untreated vs Cis + 5-FU</b>	>.999	***	***	>.999	>.999	.267
<b>Untreated vs Cis + 5-FU + 5mg/mL</b>	*	**	.950	.376	>.999	>.999
<b>Untreated vs Cis+ 5-FU + 10mg/mL FWGE</b>	***	.5067	***	**	***	***

Table 5: Effects of treatments with Chemotherapeutics associated or less with FWGE at 5 and 10 mg/mL on HSC-3 and SAS evaluated with MTT assay at different timepoints (24, 48 and 72 hours)

Cis: Cisplatin; 5-Fu: 5-Fluorouracil; FWGE: Fermented Wheat Germ Extract

p-values of multiple comparisons; significant results in bold. \* p< 0.05; \*\* p< 0.01; \*\*\*p< 0.001.

### 3.3 Discussion

Several natural compounds have been analysed in the last few years, exploring their potential anti-cancer properties, that can be exploited for disease prevention [64] or in order to make the current cancer treatment more effective and reduce the side effects that usually accompany anti-cancer therapies.[65, 66]

Different molecules extracted from plants or herbs showed, at least in pre-clinical studies, to have an inhibitory effects on various tumor cells.[65] The extract of wheat germ fermented by *Saccharomyces cerevisiae* has been found to contain a high amount of benzoquinone that seems to exert an antiproliferative and cytotoxic activity against several tumor cells.[42, 67]

In this study, the effects of FWGE on some highly aggressive OTSCC cell lines, such as HSC-3, SAS and SCC-25, were investigated. The experiments were set to analyze whether treating cancer cells with different concentrations of FWGE could affect their proliferative, invasive and migration activities, representing important aspects featuring metastatic capacity of the cancers. Furthermore, the combination of FWGE with chemotherapeutic drugs cisplatin and 5-fluorouracil was evaluated in terms of effect on cellular viability.

The results of MTT assay revealed that OTSCC cells are sensitive, albeit to varying degrees, to the treatment with FWGE. In particular, the treatment with the lowest concentration (2mg/ml) of FWGE produced no results on cancer cells viability, compared to the untreated cells. On the contrary, higher concentrations (5 and 10mg/ml) determined a significant reduction of cell viability in both the HSC-3 and SCC-25 cell lines. Concerning treatment on SAS, no variation in their viability emerged upon treatment with 5mg/ml FWGE, while a significant effect was detected for the highest concentration (10mg/ml).

The invasion and migration capacities of treated (2, 5 and 10mg/ml FWGE) and untreated HSC-3 and SAS cells were investigated using the Transwells® method. For the invasion assay the gelatinous leiomyoma matrix Myogel[60, 61] was used, since it has been demonstrated to contain various components, such as MMP-2, tenascin-C and collagen types XII and XIV, which are lacking in Matrigel®. Furthermore, the composition of myoma tissue shows a very similar characteristics with the metastatic niche[68], making myoma models suitable for preclinic drug testing.[69]

In this experiment, the treatment of HSC-3 cells with the concentrations at 5 and 10mg/ml of FWGE resulted in a significant reduction of migration. SAS cells shown to be more resistant to the FWGE. Only the treatment with the highest concentration (10mg/ml) of compound had an effect in decreasing the quantity of cells that managed to overcome the

membrane in their migration towards the nutritive components. These results were also confirmed in the Myogel invasion assay.

In order to further evaluate the invasion capacity of OTSCC cells, spheroid assay was conducted with HSC-3, SAS and SCC-25 cells. The three examined cell lines are characterized by a different proliferation and invasion capacity. The results were very similar to those of the Transwell migration and invasion assays. In particular, the invasive capacity of all cell lines was inhibited by the highest concentration (10 mg/ml) of FWGE and no effect was observed for the 2 mg/ml concentration. The concentration of 5 mg/ml had different effects depending on the OTSCC cell line. In particular, in the SAS it did not produce any significant effect. The invasive capacity of SCC-25 was strongly inhibited by this concentration. Instead, the HSC-3 exhibited an intermediate behavior, showing sensitivity in the first 4 days of treatment which was no longer evident on day 7 of observation. This confirms a different aggressiveness of the cells, observed already in previous studies [70, 71], and demonstrates that carcinomas, which appear clinically similar, can display different biological phenotypes.

Yang et al. evaluated the action of Avemar<sup>®</sup> on Oral squamous cell carcinoma (SCC-4 cell line) obtaining similar results, even if the inhibitory effects were reached with lower concentration.[30] Such result, however, may be due to the different product used in the experiment, as well as the cell line that may be more sensitive to the compound.

Cisplatin and 5-fluorouracil are chemotherapeutics frequently used for the treatment of advanced oral cancer.[72, 73] Despite the wide use, their therapeutic action is accompanied by multiple side effects and cancers frequently show resistance to the treatment. Several studies have been conducted to investigate the mechanisms of resistance that cancer cells develop to survive treatment with such molecules.[74, 75] Moreover, additional compounds have been proposed to enhance chemosensitivity of OSCC towards cisplatin and 5-

fluorouracil.[76, 77] Results obtained in this study clearly demonstrated that FWGE is able to enhance the capacity of chemotherapeutics in inhibit OTSCC cell viability. Indeed, combined treatment with chemotherapeutics and FWGE at high concentration (10mg/mL) exerted significantly higher inhibitory effects on cancer cell viability, compared to treatment with chemotherapy or FWGE alone. A particular behavior, however, was observed for the combination of FWGE with 5-FU. It seems that the combination of the chemotherapy with low concentration FWGE (5 mg / ml) produces an effect that promotes the proliferation of cancer cells, although these increases were never statistically significant. A similar effect was noted by Mueller et al.[42] in the treatment of human colon cancer cell lines HT29 and HCT-8, where if the treatment with FWGE preceded that with 5-FU, a trend to antagonism between compounds was observed. Regarding all the other combinations, a synergistic effect was observed in terms of cell growth inhibition.

Further studies are needed to identify optimal combinations that can give better efficacy on oral cancer cells as well as to understand the mechanisms underlying such action.

## RESEARCH OF DIAGNOSTIC AND PROGNOSTIC BIOMARKERS IN OSCC

In order to better understand features of Oral cancer, some molecular aspects were investigated. In particular, expressions of Musashi 2 (MSI2) and programmed death ligand 1 (PD-L1) in Oral Squamous Cell Carcinoma (OSCC) were evaluated and their correlation to clinical-pathological variables and prognosis assessed. Furthermore, mutations of the tumour-suppressor gene TP53 were analysed and correlated with known clinicopathological variables using a bioinformatics approach.

### **4. IMMUNOHISTOCHEMICAL ANALYSIS OF MUSASHI-2 AND CYCLIN-D1 EXPRESSION IN PATIENTS WITH ORAL SQUAMOUS CELLS CARCINOMA**

#### **4.1 Introduction**

Changes in the DNA sequence, accumulation of somatic mutations and epigenetic events are the main mechanisms that are involved in tumor progression. In particular, epigenetic and post-transcriptional events, gained an important role in cancer [78]. Key-regulators of these mechanisms are the RNA-Binding Proteins (RBPs) that cause variations in protein expression, due to their involvement in splicing, mRNA-polyadenylation, editing, and r-tRNA stabilization [79]. Musashi-2 (MSI2) is one of the most studied RBPs. In particular, different studies evaluated its role in cancer. For example, MSI2 overexpression was linked to an increase of invasion and metastasis in non-small cell lung carcinoma, whereas its depletion showed a decrease of epithelia-mesenchymal transition [80]. In bladder cancer, the differentiation antagonizing non-protein coding RNA (DANCR) long non-coding RNA (lncRNA) acts by sponging miR-149 increasing the expression of MSI2, getting worse a malignant phenotype [81]. In addition, MSI2 seems to be involved in patients' prognosis,

resulting as prognostic factor in gastric [82] and cervical cancer [83]; in lung cancer, MSI2 emerged as a novel therapeutic target. Several other factors that are responsible of the regulation of cell proliferation and cell cycle control have been proposed as diagnostic, prognostic, and therapeutic markers for certain malignancies. Among these, the cyclin D1 has been deeply investigated and were shown to be essential for the tumorigenesis of melanoma, breast cancer, and colon and oral squamous cell carcinoma (OSCC) [84]. Cyclin D1 belongs to the family of Cyclins and it is essential in the regulation of cell proliferation, DNA repair, and cell migration control [85]. The aim of this study was to investigate the expression of MSI2 in OSCC samples, through a histologic and bioinformatics analysis in order to evaluate its correlation to clinic-pathological variables and prognosis. Furthermore, a staining for Cyclin-D1 has been performed on OSCC tissue microarray (TMA) and the correlation of Cyclin D1 expression with MSI2 was investigated.

## 4.2 Materials and methods

### *Analysis of MSI2 Expression and Methylation in The Cancer Genome Atlas (TCGA)*

The gene expression RNAseq data HTSeq-Fragments Per Kilobase Million (FPKM) were downloaded from UCSC Xena Browser (<https://xena.ucsc.edu/>) [86]. Data were downloaded for MSI2, MKI67, and CCND1 mRNA expression. This platform was also used to access and download the methylation profile quantification for MSI2 ([https://gdc.xenahubs.net/download/TCGA-HNSC/Xena\\_Matrices/TCGA-HNSC.methylation450.tsv.gz](https://gdc.xenahubs.net/download/TCGA-HNSC/Xena_Matrices/TCGA-HNSC.methylation450.tsv.gz); Full metadata—Illumina Human Methylation 450 expressed as beta unit). Data were organized in Microsoft Excel sheet and then pasted in cBioPortal Int. J. Mol. Sci. 2020, 21, 121 7 of 9 for Cancer genomics in order to display visually the patients' profile (<http://www.cbioportal.org>) [87]. Clinic-pathological and follow-up information were downloaded from Genomic Data Commons (GDC) Data Portal (<https://portal.gdc.cancer.gov/>) [88].

The reporting recommendations for tumor marker prognostic studies (REMARK guidelines) [89] were taken as a reference for carrying out this study. All of the patients filled written informed consent for the use of their samples, according to the institutional regulations and the ethics committee of the National Cancer Institute “Giovanni Pascale”, as “Bio-Banca Istituzionale BBI” Deliberation NO. 15 del 20 Jan. 2016, approved and registered the study. We decided to exclude patients with HPV-positive tumors and those arising from the base of the tongue, tonsils, oropharynx, and lips. Patients with a follow-up lower than eight months were also excluded. A total of 122 patients were included in this study. Of them, 103 reported follow-up information (from 8 to 150 months—mean of 47.34 S.D. 34.609), meanwhile the microarray tissue was not evaluable for 14 patients. None of the patients had undergone treatments prior to tissue collection. The patients were diagnosed of OSCC and 7<sup>th</sup> American Joint Committee on Cancer (AJCC) staging system was applied. An evaluation of 13 mucosae samples from healthy subjects has been also performed. The paraffin blocks were cored in a 0.6 mm support (area of 0.28 mm<sup>2</sup>) and then transferred to the recipient master block while using Galileo TMA CK 3500® Tissue Microarrayer. As the control, we used an H&E staining of a 4-m TMA section. Immuno-histochemical staining was performed by using a mouse monoclonal antibody (Ab), which was supplied by abcam (Mouse monoclonal Anti-MSI2 antibody [OTI2F10]—ab156770), in addition staining for Cyclin-D1 (Ventana-Roche, SP4-R) and Ki-67 (Ventana-Roche) was also performed. We used an automated staining device (Ventana-Roche), with a streptavidin-biotin horseradish peroxidase technique (LSABHRP), in order to uncover the primary Abs. An optical microscope (OLYMPUS BX53, at 200) detected immune-stained spots in four high power fields (HPFs) and they were analyzed by ISE TMA Software (Integrated System Engineering, Milan, Italy). Two of the authors (GP and GT) performed the observational

quantification analysis in a joint session. Detre S. et al. method was applied to assess the scoring of immunostaining [90]. The intensity (I) of expression was scored from 0 to 3 (0 = no staining; 1 = yellow; 2 = light brown; and, 3 = black brown/black). The relative number of the positive stained cells (%) was scored from 0 to 4 (0 = 0%; 1 < 10%; 2 = 10-50%; 3 = 51-80%; 4 > 80%).

All of the samples resulted in only being stained in the cytoplasm. We decided to categorize patients in negative/positive tumors because of the relative low expression of MSI2 in OSCC.

### **4.3 Results**

#### *Analysis of MSI2 Mutations, Gene Methylation and mRNA Expression in TCGA Database*

A total 241 patients' records were included in this analysis after extracting and matching clinic-pathological data from the TCGA database. Table 1 summarizes the main clinical-pathological characteristics of the included patients. DNA mutations and copy number alterations were not detected for the MSI2 gene in patients with OSCC included in the TCGA database (0/241, 0%). The expression of MSI2 mRNA ( $\log_2(\text{fpkm}+1)$ ) was relatively low ranging from 0.2785 to 2.7117 with a mean of 1.270734 (S.E. 0.030) and a median of 1.40673. According to the median value, patients were divided in low ( $\leq 1.40673$ ) and high ( $> 1.40673$ ) MSI2 mRNA expression. Methylation status, measured in beta unit, showed a hyper methylated condition of the gene in all of the patients analyzed, the values of gene methylation ranged from 0.6802 to 0.9910 with a mean of 0.974483 (S.E. 0.0018993). The Spearman rank correlation test did not show a significant correlation between mRNA expression and methylation status of the gene ( $\rho = -0.44$ ;  $p = 0.498$ ); however, a higher methylation status was detected for the low-expression group with results that were close to the statistical significance (Mann–Whitney  $p = 0.095$ ). MSI2 mRNA expression correlated

with Grading ( $\rho = 0.169$ ;  $p = 0.009$ ) and showed a differential expression according to the gender (Mann–Whitney  $p = 0.001$ ) with males' samples showing a higher expression, while MSI2 methylation profile correlated to the age of patients ( $\rho = 0.140$ ;  $p = 0.03$ ) (Table 2). Univariate and multivariate analyses were performed, aiming to investigate whether MSI2 mRNA expression in the TCGA database was able to predict prognosis. The results of the univariate analysis were promising, showing a significant association between MSI2 mRNA expression (High vs low) and overall survival (Hazard Ratio, HR = 1.488; 95% C.I. 1.013–2.185;  $p = 0.045$ ); furthermore, the results of the multivariate analysis (HR = 1.437; 95% C.I. 0.952–1.970;  $p = 0.084$ ) were close to the threshold of statistical significance. Conversely MSI2 mRNA expression did not correlate with disease free survival (HR = 0.827; 95% C.I. 0.443–1.542;  $p = 0.549$ ) in OSCC patients.

<b>Clinic-Pathological Information</b>	<b>Groups</b>	<b>Number of Patients</b>
<b>Age</b>	≤65 years old	144/241
	> 65 years old	97/241
<b>Gender</b>	Male	158/241
	Female	83/241
<b>Grade</b>	1	43/241
	2	147/241
	3	51/241
<b>Stage</b>	1–2	76/241
	3–4	165/241
<b>Subsite</b>	Tongue	103/241
	Gingivo-buccal	30/241

	Floor of the mouth	46/241
	Others	62/241

Table 1. Clinical-pathological characteristics of patients included in The Cancer Genome Atlas (TCGA) analysis.

Variable	Age	Grade	Stage	Gender	Perineural Invasion	MSI2 Methylation	MSI2 mRNA expression	Ki-67 mRNA expression	Cyclin-D mRNA expression
Age	$\rho = 1$ p-value = 1	0,088 0,175	-0,084 0,197	<b>0,243</b> <b>0,001**</b>	0,060 0,414	<b>0,140</b> <b>0,03*</b>	-0,121 0,06	-0,069 0,287	0,033 0,607
Grader		$\rho = 1$ p-value = 1	-0,003 0,959	-0,066 0,307	0,100 0,176	-0,094 0,146	<b>0,169</b> <b>0,009**</b>	-0,105 0,105	0,053 0,418
Stage			$\rho = 1$ p-value = 1	-0,026 0,686	<b>0,199</b> <b>0,006**</b>	-0,031 0,632	-0,035 0,587	0,038 0,561	-0,062 0,340
Gender				$\rho = 1$ p-value = 1	-0,090 0,907	-0,045 0,485	<b>-0,220</b> <b>0,001**</b>	0,042 0,520	0,043 0,505
Perineural Invasion					$\rho = 1$ p-value = 1	<b>-0,178</b> <b>0,014*</b>	0,033 0,650	-0,132 0,071	-0,038 0,606
MSI2 Methylation						$\rho = 1$ p-value = 1	-0,044 0,498	0,094 0,144	0,027 0,673
MSI2 mRNA expression							$\rho = 1$ p-value = 1	-0,093 0,150	0,003 0,963
Ki-67 mRNA expression								$\rho = 1$ p-value = 1	<b>0,253</b> <b>0,000**</b>
Cyclin-D mRNA expression									$\rho = 1$ p-value = 1

Table 2. Spearman rank correlation for the 241 Oral Squamous Cell Carcinoma (OSCC) patients included in the TCGA database. \*  $p < 0.05$ ; \*\*  $p < 0.001$ .

### *Immunohistochemical Analysis of MSI2 Expression on TMA*

The IHC analysis of MSI2 protein expression was performed on a total of 108 patient' samples included in the TMA; such patients had been treated at the National Cancer Institute "Giovanni Pascale" between 1997 and 2012. Table 3 reports the clinical pathological information of patients included in the cohort. An analysis of protein expression in the TMA samples revealed that MSI2 is not frequently expressed in OSCC, in fact 58.3% (63/108) cases analyzed resulted in being negative for MSI2 expression. Of the remaining 41.7% (45/108) samples, only 5.6% (6/108) showed higher level of MSI2 expression. The presence of MSI2 expression directly correlated with Cyclin-D1 expression ( $\rho = 0.279$ ; Chi-Squared  $p$ -value = 0.022) (Table 4), this last one resulted to be higher expressed in males than in females (Mann–Whitney  $p$ -value = 0.024). The presence of MSI2 expression in the TMA cohort did not correlate with overall survival (HR = 0.575; 95% C.I. 0.278–1.190;  $p = 0.136$ ) (Table 5). In the 13 oral healthy mucosae analyzed the expression of MSI2 was faint and mainly confined to the basal layer with a percentage of expression lower than 5% of the whole number of epithelial cells (Figure 1).

<b>Clinic-pathological information</b>	<b>Groups</b>	<b>Number of patients</b>
<b>Age</b>	≤ 65 years old	45/108
	> 65 years old	63/108

<b>Gender</b>	Male	79/108
	Female	29/108
<b>Grade</b>	1	22/108
	2	50/108
	3	36/108
<b>Stage</b>	1-2	35/108
	3-4	73/108
<b>Subsite</b>	Tongue	67/108
	Gingivo-buccal	23/108
	Floor of the mouth	13/108
	Others	5/108

Table 3. Clinical-pathological characteristics of patients included in the immunoistochemical analysis.

Variable	Age	Grade	Stage	Gender	MSI2 expression (Neg/Pos)	Cyclin-D1 expression	Ki-67 expression
<b>Age</b>	$\rho = 1$	0,049	-0,151	-0,062	-0,006	0,021	0,148
	p-value = 1	0,617	0,122	0,528	0,955	0,865	0,226
<b>Grade</b>	$\rho = 1$	0,098	0,034	0,223	0,060	<b>0,398</b>	
	p-value = 1	0,313	0,726	-0,066	-0,044	<b>0,001*</b>	

<b>Stage</b>			$\rho = 1$	-0,008	0,497	0,721	-0,004
			p-value = 1	0,993	0,676	0,468	0,977
<b>Gender</b>			$\rho = 1$	-0,088	-0,277	-0,285	
			p-value = 1	0,364	<b>0,023*</b>	<b>0,031*</b>	
<b>MSI2 expression (Neg/Pos)</b>			$\rho = 1$	<b>0,279</b>	0,122		
			p-value = 1	<b>0,022*</b>	0,315		
<b>Cyclin-D1 expression</b>			$\rho = 1$	<b>0,485</b>			
			p-value = 1	<b>0,000**</b>			
<b>Ki-67 expression</b>			$\rho = 1$				
			p-value = 1				

Table 4. Spearman rank correlation for patients included in the TMA. Age, Cyclin-D1 and Ki-67 were included as continuous variables, while Grade, Stage, Gender, and MSI2 as categorical variables. \*  $p < 0.05$ ; \*\*  $p < 0.001$ .

	<i>Overall Survival</i>		
Variables	<i>Hazard Ratio</i>	<i>95,0% C.I.</i>	<i>p-value</i>
Gender	1,904	0,964-3,759	0,064
Grade	1,162	0,706-1,911	0,555
Age	1,018	0,986-1,052	0,274
Stage	2,968	1,844-4,779	0,000*
MSI2 (Pos/Neg)	0,621	0,299-1,288	0,201

Table 5. Multivariate Cox regression analysis for MSI2 adjusted for other clinic-pathological parameters. \*  $p < 0.05$ .

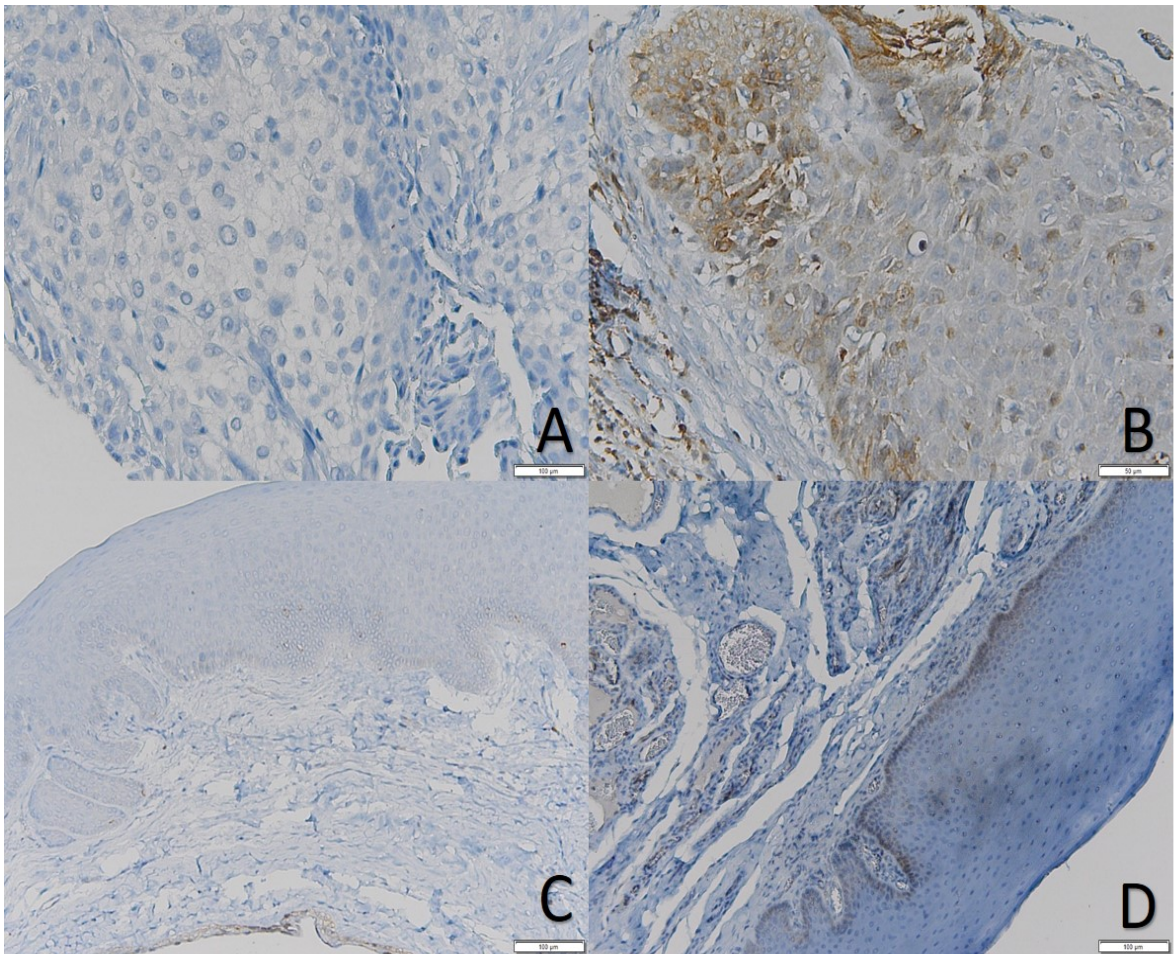


Figure 1: (A) Negative OSCC for MSI2; (B) Basal MSI2 positivity intensity +2; (C) 40% Normal mucosa negative for MSI2 with mild positivity in a ductal epithelium; and, (D) normal mucosa mild positive for MSI2 in the basal layer.

#### 4.4 Discussion

OSCC represents more than 90% of oral cancers and it is one of the most aggressive cancers, being characterized by a mortality rate reaching 50% of patients on average [91]. Continuous efforts are made to better understand the processes that lead to its onset and progression, as well as to the discovering of potential targets for its therapy. Similarly to other solid tumors, the onset of OSCC results from the accumulation of a certain number of genetic or epigenetic alterations into the cells, which cause cell cycle dysregulation and uncontrolled cell proliferation [92]. Recently, the new “omic” sciences provided a great amount of data that characterize the tumors at the molecular level and that can lead to discovering specific biomarkers that could make the tumor treatment more efficient, precise, and predictable [93]. A great contribution has been obtained from bioinformatics that allowed for analyzing this enormous amount of data, giving them a clinical significance [94]. Musashi RNA-binding protein 2 (MSI-2) has been demonstrated to be involved in several solid and blood cancers, where its expression emerged to be higher than in normal tissues and correlate with the prognosis [95]. Its role seems to be explicated in different processes, among which: epithelial-mesenchymal transition, migration, invasion, cell proliferation, and drug resistance [95]. While for many tumors, such as those arising from breast [96], cervical [83], colon [97], lung [80], etc. the role of MSI-2 proteins has been extensively studied and some target therapies proposed, no results regarding the role of MSI-2 in OSCC are reported in the literature. In this work, we combined both a bioinformatics analysis of data that were extracted from electronic TCGA database and an immunohistochemical evaluation of our samples to better understand the role of MSI-2 in oral cancer. The first interesting result emerged from the analysis of genomic data revealed that no DNA mutations and copy

number alterations are detected for the MSI2 gene in patients with OSCC. A hyper methylated condition of the gene emerged in all the patients from the investigation of epigenetic modifications. The analysis of transcriptomic data showed a relatively low expression of MSI2 mRNA in the OSCC samples. However, the mRNA expression did not result to be significantly correlated to the methylation status of the gene.

The associations between its mRNA expression and some clinicopathological characteristics of patients have been analyzed to explore the clinical value of MSI2. The analysis revealed that MSI2 mRNA expression correlates with tumor grading and males show a higher level of MSI2 mRNA expression when compared to female patients. No other clinical features seemed to significantly correlate with MSI2 mRNA expression.

As to our knowledge, no difference between sexes has been highlighted in the literature until now regarding the expression of these regulating molecules. Nevertheless, in our study Males showed significantly higher expression levels of both MSI2 and Cyclin-D1. Such results emerged from the analysis of TCGA database and they have been confirmed by our samples. This could be the decisive contribution that big data can give us in the path towards increasingly personalized medicine [94].

Another question of this work aimed to investigate whether the expression of MSI2 in OSCC patients could predict the prognosis. The results emerged from correlation analysis lay for a significant association between high MSI2mRNAexpression and poor overall survival rate; meanwhile, the disease free survival seems not to be correlated with the MSI2 mRNA expression level. We performed the immunohistochemical evaluation of healthy mucosae and OSCC samples to determine the expression levels of MSI2, in parallel with this bioinformatic analysis. It was of great interest to discover that the protein expression of MSI2 was low or even absent both in healthy samples and OSCC TMA and it did not correlate with any prognostic behavior. These data, combined with those deriving from TCGA

analysis, lead us to affirm that, unlike many other cancers [82, 98, 99], for OSCC the expression of MSI2 appears to be a poor prognostic biomarker. In addition to these results, some information regarding the potential biological functions of MSI2 in oral cancer emerged from the evaluation of the TMAs. In particular, the presence of MSI2 expression directly correlated with Cyclin-D1 expression. Cyclin-D1 is a protein that plays a crucial role in cell cycle regulation, including cell proliferation and growth, as well as DNA repair and cell migration control [100]. Its key role in tumorigenesis of several tumors, among which oral cancer, has been proposed [85], and a poor prognosis correlated to its overexpression [101]. Several mechanisms of cyclin D1 overexpression in OSCC have been identified. They range from amplification to polymorphisms and mutational events involving the oncogene CCND1, but a fundamental role of some signaling pathway intermediaries has been also suggested [102]. Zhang et al. [103] demonstrated in their study how MSI2 silencing inhibited leukemic cell growth and caused a decreasing of Cyclin D1 expression. Han et al. [104] drew the same conclusions, showing how the MSI2 silencing induced cell cycle arrest in G0/G1 phase, with decreased Cyclin D1 and increased p21 expression. In the same way, a study investigating the role of MSI2 in Hematopoietic stem cell activity discovered a close correlation between the expression profile of MSI2 and that of Cyclin D1 [105]. Given the results of our study, in a similar manner, MSI2 could affect the Cyclin D1 expression in the cells of OSCC, but further studies are needed to affirm this.

## **5. META-ANALYSIS OF PD-L1 EXPRESSION IN TUMOUR CELLS AND ITS CORRELATION WITH PROGNOSIS OF PATIENTS SUFFERING FOR ORAL SQUAMOUS CELLS CARCINOMA.**

### **5.1 Introduction**

Cancer cells can negatively regulate the immune response through the activation of inhibitory immune checkpoints. To date, different inhibitory immune checkpoints have been studied, including cytotoxic T-lymphocyte protein 4 (CTLA4), programmed cell death protein 1 (PD-1), lymphocyte activation gene-3 (LAG3), T-cell immunoglobulin-3 (TIM3) and T-cell immunoglobulin and ITIM domain (TIGIT).[106] In this article, we focused on the PD-1 immune checkpoint as the pharmacological inhibition of this immune checkpoints has recently demonstrated to improve the survival rate of patients with head and neck squamous cells carcinoma (HNSCC)[107], while the power of evidence is still weak regarding the clinical efficacy of the pharmacological inhibition of the other immune checkpoints above mentioned. In particular, we reviewed studies focused on the analysis of the programmed cell death ligand-1 (PD-L1) as a prognostic factor of patients suffering for OSCC. PD-L1 is a cell surface glycoprotein which induces both anergy and apoptosis of T cells through the activation of PD-1 receptors located on their surface.[108] The biological importance of the PD-1 receptors influences significantly the immune responses because of a diffused ligand distribution in the body. In fact, such axis showed to play a crucial role in autoimmunity,[108] tumour immunity,[109] infectious immunity [110] and allergy.[111] PD-L1 is commonly expressed in some healthy tissues since it is involved in the normal immunological homeostasis.[112] However, in many types of cancer, the expression of PD-L1 on tumour cells is remarkably higher. This overexpression seems to be present also in subsets of immune cells, including B and T cells, macrophages and dendritic cells.[110] Several studies demonstrated a strong correlation between PD-L1 expression on various tumour cells and a worse patients' prognosis.[113-116] Many studies have also been

conducted to discover a possible role of the PD-1/PD-L1 axis in the biology of OSCC.[117, 118] Its potential clinical and pathological implication has also been investigated providing, however, non-homogeneous conclusions.

The aim of the present study was to systematically review the literature and perform a meta-analysis on the available data in order to summarize the possible correlations between PD-L1 expression and the prognosis of patients suffering for OSCC.

## **5.2 Materials and methods**

### *Protocol and Registration*

This systematic review has been carried out following the guidelines of the “Preferred Reporting Items for Systematic Reviews and Meta-Analyses” (PRISMA) guidelines[37] and the Cochrane Handbook.[119] In addition, the protocol for the development of this review was prospectively registered on the online database PROSPERO (International prospective register of systematic reviews) with the registration number CRD42018090716.

### *Eligibility criteria*

The inclusion criteria were the following: (a) both prospective and retrospective clinical cohort studies, written in English language, regarding the immunohistochemical evaluation of PD-L1 expression in samples from OSCC patients; (b) at least 20 patients were included in each study; (c) studies which analysed the prognosis calculating the hazard ratio (HR) and its 95% confidence interval (95% CI) for at least one of the following: overall survival (OS), disease-free survival (DFS), disease-specific survival (DSS), gender and lymph node metastasis. Some studies reported the HR and 95% CI in the article. Others only reported the Kaplan-Meier graph. In this case, the HR and 95% CI were extracted by Kaplan-Meier graph using the method reported by Tierney et al.[119] If the article did not report both HR and 95% CI, or the Kaplan-Meier graph, author was contacted by email. By this last method,

we got the HR and 95% CI for two studies.[120, 121] Studies on non-human model, case series with less than 20 patients and case reports were not considered for the inclusion in this review. No restrictions were applied about the year of publication.

#### *Information sources and search strategy*

Two authors (GT and KZ) performed an independent direct online search on the following databases: PUBMED, SCOPUS and Web of Science. The research process was carried out by two reviewers in an independent manner. MeSH terms and free text words were combined using Boolean operators (AND, OR). The following protocol was used: (((PD-L1 OR Programmed Death Ligand 1 OR checkpoint inhibitor OR immune system))) AND ((OSCC OR "oral cancer" OR Tongue OR gingiva))) AND ((survival OR prognosis OR biomarker)).

#### *Study selection, data collection process and data items*

The selection process was performed in two rounds. In the first round, authors screened the studies reading only title and abstract of publications, while in the second phase, a full-text evaluation was performed. In case of disagreement between reviewers, a final decision for the inclusion was taken in a joint session with a third author (VCAC). This author also calculated a value of k statistic to show the level of reviewers' agreement. At the end of the selection process, papers fulfilling all inclusion criteria were included in the quantitative synthesis. Data extraction was performed using an ad hoc extraction sheet by two authors (VCAC and CA) in a joint session and controlled by a third author (GT). For each study, the following data were extracted: name of the first author, year of publication, name of the country where the study was performed, classification used for staging, number of patients included, cut-off values, gender, staging, tumour size, rate of lymph node metastasis, HRs and 95% CI for the survival outcomes considered.

### *Risk of bias assessment*

The risk of bias of the included studies was evaluated using a classification derived from the Reporting Recommendations for Tumour Marker Prognostic Studies (REMARK),[122] as previously reported by Almangush et al.[123] The scale consists of six parameters evaluating (a) samples, (b) clinical data of the cohort, (c) immunohistochemistry, (d) prognosis, (e) statistics and (f) classical prognostic factors. In addition, each parameter was considered as adequate, inadequate or not evaluable on the basis of the REMARKS guidelines. In addition, analysis of the risk of biases across studies was investigated through Q and I<sup>2</sup> tests. A P-value of Q-statistic <0.05 was considered significant for the presence of heterogeneity. The Higgins index was also assessed and classified as follows: low heterogeneity (<30%), medium heterogeneity (30%-60%) and high heterogeneity (>60%).[119]

### *Summary measures and planned methods for analyses*

For the pooled analysis of PD-L1 expression as prognostic factor in OSCC patients, the natural logarithm of HR and its standard error (SE) were calculated and entered into the software: Review Manager version 5.2.8 (Cochrane Collaboration, Copenhagen, Denmark; 2014). The inverse of variance test was used to calculate the overall effect. Results of the meta-analysis were summarized in forest plots, and a P-value lower than 0.05 was considered as threshold of statistical significance for all the tests performed in this meta-analysis. Sensitivity analyses were performed for the outcomes OS and DFS omitting articles on the basis of risk of bias, cut-off and geography, hence repeating meta-analysis through a random effect model.

## **5.3 Results**

### *Study selection*

A total of 1137 records were screened by title and abstract. Of these, only 27 overcame the first selection process and were included in the full-text evaluation. Among these, only 10 studies met the inclusion criteria and were included in the meta-analysis.[117, 120, 121, 124-130] The flow chart of the selection process is reported in Figure 1, while reasons for exclusion of the remaining 17 articles are provided in Table S2.[129, 131-146] The value of k-statistic was 0.8196 revealing an excellent level of agreement between reviewers (major details are available in Table S1 a,b).

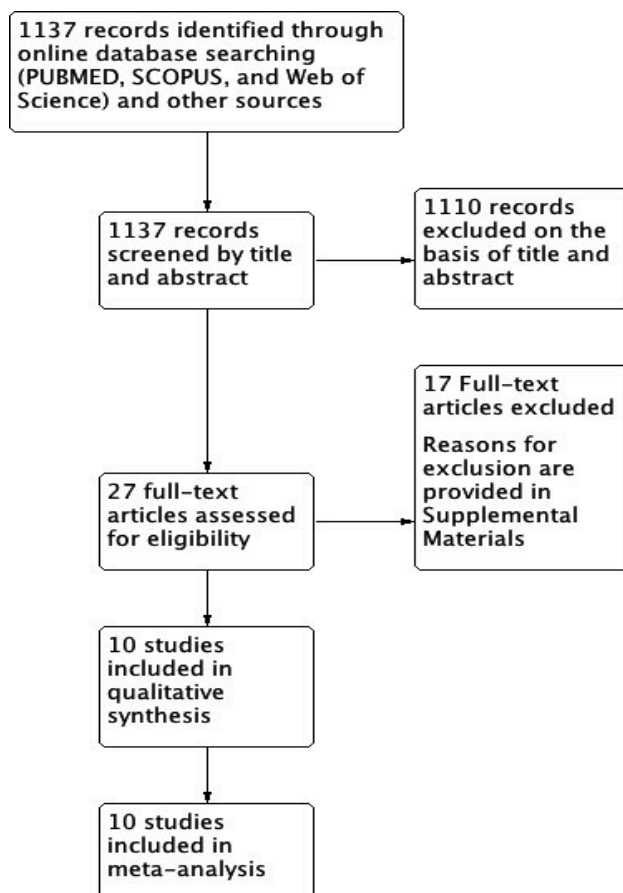


Figure 1: Flowchart for inclusion of studies in the metaanalysis.

### *Study features and risk of bias within studies*

A total of 1060 patients were analysed in the 10 studies included in the meta-analysis.[117, 121, 124-128] Five studies were performed in Asia,[117, 124-126, 129] two in Europe,[128,

130] while the remaining three in other parts of the world (Brazil,[121] Australia[127] and USA[120]). The year of publication ranged from 2011 to 2018. Multivariate analysis was performed in two studies,[121, 125] while the remaining eight [117, 124, 126-130, 147] reported only results for univariate analysis. Three studies fully respected the REMARKS guidelines,[117, 124, 125] while the remaining seven proved to be lacking in some of the parameters analysed.[120, 121, 126-130, 147] Absence of risk of bias was detected only for the immunohistochemistry, while some deficiencies were present for the others parameters. Results of the risk of bias for each of the included study are reported in Table 1.

Author/year	Country	Samples	Clinical data	Immunohistochemistry	Prognostication	Statistics	Classical Prognostic Factors
<i>Ahn/2016</i>	Korea	A	A	A	A	A	A
<i>Cho/2011</i>	Korea	A	A	A	A	A	A
<i>Kogashiwa/2017</i>	Japan	A	A	A	A	A	A
<i>Lin/2015</i>	Taiwan	I	A	A	A	A	A
<i>Oliveira-Costa/2015</i>	Brazil	I	A	A	I	I	A
<i>Satgunaseelan/2016</i>	Australia	A	A	A	I	I	I
<i>Straub/2016</i>	Germany	A	A	A	I	I	I
<i>Hirai/2016</i>	Japan	I	A	A	I	A	A
<i>Troeltzsch/2016</i>	Germany	A	A	A	I	A	A
<i>Mattox/2017</i>	USA	I	I	A	I	I	I

**Table 1:** Evaluation criteria used to assess the quality of studies included in the meta-analysis according to the REMARK guidelines – Included Studies for which: A: Adequate; I: Inadequate; N/A: no description.

<b>Study Selection</b>	<b>Reviewer #1</b>	<b>Reviewer #2</b>
Ahn/2017	I	I
Chen/2012	E	E
Chen/2015	U	U
Cho/2011	I	I
Foy/2017	U	U
Fuse/2016	E	E
Hanna/2017	I	I
Hirai/2017	U	U
Jiang/2016	E	E
Katou/2007	E	E
Kogashiwa/2017	I	I
Kubota/2017	E	I
Lanzel/2016	E	E
Lin/2015	I	I
Malaspina/2011	E	E
Marusc/2018	E	E
Mattox/2017	E	I
Oliveira-Costa/2015	I	I
Poropatich/2017	E	E

Ritprajak/2015	E	E
Satgunaseelan/2016	U	I
Stasikowskakanicka/2017	E	E
Straub/2016	I	I
Takahashi/2016	E	E
Troeltzsch/2016	U	U
Weber/2017	E	E
Wu/2017	E	E

Table S1(a): List of studies to be included in the meta-analysis for the k-agreement calculation.

<b>REVIEWER #1</b>	<b>REVIEWER #2</b>				
		<b>INCLUDE</b>	<b>EXCLUDE</b>	<b>UNSURE</b>	<b>TOTAL</b>
	<b>INCLUDE</b>	7	0	0	7
	<b>EXCLUDE</b>	2	13	0	15
	<b>UNSURE</b>	1	0	4	5
	<b>TOTAL</b>	10	13	4	27

Table S1(b): List of studies to be included in the meta-analysis for the k-agreement calculation.

Study	Reasons for exclusion
Chen/2012	Not in human
Chen/2015	PD-L1 expression in necrosis-samples
Foy/2017	Uncompleted Data (no email answer)
Fuse/2016	Not in human
Hanna/2017	Data-characterization on gender and not on PD-L1 expression level
Jiang/2016	Not performed survival analysis

Katou/2007	Not performed survival analysis
Kubota/2017	Survival analysis was not performed according to PD-L1 expression on tumor cells
Lanzel/2016	Not in human
Malaspina/2011	Not performed survival analysis
Maruse/2018	Disease-specific survival analysis
Poropatich/2017	Head and Neck SCC
Ritprajak/2015	Not performed survival analysis
Stasikowskakanicka/2017	Not performed survival analysis
Takahashi/2016	Survival analysis was not performed according to PD-L1 expression on tumor cells
Weber/2017	Not performed survival analysis
Wu/2017	Not performed survival analysis

Table S2: List of excluded studies and reasons for their exclusion.

### *Synthesis of results and risk of bias across studies*

Meta-analysis of seven studies revealed no significant correlation between high/low expression of PD-L1 and OS (HR, 0.60; 95% CI: [0.33, 1.10]; P = 0.10). A high rate of heterogeneity was detected (I<sup>2</sup> = 89%), and for such reason, a random effects model was used. Meta-analysis of studies for DFS revealed no statistical significant differences between the expression of PD-L1 in the tumour cells and DFS (HR, 0.62; 95% CI: [0.21, 1.88]; P = 0.40). Also for DFS, results obtained on the analysis of three studies showed a high rate of heterogeneity (I<sup>2</sup> = 81%). No significant differences were also detected for the rate of lymph node metastasis (HR, 1.15; 95% CI: [0.74, 1.81]; P = 0.53). On the basis of the extracted

data, meta-analysis was also performed for the secondary outcomes: gender and tumour size. Results for DSS (Figure S1) revealed the absence of a statistical difference between the high and low expression of PD-L1 (HR, 2.05; 95% CI: [0.53, 7.86]; P = 0.29). The cumulative Odds Ratio (OR) for gender status showed that high expression of PD-L1 is two times more frequent in female patients (OR, 0.5; 95% CI: [0.36, 0.69]; P < 0.0001). The rate of heterogeneity was I<sup>2</sup> = 0%, and for such reason, a fixed effects model was used. Summary effect size for OS did not substantially change in sensitivity analyses performed including only studies at low risk of bias (HR = 0.55 [0.24, 1.28] P = 0.17), with an equal cut-off (intensity > 2) (HR = 0.73 [0.27, 1.98] P = 0.54) and performed only in Asia (HR = 0.55 [0.24, 1.28] P = 0.17) (Figure S2). Sensitivity analysis was not performed for DFS and DSS because of the little number of studies included. Characteristics of included studies and their relative results are summarized in Tables 2, 3 and 4.

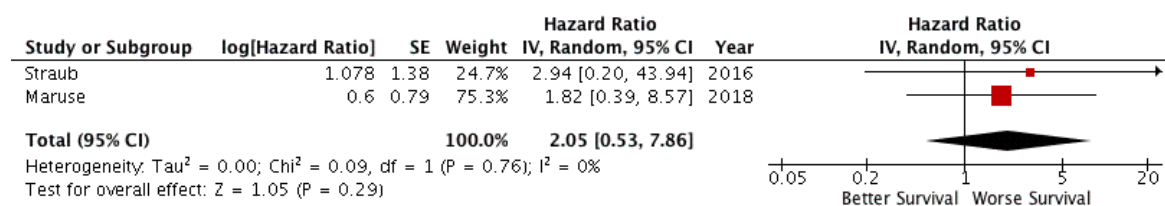


Figure S1: Forest plot for the association of higher PD-L1 expression with Disease specific survival.

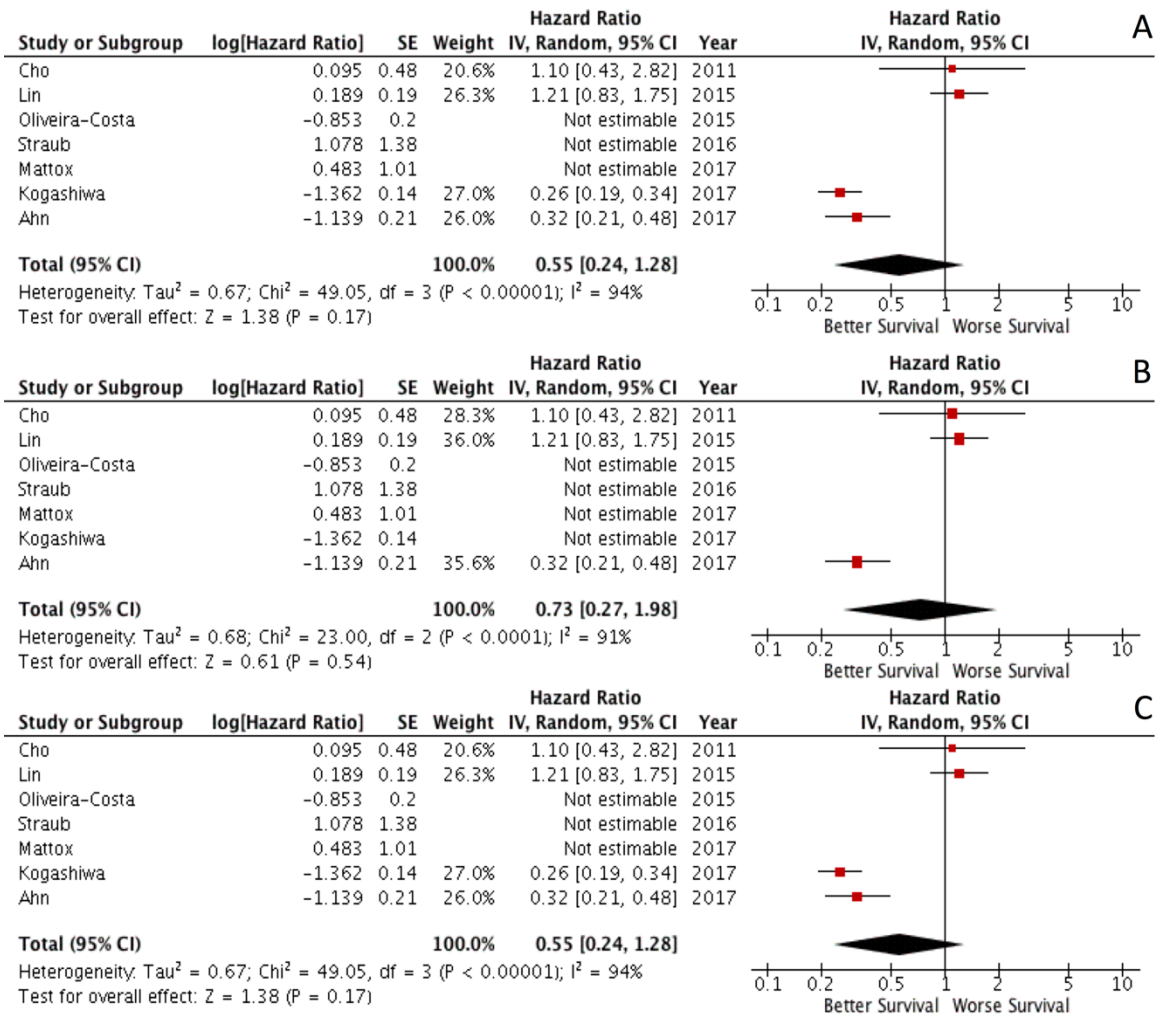


Figure S2: Forest plot for the association of higher PD-L1 expression with overall survival (OS) for studies (A) at low risk of bias; (B) with an equal cut-off (intensity > 2) and (C) studies performed only in Asia.

Study	Year	Country	N <sup>o</sup> of patients	Staging edition	Detection Method	Cut-off
Ahn H.	2017	South Korea	68	7th AJCC	IHC	Intensity >2
Cho Y-A.	2011	South Korea	45	7th AJCC	IHC	Score >2
Kogashiwa Y.	2017	Japan	84	N/A	IHC	> 5% of tumor cells
Lin Y-M.	2015	Taiwan	305	7th AJCC	IHC	Score >2

Oliveira-Costa J. P.	2015	Brazil	96	N/A	IHC	> 5% of tumor cells
Satgunaseelan L.	2016	Australia	217	7th AJCC	IHC	> 5% of tumor cells
Straub M.	2016	Germany	80	7th AJCC	IHC	> 5% of tumor cells
Mattox A. K.	2017	USA	53	N/A	IHC	> 1% of membranous PD-L1 expression by tumor and/or immune cells
Hirai M.	2016	Japan	24	N/A	IHC	> 10% of tumour cells
Troeltzsch M.	2016	Germany	88	7th AJCC	IHC	Score >2

Table 2: Main characteristics of included studies. N/A: not reported.

<i>Study</i>	<i>Follow-up</i>	<i>Overall Survival</i>		<i>Disease Free Survival</i>		<i>HR Estimation</i>
		<i>HR</i>	<i>95% C.I.</i>	<i>HR</i>	<i>95%CI</i>	
Ahn H.	44.3 mean (2.1 to 122 months)	0.32	(0.11-0.94)	0.25	(0.06-1.12)	Reported
Cho Y-A.	over 125 months/not reported	1.10	N/A	N/A	N/A	Calculated
Kogashiwa Y.	40.6 mean (3.8 to 89.6 months)	0.256	(0.101-0.646)	N/A	N/A	Reported
Lin Y-M.	45,6 mean (1,2 to 133,2 months)	1.209	(0.890-1.643)	N/A	N/A	Reported
Oliveira-Costa J. P.	20 mean (4 to 108 months)	0.426	(0.186-0.977)	N/A	N/A	Reported

Satgunaseelan L.	22 median (1 to 144 months)	N/A	N/A	1.46	N/A	Calculated
Straub M.	31 mean (2 to 63 months)	N/A	N/A	2.11	(1.00-4.43)	Calculated
Mattox A. K.	N/A	1.622	(0.5 – 4.464)	N/A	N/A	Reported
Hirai M.	N/A	N/A	N/A	N/A	N/A	N/A
Troeltzsch M.	N/A	N/A	N/A	N/A	N/A	N/A

Table 3: Synthesis of data extracted from the included studies related to outcomes pooled in the meta-analysis.

<b>PD-L1 Expression</b>									
<b>Study</b>	<b>Country</b>	<b>High with LNM</b>	<b>Low with LNM</b>	<b>High in male</b>	<b>Low in male</b>	<b>High in female</b>	<b>Low in female</b>	<b>High expression</b>	<b>Low expression</b>
Ahn H.	South Korea	N/A	N/A	N/A	N/A	N/A	N/A	45	23
Cho Y-A.	South Korea	8	8	18	14	8	5	26	19
Kogashiwa Y.	Japan	31	29	24	33	20	7	44	40
Lin Y-M.	Taiwan	52	64	93	143	40	29	133	172
Oliveira-Costa J. P.	Brazil	Unclear	Unclear	Unclear	Unclear	Unclear	Unclear	Unclear	Unclear
Satgunaseelan L.	Australia	18	76	17	113	23	64	40	177

Straub M.	Germany	26	19	23	31	13	13	36	44
Hirai M.	Japan	1	4	N/A	N/A	N/A	N/A	13	11
Troeltzsch M.	Germany	18	27	13	35	13	27	26	62
Mattox A. K.	USA	N/A							

Table 4: PD-L1 expression in Lymph-node metastasis (LNM) and Gender Status patients. N/A: not reported; unclear: data were reported but they were not clear.

## 5.4 Discussion

PD-L1, also known as B7-H1 or CD274, is a cell surface glycoprotein, which leads to T-cell inactivity or apoptosis by binding PD-1, a receptor expressed by the T lymphocytes [117]. The interaction between PD-1/PD-L1 leads to immune system impairment through a range of mechanisms, which often differs between tumor types. Once PD-1 binds to PD-L1, an inhibitory signal is induced. This happens through the phosphorylation of the tyrosine residue in the immunoreceptor tyrosine-based switch motif, leading to the recruitment of SH2-domain containing tyrosine phosphatase 2 (SHP-2) to the cytoplasmic domain of PD-1, which then down-regulates CD28-mediated PI3K activity. These events, ultimately, lead to reduction of Akt activation, which is involved in the proliferation and cytokine production from the immunity cells [148, 149]. PD-1 activation is also linked to inhibition of the anti-apoptotic protein Bcl-xL [150]. In OSCC, many studies showed different links between PD-1/PD-L1 pathway and other molecules. Chen et al. reported in an in-vitro study that IFN- $\gamma$  causes an increase of PD-L1 expression on the surface of the OSCC cell line, through PKD2 signaling pathway [132]. However, this seems to contradict the description of the inhibitory effect of INF- $\gamma$  on cancer proliferation, showing an opposite role as cancer immune resistance [151]. Ahn et al. performed an immunohistochemical study on OSCC samples demonstrating that miR-197 expression is inversely correlated with PD-L1 expression. This

relation had been already showed in non-small cell lung cancer (NSCLC), where miR-197 blocks the cyclin-dependent kinase CKS1B, which is linked to PD-L1 expression through STAT3 signal [124]. Jingjing et al. [152] reported that protein level of PD-L1 in OSCC cell line is higher than normal oral mucosa cell line, while no differences were highlighted in the PD-L1 mRNA. They justified these statements by showing that ubiquitination could be the main mechanism involved in the PD-L1 expression in OSCC cell lines, targeting USP9X as the main molecule acting as deubiquitinase and this mechanisms lead to the PD-L1 protein accumulation.

The literature is still lacking of studies regarding action and role of PD-1/PD-L1 pathway in OSCC cells. Recently, there has been growing interest about the PD-L1 expression in Tumor Associated Macrophages (TAM) and Fibroblasts. Next studies should integrate findings coming from both tumor and peritumoral microenvironment PD-L1 expression to improve the understanding of its role in OSCC prognosis.

Different studies showed that tumor cells could express on their surface PD-L1, suggesting a potential role of this protein in reducing the anticancer immune response [117]. These findings improved the research in anticancer drug development, which could interact with the PD-1/PD-L1 pathway.

On November 2016, the FDA approved a new pharmacological principle, Nivolumab for the treatment of recurrent or metastatic head and neck squamous cell carcinoma. Nivolumab stands for a human IgG4 PD-1 immune checkpoint inhibitor antibody, which selectively counters the link between PD-1 and its ligand (PD-L1), promoting the action of T-cell function [153]. Although the promising role of these new drugs, there are still problems about their controversial activity, above all the different mechanisms, in which PD-1/PD-L1 could also be involved in different cancer types. For example, for the NSCLC not all tumors expressing PD-L1 respond to PD-1/PD-L1 inhibitors. Conversely, some PD-L1-negative

tumors can respond to these agents [154]. However, the predictive role of PD-L1 expression in tumor samples is still controversial [155].

In this study, we focused on the analysis of PD-L1 expression in OSCC tissue as a prognostic (and not predictive) biomarker. In fact, such marker has demonstrated to be an independent prognostic factor in different cancer types, including: NSCLC [156], renal cell carcinoma [157], and breast cancer [158]. However, there are conflicting evidences in relation to the prognostic value of PD-L1 in different types of cancer [159-161]. Results of this study failed to reveal a correlation between the expression of PD-L1 in tissues and a poor prognostic of OSCC patients. For both OS and DFS the rate of heterogeneity among studies resulted to be very high, demonstrating that the results of the included studies are strongly conflicting among each other (Figure 2 A/B).

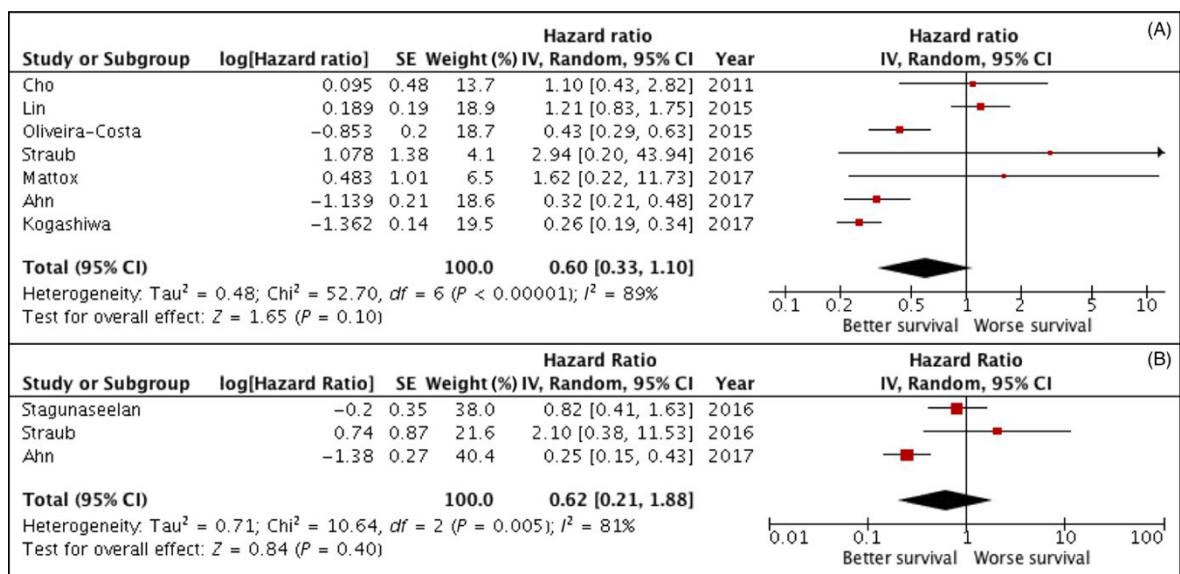


Figure 2 (A/B): Forest plot for the association of higher PD-L1 expression with overall survival (A) and disease-free survival (B).

No differences were also detected for the rate of lymph node metastasis in patients with higher PD-L1 expression (Figure 3).

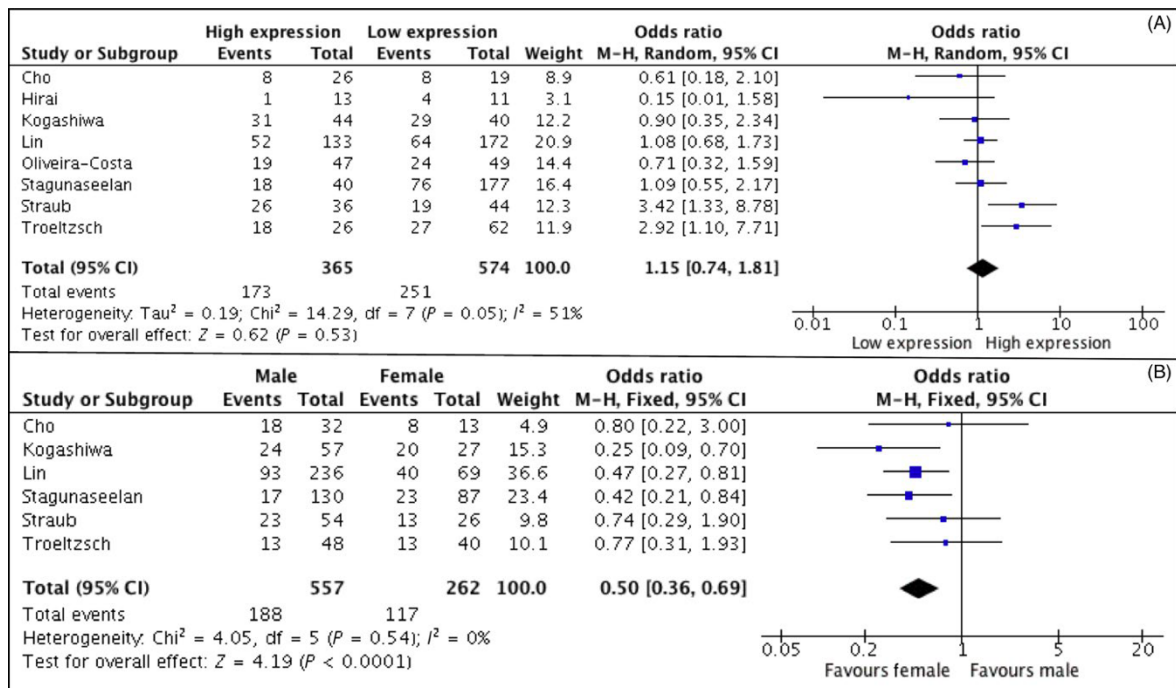


Figure 3 (A/B): Forest plot showing the association of higher PD-L1 expression with lymph node metastasis (A) and gender status (B).

Our findings are in discordance with the results of a previous meta-analysis on head and neck cancers, in which authors revealed a significant association between PD-L1 expression and poor prognosis in a subgroup analysis [162]. Such discrepancy is in part due to the inclusion of the meta-analysis of two recently published studies in which PD-L1 expression correlated with a better prognosis [124, 125].

The lack of correlation between PD-L1 expression and OS appears to contrast with the prognostic value that is attribute to this marker, based on its immunosuppressive function. Several studies regarding other tumor types found the same results, suggesting a more complex function of PD-L1 in immunosurveillance signaling [163]. A possible explanation is that PD-L1 expression by cancer cells can be considered as a marker of an active host antitumor immune response [164]. Another way to address the issue is to consider the heterogeneity of tumor microenvironment in different tumor types. In fact, a classification of tumors into 4 types based on the presence of PD-L1 positivity and/or tumor-infiltrating lymphocytes has been proposed [164, 165]. In some tumors like NSCLC, oncogenes may be more important drivers of tumor PD-L1 expression compared to other tumors, like

melanoma, in which it seems more influenced by infiltrating immune cells [165]. Furthermore, as reported by Lyford-Pike et al., in head and neck squamous cell carcinoma the expression of PD-L1 may be driven by both oncogenic and adaptive immune resistance mechanisms in the same lesion [166].

Therefore, the evaluation of PD-L1 expression alone as prognostic marker can be misleading, suggesting the need for the integration of other immune markers to obtain a better patient stratification. This action should consider the different phases, which are linked to patients' management. In this view, according to Brigas G. et al. [167], the use of small biopsies misclassified up to the 35% of PD-L1 assessments in advanced NSCLC. The biopsy sample undergoes different processes for the evaluation of PD-L1 expression. De Meulenaere et al.<sup>[168]</sup> reported that pathologists can find hurdles in the choice of assay, antibody and cut-off/score selection of PD-L1 expression. In this study, authors' compared the results of PD-L1 expression coming from biopsy samples versus resection specimens and a poor agreement emerged. Another study<sup>[169]</sup>, on the other hand, showed that the VENTANA PD-L1 (SP263) assay was characterized by high reproducibility, meanwhile tumor infiltrating PD-L1 immune cells were more variable within and between blocks and across cut-offs. These data are important for the concept of precise-medicine, according also to the evidence that microenvironment has an important role in PD-L1 expression and tumor behavior, as showed in other kind of cancers<sup>[170]</sup> and in OSCC[129, 133, 136]. According to these statements, future research should focus on the validation and standardization of all steps, from biopsy, IHC assay and tumor microenvironment evaluation for the selection of patients, who can undergo anti PD-L1 therapy.

In order to investigate the influence of specific parameters on the results of this study, we also performed sensitivity analysis for risk of bias, cut-off values, and geography. Summary effect size did not substantially change in sensitivity analyses performed including only studies at low risk of bias, performed in Asia and reporting the same cut-off value. Results

of this study revealed a significant association between PD-L1 expression and female gender. In fact, in women higher expression of PD-L1 seems to be more common as already reported for NSCLC [171, 172]. In these studies, the female subset of patient also corresponds to patients who are more likely to harbour EGFR mutations, suggesting a relationship between PD-L1 expression and altered EGFR signalling pathway [173]. A recent meta-analysis revealed that the magnitude of benefit of patients treated with immunotherapy is sex-dependent, in particular women have lower rates of positive response to the treatment [174]. However, it is not clear whether such different outcomes are due to the more frequent expression of PD-L1 in females or to other sex-related mechanism. Such findings underline the importance of performing future studies aiming to compare sex-related expression as independent prognostic factor, in order to clarify whether PD-L1 could be considered a prognostic factor in men but not in women.

Furthermore, as previously mentioned, there is a complex relationship between PD-L1 expression and the presence and pattern of inflammatory infiltrate. This must be considered in the evaluation of prognostic significance of PD-L1, because peritumoral inflammatory process seems to be more intense in female patients with OSCC, mainly due to postmenopausal inflammatory state [117].

Analysis of risk of bias in the included studies revealed deficiencies in some parameters of the REMARKS guidelines. In particular, the authors recorded ambiguity in some of the included studies in the distinction between OS and disease-specific survival. As it is known, in the calculation of OS, death for any reason is taken into consideration while in disease-specific survival only deaths for cancer are considered. It is to underline that direct contact of authors helped to clarify such discrepancy for two of the included studies [120, 121]. To note, such meta-analysis presents some limits, first of all it relied on published results rather than on individual patients' data. In addition, it presented, for the survival outcomes considered in the meta-analysis, a very high rate of heterogeneity was detected, that strongly

limits the quality of evidences despite the inclusion of an adequate number of studies performed in a good quality manner. Such heterogeneity could reflect the wide variation of PD-L1 expression in the population that limits its use as prognostic biomarker in clinical practice. It should be stressed that such results are not related to the analysis of PD-L1 expression as predictor of response to checkpoint inhibitors, such topic should be evaluated in further studies with different design.

## **6. COMPUTATIONAL ANALYSIS OF TP53 MUTATIONAL LANDSCAPE UNVEILS KEY PROGNOSTIC SIGNATURES AND DISTINCT PATHOBIOLOGICAL PATHWAYS IN HEAD AND NECK SQUAMOUS CELL CANCER.**

### **6.1 Introduction**

Mutations of the tumour-suppressor gene TP53 are among the most common genomic alterations occurring in malignancy, including head and neck squamous cell carcinoma (HNSCC). HNSCC frequently presents as a locally advanced disease,[175] and is characterised by biologically and molecularly diverse groups of tumours. More than 90% of HNSCCs involve the mucosal surfaces of the oral cavity, oropharynx and larynx.[176] Several studies have shown that such carcinogens contribute to the mutational profile of TP53.[177-180] TP53 encodes p53, a protein that regulates the expression of a vast array of target genes. In early studies, p53 was considered an oncogene because of the lower expression level in normal cells compared with the cancerous one.[181] In 1989, Levine et al. showed that wild-type p53 works as an oncosuppressor.[182] Because of its important role in cancer biology, p53 has been defined “the guardian of the genome”. The protein is involved in different cellular functions, such as apoptosis, differentiation and cell-cycle control. In addition, it plays a central role in the control of cell proliferation and death in response to various urges like DNA damage, hypoxia, oxidative stress, DNA mutations and nutrient deprivation.[183] Not surprisingly, TP53 gene alterations are frequent in a large proportion of human cancers, and occur in a tissuespecific manner. For example, TP53 mutation rates vary from 2.2% in renal cell carcinoma to 89% and 94.9% in endometrial carcinoma and serous ovarian cancers, respectively.[184] Inherited TP53 mutations lead to a wide spectrum of early-onset cancers.[185] In contrast to other tumour-suppressor genes that are mainly altered by truncating mutations, the majority of TP53 mutations are missense substitutions (75%). Other alterations include frameshift insertions and deletions (9%), nonsense mutations (7%), silent mutations (5%) and other infrequent alterations.[186]

However, whether different types of TP53 mutations bear distinct clinical and pathophysiological significance in HNSCC has not been elucidated so far. Structurally, p53 is a multifunctional 393-residue protein; it is encoded by a gene localised on chromosome 17p13.1 and is composed of 25,772 bases. The protein is constituted by three subunits: N-terminal, Core domain and C-terminal. The N-terminal subunit is composed of a transactivation domain (residues 1–42) and a proline-rich domain (residues 63–97). The central core domain (residues 98–292) is composed of a single unit that contains sequence-specific DNA-binding activity of p53 (DNA-binding domain). The C-terminal domain is characterised of a flexible linker region (residues 293–323), a tetramerisation domain (residues 324–355) and C-terminal regulatory domain (residues 363–393) that undergoes a number of post-translational modifications such as acetylation and phosphorylation.[187, 188] A growing body of evidence now suggests that differential mutational profiles of TP53 gene can influence disease prognosis in several types of tumours; for example, distinct TP53 mutations are independent predictors of survival in CD20+ lymphomas.[189] The same results have also been reported for ALK+ NSCLC,[190] hepatocellular carcinoma, HNSCC, acute myeloid leukaemia, clear-cell renal cell carcinoma (RCC), papillary RCC, uterine endometrial carcinoma and thymoma.[191] Whether mutations in p53 subdomains differentially affect disease prognosis, however, has not been elucidated so far. The aim of this study was to investigate the mutational landscape of TP53, and to correlate these molecular features with clinical variables. To do so, we used a bioinformatics approach by analysing data from The Cancer Genome Atlas (TCGA) database.[192] The results from this analysis revealed that a wide landscape of TP53 mutations exists in HNSCC and, for the first time, demonstrated that these mutations are associated with distinct clinical behaviour in a site-specific manner.

## **6.2 Materials and methods**

### *Data source and data collection*

This study has been performed according to the Recommended Guidelines for Validation, Quality Control and Reporting of TP53 Variants Clinical Practice.[193] TCGA data have been accessed and downloaded through UCSC Xena Browser (<https://xena.ucsc.edu/>). Data for mRNA expression profile of TP53 gene (ENSG00000141510) were downloaded as RNAseq data HTSeq-Fragments Per Kilobase Million (FPKM)— dataset ID TCGA-HNSC/Xena\_Matrices/TCGA-HNSC.htseq\_fpkm.tsv, and the mutational profile with the variant-allele frequency (VAF), such as the type of mutation (MuTect2 Variant Aggregation and Masking—dataset ID TCGA-HNSC/Xena\_Matrices/TCGA-HNSC.mutect2\_snv.tsv). The mutation dataset was also download from the cBioPortal for cancer genomics website. This website was also useful for downloading the RPPA-Z-score expression of p53 protein (<http://www.cbioportal.org>).[87] In this analysis, only patients with a single mutation of the TP53 gene were included. Patients with double mutations on the same gene or mismatching mutation type in the two datasets were excluded. At the end of the inclusion process, 415 patients' profiles were eligible for statistical analysis. Genomic Data Commons (GDC) Data Portal (<https://portal.gdc.cancer.gov/>) was used to download clinical and follow-up information. Data were pasted and organised in SPSS 21.0 in order to perform the statistical analysis for the evaluation of clinical and prognostic correlations. The amino-acid sequence changes were assessed and used to classify mutation profiles according to the secondary structure of p53 protein. In the Research Collaboratory for Structural Bioinformatics Protein Data Bank (RCSB-PDB), it was possible to retrieve the Secondary Structure data for the TP53 protein (<https://www.rcsb.org/pdb/explore/remediatedSequence.do?params.showJmol=false&structureId=3Q01>).[194]

Data grouping Of 415 patients with HNSCC included in the study (Supplementary Table 1A–D), 129 patients had no mutations in the TP53 gene and were defined as “wild type” (WT); meanwhile, 286 patients had one single mutation in the gene sequence (MUT) (of

these, 51 patients had a frameshift mutation, 8 an inframe mutation, 152 a missense mutation, 26 a splice-site mutation and 49 patients had a stop mutation). The p53 mRNA expression for 411 patients ( $\log_2(\text{fpkm} + 1)$ ) in the TCGA Database ranged between 0.71 and 6.47 with a mean of 3.740184 (S.D. 1.2168926) and a median of 3.88. The p53 RPPA-Z-score protein was available for only 173 patients and ranged from  $-4.3211$  to  $3.0036$  with a mean of  $-0.001732$  (S.D. 0.91044) and a median of  $-0.0933$ . Both for mRNA expression and RPPA-Z score, patients were classified as high and low expression using the median as threshold. It is important to note that RPPA-Z-score protein was available for only 173 patients, and it is not representative of the whole cohort.

Patients were also divided according to VAF, intended as the proportion of DNA molecules bringing the variant. From 40 to 64% VAF, patients were classified as being heterozygous loci; meanwhile, 65–100% VAF patients were grouped as homozygous loci.[195] VAF was reported for 271 patients and ranged from 5 to 97% with a mean of 46.73% (S.D. 19.33%). In order to further evaluate the relation of the location and the type of mutation with the clinicopathological characteristics, patients were divided according to:

1. The position of the mutated base on the DNA sequence of the gene, such as in the N-terminal transactivation domain (residues 1–97), in the DNA-binding domain (residues 98–292) and in the C-terminal domain (residues 293–393).[187] In total, 19 patients had a mutation in the Nterminal domain, 37 patients in the C-terminal domain and 230 patients in the DNA-binding domain. In total, 152 of 230 mutations in the DNA-binding domain were missense.
2. The secondary structure extracted from the RCSB-PDB, such as mutation affecting the helix region (3/10 helix, alpha-helix structure), a strand region (beta bridge, beta strand), a turn region (turn, bend) [196] and an unknown region, for which no secondary structure is assigned.

3. Well-known hotspot mutations, such as the ones occurring in the residues 175, 245, 248, 273 and 282.[197] In particular, residue R175 was affected in 5 patients, G245 in 7 patients, R248 in 11 patients, R273 in 14 patients and R282 in 6 patients (43 hotspot mutations/286 total mutations). In addition to these frequent spots, we decided to include new residues, which were also frequently mutated; only residues involved in at least six patients included in the cohort were also included as new hotspots mutations; such sites were H179 (seven patients), H193 (six patients), R196 (eight patients) and R213 (seven patients).

4. The residues involved in the zinc ion ligand, such as C176, H179, C238 and C242, which were involved in 17 on 286 patients.

5. Mutations were classified according to the type of singleamino-acid substitution, such as transition and transversion.

In order to investigate random deamination[198] or tobacco smoke- related mechanisms of mutations,[199] transitions of C–T in CpG islands and transversions of G:C–T:A were also highlighted. In addition, mutations involving CpG sites, reported in <http://p53.iarc.fr/p53Sequence.aspx>, were also investigated.

6. Mutations in conserved residues were compared with their non-conserved sites, according to a previously reported analysis by Martin et al.[200] Conserved residues were retrieved from their online platform at <http://bioinf.org.uk/p53/analysis/index.html#conserved>, such as pro98, phe113, lys120, ser121, val122, thr125, ser127, leu130, lys132, leu137, lys139, pro142, pro151, pro152, arg158, ala159, lys164, val172, val173, arg175, pro177, his178, his179, arg196, glu198, gly199, tyr205, asp208, ser215, val216, val218, pro219, tyr220, glu221, pro223, thr230, asn239, ser240, ser241, cys242, met243, gly244, gly245, asn247, arg249, ile251, thr253, leu257, gly262, leu265, gly266, arg267, phe270, glu271, val272, cys275, ala276, cys277, pro278, gly279, arg280, asp281 and arg282.

7. Martin et al. also characterised amino-acid substitutions according to their ability to donate or accept hydrogen bonds. The amino acids K, R and W are only able to donate H<sup>+</sup>;

meanwhile, E and D are only able to accept hydrogen bonds. The amino acids H, N, Q, S, T and Y are both able to accept and donate as reported by Baker et al.[201] Patients were classified as missense-disruptive mutation with substitution of K, R and W with E and D and vice versa, or in the case of forming H<sup>+</sup> bond amino acids, substituted by nonforming H<sup>+</sup> bonds.

8. We also categorised two further amino-acid substitutions, such as (1) mutations resulting in a substitution by proline, and (2) mutations from native glycine in residues at codons 117, 154, 187, 244, 245 and 262. These kinds of mutations, because of their sidechain features, are more restricted in the allowed conformations.[200]

a) All these analyses were performed in the TCGA database of patients with squamous cell carcinoma of the head and neck (HNSCC). Patients were further categorised into four main subgroups:[202]

1. Oral cavity (OC), such as alveolar ridge, buccal mucosa, floor of the mouth, hard palate, oral tongue, general oral cavity and lips
2. Oropharynx (OP), such as base of the tongue, oropharynx and tonsils
3. Hypopharynx (HP)
4. Larynx (L)

Data were also download for oesophagus and lung squamous cell carcinoma, in order to investigate and compare the TP53 mutational landscape among these groups of cancers. UCLA, TCGA and ICGC oesophagus databases from cBioPortal and TCGA (PanCancer Atlas) lung squamous cell carcinoma, were downloaded following the previous described criteria, including only patients with histologically confirmed squamous cell carcinoma. Interactome–genome–transcriptome network analysis based on co-alteration data In order to highlight co-differential gene network between WT and MUT groups, we combined interactome–transcriptome analysis [203] and interactome–genome analysis to construct dynamic, tumour-specific networks based on predicted changes of p53 interactors resulting

from genetic (mutations, CNA) or transcriptional (mRNA expression) modifications occurring in the same HNSCC cohorts. Specifically, patients were compared according to WT/MUT and subsite (OC, OP, HP and L) to evaluate if different genes/pathways were modified in relation to the distinct mutational profile of TP53 at different subsites. cBioPortal gene network tool highlights alterations per each gene, such as mutations, CNA or mRNA dysregulation. Moreover, cBioPortal gene network tool was used to build the interactome by filtering the interactions according to “controls state change of”, “controls transport of”, “controls of phosphorylation of”, “control expression of”, “in complex with” and “neighbour of”. This analysis was also performed between HPV-positive and HPV-negative OP tumours. When more than 50 neighbour genes existed in the network, these were ranked by genomic alteration frequency within the selected group of patients. To provide an effective visualisation of networks that highlighted the most relevant genes to the query, we adopted an alteration frequency of 16.9% as cut-off [87]. For HP subgroup, a 33.3% cut-off was applied because of the low number of patients included. Gene ontology (GO) analysis to evaluate the main pathway alterations in each subgroup analysis was performed by using <http://geneontology.org/> tool [204] and retrieving the results from PANTHER.[205]

Gene, percentage and type of both alteration and cell function are summarised in Supplemental material (Supplementary Table 3A–J), by including only the results with a fold enrichment over ten.

#### *Statistical analysis*

Because of the non-normal distribution of variables, nonparametric tests were used (normal distribution of variables was explored through Shapiro–Wilk normality test). Spearman rankcorrelation analysis was performed to investigate the relation between the expression profile of p53, the mutational profile and the clinicopathological characteristics. For dichotomous variables, chi-square test was used. The difference in expression between

groups was further investigated through the non-parametric test of Mann–Whitney or by Kruskal–Wallis one-way or two-way ANOVA test. Bonferroni–Holm false-discovery rate was applied to correct for multiple comparisons. Kaplan–Meier analysis with log-rank test was applied to explore differences in the overall and disease-free survival by univariate analysis. In order to estimate the effect of clinicopathological variables, a multivariate Cox regression model was built, including the following parameters as covariates: age, gender, staging and grading. All tests were performed by using SPSS 21.0 and STATA 16.0; only  $P < 0.05$  results were considered statistically significant.

#### *Survival prediction algorithm*

We generated an algorithm based on modifications of the algorithm previously reported by Poeta et al.[206] In Poeta’s algorithm, patients are grouped as bringing a TP53-disruptive mutation versus conservative mutation. Stop, frameshift, inframe and splice mutations are classified as disruptive, together with missense mutations in L2–L3 segment of the protein (codons 163–195 and 236–251) with changes in charge or polarity of the substituted amino acid. Any missense mutation outside L2–L3 segment or in L2–L3 segment without changes in charge or polarity, are considered conservative. First, we applied this algorithm to TCGA head and neck cancer, and then we implemented this model in order to highlight patients at high risk of death, according to deleterious missense substitutions in the secondary structure of the protein. Mutations were reclassified as disruptive if

- in homozygous loci, such as DNA–VAF from 65 to 100%;[195]
- in zinc ligand involved;
- changing from K, R and W to E and D and vice versa, or in the case of forming H<sup>+</sup> bond amino acids, substituted by nonforming H<sup>+</sup> bonds;
- affecting an amino acid in a non-assigned secondary structure (unknown, as reported in RCSB-PDB <http://www.rcsb.org/pdb/explore/remediatedSequence.do?structureId=1TUP>).

Mutations were reclassified as conservative if assigned to any other secondary structure,

when maintaining their ability to donate or accept hydrogen bonds. Harrell's C-statistic, AIC (Akaike information criterion) and BIC (Bayesian information criterion) were used to assess possible improvements of the prediction model.

Clinic-pathological information	Groups	Number of patients (OC)
Age	≤ 65 years old	153/245
	> 65 years old	92/245
Gender	Male	162/246
	Female	84/246
Grade	1-2	192/244
	3	52/244
Stage	I-II	74/241
	III-IV	167/241
Subsite	Alveolar ridge	15/246
	Buccal mucosa	15/246
	Floor of the mouth	46/246
	Hard palate	5/246
	Oral cavity	58/246
	Oral tongue	104/246
	Lips	3/246
Mutational status for TP53	Wild-type	70/246

Mutated	176/246
---------	---------

Supplementary Table 1 (A): Clinic-pathological characteristics of included patients with squamous cell carcinoma of the oral cavity (OC);

Clinic-pathological information	Groups	Number of patients (L)
Age	≤ 65 years old	60/90
	> 65 years old	30/90
Gender	Male	72/90
	Female	18/90
Grade	1-2	65/86
	3	21/86
Stage	I-II	11/86
	III-IV	75/86
Mutational status for TP53	Wild-type	12/90
	Mutated	78/90

Supplementary Table 1 (B): Clinic-pathological characteristics of included patients with squamous cell carcinoma of the larynx (L);

Clinic-pathological information	Groups	Number of patients (OP)
Age	≤ 65 years old	50/62
	> 65 years old	12/62
Gender	Male	52/62
	Female	10/62

Grade	1-2	33/52
	3	19/52
Stage	I-II	15/60
	III-IV	45/60
Subsite	Base of the tongue	20/62
	Oropharynx	6/62
	Tonsils	36/62
HPV Status	Negative	6/32
	Positive	26/32
Mutational status for TP53	Wild-type	43/62
	Mutated	19/62

Supplementary Table 1 (C): Clinic-pathological characteristics of included patients with squamous cell carcinoma of the oropharynx (OP);

Clinic-pathological information	Groups	Number of patients (HP)
Age	≤ 65 years old	6/9
	> 65 years old	3/9
Gender	Male	6/9
	Female	3/9
Grade	1-2	5/9
	3	4/9
Stage	I-II	0/9

	III-IV	9/9
HPV Status	Negative	2/3
	Positive	1/3
Mutational status for TP53	Wild-type	4/9
	Mutated	5/9

Supplementary Table 1 (D): Clinic-pathological characteristics of included patients with squamous cell carcinoma of the hypopharynx (HP).

Wild-type TP53 in OSCC			
Gene	Protein	Frequency and alteration type	Cell function
CDKN2A	P16 <sup>INK4A</sup>	<p><b>47.1%</b></p> <p>40% Homozygous deletion</p> <p>1.4% mRNA upregulation</p> <p>5.7% mutation</p>	Cell aging; regulation of establishment of protein localization to mitochondrion; positive regulation of cellular protein localization.
DROSHA	Ribonuclease III	<p><b>25.7%</b></p> <p>22.9% mRNA upregulation</p> <p>2.9% mRNA downregulation</p>	Not reported
TP63	Tumor protein 63	<p><b>20.0%</b></p> <p>8.6% Amplification</p> <p>12.9% mRNA upregulation</p> <p>2.9% mutation</p>	Cell aging; intrinsic apoptotic signaling pathway in response to DNA damage; regulation of establishment of protein localization to mitochondrion; positive regulation of cellular protein localization.

PMS2	Mismatch repair endonuclease PMS2	<b>18.6%</b> 1.4% Amplification 15.7% mRNA upregulation 4.3% mutation	Cellular response to DNA damage stimulus.
CDK9	Cyclin-dependent kinase 9	<b>17.1%</b> 17.1% Amplification 1.4% mRNA upregulation	Cellular response to DNA damage stimulus.
DDB2	DNA damage-binding protein 2	<b>17.1%</b> 4.3% Amplification 11.4% mRNA upregulation 1.4% mutation	Cellular response to DNA damage stimulus.
EPHA2	Ephrin type-A receptor 2	<b>17.1%</b> 1.4% Homozygous deletion 8.6% mRNA upregulation 8.6% mutation	Intrinsic apoptotic signaling pathway in response to DNA damage; positive regulation of cellular protein localization.

Supplemental material Table 3 (A): Gene ontology and network analysis for wild-type TP53 in OSCC; “Not reported” means the reported gene was not included in any Gene ontology result.

<b>Mutated TP53 in OSCC</b>			
<b>Gene</b>	<b>Protein</b>	<b>Frequency and alteration type</b>	<b>Cell function</b>
CDKN2A	P16 <sup>INK4A</sup>	<b>63.1%</b> 34.7% Homozygous deletion	Regulation of protein export from nucleus; regulation of signal transduction by p53 class mediator; regulation of cell cycle G1/S phase transition; negative regulation of cell cycle process;

		29.5% mutation	
TP63	Tumor protein 63	<b>35.2%</b> 17.6% Amplification 20.5% mRNA upregulation 0.6% mRNA downregulation 3.4% mutation	Negative regulation of cellular senescence; Negative regulation of cell aging; positive regulation of mitochondrial outer membrane permeabilization involved in apoptotic signaling pathway; regulation of signal transduction by p53 class mediator; regulation of cell cycle G1/S phase transition;
NDRG1	Protein NDRG1	<b>25.6%</b> 9.7% Amplification 19.9% mRNA upregulation	Cellular response to DNA damage stimulus
GSK3B	Glycogen synthase kinase-3 beta	<b>25.6%</b> 3.4% Amplification 22.2% mRNA upregulation 0.6% mRNA downregulation	Positive regulation of mitochondrial outer membrane permeabilization involved in apoptotic signaling pathway; regulation of protein export from nucleus; negative regulation of apoptotic process
SNAI2	Snail family transcriptional repressor 2	<b>23.8%</b> 9.7% Amplification 17.6% mRNA upregulation	Regulation of signal transduction by p53 class mediator; negative regulation of apoptotic process;
BCL6	B-cell lymphoma 6 protein	<b>23.3%</b> 16.5% Amplification 10.2% mRNA upregulation	Negative regulation of cell aging; negative regulation of cell cycle process; cellular response to DNA damage stimulus; negative regulation of apoptotic process;
CCNK	Cycline K	<b>22.7%</b> 2.3% Amplification 0.6% Homozygous deletion	Negative regulation of cell cycle process; cellular response to DNA damage stimulus

		18.2% mRNA upregulation 3.4% mRNA downregulation 0.6% mutation	
DROSHA	Ribonuclease III	<b>22.7%</b> 5.1% Amplification 18.8% mRNA upregulation 1.7% mRNA downregulation 0.6% mutation	Not reported
PRKDC	DNA-dependent protein kinase catalytic subunit	<b>22.7%</b> 7.4% Amplification 13.6% mRNA upregulation 5.7% mutation	Negative regulation of cell aging; regulation of cell cycle G1/S phase transition; negative regulation of cell cycle process; cellular response to DNA damage stimulus; negative regulation of apoptotic process
RRM2B	Ribonucleoside-diphosphate reductase subunit M2 B	<b>18.8%</b> 7.4% Amplification 14.8% mRNA upregulation	Regulation of signal transduction by p53 class mediator; cellular response to DNA damage stimulus; negative regulation of apoptotic process
HIRA	Protein HIRA	<b>18.1%</b> 4.5% Amplification 0.6% Homozygous deletion 12.5% mRNA upregulation 3.4% mRNA downregulation 1.1% mutation	Not reported

Supplemental material Table 3 (B): Gene ontology and network analysis for mutated TP53 in OSCC; “Not reported” means the reported gene was not included in any Gene ontology result.

Wild-type TP53 in Oropharynx			
Gene	Protein	Frequency and alteration type	Cell function
PCNA	Proliferating cell nuclear antigen	<p><b>47.7%</b> 2.3% Homozygous deletion 45.5% mRNA upregulation</p>	<p>DNA damage response, signal transduction by p53 class mediator; negative regulation of cell cycle process; mismatch repair; rhythmic process; DNA damage response, signal transduction by p53 class mediator resulting in cell cycle arrest; signal transduction involved in mitotic G1 DNA damage checkpoint; negative regulation of cell cycle G1/S phase transition; G1 DNA damage checkpoint; signal transduction involved in DNA damage checkpoint; negative regulation of G1/S transition of mitotic cell cycle; positive regulation of DNA repair; postreplication repair; cellular response to hydrogen peroxide</p>
BCL6	B-cell lymphoma 6 protein	<p><b>45.5%</b> 27.3% Amplification 25% mRNA upregulation 2.3% mutation</p>	<p>B cell differentiation; negative regulation of immunoglobulin production; regulation of chromatin; negative regulation of cellular senescence; negative regulation of apoptotic process; negative regulation of cell cycle process; regulation of B cell apoptotic process; positive regulation of histone deacetylation; negative regulation of cell-matrix adhesion; regulation of regulatory T cell differentiation; regulation of isotype switching; regulation of T-helper cell differentiation</p>
FAS	Tumor necrosis factor receptor superfamily member 6	<p><b>36.4%</b> 6.8% Homozygous deletion 27.3% mRNA upregulation 2.3% mutation</p>	<p>negative regulation of apoptotic process; necroptotic process; negative regulation of extrinsic apoptotic signaling pathway; activation of cysteine-type endopeptidase activity involved in apoptotic process; fatty acid biosynthetic process; cellular response to starvation</p>
GSK3B	Glycogen synthase kinase-3 beta	<p><b>34.1%</b> 6.8% Amplification 29.5% mRNA upregulation 2.3% mRNA downregulation</p>	<p>ER overload response; ER-nucleus signaling pathway; regulation of mitochondrial outer membrane permeabilization involved in apoptotic signaling pathway; positive regulation of protein export from nucleus; negative regulation of apoptotic process; negative regulation of protein acetylation; rhythmic process; extrinsic apoptotic signaling pathway in absence of ligand; peptidyl-threonine phosphorylation; peptidyl-serine phosphorylation; protein autophosphorylation</p>

TP63	Tumor protein 63	<p><b>34.1%</b> 25% Amplification 13.6% mRNA upregulation 2.3% mRNA downregulation 2.3% mutation</p>	<p>cell aging; aging; negative regulation of cellular senescence; positive regulation of protein insertion into mitochondrial membrane involved in apoptotic signaling pathway; regulation of mitochondrial outer membrane permeabilization involved in apoptotic signaling pathway; negative regulation of intracellular estrogen receptor signaling pathway; intrinsic apoptotic signaling pathway in response to DNA damage by p53 class mediator; intrinsic apoptotic signaling pathway by p53 class mediator; regulation of fibroblast apoptotic process; morphogenesis of embryonic epithelium</p>
TSC2	TSC Complex subunit 2	<p><b>31.8%</b> 31.8% mRNA upregulation</p>	<p>negative regulation of mitophagy; negative regulation of phosphatidylinositol 3-kinase signaling; protein kinase B signaling; morphogenesis of embryonic epithelium</p>
BRCA1	Breast cancer type 1 susceptibility protein	<p><b>31.8%</b> 29.5% mRNA upregulation 2.3% mutation</p>	<p>positive regulation of histone H3-K9 methylation ; regulation of chromatin organization; negative regulation of intracellular estrogen receptor signaling pathway; DNA damage response, signal transduction by p53 class mediator; negative regulation of apoptotic process; negative regulation of cell cycle process; positive regulation of histone H3-K4 methylation; negative regulation of protein acetylation; signal transduction involved in DNA damage checkpoint; negative regulation of G1/S transition of mitotic cell cycle; regulation of cell cycle G2/M phase transition; G2 DNA damage checkpoint; positive regulation of DNA repair; postreplication repair; negative regulation of reactive oxygen species metabolic process; negative regulation of extrinsic apoptotic signaling pathway; negative regulation of G0 to G1 transition; fatty acid biosynthetic process</p>
BCL2	B-cell lymphoma 2	<p><b>29.5%</b> 29.5% mRNA upregulation</p>	<p>B cell lineage commitment; B cell differentiation; lymphoid progenitor cell differentiation; cell aging; aging; positive regulation of protein insertion into mitochondrial membrane involved in apoptotic signaling pathway; regulation of mitochondrial outer membrane permeabilization involved in apoptotic signaling pathway; T cell lineage commitment; negative regulation of signal transduction by p53 class mediator; negative regulation of intrinsic apoptotic signaling pathway by p53 class mediator; negative regulation of apoptotic</p>

			<p>process; negative regulation of cell cycle process; response to UV-B; regulation of myeloid cell apoptotic process; release of cytochrome c from mitochondria; intrinsic apoptotic signaling pathway in response to endoplasmic reticulum stress; negative regulation of cell cycle G1/S phase transition; negative regulation of G1/S transition of mitotic cell cycle; response to gamma radiation; extrinsic apoptotic signaling pathway in absence of ligand; response to iron ion; peptidyl-threonine phosphorylation; response to ischemia; negative regulation of reactive oxygen species metabolic process; negative regulation of extrinsic apoptotic signaling pathway in absence of ligand; negative regulation of extrinsic apoptotic signaling pathway; peptidyl-serine phosphorylation; regulation of viral genome replication; cellular response to starvation</p>
MDM2	E3 ubiquitin protein ligase MDM2	<p><b>29.5%</b> 29.5% mRNA upregulation</p>	<p>cellular response to actinomycin D; cellular response to UV-C; amyloid fibril formation; positive regulation of protein export from nucleus; DNA damage response, signal transduction by p53 class mediator; negative regulation of DNA damage response, signal transduction by p53 class mediator; negative regulation of signal transduction by p53 class mediator; regulation of DNA damage response, signal transduction by p53 class mediator; negative regulation of intrinsic apoptotic signaling pathway by p53 class mediator; negative regulation of apoptotic process; negative regulation of cell cycle arrest; negative regulation of cell cycle process; DNA damage response, signal transduction by p53 class mediator resulting in cell cycle arrest; signal transduction involved in mitotic G1 DNA damage checkpoint; negative regulation of cell cycle G1/S phase transition; G1 DNA damage checkpoint; signal transduction involved in DNA damage checkpoint; negative regulation of G1/S transition of mitotic cell cycle; response to gamma radiation; response to iron ion; cellular response to hydrogen peroxide; positive regulation of smooth muscle cell proliferation; protein sumoylation</p>
LMNB1	Lamin-B1	<p><b>29.5%</b> 29.5% mRNA upregulation</p>	Not reported

PTEN	Phosphatidylinositol 3,4,5-trisphosphate 3-phosphatase and dual-specificity protein phosphatase PTEN	<p><b>27.3%</b> 15.9% Homozygous deletion 18.2% mRNA downregulation 9.1% mutation</p>	Aging; negative regulation of phosphatidylinositol 3-kinase signaling; negative regulation of apoptotic process; negative regulation of cell cycle process; regulation of B cell apoptotic process; regulation of myeloid cell apoptotic process; circadian behavior; rhythmic process; negative regulation of cell cycle G1/S phase transition; negative regulation of G1/S transition of mitotic cell cycle; regulation of ubiquitin protein ligase activity; negative regulation of cell-matrix adhesion; negative regulation of cyclin-dependent protein serine/threonine kinase activity; protein kinase B signaling; transcription initiation from RNA polymerase II promoter
DGCR8	Microprocessor complex subunit DGCR8	<p><b>27.3%</b> 25% mRNA upregulation 2.3% mutation</p>	primary miRNA processing; production of miRNAs involved in gene silencing by miRNA; miRNA metabolic process
TP73	Tumor protein P73	<p><b>27.3%</b> 2.3% Homozygous deletion 25% mRNA upregulation</p>	positive regulation of protein insertion into mitochondrial membrane involved in apoptotic signaling pathway; regulation of mitochondrial outer membrane permeabilization involved in apoptotic signaling pathway; intrinsic apoptotic signaling pathway in response to DNA damage by p53 class mediator; intrinsic apoptotic signaling pathway by p53 class mediator; mismatch repair; regulation of gliogenesis
TRIM28	Transcription intermediary factor 1-beta	<p><b>27.3%</b> 27.3% mRNA upregulation</p>	regulation of chromatin; positive regulation of DNA repair; positive regulation of protein localization to nucleus; protein sumoylation; regulation of viral genome replication; transcription initiation from RNA polymerase II promoter; protein autophosphorylation; epithelial to mesenchymal transition
BCL2L14	Apoptosis facilitator BCL-2-like protein 14	<p><b>25%</b> 4.5% Amplification 20.5% mRNA upregulation</p>	Not reported
DYRK1A	Dual specificity tyrosin phosphorylation regulated forkhead box A1	<p><b>25%</b> 22.7% mRNA upregulation 2.3% mutation</p>	negative regulation of DNA damage response, signal transduction by p53 class mediator; negative regulation of signal transduction by p53 class mediator; regulation of DNA damage response, signal transduction by p53 class mediator; rhythmic process; peptidyl-threonine phosphorylation; peptidyl-serine phosphorylation; protein autophosphorylation
CCNK	Cyclin K	<p><b>25%</b> 4.5% Homozygous deletion</p>	negative regulation of cell cycle arrest; regulation of viral genome replication

		4.5% mRNA upregulation 20.5% mRNA downregulation	
AGO4	Protein argonaute 4	<b>25%</b> 15.9% mRNA upregulation 9.1% mutation	production of miRNAs involved in gene silencing by miRNA; pre-miRNA processing; miRNA metabolic process; negative regulation of apoptotic process
MSH2	Muts Homolog II	<b>22.7%</b> 22.7% mRNA upregulation	B cell differentiation; aging; regulation of helicase activity; intrinsic apoptotic signaling pathway in response to DNA damage by p53 class mediator; intrinsic apoptotic signaling pathway by p53 class mediator; negative regulation of apoptotic process; response to UV-B; determination of adult lifespan; mismatch repair; somatic recombination of immunoglobulin gene segments; response to X-ray; regulation of isotype switching; postreplication repair
PRKAB1	5'-AMP-activated protein kinase subunit beta-1	<b>22.7%</b> 22.7% mRNA upregulation	fatty acid biosynthetic process
PRKDC	DNA-dependent protein kinase catalytic subunit	<b>22.7%</b> 22.7% mRNA upregulation	negative regulation of immunoglobulin production B cell lineage commitment; B cell differentiation; lymphoid progenitor cell differentiation; negative regulation of cellular senescence; T cell lineage commitment; negative regulation of apoptotic process; negative regulation of cell cycle process; rhythmic process; signal transduction involved in mitotic G1 DNA damage checkpoint; negative regulation of cell cycle G1/S phase transition; G1 DNA damage checkpoint; signal transduction involved in DNA damage checkpoint; negative regulation of G1/S transition of mitotic cell cycle; somatic recombination of immunoglobulin gene segments; response to gamma radiation; positive regulation of DNA repair; peptidyl-serine phosphorylation; regulation of fibroblast proliferation
CDK1	Cycline-dependent kinase 1	<b>20.5%</b> 20.5% mRNA upregulation	cell aging; aging; DNA damage response, signal transduction by p53 class mediator; negative regulation of apoptotic process; negative regulation of cell cycle process; rhythmic process; DNA damage response, signal transduction by p53 class mediator resulting in cell cycle arrest; signal transduction involved in mitotic G1 DNA damage checkpoint; negative regulation of cell cycle G1/S phase transition; G1 DNA damage checkpoint; signal transduction

			involved in DNA damage checkpoint; negative regulation of G1/S transition of mitotic cell cycle; regulation of cell cycle G2/M phase transition; G2 DNA damage checkpoint; peptidyl-threonine phosphorylation; cellular response to hydrogen peroxide; peptidyl-serine phosphorylation; positive regulation of protein localization to nucleus; transcription initiation from RNA polymerase II promoter; regulation of gliogenesis
MDM4	Protein MDM4	<b>20.5%</b> 2.3% Amplification 20.5% mRNA upregulation	DNA damage response, signal transduction by p53 class mediator; negative regulation of apoptotic process; negative regulation of cell cycle arrest; negative regulation of cell cycle process; DNA damage response, signal transduction by p53 class mediator resulting in cell cycle arrest; signal transduction involved in mitotic G1 DNA damage checkpoint; negative regulation of cell cycle G1/S phase transition; G1 DNA damage checkpoint; signal transduction involved in DNA damage checkpoint; negative regulation of G1/S transition of mitotic cell cycle
MAPKAPK2	MAP kinase-activated protein kinase 2	<b>20.5%</b> 2.3% Amplification 18.2% mRNA upregulation 2.3% mRNA downregulation	peptidyl-serine phosphorylation; protein autophosphorylation
DROSHA	Drosha Ribonuclease III	<b>20.5%</b> 2.3% Amplification 20.5% mRNA upregulation	primary miRNA processing; production of miRNAs involved in gene silencing by miRNA; pre-miRNA processing, miRNA metabolic process; regulation of regulatory T cell differentiation
RRM2B	Ribonucleoside-disphosphate reductase subunit M2 B	<b>20.5%</b> 2.3% Amplification 18.2% mRNA upregulation	negative regulation of signal transduction by p53 class mediator; negative regulation of intrinsic ; apoptotic signaling pathway by p53 class mediator; negative regulation of apoptotic process
CDKN2A	P16 <sup>INK4A</sup>	<b>18.2%</b> 2.3% Homozygous deletion 13.6% mRNA upregulation 2.3% mutation	amyloid fibril formation; regulation of apoptotic DNA fragmentation; regulation of execution phase of apoptosis; replicative senescence; cell aging; aging; regulation of DNA damage response, signal transduction by p53 class mediator; negative regulation of cell cycle process; regulation of myeloid cell apoptotic process; negative regulation of cell cycle G1/S phase transition; negative regulation of G1/S transition of mitotic cell cycle; regulation of ubiquitin protein ligase activity; negative regulation of cell-matrix adhesion; regulation of cell cycle G2/M phase

			transition; negative regulation of cyclin-dependent protein serine/threonine kinase activity; positive regulation of protein localization to nucleus; protein sumoylation; activation of cysteine-type endopeptidase activity involved in apoptotic process; chromatin assembly
E2F2	Transcription factor E2F2	<b>18.2%</b> 18.2% mRNA upregulation	intrinsic apoptotic signaling pathway by p53 class mediator; transcription initiation from RNA polymerase II promoter
CSNK2A1	Casein kinase II subunit alfa	<b>18.2%</b> 2.3% Homozygous deletion 6.8% mRNA upregulation 9.1% mRNA downregulation 2.3% mutation	negative regulation of apoptotic process; rhythmic process; peptidyl-threonine phosphorylation; peptidyl-serine phosphorylation
CX3CL1	Fractalkine	<b>18.2%</b> 2.3% Homozygous deletion 15.9% mRNA upregulation	Aging; negative regulation of apoptotic process; positive regulation of transforming growth factor beta production; negative regulation of cell-matrix adhesion; response to ischemia; negative regulation of extrinsic apoptotic signaling pathway in absence of ligand; negative regulation of extrinsic apoptotic signaling pathway; positive regulation of smooth muscle cell proliferation
APAF1	Apoptotic protease-activating factor 1	<b>18.2%</b> 18.2% mRNA upregulation	regulation of apoptotic DNA fragmentation; regulation of execution phase of apoptosis; aging; negative regulation of cell cycle process; intrinsic apoptotic signaling pathway in response to endoplasmic reticulum stress; negative regulation of G0 to G1 transition; activation of cysteine-type endopeptidase activity involved in apoptotic process; morphogenesis of embryonic epithelium
MYB	Proliferation marker protein Ki-67	<b>18.2%</b> 15.9% mRNA upregulation 2.3% mutation	positive regulation of histone H3-K9 methylation; regulation of chromatin; positive regulation of histone H3-K4 methylation; positive regulation of transforming growth factor beta production; regulation of T-helper cell differentiation; cellular response to hydrogen peroxide; regulation of fibroblast proliferation; positive regulation of smooth muscle cell proliferation; regulation of gliogenesis
CABIN1	Calcineurin-binding protein cabin-1	<b>17.5%</b> 20.5% mRNA upregulation 4.5% mutation	chromatin assembly

Supplemental material Table 3 (C): Gene ontology and network analysis for wild-type TP53 in OP; “Not reported” means the reported gene was not included in any Gene ontology result.

<b>Mutated TP53 in Oropharynx</b>			
<b>Gene</b>	<b>Protein</b>	<b>Frequency and alteration type</b>	<b>Cell function</b>
CDKN2A	P16 <sup>INK4A</sup>	<b>78.9%</b> 57.9% Homozygous deletion 21.1% mutation	replicative senescence; cell aging; negative regulation of developmental process; regulation of protein export from nucleus; negative regulation of cell cycle process; negative regulation of cell-matrix adhesion; positive regulation of apoptotic process; negative regulation of B cell activation; regulation of signal transduction by p53 class mediator; apoptotic mitochondrial changes; cell cycle arrest; G1/S transition of mitotic cell cycle; chromatin assembly; positive regulation of protein modification by small protein conjugation or removal; negative regulation of cell growth
TP63	Tumor protein 63	<b>52.6%</b> 42.1% Amplification 21.1% mRNA upregulation	cell aging; negative regulation of cellular senescence; negative regulation of developmental process; morphogenesis of an epithelial fold; positive regulation of protein insertion into mitochondrial membrane involved in apoptotic signaling pathway; positive regulation of mitochondrion organization; positive regulation of apoptotic process; regulation of mitochondrial outer membrane permeabilization involved in apoptotic signaling pathway; regulation of signal transduction by p53 class mediator; regulation of intracellular estrogen receptor signaling pathway; negative regulation of epithelial cell differentiation; stem cell differentiation; positive regulation of epithelial cell proliferation
NDRG1	Protein NDRG1	<b>42.1%</b> 10.5% Amplification 36.8% mRNA upregulation	cellular response to hypoxia; DNA damage response, signal transduction by p53 class mediator
BCL6	B-cell lymphoma 6 protein	<b>36.38%</b> 26.3% Amplification 15.8% mRNA upregulation	negative regulation of cellular senescence; negative regulation of developmental process; positive regulation of histone deacetylation; regulation of histone modification; positive regulation of protein deacetylation; negative regulation of cell cycle process; negative regulation of cell-matrix adhesion; positive regulation of apoptotic process; negative regulation of lymphocyte apoptotic process; regulation of regulatory T cell differentiation; negative regulation of

			B cell activation; negative regulation of cell growth
DROSHA	Drosha ribonuclease III	<b>36.8%</b> 15.8% Amplification 26.3% mRNA upregulation 5.3% mutation	regulation of regulatory T cell differentiation
PRKAB2	Protein kinase AMP-activated non-catalytic subunit beta 2	<b>26.3%</b> 10.5% Amplification 15.8% mRNA upregulation	regulation of signal transduction by p53 class mediator; regulation of autophagy; cell cycle arrest; regulation of macroautophagy
SKP2	S-phase kinase associated protein 2	<b>26.3%</b> 15.8% Amplification 15.8% mRNA upregulation	regulation of intracellular estrogen receptor signaling pathway; G1/S transition of mitotic cell cycle; positive regulation of protein modification by small protein conjugation or removal; protein deubiquitination
CCNK	Cyclin K	<b>26.3%</b> 15.8% mRNA upregulation 10.5% mRNA downregulation	negative regulation of cell cycle arrest; negative regulation of cell cycle process; transcription, DNA-templated; positive regulation of DNA-templated transcription, elongation; ncRNA transcription
STEAP3	STEAP3 metalloredutase	<b>26.3%</b> 26.3% mRNA upregulation	iron ion homeostasis
HIF1A	Hypoxia inducible factor 1 subunit alpha	<b>21.1%</b> 5.3% Amplification 10.5% mRNA upregulation 15.8% mutation	positive regulation of transcription from RNA polymerase II promoter in response to hypoxia; cellular response to hypoxia; regulation of thymocyte apoptotic process; negative regulation of developmental process; morphogenesis of an epithelial fold; positive regulation of glycolytic process; positive regulation of cellular catabolic process; regulation of carbohydrate metabolic process; positive regulation of mitochondrion organization; mRNA transcription; transcription, DNA-templated; negative regulation of lymphocyte apoptotic process; regulation of cellular respiration; positive regulation of pri-miRNA transcription by RNA polymerase II; regulation of autophagy of mitochondrion; regulation of autophagy; iron ion homeostasis; positive regulation of autophagy; stem cell differentiation; protein deubiquitination; regulation of macroautophagy; cellular response to interleukin-1; positive regulation of epithelial cell proliferation
PPP2CB	Protein phosphatase 2 catalytic subunit beta	<b>21.1%</b> 5.3% Homozygous deletion 10.5% Amplification 5.3% mRNA upregulation	apoptotic mitochondrial changes; positive regulation of binding

		5.3% mRNA downregulation	
YY1	YY1 transcription factor	<b>21.1%</b> 21.1% mRNA upregulation	response to UV-C; response to UV; negative regulation of developmental process; positive regulation of pri-miRNA transcription by RNA polymerase II; negative regulation of cell growth; protein deubiquitination; cellular response to interleukin-1; double-strand break repair; regulation of cell growth involved in cardiac muscle cell development
SERPINE1	Serpin family E member 1	<b>21.1%</b> 15.8% Amplification 10.5% mRNA upregulation	replicative senescence; cell aging; negative regulation of developmental process; negative regulation of smooth muscle cell migration; regulation of smooth muscle cell migration; negative regulation of cell-matrix adhesion; negative regulation of epithelial cell differentiation; circadian rhythm
MYC	MYC proto-oncogene	<b>21.1 %</b> 21.1% Amplification	cellular response to hypoxia; response to UV; negative regulation of developmental process; regulation of smooth muscle cell migration; positive regulation of glycolytic process; positive regulation of cellular catabolic process; regulation of carbohydrate metabolic process; positive regulation of apoptotic process; transcription, DNA-templated; beta-catenin-TCF complex assembly; regulation of cellular respiration; liver regeneration; iron ion homeostasis; cell cycle arrest; G1/S transition of mitotic cell cycle; positive regulation of binding; response to ionizing radiation; protein deubiquitination; cellular response to interleukin-1; positive regulation of epithelial cell proliferation
PRMT5	Protein arginine methyltransferase 5	<b>21.1%</b> 21.1 mRNA upregulation	negative regulation of developmental process; regulation of DNA methylation; regulation of DNA methylation; transcription, DNA-templated; liver regeneration; regulation of signal transduction by p53 class mediator; circadian rhythm
CDK9	Cyclin dependent kinase 9	<b>21.1%</b> 10.5% Amplification 21.1% mRNA upregulation	regulation of histone modification; negative regulation of cell cycle arrest; negative regulation of cell cycle process; transcription, DNA-templated; positive regulation of DNA-templated transcription, elongation; ncRNA transcription; positive regulation of binding; positive regulation of protein modification by small protein conjugation or removal

GSK3B	GSK-3 beta, GSK3beta isoform, serine/threonine-protein kinase GSK3B	<b>21.1%</b> 5.3% Amplification 15.8% mRNA upregulation	ER overload response; negative regulation of developmental process; positive regulation of protein export from nucleus; regulation of protein export from nucleus; positive regulation of cellular catabolic process; regulation of carbohydrate metabolic process; positive regulation of mitochondrion organization; positive regulation of apoptotic process; regulation of mitochondrial outer membrane permeabilization involved in apoptotic signaling pathway; regulation of autophagy; negative regulation of epithelial cell differentiation; circadian rhythm; regulation of glucose metabolic process; positive regulation of autophagy; positive regulation of binding
KAT5	Lysine acetyltransferase 5	<b>21.1%</b> 5.3% Amplification 21.1% mRNA upregulation	DNA damage response, signal transduction by p53 class mediator resulting in transcription of p21 class mediator; DNA damage response, signal transduction by p53 class mediator; positive regulation of cellular catabolic process; beta-catenin-TCF complex assembly; regulation of signal transduction by p53 class mediator; regulation of autophagy; positive regulation of autophagy; response to ionizing radiation; double-strand break repair
HIRA	Histone cell cycle regulator	<b>21.1%</b> 5.3% Amplification 15.8% mRNA upregulation	transcription, DNA-templated; chromatin assembly
XRRC5	X-ray repair cross complementing 5	<b>21.1%</b> 10.5% mRNA upregulation 10.5% mRNA downregulation 4.2% mutation	Not reported
IGFBP3	Insulin like growth factor binding protein 3	<b>21.1%</b> 21.1% mRNA upregulation	negative regulation of smooth muscle cell migration; regulation of smooth muscle cell migration; regulation of carbohydrate metabolic process; positive regulation of apoptotic process; regulation of glucose metabolic process
TTC5	Tetratricopeptide repeat domain 5	<b>21.1%</b> 21.1% mRNA upregulation	regulation of signal transduction by p53 class mediator

Supplemental material Table 3 (D): Gene ontology and network analysis for mutated TP53 in OP; “Not reported” means the reported gene was not included in any Gene ontology result.

<b>Wild-type TP53 in Larynx</b>			
<b>Gene</b>	<b>Protein</b>	<b>Frequency and alteration type</b>	<b>Cell function</b>
CDKN2A	P16 <sup>INK4A</sup>	<b>41.6%</b> 41.6% Homozygous deletion	regulation of signal transduction by p53 class mediator; DNA conformation change; positive regulation of apoptotic process;
CCNK	Cycline K	<b>33.3%</b> 8.3% mRNA upregulation 25.0% mRNA downregulation	Not reported
BCL6	B-cell lymphoma 6 protein	<b>33.3%</b> 25.0% Amplification 16.7% mRNA upregulation	positive regulation of apoptotic process;
SH2D1A	SH2 domain-containing protein 1A	<b>33.3%</b> 16.7% mRNA upregulation 16.7% mutation	positive regulation of innate immune response
TP63	Tumor protein 63	<b>33.3%</b> 25.0% Amplification 16.7% mRNA upregulation	regulation of signal transduction by p53 class mediator; positive regulation of apoptotic process
CSNK2A1	Casein kinase II subunit alfa	<b>33.3%</b> 8.3% mRNA upregulation 16.7% mRNA downregulation 8.3% mutation	regulation of signal transduction by p53 class mediator; peptidyl-serine phosphorylation; rhythmic process
MAPK13	Mitogen-activated protein kinase 13	<b>25%</b> 16.7% mRNA upregulation 8.3% mutation	stress-activated MAPK cascade; peptidyl-serine phosphorylation;
FDXR	NADPH: adrenodoxin oxidoreductase, mitochondrial	<b>25%</b> 25.0% mRNA upregulation	Not reported
GSK3B	Glycogen synthase kinase-3 beta	<b>25%</b> 16.7% Amplification 8.3% mRNA upregulation	peptidyl-serine phosphorylation; rhythmic process; positive regulation of apoptotic process;
UBB	Polyubiquitin-B	<b>25%</b> 8.3% mRNA upregulation 16.7% mRNA downregulation	stress-activated MAPK cascade; regulation of signal transduction by p53 class mediator; activation of innate immune response; positive regulation of innate immune response; positive regulation of apoptotic process;
NEDD8	NEDD8	<b>25%</b> 8.3% Amplification 16.7% mRNA upregulation	Not reported
TRAF6	TNF receptor-associated factor 6	<b>25%</b> 8.3% mRNA upregulation 16.7% mRNA downregulation	stress-activated MAPK cascade; activation of innate immune response; positive regulation of innate immune response; positive regulation of apoptotic process;
CREBBP	CREB-binding protein	<b>25%</b> 8.3% mRNA upregulation 16.7% mRNA downregulation	activation of innate immune response; positive regulation of innate immune response; rhythmic process

ASF1A	Histone chaperone ASF1A	<b>25%</b> 16.7% mRNA upregulation 8.3% mRNA downregulation	DNA conformation change
MAPKAPK2	MAP kinase-activated protein kinase 2	<b>25%</b> 25.0% mRNA upregulation	stress-activated MAPK cascade; peptidyl-serine phosphorylation; activation of innate immune response; positive regulation of innate immune response;
DYRK1A	Dual specificity tyrosine-phosphorylation-regulated kinase 1A	<b>25%</b> 8.3% Amplification 8.3% mRNA upregulation 16.7% mRNA downregulation	regulation of signal transduction by p53 class mediator; peptidyl-serine phosphorylation; rhythmic process
XRCC5	X-ray repair cross-complementing protein 5	<b>25%</b> 8.3% Homozygous deletion 8.3% mRNA upregulation 16.7% mRNA downregulation	activation of innate immune response; positive regulation of innate immune response; DNA conformation change;
NDRG1	Protein NDRG1	<b>25%</b> 25.0% mRNA upregulation	Not reported

Supplemental material Table 3 (E): Gene ontology and network analysis for wild-type TP53 in L; “Not reported” means the reported gene was not included in any Gene ontology result.

<b>Mutated TP53 in Larynx</b>			
<b>Gene</b>	<b>Protein</b>	<b>Frequency and alteration type</b>	<b>Cell function</b>
CDKN2A	P16 <sup>INK4A</sup>	<b>56.4%</b> 33.3% Homozygous deletion 1.3% mRNA upregulation 23.1% mutation	cell aging; regulation of signal transduction by p53 class mediator; regulation of cysteine-type endopeptidase activity involved in apoptotic process; regulation of DNA metabolic process; regulation of hemopoiesis; regulation of growth; regulation of cell cycle process
TP63	Tumor protein 63	<b>52.5%</b> 35.9% Amplification 26.9% mRNA upregulation 1.3% mutation	negative regulation of cellular senescence; positive regulation of mitochondrial outer membrane permeabilization involved in apoptotic signaling pathway; cell aging; regulation of signal transduction by p53 class mediator; regulation of cysteine-type endopeptidase activity involved in apoptotic process; regulation of cell cycle process
BCL6	B-cell lymphoma 6 protein	<b>47.4%</b> 32.1% Amplification 25.6% mRNA upregulation 1.3% mutation	negative regulation of cellular senescence; regulation of DNA metabolic process; regulation of hemopoiesis; regulation of growth; regulation of cell cycle process
NDRG1	Protein NDRG1	<b>32%</b> 17.9% Amplification 23.1% mRNA upregulation	cellular response to hypoxia

DROSHA	Ribonuclease III	<b>30.7%</b> 5.1% Amplification 29.5% mRNA upregulation 1.3% mutation	regulation of hemopoiesis
PRKDC	DNA-dependent protein kinase catalytic subunit	<b>28.2%</b> 3.8% Amplification 21.8% mRNA upregulation 7.7% mutation	negative regulation of cellular senescence; response to gamma radiation; rhythmic process; regulation of growth; regulation of cell cycle process
GSK3B	Glycogen synthase kinase-3 beta	<b>24.3%</b> 6.4% Amplification 19.2% mRNA upregulation 2.6% mutation	positive regulation of mitochondrial outer membrane permeabilization involved in apoptotic signaling pathway; rhythmic process; regulation of growth;
MYC	MYC proto-oncogene protein	<b>23%</b> 23.0% Amplification	response to gamma radiation; cellular response to UV; cellular response to hypoxia; regulation of cysteine-type endopeptidase activity involved in apoptotic process; regulation of DNA metabolic process; regulation of hemopoiesis;
COP1	E3 ubiquitin protein ligase COP1	<b>21.7%</b> 1.3% Amplification 20.5% mRNA upregulation 2.6% mutation	cellular response to UV; cellular response to hypoxia; regulation of cysteine-type endopeptidase activity involved in apoptotic process;
PMS2	Mismatch repair endonuclease PMS2	<b>20.5%</b> 2.6% Amplification 17.9% mRNA upregulation 1.3% mutation	Not reported
CDK9	Cyclin-dependent kinase 9	<b>20.5%</b> 3.8% Amplification 15.4% mRNA upregulation 2.6% mRNA downregulation 2.6% mutation	regulation of DNA metabolic process; regulation of cell cycle process
CSNK2A1	Casein kinase II subunit alfa	<b>20.5%</b> 17.9% mRNA upregulation 2.6% mutation	regulation of signal transduction by p53 class mediator; regulation of cysteine-type endopeptidase activity involved in apoptotic process; rhythmic process; regulation of growth; regulation of cell cycle process
TNRC6B	Trinucleotide repeat-containing gene 6B protein	<b>20.5%</b> 1.3% Amplification 16.7% mRNA upregulation 2.6% mutation	regulation of hemopoiesis;
SKP2	S-phase kinase-associated protein 2	<b>19.2%</b> 3.8% Amplification 17.9% mRNA upregulation	Not reported
CREBBP	CREB-binding protein	<b>19.2%</b> 1.3% Homozygous deletion 11.5% mRNA upregulation 6.4% mutation	cellular response to UV; cellular response to hypoxia; rhythmic process; regulation of hemopoiesis;
WRN	Werner syndrome ATP-dependent helicase	<b>17.9%</b> 1.3% Amplification 14.1% mRNA upregulation 1.3% mRNA downregulation 3.8% mutation	response to gamma radiation; cell aging; regulation of signal transduction by p53 class mediator; regulation of DNA metabolic process; regulation of growth;

Supplemental material Table 3 (F): Gene ontology and network analysis for mutated TP53 in L; “Not reported” means the reported gene was not included in any Gene ontology result.

<b>TP53 in HPV negative Oropharynx</b>			
<b>Gene</b>	<b>Protein</b>	<b>Frequency and alteration type</b>	<b>Cell function</b>
CDKN2A	P16 <sup>INK4A</sup>	<b>83.3%</b> 50.0% Homozygous deletion 33.3% mutation	replicative senescence; positive regulation of cell aging; negative regulation of cell-matrix adhesion; negative regulation of cell cycle process; negative regulation of B cell activation; negative regulation of proteolysis; regulation of DNA damage response, signal transduction by p53 class mediator; regulation of execution phase of apoptosis; cell cycle arrest; positive regulation of protein modification by small protein conjugation or removal; regulation of cysteine-type endopeptidase activity involved in apoptotic process; regulation of cell cycle G1/S phase transition; protein stabilization; negative regulation of cell growth; negative regulation of cellular catabolic process
TP63	Tumor protein 63	<b>66.7%</b> 50% Amplification 33.3.0% mRNA upregulation	stem cell differentiation; negative regulation of cellular senescence; positive regulation of mitochondrial outer membrane permeabilization involved in apoptotic signaling pathway ; intrinsic apoptotic signaling pathway in response to DNA damage by p53 class mediator; regulation of intracellular estrogen receptor signaling pathway; negative regulation of epithelial cell differentiation; regulation of cysteine-type endopeptidase activity involved in apoptotic process; regulation of cell cycle G1/S phase transition
PRKAB2	5'-AMP-activated protein kinase subunit beta-2	<b>50%</b> 33..3% Amplification 16.7% mRNA upregulation	Lipophagy; carnitine shuttle; fatty acid transmembrane transport; cell cycle arrest; regulation of macroautophagy; regulation of autophagy
BCL6	B-cell lymphoma 6 protein	<b>50%</b> 33.3% Amplification 16.7% mRNA upregulation	negative regulation of cell-matrix adhesion; negative regulation of cellular senescence; positive regulation of histone deacetylation; regulation of protein deacetylation; negative regulation of cell cycle process; regulation of regulatory T cell differentiation; negative regulation of B cell activation; negative regulation of DNA replication; regulation of Notch signaling pathway; negative regulation of cell growth; regulation of inflammatory response
NDRG1	Protein NDRG1	<b>50%</b> 16.7% Amplification 33.3% mRNA upregulation	cellular response to hypoxia

SERPINE1	Serpin family E member 1	<b>33.3%</b> 33.3% Amplification 16.7% mRNA upregulation	replicative senescence; negative regulation of cell-matrix adhesion; negative regulation of protein processing; negative regulation of proteolysis; negative regulation of extrinsic apoptotic signaling pathway via death domain receptors; circadian rhythm; regulation of inflammatory response; negative regulation of hydrolase activity
XRCC5	X-ray repair cross-complementing protein 5	<b>33.3%</b> 16.7% mRNA upregulation 16.7% mRNA downregulation	hematopoietic stem cell differentiation; stem cell differentiation; response to salt stress; response to ionizing radiation; cellular response to gamma radiation; regulation of DNA biosynthetic process
CREBBP	CREB-binding protein	<b>33.3%</b> 33.3% mRNA upregulation	regulation of Notch signaling pathway; circadian rhythm; cellular response to hypoxia; transcription initiation from RNA polymerase II promoter
SKP2	S-phase kinase-associated protein 2	<b>33.3%</b> 33.3% mRNA upregulation	regulation of intracellular estrogen receptor signaling pathway; positive regulation of protein modification by small protein conjugation or removal
GSK3B	Glycogen synthase kinase-3 beta	<b>33.3%</b> 16.7% Amplification 16.7% mRNA upregulation	ER overload response; ER-nucleus signaling pathway; positive regulation of protein export from nucleus; positive regulation of mitochondrial outer membrane permeabilization involved in apoptotic signaling pathway; negative regulation of epithelial cell differentiation; regulation of circadian rhythm; regulation of proteasomal ubiquitin-dependent protein catabolic process; circadian rhythm; regulation of autophagy; positive regulation of binding; negative regulation of hydrolase activity
DROSHA	Ribonuclease III	<b>33.3%</b> 33.3% mRNA upregulation	regulation of regulatory T cell differentiation; regulation of inflammatory response
BDNF	brain derived neurotrophic factor	<b>33.3%</b> 33.3% mRNA upregulation	positive regulation of binding; positive regulation of peptidyl-tyrosine phosphorylation
PMS2	Mismatch repair endonuclease PMS2	<b>33.3%</b> 33.3% mRNA upregulation	Not reported
HGF	Hepatocyte growth factor	<b>33.3%</b> 33.3% Amplification	regulation of neuron projection regeneration; negative regulation of proteolysis; negative regulation of extrinsic apoptotic signaling pathway via death domain receptors; regulation of DNA biosynthetic process; regulation of cysteine-type endopeptidase activity involved in apoptotic process; regulation of autophagy; positive regulation of peptidyl-tyrosine phosphorylation; negative regulation of cellular catabolic process; regulation of inflammatory response; negative regulation of hydrolase activity

USP7	Ubiquitin carboxyl-terminal hydrolase 7	<b>33.3%</b> 16.7% Amplification 33.3% mRNA upregulation	negative regulation of proteolysis; regulation of circadian rhythm; regulation of proteasomal ubiquitin-dependent protein catabolic process; protein stabilization; negative regulation of cellular catabolic process
CDK9	Cyclin-dependent kinase 9	<b>33.3%</b> 16.7% Amplification 33.3% mRNA upregulation	negative regulation of cell cycle arrest; negative regulation of cell cycle process; positive regulation of DNA-templated transcription, elongation; ncRNA transcription; positive regulation of protein modification by small protein conjugation or removal; positive regulation of binding; transcription initiation from RNA polymerase II promoter
CCNK	Cyclin K	<b>33.3%</b> 33.3% mRNA downregulation	negative regulation of cell cycle arrest; negative regulation of cell cycle process; positive regulation of DNA-templated transcription, elongation; ncRNA transcription
PRKAA2	5'-AMP-activated protein kinase catalytic subunit alfa-2	<b>33.3%</b> 16.7% Amplification 16.7% mRNA upregulation	Lipophagy; carnitine shuttle; fatty acid transmembrane transport; regulation of protein deacetylation; cellular response to glucose starvation; regulation of circadian rhythm; cell cycle arrest; regulation of macroautophagy; regulation of autophagy
MAP4K4	Mitogen-activated protein kinase kinase kinase kinase 4	<b>33.3%</b> 33.3% mRNA upregulation	negative regulation of cell-matrix adhesion; regulation of neuron projection regeneration
COP1	E3 ubiquitin protein ligase COP1	<b>33.3%</b> 16.7% Amplification 33.3% mRNA upregulation	cellular response to UV-C; response to ionizing radiation; negative regulation of protein processing; negative regulation of proteolysis; regulation of proteasomal ubiquitin-dependent protein catabolic process; cellular response to hypoxia; regulation of cysteine-type endopeptidase activity involved in apoptotic process; negative regulation of hydrolase activity

Supplemental material Table 3 (G): Gene ontology and network analysis for HPV negative TP53 in OP; “Not reported” means the reported gene was not included in any Gene ontology result.

<b>TP53 in HPV positive Oropharynx</b>			
<b>Gene</b>	<b>Protein</b>	<b>Frequency and alteration type</b>	<b>Cell function</b>
PCNA	Proliferating cell nuclear antigen	<b>50%</b> 3.7% Homozygous deletion 48.1% mRNA upregulation	response to UV; regulation of deoxyribonuclease activity; negative regulation of cell cycle process; DNA damage response, signal transduction by p53 class mediator resulting in cell cycle arrest; mismatch repair; regulation of transcription involved in G1/S transition of mitotic cell cycle; liver regeneration; positive regulation of DNA repair; postreplication repair;

			cellular response to hydrogen peroxide; nucleotide-excision repair
FAS	Tumor necrosis factor receptor superfamily member 6	<b>37.0%</b> 7.4% Homozygous deletion 25.9% mRNA upregulation 3.7% mutation	positive regulation of apoptotic process; negative regulation of apoptotic signaling pathway; necroptotic process; regulation of extrinsic apoptotic signaling pathway via death domain receptors; regulation of extrinsic apoptotic signaling pathway; regulation of cysteine-type endopeptidase activity involved in apoptotic process; fatty acid biosynthetic process
BCL6	B-cell lymphoma 6 protein	<b>37.0%</b> 18.5% Amplification 25.9% mRNA upregulation	negative regulation of B cell apoptotic process; regulation of leukocyte apoptotic process; positive regulation of apoptotic process; negative regulation of cell cycle process; positive regulation of histone deacetylation; negative regulation of cell-matrix adhesion; regulation of cell-matrix adhesion; regulation of regulatory T cell differentiation; regulation of isotype switching; negative regulation of cell growth
DGCR8	Microprocessor complex subunit DGCR8	<b>37.0%</b> 37.0% mRNA upregulation	primary miRNA processing; production of miRNAs involved in gene silencing by miRNA; miRNA metabolic process
BRCA1	Breast cancer type 1 susceptibility protein	<b>33.3%</b> 29.6% mRNA upregulation 3.7% mutation	positive regulation of histone H3-K9 methylation; negative regulation of intracellular estrogen receptor signaling pathway; regulation of intracellular estrogen receptor signaling pathway; DNA damage response, signal transduction by p53 class mediator resulting in transcription of p21 class mediator; intrinsic apoptotic signaling pathway in response to DNA damage; negative regulation of cell cycle process; positive regulation of histone H3-K4 methylation; negative regulation of protein acetylation; negative regulation of apoptotic signaling pathway; regulation of protein ubiquitination; regulation of DNA methylation; negative regulation of G2/M transition of mitotic cell cycle; G2 DNA damage checkpoint; positive regulation of DNA repair; postreplication repair; negative regulation of reactive oxygen species metabolic process; regulation of extrinsic apoptotic signaling pathway via death domain receptors; regulation of extrinsic apoptotic signaling pathway; protein autoubiquitination; fatty acid biosynthetic process
CCNK	Cycline K	<b>33.3%</b> 3.7% Homozygous deletion 11.1% mRNA upregulation	negative regulation of cell cycle arrest; negative regulation of cell cycle process; regulation of viral genome replication

		22.2% mRNA downregulation	
GSK3B	Glycogen synthase kinase-3 beta	<b>33.3%</b> 7.4% Amplification 29.6% mRNA upregulation 3.7% mRNA downregulation	ER overload response; positive regulation of apoptotic process; positive regulation of protein insertion into mitochondrial membrane involved in apoptotic signaling pathway; regulation of nucleocytoplasmic transport; peptidyl-threonine phosphorylation; negative regulation of protein acetylation; regulation of cell-matrix adhesion; protein autophosphorylation; protein sumoylation
PTEN	Phosphatidylinositol 3,4,5-trisphosphate 3-phosphatase and dual-specificity protein phosphatase PTEN	<b>29.6%</b> 14.8% Homozygous deletion 22.2% mRNA downregulation 11.1% mutation	regulation of leukocyte apoptotic process; negative regulation of phosphatidylinositol 3-kinase signaling; positive regulation of apoptotic process; negative regulation of cell cycle process; negative regulation of cardiac muscle cell proliferation; regulation of cardiac muscle tissue growth; negative regulation of phagocytosis; regulation of ubiquitin protein ligase activity; regulation of protein ubiquitination; negative regulation of cell-matrix adhesion; regulation of cell-matrix adhesion; negative regulation of epithelial to mesenchymal transition; negative regulation of cyclin-dependent protein serine/threonine kinase activity; positive regulation of ubiquitin-protein transferase activity; regulation of extrinsic apoptotic signaling pathway via death domain receptors; regulation of extrinsic apoptotic signaling pathway; protein sumoylation
CDK1	Cycline-dependent kinase 1	<b>29.6%</b> 29.6% mRNA upregulation	Golgi disassembly; histone phosphorylation; mitotic nuclear envelope disassembly; cell aging; protein localization to kinetochore; protein localization to chromosome, centromeric region; mitotic prophase; negative regulation of cell cycle process; regulation of cardiac muscle tissue growth; DNA damage response, signal transduction by p53 class mediator resulting in cell cycle arrest; peptidyl-threonine phosphorylation; negative regulation of G2/M transition of mitotic cell cycle; G2 DNA damage checkpoint; cellular response to hydrogen peroxide
TP63	Tumor protein 63	<b>29.6%</b> 18.5% Amplification 11.1% mRNA upregulation 3.7% mRNA downregulation	prostate glandular acinus development; cell aging; epithelial cell differentiation involved in prostate gland development; positive regulation of apoptotic process; positive regulation of protein insertion into mitochondrial membrane involved in apoptotic signaling pathway; negative regulation of intracellular estrogen

			receptor signaling pathway; regulation of intracellular estrogen receptor signaling pathway; intrinsic apoptotic signaling pathway in response to DNA damage; neuron apoptotic process; prostate gland epithelium morphogenesis; hair follicle morphogenesis; chromatin remodeling; regulation of cysteine-type endopeptidase activity involved in apoptotic process
CDKN2A	P16 <sup>INK4A</sup>	<b>25.9%</b> 3.7% Homozygous deletion 22.2% mRNA upregulation	amyloid fibril formation; regulation of leukocyte apoptotic process; replicative senescence; cell aging; positive regulation of apoptotic process; regulation of nucleocytoplasmic transport; negative regulation of cell cycle process; regulation of ubiquitin protein ligase activity; regulation of protein ubiquitination; negative regulation of cell-matrix adhesion; regulation of cell-matrix adhesion; negative regulation of cyclin-dependent protein serine/threonine kinase activity; cell cycle arrest; chromatin remodeling; negative regulation of cell growth; regulation of cysteine-type endopeptidase activity involved in apoptotic process
TRIM28	Transcription intermediary factor 1-beta	<b>25.9%</b> 25.9% mRNA upregulation	regulation of nucleocytoplasmic transport; positive regulation of DNA repair; positive regulation of DNA binding; protein autophosphorylation; regulation of viral genome replication
DROSHA	Ribonuclease III	<b>25.9%</b> 25.9% mRNA upregulation	primary miRNA processing; production of miRNAs involved in gene silencing by miRNA; pre-miRNA processing; miRNA metabolic process; regulation of regulatory T cell differentiation
MDM2	E3 ubiquitin protein ligase MDM2	<b>25.9%</b> 25.9% mRNA upregulation	cellular response to actinomycin D; cellular response to UV-C; response to UV; amyloid fibril formation; regulation of nucleocytoplasmic transport; negative regulation of DNA damage response, signal transduction by p53 class mediator; negative regulation of cell cycle arrest; negative regulation of cell cycle process; DNA damage response, signal transduction by p53 class mediator resulting in cell cycle arrest; negative regulation of intrinsic apoptotic signaling pathway by p53 class mediator; negative regulation of apoptotic signaling pathway; response to iron ion; cellular response to hydrogen peroxide; protein autoubiquitination; regulation of cysteine-type endopeptidase activity involved in apoptotic process

TP73	Tumor protein P73	<p><b>25.9%</b> 3.7% Homozygous deletion 22.2% mRNA upregulation</p>	<p>positive regulation of apoptotic process; positive regulation of protein insertion into mitochondrial membrane involved in apoptotic signaling pathway; intrinsic apoptotic signaling pathway in response to DNA damage; negative regulation of cardiac muscle cell proliferation; regulation of cardiac muscle tissue growth; mismatch repair; positive regulation of oligodendrocyte differentiation; cell cycle arrest</p>
LMNB1	Lamin-B1	<p><b>25.9%</b> 25.9% mRNA upregulation</p>	Not reported
BCL2L14	Apoptosis faciliator BCL-2-like protein 14	<p><b>25.9%</b> 25.9% mRNA upregulation</p>	<p>positive regulation of apoptotic process; regulation of extrinsic apoptotic signaling pathway</p>
PRMT5	Protein arginine N-methyltransferase 5	<p><b>22.2%</b> 11.1% mRNA upregulation 7.4% mRNA downregulation 3.7% mutation</p>	<p>histone H4-R3 methylation; peptidyl-arginine omega-N-methylation; positive regulation of oligodendrocyte differentiation; regulation of DNA methylation; liver regeneration</p>
MDM4	Protein MDM4	<p><b>22.2%</b> 22.2% mRNA upregulation</p>	<p>negative regulation of cell cycle arrest; negative regulation of cell cycle process; DNA damage response, signal transduction by p53 class mediator resulting in cell cycle arrest</p>
BCL2	Apoptosis regulator BCL-2	<p><b>22.2%</b> 22.2% mRNA upregulation</p>	<p>response to UV; cell aging; positive regulation of apoptotic process; positive regulation of protein insertion into mitochondrial membrane involved in apoptotic signaling pathway; intrinsic apoptotic signaling pathway in response to DNA damage; negative regulation of cell cycle process; response to UV-B; neuron apoptotic process; negative regulation of CD4-positive, alpha-beta T cell differentiation; peptidyl-threonine phosphorylation; release of cytochrome c from mitochondria; negative regulation of intrinsic apoptotic signaling pathway by p53 class mediator; negative regulation of apoptotic signaling pathway; hair follicle morphogenesis; regulation of cell-matrix adhesion; response to iron ion; negative regulation of reactive oxygen species metabolic process; regulation of extrinsic apoptotic signaling pathway; negative regulation of cell growth; regulation of viral genome replication</p>
AURKB	Aurora kinase B	<p><b>22.2%</b> 22.2% mRNA upregulation</p>	<p>response to UV; histone-serine phosphorylation; histone phosphorylation; negative regulation of B cell apoptotic process; regulation of leukocyte apoptotic process; protein localization to kinetochore; protein localization to chromosome, centromeric region; negative regulation of cell cycle process; attachment of</p>

			spindle microtubules to kinetochore; negative regulation of G2/M transition of mitotic cell cycle; regulation of chromosome separation; protein autophosphorylation
HMGB1	High mobility group protein B1	<b>22.2%</b> 22.2% mRNA upregulation	regulation of deoxyribonuclease activity; positive regulation of apoptotic process; regulation of RNA polymerase II transcriptional preinitiation complex assembly; negative regulation of CD4-positive, alpha-beta T cell differentiation; negative regulation of phagocytosis; positive chemotaxis; positive regulation of DNA repair; positive regulation of DNA binding; chromatin remodeling; lymphocyte activation involved in immune response; regulation of cysteine-type endopeptidase activity involved in apoptotic process
DDB2	DNA damage-binding protein 2	<b>22.2%</b> 22.2% mRNA upregulation	response to UV; protein autoubiquitination; nucleotide-excision repair
AGO4	Protein argonaute 4	<b>22.2%</b> 14.8% mRNA upregulation 7.4% mutation	production of miRNAs involved in gene silencing by miRNA; pre-miRNA processing; miRNA metabolic process
YY1	Transcriptional repressor protein YY1	<b>22.2%</b> 3.7% Homozygous deletion 7.4% mRNA upregulation 11.1% mRNA downregulation	response to UV; regulation of cardiac muscle tissue growth; negative regulation of cell growth
TSC2	Tuberin	<b>22.2%</b> 22.2% mRNA upregulation	negative regulation of mitophagy; negative regulation of phosphatidylinositol 3-kinase signaling; positive chemotaxis
MYB	Proliferation marker protein Ki-67	<b>22.2%</b> 18.5% mRNA upregulation 3.7% mutation	positive regulation of histone H3-K9 methylation; positive regulation of apoptotic process; positive regulation of histone H3-K4 methylation; positive regulation of transforming growth factor beta production; cellular response to hydrogen peroxide; chromatin remodeling
CSNK1G2	Casein kinase I isoform gamma-2	<b>18.5%</b> 18.5% mRNA upregulation	peptidyl-threonine phosphorylation; protein autophosphorylation
MAPKAPK2	MAP kinase-activated protein kinase 2	<b>18.5%</b> 14.8% mRNA upregulation 3.7% mRNA downregulation	protein autophosphorylation
PIN1	Peptidyl-prolyl cis-trans isomerase NIMA-interacting 1	<b>18.5%</b> 18.5% mRNA upregulation	positive regulation of apoptotic process; regulation of cell growth involved in cardiac muscle cell development; regulation of cardiac muscle tissue growth; regulation of protein ubiquitination; positive regulation of ubiquitin-protein transferase activity

CX3CL1	Fractalkine	<b>18.5%</b> 3.7% Homozygous deletion 14.8% mRNA upregulation	synapse pruning; positive regulation of transforming growth factor beta production; negative regulation of apoptotic signaling pathway; regulation of cell-matrix adhesion; positive chemotaxis; regulation of extrinsic apoptotic signaling pathway
PRMT1	Protein arginine N-methyltransferase 1	<b>18.5%</b> 18.5% mRNA upregulation	histone H4-R3 methylation; peptidyl-arginine omega-N-methylation; negative regulation of cell cycle process; DNA damage response, signal transduction by p53 class mediator resulting in cell cycle arrest
CABIN1	Calcineurin-binding protein cabin-1	<b>18.5%</b> 18.5% mRNA upregulation	Not reported
RB1	Retinoblastoma-associated protein	<b>18.5%</b> 3.7% Homozygous deletion 7.4% mRNA downregulation 14.8% mutation	protein localization to chromosome, centromeric region; mitotic prophase; negative regulation of cell cycle process: neuron apoptotic process; attachment of spindle microtubules to kinetochore; negative regulation of apoptotic signaling pathway; regulation of transcription involved in G1/S transition of mitotic cell cycle; positive regulation of DNA binding; regulation of chromosome separation; cell cycle arrest; chromatin remodeling
DYRK1A	Dual specificity tyrosine-phosphorylation-regulated kinase 1A	<b>18.5%</b> 18.5% mRNA upregulation	negative regulation of DNA damage response, signal transduction by p53 class mediator; peptidyl-threonine phosphorylation; protein autophosphorylation
CDK5	Cyclin-dependent-like kinase 5	<b>18.5%</b> 7.4% Homozygous deletion 11.1% mRNA upregulation	synapse pruning; histone phosphorylation; positive regulation of apoptotic process; regulation of nucleocytoplasmic transport; neuron apoptotic process; peptidyl-threonine phosphorylation; regulation of protein ubiquitination; protein autophosphorylation; protein sumoylation; negative regulation of cell growth
CSNK2A1	Casein kinase II subunit alfa	<b>18.5%</b> 3.7% Homozygous deletion 14.8% mRNA downregulation 3.7% mutation	peptidyl-threonine phosphorylation; negative regulation of apoptotic signaling pathway; regulation of chromosome separation; regulation of cysteine-type endopeptidase activity involved in apoptotic process
PRKAB1	5'-AMP-activated protein kinase subunit beta-1	<b>18.5%</b> 18.5% mRNA upregulation	cell cycle arrest; fatty acid biosynthetic process
VRK1	Serine/threonine-protein kinase VRK1	<b>18.5%</b> 3.7% Homozygous deletion 14.8% mRNA upregulation	Golgi disassembly; histone-serine phosphorylation; histone phosphorylation; mitotic nuclear envelope disassembly; peptidyl-threonine phosphorylation; protein autophosphorylation
MSH2	DNA mismatch repair protein MSH2	<b>18.5%</b> 18.5% mRNA upregulation	response to UV; regulation of helicase activity; intrinsic apoptotic signaling pathway in response to DNA damage; response to UV-B; mismatch repair;

			regulation of isotype switching; postreplication repair; cell cycle arrest; lymphocyte activation involved in immune response
CCNG1	Cyclin-G1	<b>18.5%</b> 18.5% mRNA upregulation	Not reported
FOXA1	Forkhead box A1	<b>18.5%</b> 3.7% Homozygous deletion 14.8% mRNA upregulation	prostate glandular acinus development; epithelial cell differentiation involved in prostate gland development; positive regulation of apoptotic process; regulation of intracellular estrogen receptor signaling pathway; prostate gland epithelium morphogenesis; negative regulation of epithelial to mesenchymal transition; chromatin remodeling

Supplemental material Table 3 (H): Gene ontology and network analysis for HPV positive TP53 in OP; “Not reported” means the reported gene was not included in any Gene ontology result.

<b>Wild-type TP53 in HP</b>			
<b>Gene</b>	<b>Protein</b>	<b>Frequency and alteration type</b>	<b>Cell function</b>
CDKN2A	P16 <sup>INK4A</sup>	<b>75.0%</b> 50.0% Homozygous deletion 25.0% mRNA upregulation	apoptotic mitochondrial changes; regulation of apoptotic DNA fragmentation; replicative senescence; regulation of DNA damage response, signal transduction by p53 class mediator; regulation of signal transduction by p53 class mediator; regulation of cell cycle G1/S phase transition; negative regulation of mitotic cell cycle; regulation of protein export from nucleus; regulation of mitochondrial membrane potential; activation of cysteine-type endopeptidase activity involved in apoptotic process; negative regulation of cell-substrate adhesion; organelle disassembly; regulation of cell-matrix adhesion; G1/S transition of mitotic cell cycle; Ras protein signal transduction; negative regulation of proteolysis
PLK3	Polo like kinase 3	<b>75.0%</b> 50.0% mRNA upregulation	positive regulation of chaperone-mediated autophagy; negative regulation of apoptotic process; regulation of signal transduction by p53 class mediator; DNA damage response, signal transduction by

		25.0% mutation	p53 class mediator resulting in cell cycle arrest; regulation of cell cycle G1/S phase transition; G1 DNA damage checkpoint; negative regulation of mitotic cell cycle; organelle disassembly; regulation of cytokinesis; G1/S transition of mitotic cell cycle
BCL2L1	BCL2 like 1	75.0% 50.0% Amplification 75.0% mRNA upregulation	apoptotic mitochondrial changes; extrinsic apoptotic signaling pathway; release of cytochrome c from mitochondria; mitochondrion morphogenesis; neuron apoptotic process; cellular response to gamma radiation; response to gamma radiation; extrinsic apoptotic signaling pathway in absence of ligand; negative regulation of extrinsic apoptotic signaling pathway in absence of ligand; negative regulation of apoptotic process; negative regulation of mitotic cell cycle; positive regulation of intrinsic apoptotic signaling pathway; intrinsic apoptotic signaling pathway in response to DNA damage; regulation of mitochondrial membrane potential; ovarian follicle development; negative regulation of autophagy; regulation of response to endoplasmic reticulum stress; regulation of cytokinesis; negative regulation of neuron apoptotic process; male gonad development; cellular response to organonitrogen compound
CX3CL1	Fractalkine	50.0% 50.0% mRNA upregulation	positive regulation of calcium-independent cell-cell adhesion; regulation of neuroblast proliferation; regulation of stem cell proliferation; negative regulation of extrinsic apoptotic signaling pathway in absence of ligand; negative regulation of apoptotic process; positive regulation of release of sequestered calcium ion into cytosol; response to ischemia; negative regulation of cell-substrate adhesion; negative regulation of neuron apoptotic process; regulation of cell-matrix adhesion; negative regulation of neurogenesis
BAX	BCL2 associated X	50.0% 50.0% mRNA upregulation	release of matrix enzymes from mitochondria; apoptotic mitochondrial changes; B cell receptor apoptotic signaling pathway; extrinsic apoptotic signaling pathway; regulation of

			<p>apoptotic DNA fragmentation; release of cytochrome c from mitochondria; positive regulation of execution phase of apoptosis; mitochondrion morphogenesis; neuron apoptotic process; regulation of mitochondrial membrane permeability involved in apoptotic process; response to gamma radiation; positive regulation of release of cytochrome c from mitochondria; extrinsic apoptotic signaling pathway in absence of ligand; intrinsic apoptotic signaling pathway in response to endoplasmic reticulum stress; negative regulation of apoptotic process; positive regulation of mitochondrial outer membrane permeabilization involved in apoptotic signaling pathway; DNA damage response, signal transduction by p53 class mediator resulting in cell cycle arrest; regulation of cell cycle G1/S phase transition; G1 DNA damage checkpoint; negative regulation of mitotic cell cycle; positive regulation of intrinsic apoptotic signaling pathway; positive regulation of release of sequestered calcium ion into cytosol; intrinsic apoptotic signaling pathway in response to DNA damage; regulation of mitochondrial membrane potential; ovarian follicle development; activation of cysteine-type endopeptidase activity involved in apoptotic process; regulation of response to endoplasmic reticulum stress; negative regulation of neuron apoptotic process; male gonad development</p>
NGFR	Nerve growth factor receptor	<p><b>50.0%</b> 50.0% mRNA upregulation</p>	<p>neuron apoptotic process; positive regulation of pri-miRNA transcription by RNA polymerase II; negative regulation of apoptotic process; activation of cysteine-type endopeptidase activity involved in apoptotic process; Ras protein signal transduction; negative regulation of neurogenesis; negative regulation of proteolysis; cellular response to organonitrogen compound</p>

Supplemental material Table 3 (I): Gene ontology and network analysis for wild-type TP53 in HP; “Not reported” means the reported gene was not included in any Gene ontology result.

<b>Mutated TP53 in HP</b>			
<b>Gene</b>	<b>Protein</b>	<b>Frequency and alteration type</b>	<b>Cell function</b>
CDKN2A	P16 <sup>INK4A</sup>	<p><b>80.0%</b></p> <p>60.0% Homozygous deletion</p> <p>20.0% mutation</p>	<p>Autophagy; replicative senescence; regulation of DNA damage response, signal transduction by p53 class mediator; regulation of signal transduction by p53 class mediator; negative regulation of protein phosphorylation; protein destabilization; apoptotic mitochondrial changes; activation of cysteine-type endopeptidase activity involved in apoptotic process; chromatin assembly; positive regulation of response to DNA damage stimulus; negative regulation of G1/S transition of mitotic cell cycle; regulation of nucleocytoplasmic transport; cell cycle arrest; negative regulation of catabolic process</p>
DDIT4	DNA damage inducible transcript 4	<p><b>60.0%</b></p> <p>60.0% mRNA upregulation</p>	<p>negative regulation of ATP metabolic process; regulation of ATP metabolic process; negative regulation of peptidyl-serine phosphorylation; negative regulation of protein phosphorylation; intrinsic apoptotic signaling pathway in response to DNA damage by p53 class mediator; regulation of glycolytic process; negative regulation of small molecule metabolic process; negative regulation of catabolic process</p>
PMS2	Mismatch repair endonuclease PMS2	<p><b>60.0%</b></p> <p>20.0% Amplification</p> <p>40.0% mRNA upregulation</p> <p>20.0% mutation</p>	DNA repair
PRKAB2	Protein kinase AMP-activated non-catalytic subunit beta 2	<p><b>60.0%</b></p> <p>20.0% Homozygous deletion</p> <p>20.0% Amplification</p>	<p>Lipophagy; autophagy; regulation of signal transduction by p53 class mediator; regulation of macroautophagy; cell cycle arrest; fatty acid biosynthetic process</p>

		20.0% mRNA upregulation	
SNAI2	Snail family transcriptional repressor 2	<p><b>60.0%</b></p> <p>40.0% Amplification</p> <p>40.0% mRNA upregulation</p>	<p>regulation of branching involved in salivary gland morphogenesis; stem cell differentiation; negative regulation of stem cell proliferation; regulation of DNA damage response, signal transduction by p53 class mediator; regulation of signal transduction by p53 class mediator; positive regulation of histone acetylation; positive regulation of chromosome organization; regulation of apoptotic signaling pathway; negative regulation of signal transduction by p53 class mediator; epithelial to mesenchymal transition; negative regulation of extrinsic apoptotic signaling pathway; negative regulation of intrinsic apoptotic signaling pathway; negative regulation of small molecule metabolic process</p>
HGF	Hepatocyte growth factor	<p><b>40.0%</b></p> <p>40.0% mRNA upregulation</p>	<p>regulation of branching involved in salivary gland morphogenesis; negative regulation of peptidyl-serine phosphorylation; negative regulation of protein phosphorylation; regulation of apoptotic signaling pathway; epithelial to mesenchymal transition; negative regulation of extrinsic apoptotic signaling pathway; regulation of DNA biosynthetic process; negative regulation of catabolic process</p>
HIF1A	Hypoxia inducible factor 1 subunit alpha	<p><b>40.0%</b></p> <p>20.0% Amplification</p> <p>20.0% mRNA upregulation</p>	<p>positive regulation of transcription from RNA polymerase II promoter in response to hypoxia; stem cell differentiation; positive regulation of autophagy of mitochondrion; regulation of ATP metabolic process; mRNA transcription; regulation of apoptotic signaling pathway; positive regulation of pri-miRNA transcription by RNA polymerase II; regulation of pri-miRNA transcription by RNA polymerase II; epithelial to mesenchymal transition; regulation of glycolytic process; negative regulation of intrinsic apoptotic signaling pathway; regulation of macroautophagy; protein deubiquitination</p>

HIRA	Histone cell cycle regulator	<b>40.0%</b> 40.0% mRNA downregulation	regulation of chromatin silencing; chromatin assembly
HIST1H1D	Histone H1.3	<b>40.0%</b> 40.0% mRNA upregulation	regulation of chromatin silencing; negative regulation of DNA metabolic process; chromatin assembly
HTT	Huntingtin	<b>40.0%</b> 40.0% mRNA downregulation	positive regulation of autophagy of mitochondrion; negative regulation of neural precursor cell proliferation; regulation of apoptotic signaling pathway; vasoconstriction; protein destabilization; negative regulation of organ growth; negative regulation of extrinsic apoptotic signaling pathway; regulation of macroautophagy; rhythmic process
CSNK2A1	Casein kinase II subunit alfa	<b>40.0%</b> 20.0% mRNA upregulation 20.0% mRNA downregulation	Autophagy; regulation of signal transduction by p53 class mediator; regulation of apoptotic signaling pathway; negative regulation of catabolic process; rhythmic process
PPP2CB	Protein phosphatase 2 catalytic subunit beta	<b>40.0%</b> 20.0% Homozygous deletion 20.0% mRNA downregulation	peptidyl-threonine dephosphorylation; apoptotic mitochondrial changes
DUSP5	Dual specificity phosphatase 5	<b>40.0%</b> 40.0% mRNA upregulation	peptidyl-threonine dephosphorylation; negative regulation of protein phosphorylation
PRKAG1	Protein kinase AMP-activated non-catalytic subunit gamma 1	<b>40.0%</b> 20.0% Homozygous deletion 20.0% mRNA upregulation 20.0% mRNA downregulation	Lipophagy; autophagy; regulation of signal transduction by p53 class mediator; regulation of ATP metabolic process; regulation of glycolytic process; regulation of macroautophagy; cell cycle arrest; fatty acid biosynthetic process

PRKDC	Protein kinase, DNA-activated, catalytic subunit	<p><b>40.0%</b></p> <p>20.0% Amplification</p> <p>20.0% mRNA upregulation</p>	B cell lineage commitment; T cell lineage commitment; negative regulation of protein phosphorylation; protein destabilization; positive regulation of response to DNA damage stimulus; negative regulation of G1/S transition of mitotic cell cycle; regulation of type I interferon production; double-strand break repair; DNA repair; rhythmic process
RRM2B	Ribonucleotide reductase regulatory TP53 inducible subunit M2B	<p><b>40.0%</b></p> <p>20.0% Amplification</p> <p>40.0% mRNA upregulation</p>	regulation of signal transduction by p53 class mediator; regulation of intrinsic apoptotic signaling pathway by p53 class mediator; regulation of apoptotic signaling pathway; negative regulation of signal transduction by p53 class mediator; negative regulation of intrinsic apoptotic signaling pathway; DNA repair
EDN2	Endothelin 2	<p><b>40.0%</b></p> <p>40.0% mRNA upregulation</p>	Vasoconstriction; fatty acid biosynthetic process
TADA2B	Transcriptional adaptor 2B	<p><b>40.0%</b></p> <p>40.0% mRNA downregulation</p>	positive regulation of histone acetylation; positive regulation of chromosome organization; protein deubiquitination
TNFRSF10B	TNF receptor superfamily member 10b	<p><b>40.0%</b></p> <p>20.0% Homozygous deletion</p> <p>20.0% mRNA upregulation</p>	regulation of apoptotic signaling pathway; intrinsic apoptotic signaling pathway in response to endoplasmic reticulum stress; negative regulation of extrinsic apoptotic signaling pathway; activation of cysteine-type endopeptidase activity involved in apoptotic process
TP53RK	TP53 regulating kinase	<p><b>40.0%</b></p> <p>40.0% mRNA upregulation</p>	regulation of signal transduction by p53 class mediator
TRIM28	Tripartite motif containing 28	<p><b>40.0%</b></p> <p>40.0% mRNA upregulation</p>	regulation of chromatin silencing; positive regulation of chromosome organization; negative regulation of DNA metabolic process; positive regulation of response to DNA damage stimulus; regulation of

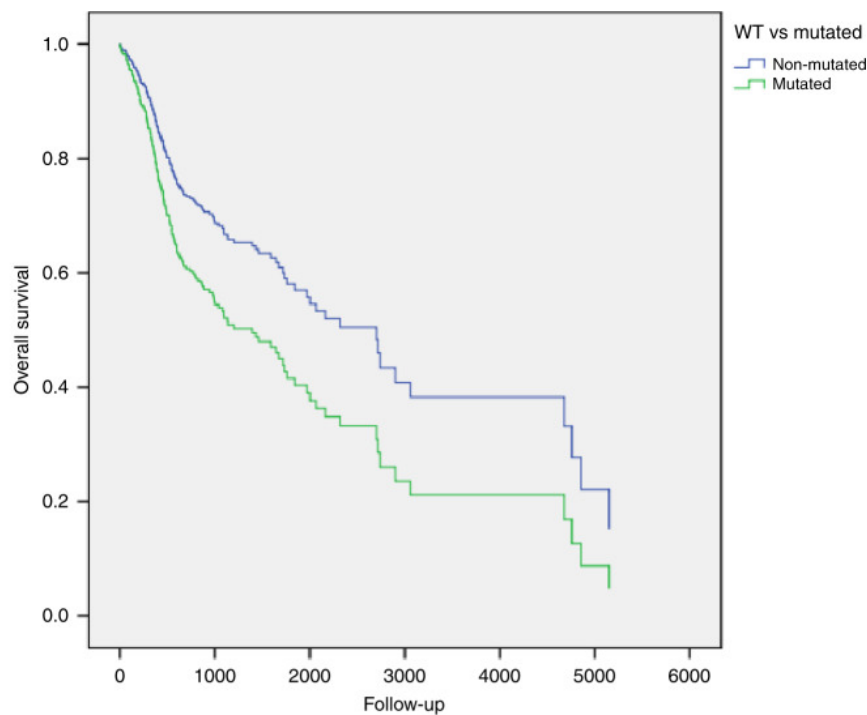
			nucleocytoplasmic transport; DNA repair
XRCC5	X-ray repair cross complementing 5	<p><b>40.0%</b></p> <p>20.0% mRNA downregulation</p> <p>20.0% mutation</p>	hematopoietic stem cell differentiation; stem cell differentiation; response to salt stress; response to X-ray; cellular response to gamma radiation; positive regulation of chromosome organization; negative regulation of DNA metabolic process; regulation of DNA biosynthetic process; regulation of type I interferon production; double-strand break repair; DNA repair
YY1	YY1 transcription factor	<p><b>40.0%</b></p> <p>20.0% mRNA upregulation</p> <p>20.0% mRNA downregulation</p>	response to UV-C; regulation of pri-miRNA transcription by RNA polymerase II; negative regulation of organ growth; regulation of type I interferon production; double-strand break repair; DNA repair; protein deubiquitination
CASP1	Caspase 1	<p><b>40.0%</b></p> <p>40.0% Amplification</p> <p>20.0% mRNA upregulation</p>	activation of cysteine-type endopeptidase activity involved in apoptotic process

Supplemental material Table 3 (J): Gene ontology and network analysis for mutated TP53 in HP. “Not reported” means the reported gene was not included in any Gene ontology result.

### 6.3 Results

*Survival analysis of TP53 mutational landscape reveals novel prognostic signatures.*

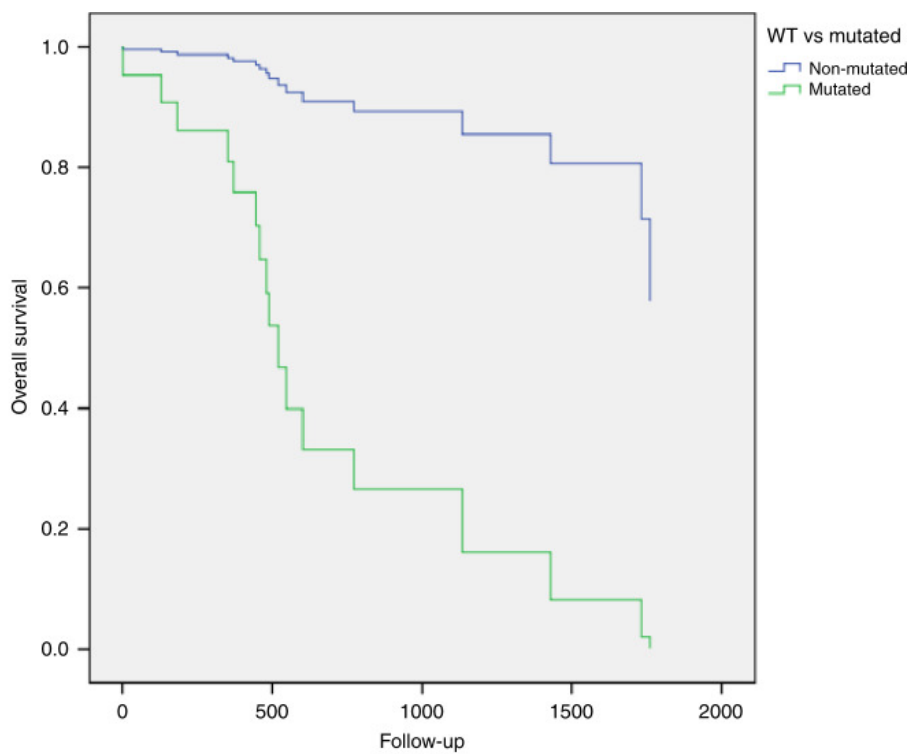
We aimed to investigate whether the presence of mutations in the TP53 gene correlated with the prognosis of HNSCC. By comparing wild-type (WT) HNSCCs with the ones with mutated TP53, univariate survival analysis showed a worse overall survival for patients carrying one mutation in TP53 gene. Multivariate Cox regression analysis confirmed that TP53 mutation was an independent prognostic factor in HNSCC patients (multivariate analysis: HR = 1.613; 95% CI: 1.119–2.325; P = 0.010) (Fig. 1).



Clinic-pathological covariates	Sig.	Hazard ratio	95% CI	
			Lower limit	Upper limit
Age	0.020	1.018	1.003	1.034
Stage	0.464	1.065	0.900	1.260
Grading	0.157	1.191	0.935	1.518
Gender	0.204	1.247	0.887	1.753
WT vs MUT	0.010	1.613	1.119	2.325

Fig. 1 Overall survival of TP53-mutated patients. Multivariate survival analysis revealed that patients with mutations (MUT) in TP53 gene sequence (green line) showed a worse survival compared to patients with wild-type (WT) TP53 (blue line).

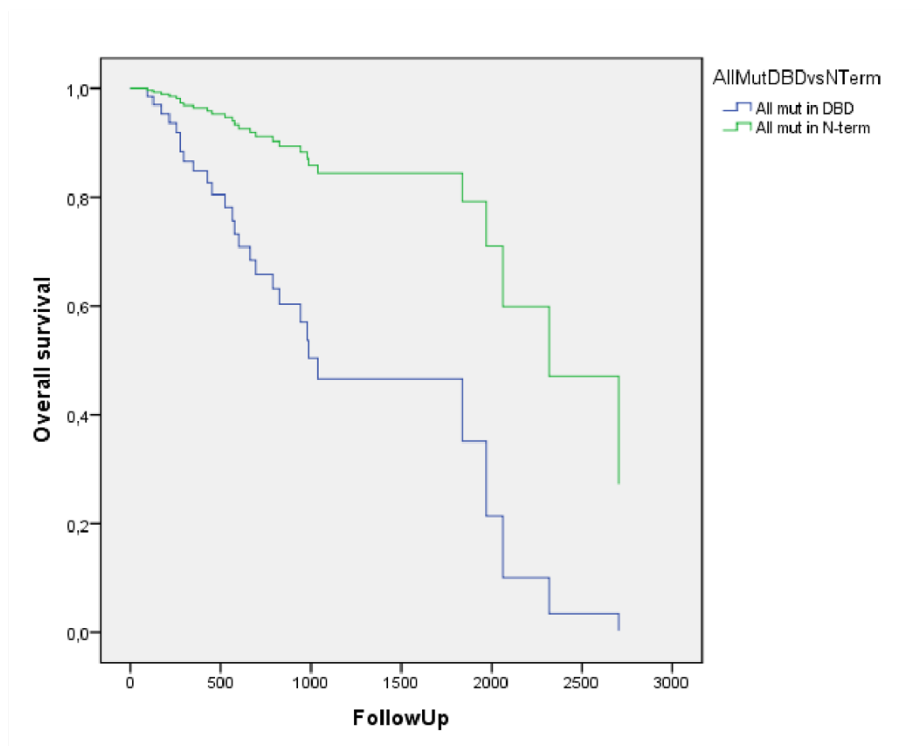
Interestingly, in the OP subgroup, the mutated profile was an independent prognostic factor of overall survival (multivariate analysis: HR = 11.657; 95% CI: 2.668–50.929; P = 0.001) (Fig. 2); meanwhile, it was close to the threshold of statistical significance for disease-free survival (multivariate analysis: HR = 5.773; 95% CI: 0.896–37.174; P = 0.065).



Clinic-pathological covariates	Sig.	Hazard ratio	95% CI	
			Lower limit	Upper limit
Age	0.801	1.008	0.951	1.068
Stage	0.632	1.145	0.659	1.988
Grading	0.228	1.989	0.651	6.074
Gender	0.172	2.190	0.712	6.736
Mutated vs WT	0.001	11.657	2.668	50.929

Fig. 2 Overall survival of patients with oropharynx squamous cell carcinoma. Multivariate survival analysis, including only oropharynx squamous cell carcinoma, revealed that subjects with mutations (MUT) in TP53 gene sequence (green line) had a worse survival compared to patients with wild-type (WT) TP53 (blue line).

Next, we investigated whether there was an association between specific characteristics of the mutation and patients' survival, as follows. Structural domains. When analysing TP53 mutations according to the predicted p53 domains affected (N-terminal, C-terminal or DNA-binding domain), no differences in survival emerged in subgroups, except larynx, where at the univariate analysis, patients with mutations in the DNA-binding domain had a worse overall survival than those with mutations in the N-terminal segment of the gene (multivariate analysis: HR = 0.223; 95% CI: 0.050–0.998; P = 0.050) (Supplementary Fig. 1).

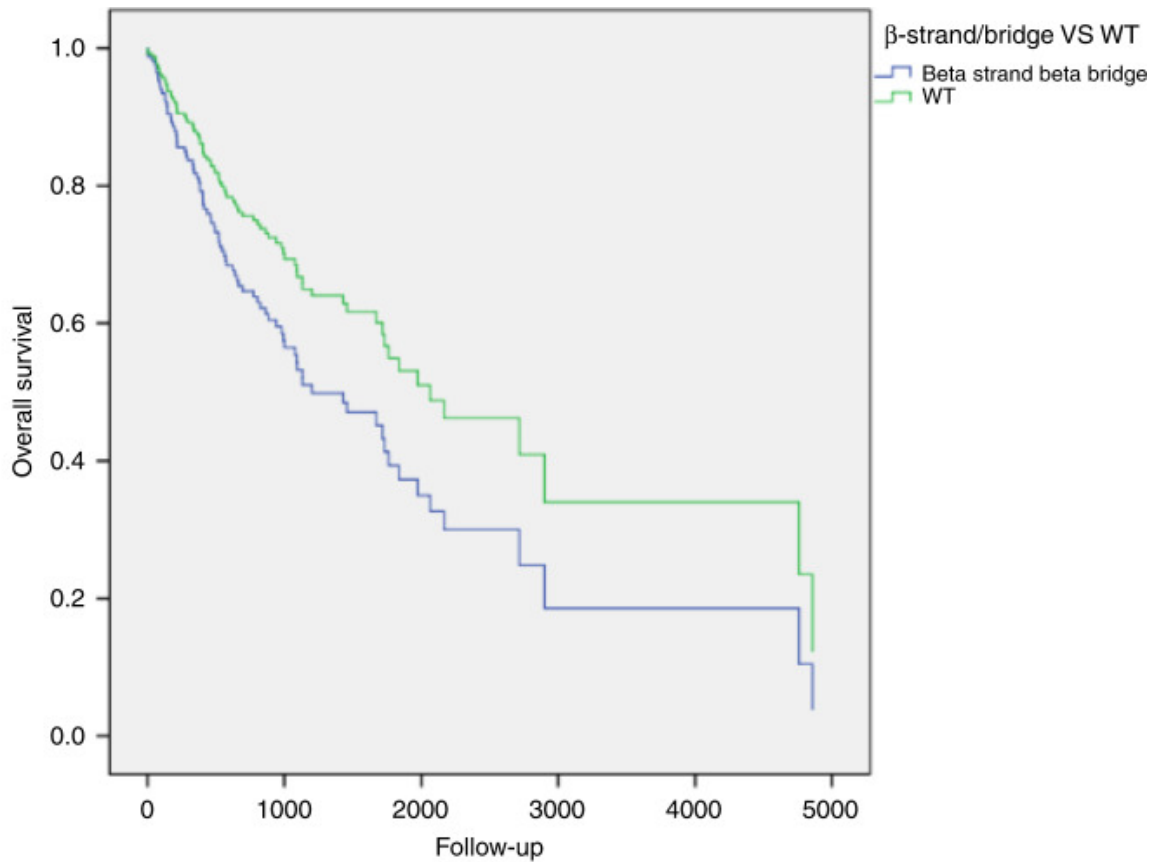


Clinic-pathological covariates	Sig.	Hazard Ratio	95% C.I.	
			Lower limit	Upper limit
Age	0,807	0,993	0,941	1,048
Stage	0,622	1,155	0,652	2,046
Grading	0,741	0,868	0,375	2,007
Gender	0,001	4,035	1,756	9,272
DBD vs N-Term	0,050	0,223	0,050	0,998

Supplemental material Figure 1: Multivariate Overall survival in larynx for TP53 mutations in DBD versus N-term.

*Secondary structure.* TP53 mutations were then analysed according to their occurrence in the predicted secondary structure of the protein. No differences in survival emerged between WT patients and those with mutations in the helix or in turn region of the protein. Patients

with mutations in a strand region had a worse overall survival, both in HNSCC (multivariate analysis: HR = 1.559; 95% CI: 1.007–2.413; P = 0.046) (Fig. 3) and larynx (multivariate analysis: HR 0.071; 95% CI: 0.005–0.935; P = 0.044) subgroups, compared with WT.

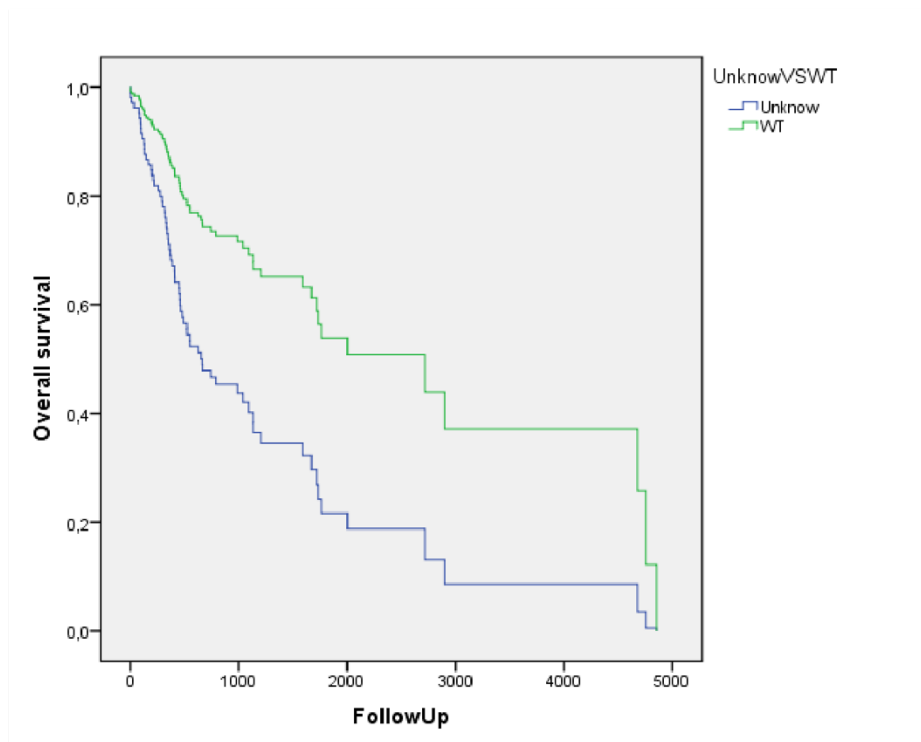


Clinic-pathological covariates	Sig.	Hazard ratio	95% C.I.	
			Lower limit	Upper limit
Age	0.215	1.014	0.992	1.036
Stage	0.730	1.043	0.822	1.323
Grading	0.723	1.061	0.765	1.471
Gender	0.481	1.189	0.735	1.923
$\beta$ -strand/bridge VS WT	0.046	1.559	1.007	2.413

Fig. 3 Overall survival of patients with TP53 mutations in  $\beta$ -strand/bridge. Multivariate survival analysis in head and neck squamous cell carcinoma, showing that patients with mutations in  $\beta$ -strand/bridge of p53 secondary structure (blue line) have a worse survival compared to patients with wild-type (WT) TP53 gene (green line).

Poor overall survival was also detected for patients with mutations in unknown regions. In particular, patients in HNSCC (multivariate analysis: HR = 2.476; 95% CI: 1.525–4.019; P

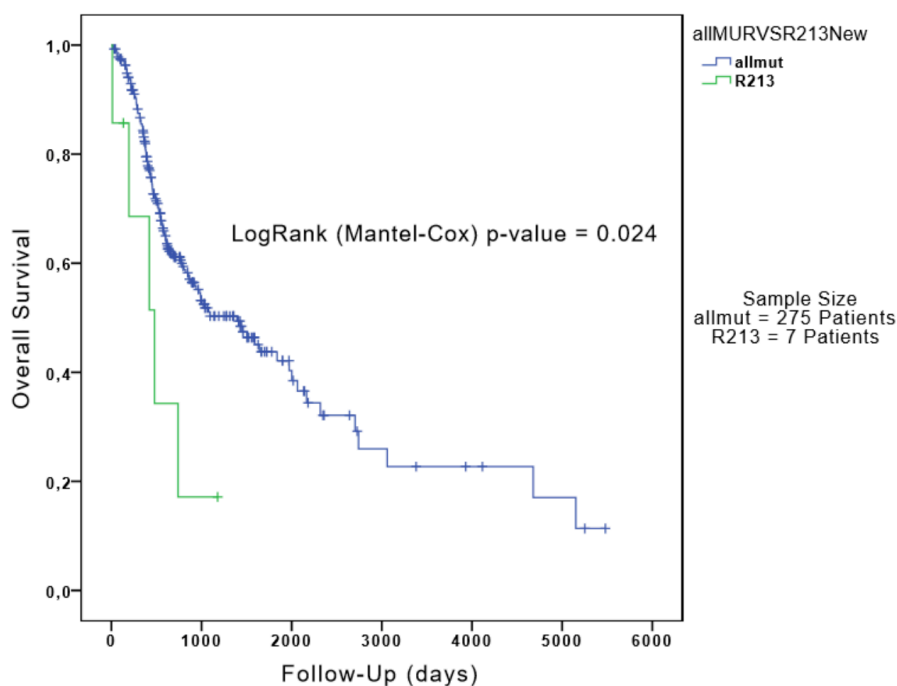
< 0.001) (Supplementary Fig. 2), OP (multivariate analysis: HR = 0.072; 95% CI: 0.011–0.490; P = 0.007) and L (univariate analysis: HR = 0.133; 95% CI: 0.03–0.598; P = 0.008) subgroups had a worse overall survival compared with the WT group.



Clinic-pathological covariates	Sig.	Hazard Ratio	95% C.I.	
			Lower limit	Upper limit
Age	0,086	1,021	0,997	1,046
Stage	0,659	1,061	0,815	1,383
Grading	0,563	1,120	0,764	1,641
Gender	0,500	0,832	0,487	1,421
Unknown vs WT	0,000	2,476	1,525	4,019

Supplemental material Figure 2: Multivariate Overall survival in HNSCC for TP53 mutations in unknown secondary structure versus wild-type.

*Hotspot mutations.* Survival analysis was also performed in order to investigate whether particular hotspot mutations could influence patients' prognosis. Specifically, the comparison was performed between hotspot mutations and non-hotspot residues. Mutations affecting the residue R175 were associated with a worse overall survival in HNSCC (multivariate analysis: HR = 6.855; 95% CI: 1.635–28.75; P = 0.008) compared with the non-hotspot group. The same result emerged from the analysis of the residue H193 (multivariate analysis: HR = 3.578; 95% CI: 1.380–9.277; P = 0.009). Finally, R213 was linked to poor overall survival in HNSCC (univariate analysis: P = 0.024) (Supplementary Fig. 3).



Supplemental material Figure 3: Univariate analysis for overall survival according to R213 MUT.

Although the results from this analysis could be clinically relevant, it should be noted that the small sample size available for this cohort bears high risk of bias; therefore, the results should be further validated in larger sample size. Type of mutation. Differences in mutation type (frameshift, missense, inframe, splice site and stop) showed variable prognostic

capabilities. In particular, missense (multivariate analysis: HR = 1.688; 95% CI: 1.129–2.526; P = 0.011) and stop (multivariate analysis: HR = 2.016; 95% CI: 1.220–3.332; P = 0.006) mutations were predictive of worse overall survival compared with WT patients in HNSCC. Variant-allele frequency. In the last analysis, HNSCC patients with higher VAF, such as those carrying the mutation in homozygous loci, reported a worse overall survival (multivariate analysis: HR = 1.747; 95% CI: 1.055–2.891; P = 0.030) and higher risk of relapse (multivariate analysis: HR = 2.421; 95% CI: 1.168–5.020; P = 0.017) compared with patients with lower VAF (i.e. mutations in heterozygous loci) (Fig. 4).

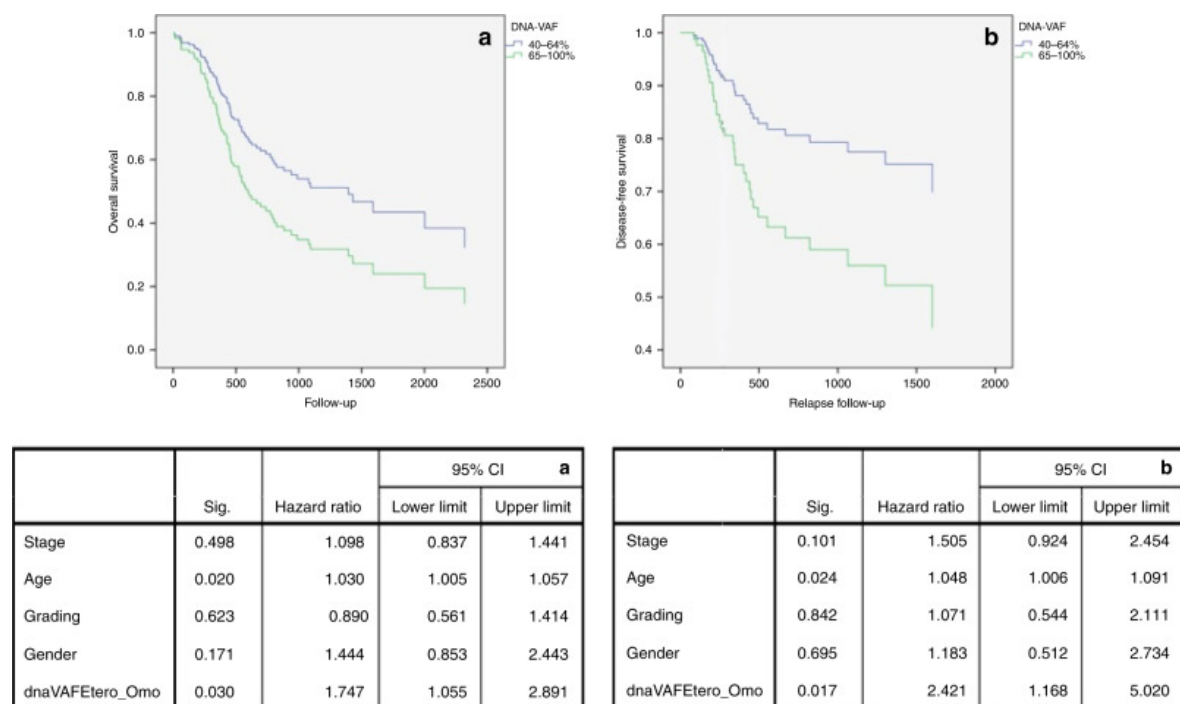


Fig. 4 Overall and Relapse-free survival according to DNA-VAF. Multivariate survival analysis for patients with head and neck squamous cell carcinoma, showing that subjects with homozygous mutations in TP53 gene sequence (green line) showed a worse overall (a) and relapse free (b) -survival, compared to patients with heterozygous mutations (blue line).

Differential mRNA expression did not influence the overall survival in HNSCC and its subgroups. Finally, because cancers arising in lung and esophagus share common histopathological characteristics with HNSCC, we compared available datasets for these groups of carcinomas. Surprisingly, the results failed to show an association between p53 mutations and prognosis. In particular, in lung squamous cell cancer, patients with wild-type TP53 had worse overall survival compared with patients with mutated p53 (multivariate

analysis: HR = 0.636; 95% CI: 0.437–0.926; P = 0.018). The results are summarised in Supplementary Table 2. Taken together, these data demonstrate that TP53 mutations are not only predictors of patient survival but, also, that different types of mutations have distinct prognostic significance in HNSCC.

Variable	Subsite	Univariate Overall Survival	Multivariate Overall Survival	Univariate Disease-Free Survival	Multivariate Disease-Free Survival
Wild-type TP53 vs Mutated	<b>Head and Neck</b>	HR = 1,586; p = 0,009	HR = 1,525; p = 0,026	HR = 1,132; p = 0,641	HR = 1,195; p = 0,535
	<b>Oral</b>	HR = 1,107; p = 0,638	HR = 1,171; p = 0,475	HR = 0,856; p = 0,632	HR = 0,844; p = 0,611
	<b>Oropharynx</b>	HR = 6,669; p = 0,001	HR = 11,657; p = 0,001	HR = 4,441; p = 0,037	HR = 5,773; p = 0,065
	<b>Hypopharynx</b>	HR = 1,691; p = 0,669	HR = 1,200; p = 0,914	HR = 1,266; p = 0,848	HR = 1,395; p = 0,801
	<b>Larynx</b>	HR = 1,669; p = 0,124	HR = 3,639; p = 0,108	HR = 1,032; p = 0,968	HR = 0,585; p = 0,638
	<b>Oesophagus</b>	HR = 1,183; p = 0,658	HR = 1,452; p = 0,660	HR = 0,835; p = 0,805	HR = 0,468; p = 0,362
	<b>Lung</b>	HR = 0,655; p = 0,026	HR = 0,636; p = 0,018	HR = 1,012; p = 0,975	HR = 0,994; p = 0,988
Low vs high mRNA expression	<b>Head and Neck</b>	HR = 0,966; p = 0,820	HR = 1,091; p = 0,581	HR = 0,918; p = 0,715	HR = 1,115; p = 0,651
	<b>Oral</b>	HR = 1,056; p = 0,774	HR = 1,038; p = 0,847	HR = 1,208; p = 0,513	HR = 1,302; p = 0,273
	<b>Oropharynx</b>	HR = 0,41; p = 0,002	HR = 0,001; p = 0,909	HR = 0,278; p = 0,112	HR = 0,210; p = 0,149

	<b>Hypopharynx</b>	HR = 2,377; p = 0,480	HR = 2,344; p = 0,691	HR = 1,818; p = 0,629	HR = 4,316; p = 0,563
	<b>Larinx</b>	HR = 1,669; p = 0,124	<b>HR = 2,142; p = 0,063</b>	HR = 1,041; p = 0,942	HR = 2,569; p = 0,164
	<b>Oesophagus</b>	HR = 0,612; p = 0,338	HR = 0,917; p = 0,886	HR = 0,912; p = 0,849	HR = 1,152; p = 0,783
	<b>Lung</b>	HR = 0,897; p = 0,459	HR = 0,941; p = 0,685	HR = 0,941; p = 0,820	HR = 1,014; p = 0,960
DNA-VAF	<b>Head and Neck</b>	<b>HR = 1,677; p = 0,031</b>	<b>HR = 1,747; p = 0,030</b>	<b>HR = 2,079; p = 0,042</b>	<b>HR = 2,421; p = 0,017</b>
	<b>Oral</b>	HR = 1,652; p = 0,143	HR = 1,469; p = 0,285	HR = 1,933; p = 0,201	<b>HR = 2,844; p = 0,061</b>
	<b>Oropharynx</b>	<b>HR = 14,065; p = 0,025</b>	<b>HR = 111,994; p = 0,023</b>	N/A	N/A
	<b>Hypopharynx</b>	N/A	N/A	N/A	N/A
	<b>Larinx</b>	HR = 1,931; p = 0,136	<b>HR = 2,660; p = 0,056</b>	HR = 3,227; p = 0,155	HR = 0,479; p = 2,637
	<b>Oesophagus</b>	HR = 1,669; p = 0,294	HR = 0,613; p = 0,514	HR = 0,580; p = 0,253	HR = 0,739; p = 0,606

	<i>Lung</i>	HR = 1,250; p = 0,317	HR = 1,359; p = 0,176	HR = 1,406; p = 0,321	HR = 1,558; p = 0,204
Mutated in Zinc ligand vs mutated in other region	<i>Head and Neck</i>	HR = 1,044; p = 0,913	HR = 0,899; p = 0,786	HR = 0,466; p = 0,078	HR = 0,505; p = 0,205
	<i>Oral</i>	HR = 1,654; p = 0,398	HR = 1,024; p = 0,968	HR = 0,436; p = 0,086	HR = 0,487; p = 0,248
	<i>Oropharynx</i>	N/A	N/A	N/A	N/A
	<i>Hypopharynx</i>	N/A	N/A	N/A	N/A
	<i>Larynx</i>	HR = 0,624; p = 0,440	HR = 0,796; p = 0,721	N/A	N/A
	<i>Oesophagus</i>	HR = 0,595; p = 0,393	HR = 0,774; p = 0,810	<b>HR = 0,313; p = 0,070</b>	HR = 0,357; p = 0,122
	<i>Lung</i>	HR = 0,834; p = 0,562	HR = 0,919; p = 0,791	HR = 0,700; p = 0,550	HR = 0,930; p = 0,907
	Mutated in Zinc ligand vs WT	<i>Head and Neck</i>	HR = 0,637; p = 0,275	HR = 0,496; p = 0,118	HR = 0,394; p = 0,052
<i>Oral</i>		HR = 1,393; p = 0,587	HR = 0,959; p = 0,947	HR = 0,491; p = 0,188	HR = 0,504; p = 0,336

	<b>Oropharynx</b>	N/A	N/A	N/A	N/A
	<b>Hypopharynx</b>	N/A	N/A	N/A	N/A
	<b>Larynx</b>	HR = 0,198; p = 0,080	HR = 0,009; p = 0,168	N/A	N/A
	<b>Oesophagus</b>	HR = 0,757; p = 0,691	N/A	HR = 0,422; p = 0,356	N/A
	<b>Lung</b>	HR = 1,291; p = 0,464	HR = 1,572; p = 0,209	HR = 0,722; p = 0,634	HR = 1,212; p = 0,798
$\alpha$ -Helix vs Wild Type	<b>Head and Neck</b>	HR = 0,816; p = 0,418	HR = 0,775; p = 0,422	HR = 0,789; p = 0,533	HR = 0,976; p = 0,956
	<b>Oral</b>	HR = 1,160; p = 0,677	HR = 1,031; p = 0,937	HR = 1,131; p = 0,804	HR = 1,243; p = 0,722
	<b>Oropharynx</b>	<b>HR = 0,178; p = 0,047</b>	HR = 0,256; p = 0,185	HR = 0,067; p = 0,059	HR = 0,005; p = 0,117
	<b>Hypopharynx</b>	N/A	N/A	N/A	N/A
	<b>Larynx</b>	HR = 0,397; p = 0,245	HR = 0,682; p = 0,746	HR = 0,786; p = 0,794	HR = 0,725; p = 0,818

	<b>Oesophagus</b>	HR = 0,820; p = 0,713	HR = 3,480; p = 0,564	HR = 2,992; p = 0,371	N/A
	<b>Lung</b>	<b>HR = 1,830; p = 0,053</b>	<b>HR = 1,830; p = 0,055</b>	HR = 1,089; p = 0,871	HR = 1,151; p = 0,789
$\alpha$ -Helix vs Turn;bend	<b>Head and Neck</b>	HR = 0,990; p = 0,977	HR = 1,233; p = 0,595	HR = 0,871; p = 0,754	HR = 1,104; p = 0,843
	<b>Oral</b>	HR = 1,028; p = 0,950	HR = 1,141; p = 0,804	HR = 0,841; p = 0,764	HR = 0,945; p = 0,942
	<b>Oropharynx</b>	HR = 0,474; p = 0,546	HR = 0,226; p = 0,899	HR = 1,618; p = 0,697	N/A
	<b>Hypopharynx</b>	N/A	N/A	N/A	N/A
	<b>Larinx</b>	HR = 1,438; p = 0,658	HR = 2,620; p = 0,358	N/A	N/A
	<b>Oesophagus</b>	HR = 1,139; p = 0,803	HR = 1,185; p = 0,860	HR = 2,043; p = 0,523	HR = 2,189; p = 0,501
	<b>Lung</b>	HR = 1,275; p = 0,446	HR = 1,345; p = 0,357	HR = 1,290; p = 0,608	HR = 1,497; p = 0,421
$\alpha$ -Helix vs Unknow	<b>Head and Neck</b>	<b>HR = 1,930; p = 0,026</b>	HR = 1,660; p = 0,130	HR = 0,978; p = 0,957	HR = 1,119; p = 0,808

	<b>Oral</b>	HR = 1,495; p = 0,296	HR = 1,273; p = 0,572	HR = 0,788; p = 0,694	HR = 0,763; p = 0,727
	<b>Oropharynx</b>	HR = 1,007; p = 0,994	N/A	HR = 0,283; p = 0,379	N/A
	<b>Hypopharynx</b>	N/A	N/A	N/A	N/A
	<b>Larynx</b>	<b>HR = 3,856; p = 0,036</b>	HR = 3,233; p = 0,138	HR = 1,578; p = 0,553	HR = 1,800; p = 0,494
	<b>Oesophagus</b>	HR = 1,153; p = 0,769	HR = 1,263; p = 0,778	HR = 4,630; p = 0,158	HR = 4,834; p = 0,199
	<b>Lung</b>	HR = 1,777; p = 0,071	<b>HR = 2,124; p = 0,024</b>	HR = 0,764; p = 0,649	HR = 0,888; p = 0,844
$\alpha$ -Helix vs $\beta$ -Strand;bridge	<b>Head and Neck</b>	HR = 1,248; p = 0,439	HR = 1,111; p = 0,726	HR = 0,719; p = 0,389	HR = 0,821; p = 0,645
	<b>Oral</b>	HR = 1,314; p = 0,439	HR = 1,108; p = 0,788	HR = 0,916; p = 0,860	HR = 1,059; p = 0,925
	<b>Oropharynx</b>	HR = 0,010; p = 0,440	HR = 0,001; p = 0,403	HR = 0,703; p = 0,775	N/A
	<b>Hypopharynx</b>	N/A	N/A	N/A	N/A

	<i>Larinx</i>	HR = 1,619; p = 0,464	HR = 1,961; p = 0,461	HR = 0,419; p = 0,292	HR = 0,914; p = 0,920
	<i>Oesophagus</i>	HR = 0,757; p = 0,563	HR = 0,626; p = 0,567	HR = 4,061; p = 0,192	HR = 2,646; p = 0,433
	<i>Lung</i>	HR = 1,164; p = 0,565	HR = 1,161; p = 0,619	HR = 1,007; p = 0,988	HR = 1,108; p = 0,825
β-Strand;bridge vs Wild Type	<i>Head and Neck</i>	<b>HR = 0,632; p = 0,032</b>	<b>HR = 0,641; p = 0,046</b>	HR = 1,020; p = 0,952	HR = 0,963; p = 0,916
	<i>Oral</i>	HR = 0,855; p = 0,543	HR = 0,893; p = 0,663	HR = 1,177; p = 0,680	HR = 1,174; p = 0,690
	<i>Oropharynx</i>	<b>HR = 0,226; p = 0,044</b>	HR = 0,701; p = 0,753	HR = 0,297; p = 0,197	HR = 0,213; p = 0,276
	<i>Hypopharynx</i>	N/A	N/A	N/A	N/A
	<i>Larinx</i>	<b>HR = 0,184; p = 0,037</b>	<b>HR = 0,071; p = 0,044</b>	HR = 1,217; p = 0,833	HR = 1,129; p = 0,935
	<i>Oesophagus</i>	HR = 1,032; p = 0,943	HR = 0,944; p = 0,966	HR = 0,835; p = 0,824	HR = 1,688; p = 0,593
	<i>Lung</i>	HR = 1,641; p = 0,026	<b>HR = 1,721; p = 0,022</b>	HR = 1,112; p = 0,807	HR = 1,049; p = 0,913

β-Strand;bridge vs Turn;bend	<b>Head and Neck</b>	HR = 0,751; p = 0,325	HR = 0,908; p = 0,751	HR = 1,141; p = 0,738	HR = 0,984; p = 0,969
	<b>Oral</b>	HR = 0,685; p = 0,281	HR = 0,751; p = 0,439	HR = 0,917; p = 0,860	HR = 0,704; p = 0,486
	<b>Oropharynx</b>	HR = 2,399; p = 0,388	N/A	HR = 4,215; p = 0,244	N/A
	<b>Hypopharynx</b>	N/A	N/A	N/A	N/A
	<b>Larynx</b>	HR = 1,090; p = 0,897	HR = 1,541; p = 0,552	HR = 0,848; p = 0,887	HR = 2,205; p = 0,594
	<b>Oesophagus</b>	HR = 1,548; p = 0,287	HR = 2,930; p = 0,240	HR = 0,743; p = 0,649	HR = 1,042; p = 0,955
	<b>Lung</b>	HR = 1,047; p = 0,843	HR = 1,019; p = 0,936	HR = 1,275; p = 0,548	HR = 1,222; p = 0,638
β-Strand;bridge vs Unknow	<b>Head and Neck</b>	<b>HR = 1,651; p = 0,023</b>	HR = 1,566; p = 0,064	HR = 1,297; p = 0,487	HR = 1,203; p = 0,646
	<b>Oral</b>	HR = 1,169; p = 0,597	HR = 1,239; p = 0,490	HR = 0,873; p = 0,797	HR = 0,690; p = 0,504
	<b>Oropharynx</b>	HR = 4,288; p = 0,216	N/A	N/A	N/A

	<b>Hypopharynx</b>	N/A	N/A	N/A	N/A
	<b>Larynx</b>	<b>HR = 3,167; p = 0,011</b>	HR = 1,689; p = 0,363	HR = 3,491; p = 0,104	HR = 2,659; p = 0,281
	<b>Oesophagus</b>	HR = 1,694; p = 0,147	<b>HR = 11,811; p = 0,019</b>	HR = 1,043; p = 0,941	HR = 1,371; p = 0,647
	<b>Lung</b>	HR = 1,520; p = 0,068	<b>HR = 1,638; p = 0,40</b>	HR = 0,901; p = 0,840	HR = 0,756; p = 0,609
Turn;bend vs Wild Type	<b>Head and Neck</b>	HR = 0,800; p = 0,456	HR = 0,753; p = 0,376	HR = 0,863; p = 0,709	HR = 0,935; p = 0,876
	<b>Oral</b>	HR = 1,148; p = 0,701	HR = 1,047; p = 0,903	HR = 1,197; p = 0,720	HR = 1,076; p = 0,886
	<b>Oropharynx</b>	<b>HR = 0,155; p = 0,032</b>	<b>HR = 0,079; p = 0,029</b>	<b>HR = 0,031; p = 0,005</b>	HR = 0,001; p = 0,075
	<b>Hypopharynx</b>	N/A	N/A	N/A	N/A
	<b>Larynx</b>	N/A	N/A	N/A	N/A
	<b>Oesophagus</b>	HR = 0,760; p = 0,576	HR = 5,900; p = 0,348	HR = 1,762; p = 0,517	HR = 1,853; p = 0,590

	<b>Lung</b>	HR =1,529; p =0,095	HR =1,577; p =0,077	HR =0,849; p =0,731	HR =0,935; p =0,893
Turn;bend vs Unknow	<b>Head and Neck</b>	<b>HR = 2,062; p = 0,016</b>	HR = 1,622; p = 0,127	HR = 1,067; p = 0,881	HR = 1,196; p = 0,709
	<b>Oral</b>	HR = 1,486; p = 0,308	HR = 1,343; p = 0,477	HR = 0,880; p = 0,834	HR = 1,034; p = 0,959
	<b>Oropharynx</b>	HR = 1,510; p = 0,662	N/A	HR = 0,134 p = 0,104	N/A
	<b>Hypopharynx</b>	N/A	N/A	N/A	N/A
	<b>Larinx</b>	HR =0,361; p =0,266	HR =0,001; p =0,959	HR = 0,845; p = 0,906	HR = 0,00; p = 0,440
	<b>Oesophagus</b>	HR = 1,204; p = 0,665	HR = 1,004; p = 0,996	HR = 1,708; p = 0,428	HR = 1,974; p = 0,333
	<b>Lung</b>	HR = 1,384; p =0,210	<b>HR = 1,680; p = 0,051</b>	HR = 0,698; p = 0,513	HR = 0,764; p = 0,629
	Unknow vs Wild Type	<b>Head and Neck</b>	<b>HR = 0,040; p = 0,000</b>	<b>HR = 0,404; p = 0,000</b>	HR = 0,793; p = 0,532
<b>Oral</b>		HR = 0,704; p = 0,250	HR = 0,711; p = 0,291	HR = 1,410; p = 0,515	HR = 1,610; p = 0,399

	<b>Oropharynx</b>	HR = 0,174; p = 0,023	HR = 0,072; p = 0,007	HR = 0,405; p = 0,467	HR = 0,123; p = 0,251
	<b>Hypopharynx</b>	HR = 0,270; p = 0,292	HR = 0,00; p = 0,965	HR = 0,342; p = 0,385	HR = 0,000; p = 0,291
	<b>Larinx</b>	HR = 0,133; p = 0,008	HR = 0,143; p = 0,092	HR = 0,313; p = 0,303	HR = 0,124; p = 0,262
	<b>Oesophagus</b>	HR = 0,698; p = 0,412	HR = 0,050; p = 0,058	HR = 0,684; p = 0,644	HR = 3,030; p = 0,596
	<b>Lung</b>	HR = 1,121; p = 0,647	HR = 1,055; p = 0,834	HR = 1,334; p = 0,614	HR = 1,553; p = 0,461
R273 in C vs H	<b>Head and Neck</b>	HR = 0,182; p = 0,056	HR = 0,254; p = 0,336	HR = 0,080; p = 0,028	HR = 0,056; p = 0,049
	<b>Oral</b>	HR = 0,280; p = 0,171	HR = 0,458; p = 0,541	HR = 0,112; p = 0,056	HR = 0,060; p = 0,076
	<b>Oropharynx</b>	N/A	N/A	N/A	N/A
	<b>Hypopharynx</b>	N/A	N/A	N/A	N/A
	<b>Larinx</b>	N/A	N/A	N/A	N/A

	<b>Oesophagus</b>	HR = 1,803; p = 0,615	N/A	N/A	N/A
	<b>Lung</b>	N/A	N/A	N/A	N/A
R248 in Q vs W	<b>Head and Neck</b>	HR = 2,049; p = 0,409	HR = 1,994; p = 0,662	HR = 0,434; p = 0,498	HR = 0,001; p = 0,611
	<b>Oral</b>	HR = 3,236; p = 0,301	HR = 10,773; p = 0,503	HR = 65,289; p = 0,610	N/A
	<b>Oropharynx</b>	N/A	N/A	N/A	N/A
	<b>Hypopharynx</b>	N/A	N/A	N/A	N/A
	<b>Larynx</b>	N/A	N/A	N/A	N/A
	<b>Oesophagus</b>	N/A	N/A	N/A	N/A
	<b>Lung</b>	N/A	N/A	N/A	N/A
Mutations in N-Term vs C-Term	<b>Head and Neck</b>	HR = 1,792; p = 0,197	HR = 2,171; p = 0,105	HR = 1,839; p = 0,448	HR = 0,827; p = 0,838

	<b>Oral</b>	HR = 1,200; p = 0,743	HR = 1,147; p = 0,816	HR = 1,014; p = 0,988	HR = 0,639; p = 0,687
	<b>Oropharynx</b>	N/A	N/A	N/A	N/A
	<b>Hypopharynx</b>	N/A	N/A	N/A	N/A
	<b>Larynx</b>	HR = 2,439; p = 0,307	HR = 2,439; p = 0,307	N/A	N/A
	<b>Oesophagus</b>	HR = 1,200; p = 0,743	N/A	N/A	N/A
	<b>Lung</b>	HR = 0,956; p = 0,919	HR = 1,134; p = 0,784	HR = 1,300; p = 0,711	HR = 1,023; p = 0,977
Mutations in DBD vs N-Term	<b>Head and Neck</b>	HR = 0,618; p = 0,195	HR = 0,781; p = 0,523	HR = 0,587; p = 0,460	HR = 0,758; p = 0,389
	<b>Oral</b>	HR = 0,985; p = 0,972	HR = 1,134; p = 0,781	HR = 0,911; p = 0,898	HR = 0,987; p = 0,986
	<b>Oropharynx</b>	N/A	N/A	N/A	N/A

	<b>Hypopharynx</b>	N/A	N/A	N/A	N/A
	<b>Larinx</b>	HR = 0,233; p = 0,054	HR = 0,223; p = 0,050	HR = 0,042; p = 0,489	N/A
	<b>Oesophagus</b>	HR = 1,388; p = 0,583	N/A	N/A	N/A
	<b>Lung</b>	HR = 1,151; p = 0,657	HR = 1,091; p = 0,785	HR = 1,199; p = 0,734	HR = 1,192; p = 0,742
Mutations in DBD vs C-Term	<b>Head and Neck</b>	HR = 1,087; p = 0,744	HR = 1,142; p = 0,610	HR = 1,148; p = 0,734	HR = 1,218; p = 0,638
	<b>Oral</b>	HR = 1,122; p = 0,734	HR = 1,293; p = 0,461	HR = 1,064; p = 0,908	HR = 1,368; p = 0,565
	<b>Oropharynx</b>	HR = 1,865; p = 0,339	HR = 1,516; p = 0,632	N/A	N/A
	<b>Hypopharynx</b>	N/A	N/A	N/A	N/A
	<b>Larinx</b>	HR = 0,659; p = 0,443	HR = 0,818; p = 0,714	HR = 0,566; p = 0,587	HR = 0,319; p = 0,287
	<b>Oesophagus</b>	HR = 0,511; p = 0,261	HR = 0,064; p = 0,027	HR = 0,390; p = 0,360	N/A

	<b>Lung</b>	HR = 1,042; p = 0,902	HR = 1,083; p = 0,821	HR = 1,526; p = 0,429	HR = 1,354; p = 0,621
G245 vs other mutations	<b>Head and Neck</b>	HR = 0,231; p = 0,145	HR = 0,300; p = 0,233	HR = 0,047; p = 0,329	HR = 0,00; p = 0,970
	<b>Oral</b>	N/A	N/A	N/A	N/A
	<b>Oropharynx</b>	N/A	N/A	N/A	N/A
	<b>Hypopharynx</b>	N/A	N/A	N/A	N/A
	<b>Larynx</b>	HR = 0,583; p = 0,596	HR = 1,367; p = 0,767	N/A	N/A
	<b>Oesophagus</b>	HR = 0,386; p = 0,195	N/A	N/A	N/A
	<b>Lung</b>	HR = 1,235; p = 0,678	HR = 1,383; p = 0,531	HR = 0,728; p = 0,662	HR = 0,705; p = 0,636
	R248 vs other mutations	<b>Head and Neck</b>	HR = 1,070; p = 0,873	HR = 1,156; p = 0,730	HR = 0,620; p = 0,421
<b>Oral</b>		HR = 1,150; p = 0,785	HR = 1,096; p = 0,859	HR = 1,628; p = 0,631	HR = 1,893; p = 0,535

	<b>Oropharynx</b>	HR = 0,502; p = 0,391	HR = 0,924; p = 0,935	HR = 0,407; p = 0,422	HR = 0,105; p = 0,323
	<b>Hypopharynx</b>	N/A	N/A	N/A	N/A
	<b>Larynx</b>	N/A	N/A	N/A	N/A
	<b>Oesophagus</b>	HR = 0,653; p = 0,557	HR = 0,270; p = 0,253	HR = 0,649; p = 0,681	HR = 0,330; p = 0,316
	<b>Lung</b>	HR = 0,596; p = 0,310	HR = 0,676; p = 0,443	<b>HR = 0,152; p = 0,011</b>	<b>HR = 0,109 p = 0,005</b>
R282 vs other mutations	<b>Head and Neck</b>	HR = 0,269; p = 0,191	HR = 0,218; p = 0,131	HR = 0,649; p = 0,669	HR = 0,501; p = 0,502
	<b>Oral</b>	HR = 2,390; p = 0,785	HR = 2,857; p = 0,301	HR = 1,019; p = 0,985	HR = 1,164; p = 0,885
	<b>Oropharynx</b>	N/A	N/A	N/A	N/A
	<b>Hypopharynx</b>	N/A	N/A	N/A	N/A
	<b>Larynx</b>	HR = 0,047; p = 0,515	N/A	N/A	N/A

	<b>Oesophagus</b>	HR = 0,553; p = 0,324	<b>HR = 0,089; p = 0,049</b>	N/A	N/A
	<b>Lung</b>	HR = 0,871; p = 0,813	HR = 0,972; p = 0,961	HR = 0,942; p = 0,953	HR = 1,010; p = 0,993
R175 vs other mutations	<b>Head and Neck</b>	<b>HR = 0,228; p = 0,004</b>	<b>HR = 0,146; p = 0,008</b>	HR = 20,346; p = 0,758	HR = 11318,19; p = 0,980
	<b>Oral</b>	HR = 0,381; p = 0,180	HR = 5,814; p = 0,089	N/A	N/A
	<b>Oropharynx</b>	N/A	N/A	N/A	N/A
	<b>Hypopharynx</b>	N/A	N/A	N/A	N/A
	<b>Larynx</b>	<b>HR = 0,100; p = 0,033</b>	<b>HR = 0,072; p = 0,022</b>	N/A	N/A
	<b>Oesophagus</b>	HR = 1,530; p = 0,558	N/A	HR = 1,277; p = 0,751	HR = 1,381; p = 0,711
	<b>Lung</b>	HR = 0,608; p = 0,329	HR = 0,469; p = 0,147	N/A	N/A
H179 vs other mutations	<b>Head and Neck</b>	HR = 3,720; p = 0,191	HR = 2,061; p = 0,473	HR = 0,390; p = 0,070	HR = 0,303; p = 0,118

	<b>Oral</b>	N/A	HR = 0,072; p = 0,973	HR = 0,500; p = 0,250	HR = 0,729; p = 0,762
	<b>Oropharynx</b>	N/A	N/A	N/A	N/A
	<b>Hypopharynx</b>	N/A	N/A	N/A	N/A
	<b>Larynx</b>	HR = 0,048; p = 0,602	N/A	N/A	N/A
	<b>Oesophagus</b>	N/A	N/A	N/A	N/A
	<b>Lung</b>	HR = 1,681; p = 0,374	HR = 2,399; p = 0,142	HR = 0,722; p = 0,654	HR = 1,088; p = 0,791
H193 vs other mutations	<b>Head and Neck</b>	HR = 0,420; p = 0,058	HR = 0.302; p = 0,015	HR = 1,050; p = 0,962	HR = 0,949; p = 0,961
	<b>Oral</b>	HR = 0,824; p = 0,787	HR = 1,689; p = 0,483	HR = 0,793; p = 0,819	HR = 0,454; p = 0,471
	<b>Oropharynx</b>	HR = 0,048; p = 0,014	HR = 0,002; p = 0,006	HR = 23,350; p = 0,643	N/A
	<b>Hypopharynx</b>	N/A	N/A	N/A	N/A

	<b>Larinx</b>	N/A	N/A	N/A	N/A
	<b>Oesophagus</b>	N/A	N/A	N/A	N/A
	<b>Lung</b>	HR = 2,059; p = 0,472	HR = 1,892; p = 0,526	N/A	N/A
R196 vs other mutations	<b>Head and Neck</b>	HR = 0,638; p = 0,442	HR = 0,461; p = 0,195	HR = 1,205; p = 0,796	HR = 1,058; p = 0,858
	<b>Oral</b>	HR = 1,503; p = 0,489	HR = 1,984; p = 0,255	HR = 1,132; p = 0,865	HR = 1,432; p = 0,634
	<b>Oropharynx</b>	N/A	N/A	N/A	N/A
	<b>Hypopharynx</b>	N/A	N/A	N/A	N/A
	<b>Larinx</b>	N/A	N/A	N/A	N/A
	<b>Oesophagus</b>	N/A	N/A	N/A	N/A
	<b>Lung</b>	N/A	N/A	N/A	N/A

R213 vs other mutations	<b>Head and Neck</b>	HR = 0,371; p = 0,030	HR = 0,438; p = 0,108	HR = 0,993; p = 0,994	HR = 1,041; p = 0,969
	<b>Oral</b>	HR = 0,399; p = 0,075	HR = 2,096; p = 0,153	N/A	N/A
	<b>Oropharynx</b>	N/A	N/A	N/A	N/A
	<b>Hypopharynx</b>	N/A	N/A	N/A	N/A
	<b>Larynx</b>	N/A	N/A	N/A	N/A
	<b>Oesophagus</b>	HR = 0,447; p = 0,183	HR = 0,419; p = 0,439	N/A	N/A
	<b>Lung</b>	HR = 0,234; p = 0,014	HR = 0,316; p = 0,053	N/A	N/A
R273 vs other mutations	<b>Head and Neck</b>	HR = 1,387; p = 0,403	HR = 0,707; p = 0,305	HR = 0,723; p = 0,455	HR = 0,696; p = 0,407
	<b>Oral</b>	HR = 1,422; p = 0,448	HR = 0,720; p = 0,483	HR = 0,631; p = 0,343	HR = 0,566; p = 0,244
	<b>Oropharynx</b>	N/A	N/A	N/A	N/A

	<b>Hypopharynx</b>	N/A	N/A	N/A	N/A
	<b>Larynx</b>	HR = 0,988; p = 0,987	HR = 1,280; p = 0,750	N/A	N/A
	<b>Oesophagus</b>	HR = 1,034; p = 0,948	HR = 1,663; p = 0,647	N/A	N/A
	<b>Lung</b>	HR = 0,808; p = 0,610	HR = 1,121; p = 0,803	HR = 1,081; p = 0,939	HR = 1,247; p = 0,829
Wild Type vs Missense	<b>Head and Neck</b>	<b>HR = 1,601; p = 0,016</b>	<b>HR = 1,688; p = 0,011</b>	HR = 1,192; p = 0,545	HR = 0,778; p = 0,439
	<b>Oral</b>	HR = 1,009; p = 0,969	HR = 1,157; p = 0,964	HR = 0,921; p = 0,815	HR = 0,953; p = 0,897
	<b>Oropharynx</b>	<b>HR = 7,417; p = 0,002</b>	<b>HR = 13,484; p = 0,001</b>	<b>HR = 11,353; p = 0,007</b>	<b>HR = 51,970; p = 0,033</b>
	<b>Hypopharynx</b>	HR = 3,464; p = 0,381	N/A	N/A	N/A
	<b>Larynx</b>	<b>HR = 6,943; p = 0,013</b>	<b>HR = 11,845; p = 0,025</b>	HR = 1,071; p = 0,936	HR = 0,731; p = 0,802
	<b>Oesophagus</b>	HR = 1,199; p = 0,647	HR = 4,083; p = 0,261	HR = 1,029; p = 0,970	HR = 0,860; p = 0,868

	<b>Lung</b>	<b>HR = 0,659; p = 0,037</b>	<b>HR = 0,647; p = 0,031</b>	HR = 0,850; p = 0,688	HR = 0,833; p = 0,652
Wild Type vs Frameshift	<b>Head and Neck</b>	HR = 1,323; p = 0,303	HR = 1,346; p = 0,314	HR = 1,427; p = 0,356	HR = 1,455; p = 0,375
	<b>Oral</b>	HR = 1,039; p = 0,915	HR = 0,791; p = 0,534	HR = 1,088; p = 0,866	HR = 1,117; p = 0,834
	<b>Oropharynx</b>	<b>HR = 8,221; p = 0,006</b>	HR = 5,872; p = 0,103	<b>HR = 32,637; p = 0,005</b>	<b>HR = 20,814; p = 0,050</b>
	<b>Hypopharynx</b>	HR = 1,732; p = 0,698	N/A	HR = 1,225; p = 0,887	N/A
	<b>Larinx</b>	HR = 1,495; p = 0,556	HR = 1,183; p = 0,875	HR = 0,400; p = 0,455	HR = 0,979; p = 0,989
	<b>Oesophagus</b>	HR = 2,208; p = 0,104	HR = 3,749; p = 0,416	N/A	N/A
	<b>Lung</b>	HR = 0,748; p = 0,300	HR = 0,4684; p = 0,190	HR = 0,788; p = 0,660	HR = 0,646; p = 0,448
	Wild Type vs Inframe	<b>Head and Neck</b>	HR = 1,683; p = 0,322	HR = 2,073; p = 0,189	HR = 0,744; p = 0,775
<b>Oral</b>		HR = 1,403; p = 0,580	HR = 1,921; p = 0,326	HR = 0,044; p = 0,520	HR = 0,000; p = 0,986

	<b>Oropharynx</b>	HR = 0,046; p = 0,760	HR = 0,001; p = 0,994	HR = 0,042; p = 0,762	N/A
	<b>Hypopharynx</b>	N/A	N/A	N/A	N/A
	<b>Larinx</b>	N/A	N/A	HR = 0,400; p = 0,455	N/A
	<b>Oesophagus</b>	HR = 0,043; p = 0,577	N/A	HR = 1,137; p = 0,917	N/A
	<b>Lung</b>	HR = 0,434; p = 0,176	HR = 0,544; p = 0,337	HR = 1,096; p = 0,931	HR = 1,267; p = 0,831
Wild Type vs Splice	<b>Head and Neck</b>	HR = 1,208; p = 0,580	HR = 0,935; p = 0,866	HR = 1,107; p = 0,839	HR = 0,914; p = 0,871
	<b>Oral</b>	HR = 1,024; p = 0,959	HR = 1,105; p = 0,830	HR = 0,641; p = 0,558	HR = 0,790; p = 0,769
	<b>Oropharynx</b>	<b>HR = 8,784; p = 0,052</b>	HR = 1,577; p = 0,836	N/A	N/A
	<b>Hypopharynx</b>	N/A	N/A	N/A	N/A
	<b>Larinx</b>	HR = 1,199; p = 0,837	HR = 0,023; p = 0,398	HR = 2,253; p = 0,484	N/A

	<b>Oesophagus</b>	HR = 1,553; p = 0,487	N/A	HR = 0,532; p = 0,530	HR = 0,283; p = 0,687
	<b>Lung</b>	HR = 0,530; p = 0,069	<b>HR = 0,486; p = 0,041</b>	HR = 1,931; p = 0,176	HR = 1,634; p = 0,364
Wild Type vs Stop	<b>Head and Neck</b>	<b>HR = 2,098; p = 0,003</b>	<b>HR = 2,016; p = 0,006</b>	HR = 0,847; p = 0,710	HR = 0,840; p = 0,707
	<b>Oral</b>	HR = 1,587; p = 0,118	HR = 1,505; p = 0,168	HR = 0,710; p = 0,521	HR = 0,625; p = 0,384
	<b>Oropharynx</b>	HR = 3,060; p = 0,310	HR = 2,169; p = 0,558	N/A	N/A
	<b>Hypopharynx</b>	HR = 0,026; p = 0,681	HR = 0,000; p = 0,866	HR = 1,225; p = 0,887	HR = 0,000; p = 0,539
	<b>Larynx</b>	<b>HR = 4,145; p = 0,05</b>	HR = 2,680; p = 0,405	HR = 1,366; p = 0,825	HR = 1,030; p = 0,991
	<b>Oesophagus</b>	HR = 0,639; p = 0,387	HR = 0,006; p = 0,210	HR = 0,763; p = 0,771	N/A
	<b>Lung</b>	HR = 0,757; p = 0,319	HR = 0,759; p = 0,337	HR = 1,411; p = 0,491	HR = 1,573; p = 0,407
Missense vs Inframe	<b>Head and Neck</b>	HR = 0,987; p = 0,980	HR = 0,860; p = 0,780	HR = 0,507; p = 0,504	HR = 1,074; p = 0,946

	<b>Oral</b>	HR = 1,338; p = 0,627	HR = 0,877; p = 0,839	HR = 0,046; p = 0,507	HR = 0,000; p = 0,987
	<b>Oropharynx</b>	HR = 0,030; p = 0,388	HR = 0,001; p = 0,989	N/A	N/A
	<b>Hypopharynx</b>	N/A	N/A	N/A	N/A
	<b>Larinx</b>	N/A	N/A	N/A	N/A
	<b>Oesophagus</b>	HR = 0,048; p = 0,528	N/A	HR = 1,186; p = 0,870	HR = 0,885; p = 0,908
	<b>Lung</b>	HR = 0,542; p = 0,301	HR = 0,572; p = 0,352	HR = 1,026; p = 0,980	HR = 1,181; p = 0,873
Missense vs Frameshift	<b>Head and Neck</b>	HR = 0,804; p = 0,392	HR = 0,912; p = 0,731	HR = 1,081; p = 0,824	HR = 1,185 p = 0,876
	<b>Oral</b>	HR = 0,917; p = 0,800	HR = 0,877; p = 0,839	HR = 1,065; p = 0,892	HR = 1,052 p = 0,919
	<b>Oropharynx</b>	HR = 0,937; p = 0,927	HR = 1,911; p = 0,537	HR = 4,213; p = 0,154	N/A
	<b>Hypopharynx</b>	HR = 0,707; p = 0,809	N/A	N/A	N/A

	<i>Larinx</i>	HR = 0,404; p = 0,104	<b>HR = 0,236; p = 0,031</b>	HR = 0,459; p = 0,478	HR = 0,196; p = 0,183
	<i>Oesophagus</i>	HR = 1,933; p = 0,559	<b>HR = 5,759; p = 0,037</b>	HR = 0,038; p = 0,337	N/A
	<i>Lung</i>	HR = 1,153; p = 0,582	HR = 1,039; p = 0,877	HR = 1,048; p = 0,919	HR = 0,987; p = 0,977
Missense vs Splice	<i>Head and Neck</i>	HR = 0,827; p = 0,559	HR = 0,721; p = 0,368	HR = 0,922; p = 0,865	HR = 0,817; p = 0,690
	<i>Oral</i>	HR = 1,234; p = 0,610	HR = 1,292; p = 0,553	HR = 0,750; p = 0,697	HR = 0,592; p = 0,503
	<i>Oropharynx</i>	HR = 1,283; p = 0,821	HR = 3,334; p = 0,685	N/A	N/A
	<i>Hypopharynx</i>	N/A	N/A	N/A	N/A
	<i>Larinx</i>	HR = 0,278; p = 0,087	HR = 0,168; p = 0,092	HR = 1,827; p = 0,418	HR = 1,117; p = 0,913
	<i>Oesophagus</i>	HR = 1,519; p = 0,394	HR = 1,592; p = 0,525	HR = 0,622; p = 0,534	HR = 0,295; p = 0,250
	<i>Lung</i>	HR = 0,794; p = 0,469	HR = 0,750; p = 0,367	<b>HR = 2,519; p = 0,018</b>	<b>HR = 2,355; p = 0,034</b>

Missense vs Stop	<b>Head and Neck</b>	HR = 1,263; p = 0,298	HR = 1,159; p = 0,519	HR = 0,650; p = 0,302	HR = 0,622; p = 0,265
	<b>Oral</b>	HR = 1,528; p = 0,121	HR = 1,387; p = 0,240	HR = 0,650; p = 0,469	HR = 0,675; p = 0,437
	<b>Oropharynx</b>	HR = 0,033; p = 0,418	HR = 0,001; p = 0,963	HR = 0,024; p = 0,418	HR = 0,006; p = 0,265
	<b>Hypopharynx</b>	HR = 0,015; p = 0,610	N/A	N/A	N/A
	<b>Larinx</b>	HR = 0,822; p = 0,699	HR = 0,673; p = 0,539	HR = 0,842; p = 0,876	HR = 0,020; p = 0,147
	<b>Oesophagus</b>	HR = 0,514; p = 0,113	HR = 0,237; p = 0,078	HR = 0,716; p = 0,244	HR = 0,793; p = 0,745
	<b>Lung</b>	HR = 1,073; p = 0,770	HR = 1,058; p = 0,822	HR = 1,604; p = 0,669	HR = 1,586; p = 0,287
Frameshift vs Inframe	<b>Head and Neck</b>	HR = 1,248; p = 0,688	HR = 0,860; p = 0,780	HR = 0,456; p = 0,455	HR = 0,475; p = 0,535
	<b>Oral</b>	HR = 1,193; p = 0,794	HR = 2,584; p = 0,477	HR = 0,039; p = 0,511	N/A
	<b>Oropharynx</b>	HR = 0,018; p = 0,403	HR = 0,002; p = 0,365	N/A	N/A

	<b>Hypopharynx</b>	N/A	N/A	N/A	N/A
	<b>Larinx</b>	N/A	HR = 8,842; p = 0,186	N/A	N/A
	<b>Oesophagus</b>	HR = 0,037; p = 0,393	N/A	N/A	N/A
	<b>Lung</b>	HR = 0,544; p = 0,362	HR = 0,389; p = 0,191	HR = 1,551; p = 0,686	HR = 0,820; p = 0,816
Frameshift vs Splice	<b>Head and Neck</b>	HR = 0,979; p = 0,957	HR = 0,793; p = 0,587	HR = 0,820; p = 0,714	HR = 0,940; p = 0,913
	<b>Oral</b>	HR = 1,340; p = 0,566	HR = 1,539; p = 0,422	HR = 0,662; p = 0,614	HR = 0,775; p = 0,788
	<b>Oropharynx</b>	HR = 2,828; p = 0,469	N/A	N/A	N/A
	<b>Hypopharynx</b>	N/A	N/A	N/A	N/A
	<b>Larinx</b>	HR = 0,597; p = 0,537	HR = 3,894; p = 0,240	HR = 0,177; p = 0,291	HR = 2,555; p = 0,449
	<b>Oesophagus</b>	HR = 0,626; p = 0,444	N/A	N/A	N/A

	<b>Lung</b>	HR = 0,637; p = 0,243	HR = 0,699; p = 0,367	HR = 2,239; p = 0,126	HR = 2,547; p = 0,080
Frameshift vs Stop	<b>Head and Neck</b>	HR = 1,572; p = 0,123	HR = 1,378; p = 0,307	HR = 0,569; p = 0,246	HR = 0,382; p = 0,070
	<b>Oral</b>	HR = 1,667; p = 0,175	HR = 1,534; p = 0,287	HR = 0,628; p = 0,448	HR = 0,375; p = 0,173
	<b>Oropharynx</b>	HR = 0,021; p = 0,435	HR = 0,001; p = 0,586	HR = 0,010; p = 0,439	HR = 0,017; p = 0,536
	<b>Hypopharynx</b>	HR = 0,026; p = 0,681	N/A	HR = 1,414; p = 0,809	N/A
	<b>Larinx</b>	HR = 2,229; p = 0,216	HR = 2,545; p = 0,237	HR = 1,633; p = 0,730	HR = 0,00; p = 0,708
	<b>Oesophagus</b>	<b>HR = 0,255; p = 0,010</b>	N/A	N/A	N/A
	<b>Lung</b>	HR = 1,061; p = 0,849	HR = 1,250; p = 0,488	HR = 1,732; p = 0,309	HR = 1,595; p = 0,409
	Inframe vs Splice	<b>Head and Neck</b>	HR = 0,812; p = 0,726	HR = 0,672; p = 0,574	HR = 1,897; p = 0,559
<b>Oral</b>		HR = 0,893; p = 0,875	HR = 0,642; p = 0,644	HR = 33,002; p = 0,607	HR = 2,473; p = 0,996

	<b>Oropharynx</b>	N/A	N/A	N/A	N/A
	<b>Hypopharynx</b>	N/A	N/A	N/A	N/A
	<b>Larynx</b>	N/A	N/A	N/A	N/A
	<b>Oesophagus</b>	HR = 26,667; p = 0,571	N/A	HR = 0,452; p = 0,521	N/A
	<b>Lung</b>	N/A	N/A	N/A	N/A
Inframe vs Stop	<b>Head and Neck</b>	HR = 1,104; p = 0,854	HR = 0,956; p = 0,939	HR = 1,325; p = 0,793	HR = 0,598; p = 0,670
	<b>Oral</b>	HR = 0,989; p = 0,985	HR = 1,056; p = 0,939	HR = 24,776; p = 0,593	N/A
	<b>Oropharynx</b>	N/A	N/A	N/A	N/A
	<b>Hypopharynx</b>	N/A	N/A	N/A	N/A
	<b>Larynx</b>	N/A	N/A	N/A	N/A

	<b>Oesophagus</b>	HR = 22,507; p = 0,657	N/A	HR = 1,149; p = 0,909	N/A
	<b>Lung</b>	N/A	N/A	N/A	N/A
Splice vs Stop	<b>Head and Neck</b>	HR = 1,694; p = 0,156	HR = 1,896; p = 0,121	HR = 0,721; p = 0,577	HR = 0,609; p = 0,436
	<b>Oral</b>	HR = 1,357; p = 0,514	HR = 1,208; p = 0,695	HR = 0,988; p = 0,988	HR = 0,534; p = 0,506
	<b>Oropharynx</b>	N/A	N/A	N/A	N/A
	<b>Hypopharynx</b>	N/A	N/A	N/A	N/A
	<b>Larynx</b>	HR = 3,065; p = 0,171	HR = 5,711; p = 0,174	HR = 0,444; p = 0,484	HR = 0,00; p = 0,927
	<b>Oesophagus</b>	HR = 2,112; p = 0,244	N/A	HR = 0,424; p = 0,484	HR = 0,674; p = 0,819
	<b>Lung</b>	HR = 1,445; p = 0,326	HR = 1,549; p = 0,257	HR = 0,699; p = 0,462	HR = 0,674; p = 0,481
V157 vs other mutations	<b>Head and Neck</b>	N/A	N/A	N/A	N/A

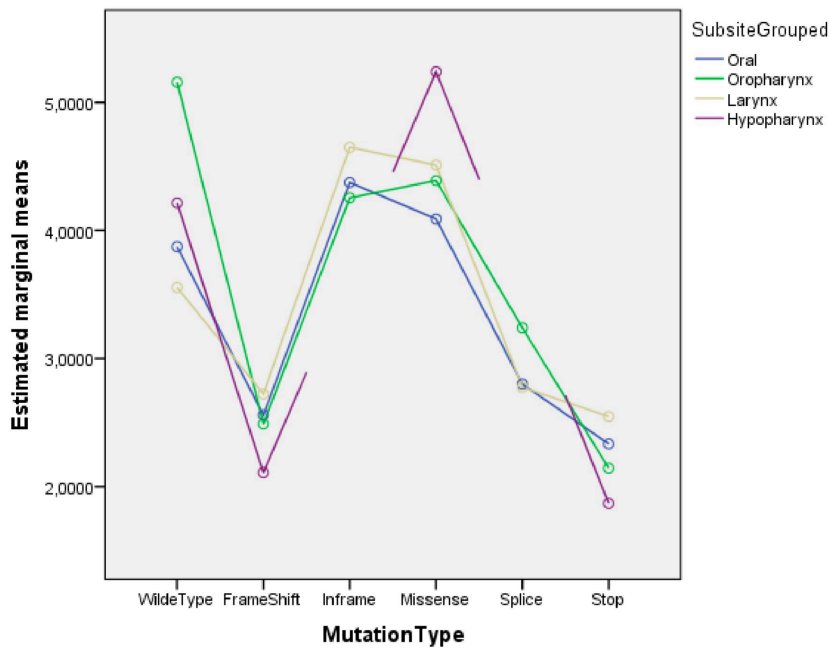
	<b>Oral</b>	N/A	N/A	N/A	N/A
	<b>Oropharynx</b>	N/A	N/A	N/A	N/A
	<b>Hypopharynx</b>	N/A	N/A	N/A	N/A
	<b>Larynx</b>	N/A	N/A	N/A	N/A
	<b>Oesophagus</b>	N/A	N/A	N/A	N/A
	<b>Lung</b>	HR = 0,824; p = 0,644	HR = 0,837; p = 0,671	HR = 0,226; p = 0,006	HR = 0,212 p = 0,004
R158 vs other mutations	<b>Head and Neck</b>	N/A	N/A	N/A	N/A
	<b>Oral</b>	N/A	N/A	N/A	N/A
	<b>Oropharynx</b>	N/A	N/A	N/A	N/A
	<b>Hypopharynx</b>	N/A	N/A	N/A	N/A

	<b>Larinx</b>	N/A	N/A	N/A	N/A
	<b>Oesophagus</b>	N/A	N/A	N/A	N/A
	<b>Lung</b>	HR = 0,739; p = 0,508	HR = 0,715; p = 0,468	HR = 0,913; p = 0,900	HR = 0,963; p = 0,958
P278 vs other mutations	<b>Head and Neck</b>	N/A	N/A	N/A	N/A
	<b>Oral</b>	N/A	N/A	N/A	N/A
	<b>Oropharynx</b>	N/A	N/A	N/A	N/A
	<b>Hypopharynx</b>	N/A	N/A	N/A	N/A
	<b>Larinx</b>	N/A	N/A	N/A	N/A
	<b>Oesophagus</b>	N/A	N/A	N/A	N/A
	<b>Lung</b>	HR = 1,795; p = 0,317	HR = 1,324; p = 0,634	HR = 1,163; p = 0,836	HR = 1,072; p = 0,925

Supplemental material Table 2: Univariate and multivariate overall and disease-free survival for head and neck, oral, oropharynx, hypopharynx, larynx, oesophagus and lung squamous cell carcinoma. HR=Hazard Ratio; p=p-value; N/A not calculable.

TP53 genotype correlates with expression profile and clinicopathological variables.

*Correlation with TP53 transcripts.* The expression of p53 mRNA differed between WT and MUT patients (Mann–Whitney  $P < 0.001$ ) in HNSCC. In the WT cohort, the expression ( $\log_2(\text{fpkm} + 1)$ ) ranged from 0.71 to 6.47 with a mean of 4.2825 and a median of 4.39. In the MUT cohort, mRNA expression varied from 0.76 to 5.85 with a mean of 3.492 and a median of 3.665. This differential expression was also reported in the OP subgroup (Mann–Whitney  $P < 0.001$ ) where in the WT cohort, the expression ranged from 2.23 to 6.47 with a mean of 5.1579 and a median of 5.21; meanwhile, for the MUT cohort, the expression reported was from 1.82 to 5.62 with a mean of 3.6789 and a median of 3.90. mRNA expression was also variable in HPV+ and HPV– tumours, in particular in OP subgroup (Mann–Whitney  $P = 0.006$ ). In HPV– tumours, the expression ranged with a mean of 3.86 and a median of 3.73; meanwhile, HPV+ tumours reported a mean of 5.2373 and a median of 5.1754. A two-way ANOVA was conducted that examined the effect of the anatomical subsite and mutational status on TP53 mRNA expression. There was a statistically significant interaction between the anatomical subsite and mutational status on mRNA expression, two-way ANOVA  $P = 0.003$ . Simple main effect analysis showed that mutational status significantly affected mRNA expression ( $P < 0.001$ ), but there were no differences between anatomical subsites ( $P = 0.684$ ). Bonferroni–Holm post hoc test showed a differential mRNA expression between OP and the other subsites (O, L and HP;  $P < 0.001$ ) and a higher mRNA expression in WT, missense and inframe MUT, compared with frameshift, splice and stop MUT ( $P < 0.001$ ) (Supplementary Fig. 4).



Supplemental material Figure 4: Two-way ANOVA showing the differential mRNA expression according to the mutational TP53 status and anatomical subsite.

mRNA expression poorly correlated with its protein expression (Spearman rank-correlation test  $\rho = 0.382$ ,  $P < 0.001$ ). Of interest, TP53 mRNA expression differed among tumour grades (Bonferroni–Holm post hoc test G1 vs G2  $P = 0.045$ ; G1 vs G3  $P < 0.001$ ; G2 vs G3  $P = 0.031$ ) with the following expression means in G1 of 3.2434, in G2 of 3.6753 and in G3 of 4.0424.

*Correlation with clinicopathological variables.*

Chi-square test showed a differential ratio between WT/MUT patients and tumour subgroup (OC, OP, HP and L) and HPV positive/negative ( $P < 0.001$ ). In total, 176/246 MUT in OC (Bonferroni post hoc test  $P = 0.08239$ ), 19/62 in OP (Bonferroni post hoc test  $P < 0.000001$ ), 5/9 in HP (Bonferroni post hoc test  $P = 0.40597$ ) and 78/90 in L (Bonferroni post hoc test  $P = 0.00002$ ); for the HPV status, 3/30 HPV-positive patients were mutated in TP53 gene; meanwhile, 52/64 were mutated in HPV-negative tumours. In addition, perineural invasion was more frequent in MUT ( $P = 0.031$ ); 28/78 WT reported perineural invasion against

101/201 MUT. This event was also notable in the OC subgroup where 21/50 WT reported perineural invasion against 82/140 MUT (P = 0.044). Interestingly, 110/143 smoking patients were mutated against 176/272 nonsmokers (P = 0.011). Spearman analysis showed a correlation between DNA-VAF and grading in HNSCC ( $\rho = 0.131$ , P= 0.035), in particular higher DNA-VAF was present in patients with higher tumour grade (Kruskal-Wallis P = 0.041—Bonferroni-Holm post hoc test G1 vs G2 P = 0.134; G1 vs G3 P = 0.059; G2 vs G3 P = 1.00). The results from Spearman analysis in head and neck cancer are shown in Supplementary Fig. 5.

Variable	TP53 mRNA expression	TP53 Z-score protein expression	DNA-VAF	N° of packs of cigarettes	Age	T-Dimensional	Stage	Grading
TP53 mRNA expression	$\rho = 1$ p-value = 1	<b>0,382</b> < <b>0,001</b>	-0,056 0,362	-0,041 0,449	-0,038 0,446	<b>-0,120</b> <b>0,017</b>	0,046 0,362	<b>0,203</b> < <b>0,001</b>
TP53 Z-score protein expression		$\rho = 1$ p-value = 1	0,078 0,394	0,074 0,403	0,103 0,177	0,020 0,796	0,17 0,826	0,00 0,998
DNA-VAF			$\rho = 1$ p-value = 1	<b>0,197</b> <b>0,004</b>	0,002 0,980	0,047 0,458	0,021 0,738	<b>0,131</b> <b>0,036</b>
N° of packs of cigarettes				$\rho = 1$ p-value = 1	<b>0,125</b> <b>0,022</b>	0,059 0,293	0,070 0,206	-0,008 0,893
Age					$\rho = 1$ p-value = 1	-0,022 0,671	-0,062 0,219	0,059 0,244
T-Dimensional						$\rho = 1$ p-value = 1	<b>0,104</b> <b>0,041</b>	0,083 0,109
Stage							$\rho = 1$ p-value = 1	0,080 0,117
Grading								$\rho = 1$ p-value = 1

Supplemental material Figure 5: Spearman's rank correlation results from linear variables.

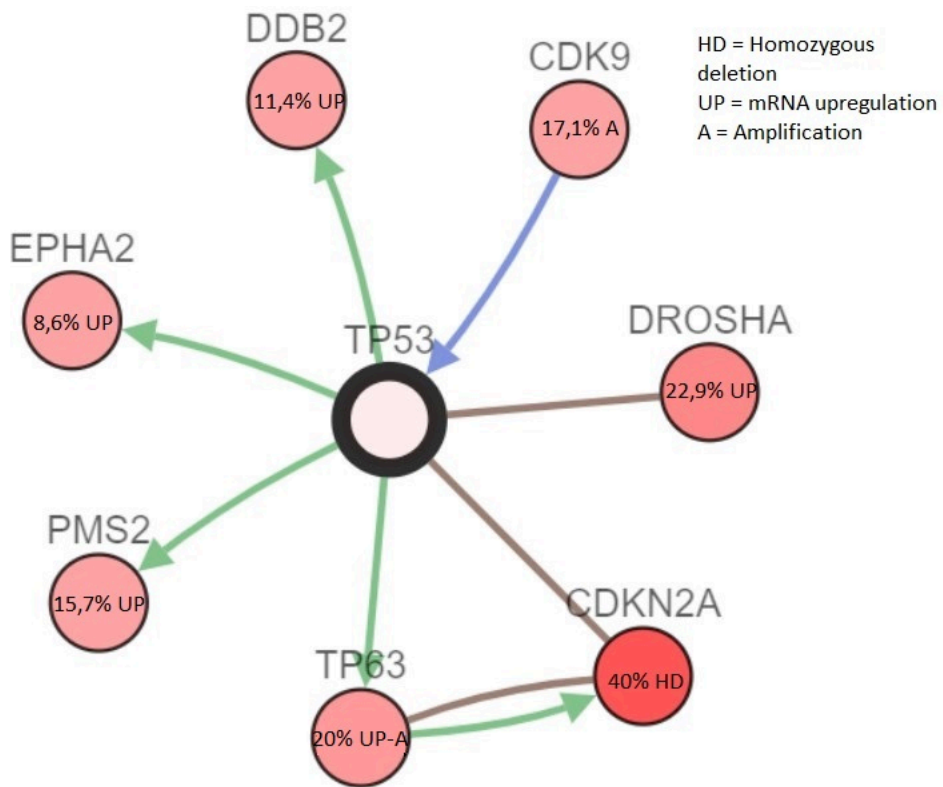
Different characteristics were also found between male and female patients. Chi-square test showed a higher RPPA-Z-score protein expression in males, compared with females, 65/119 males and 17/51 females (P = 0.011). In addition, the occurrence of hotspot mutations taken into consideration, differed between genders. Mutations in H193 occurred only in males; meanwhile, of 8 patients mutated in R196, 6/8 were female patients (chi-square test P = 0.003). R196 resulted mutated only in the OC subgroup. In the last analysis, R273 mutations were characterised by a missense mutation by a substitution of the R (arginine) amino acid

to C (cysteine) or H (histidine). Changes in C involved one male over five patients; meanwhile, H involved seven male patients over nine (chi-square test  $P = 0.036$ ). R273 missense mutations were also linked to alcohol consumption; in particular, of five patients with a change from R to C, four reported alcohol consumption in the anamnesis; meanwhile, 8/9 patients with H change did not report alcohol history (chi-square test  $P = 0.01$ ); the same result was also detected for the OC subgroup (chi-square test  $P = 0.044$ ). Cigarette consumption was also considered as a clinical variable in HNSCC. Transitions of C–T in CpG islands are reported to be a common consequence of random deamination; meanwhile, transversions of G:C–T:A are tobacco smoke-related mechanisms of mutations.[198, 199] Chi-square test ( $P = 0.018$ ) showed a lower number of transversion events in never-smoker patients (6/16) (Bonferroni post hoc test  $P = 0.00237$ ). A higher number of transversion of G:C–T:A events occurred in current smokers (24/31) (Bonferroni post hoc test  $P = 0.1815$ ) and in ex-smokers less than 15 years (20/25) (Bonferroni post hoc test  $P = 0.1423$ ). Indeed, a higher number of smoked cigarettes emerged in patients with transversions, compared with patients with transitions of C–T in CpG islands (Mann–Whitney  $P = 0.032$ ). Patients with mutations in Alpha secondary structure showed lower number of smoked packs of cigarettes, against Turn and Bend (Mann–Whitney  $P = 0.005$ ), unknown (Mann–Whitney  $P = 0.03$ ) and  $\beta$ -strand/bridge patients ( $P = 0.021$ ). Although Bonferroni–Holm post hoc test failed to find significant difference ( $P = 0.190$ ;  $P = 0.288$ ;  $P = 0.096$ , respectively), chi-square test showed a significant difference between the smoking history and the secondary structure involved. In particular, only 8/124 current smokers reported a mutation in Alpha secondary structure ( $P = 0.019$ ). Bonferroni post hoc-adjusted  $P$  values are reported in Supplementary Table 4.

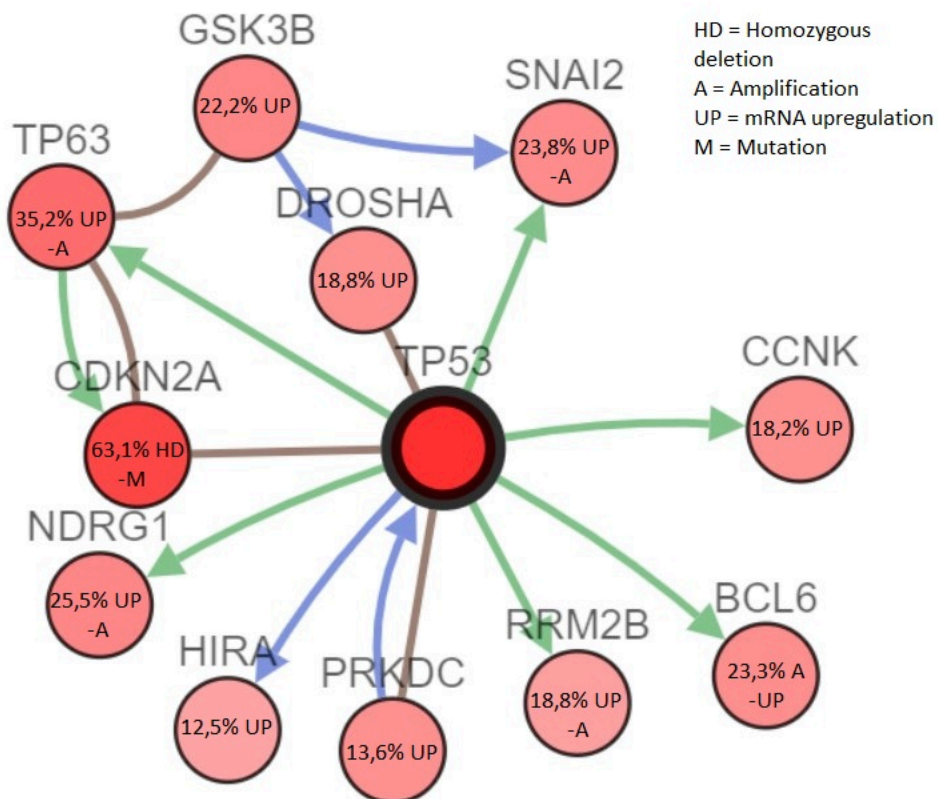
			Secondary structure					Total
			Beta-sheets	Helix	Turn_bend	Unknown	Wild-type	
Smoking History	Never-Smoker	Number	22	14	8	13	34	91
		% among smoking history	24,2%	15,4%	8,8%	14,3%	37,4%	100,0%
		Adjusted p-value	,904	,085	,254	,303	,535	
	Current-smoker	Number	39	8	13	31	33	124
		% among smoking history	31,5%	6,5%	10,5%	25,0%	26,6%	100,0%
		Adjusted p-value	0,032	0,067	0,478	0,011	0,020	
	Ex-smoker>15years	Number	13	5	7	4	25	54
		% among smoking history	24,1%	9,3%	13,0%	7,4%	46,3%	100,0%
		Adjusted p-value	,912	,734	,849	,030	,052	
	Ex-smoker<15years	Number	17	12	17	18	36	100
		% among smoking history	17,0%	12,0%	17,0%	18,0%	36,0%	100,0%
		Adjusted p-value	0,038	0,582	0,085	0,976	0,749	
Total	Number	91	39	45	66	128	369	
	% among smoking history	24,7%	10,6%	12,2%	17,9%	34,7%	100,0%	

Supplemental material Table 4: Bonferroni post-hoc adjusted p-values for Chi-square test comparisons between smoking history and secondary structure.

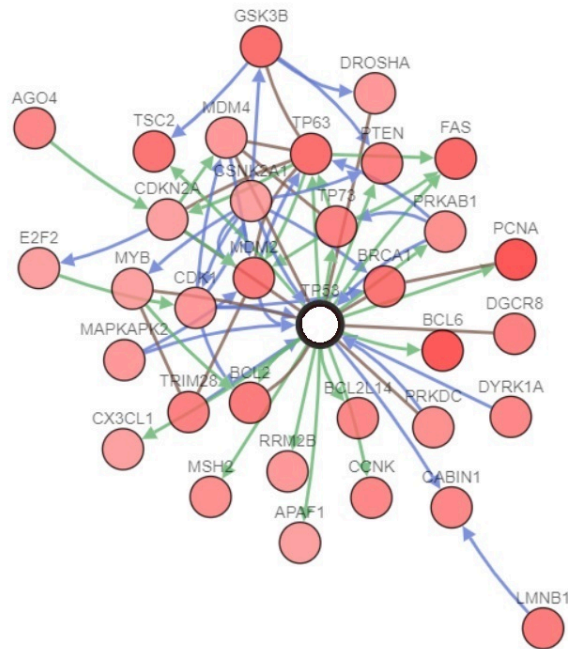
Collectively, our data show distinct correlations between TP53 genotype, p53 expression profile and clinicopathological features of HNSCC. Network analysis reveals distinct alterations in HNSCC subgroups. Interactome–genome–transcriptome analysis was undertaken to build a dynamic network that highlighted the TP53 interactors that underwent genomic (mutations, CNA) or translational (mRNA expression) modifications in HNSCC. TP53 networks differed substantially in WT- and p53-mutated HNSCC subgroups (Supplementary Fig. 6–15).



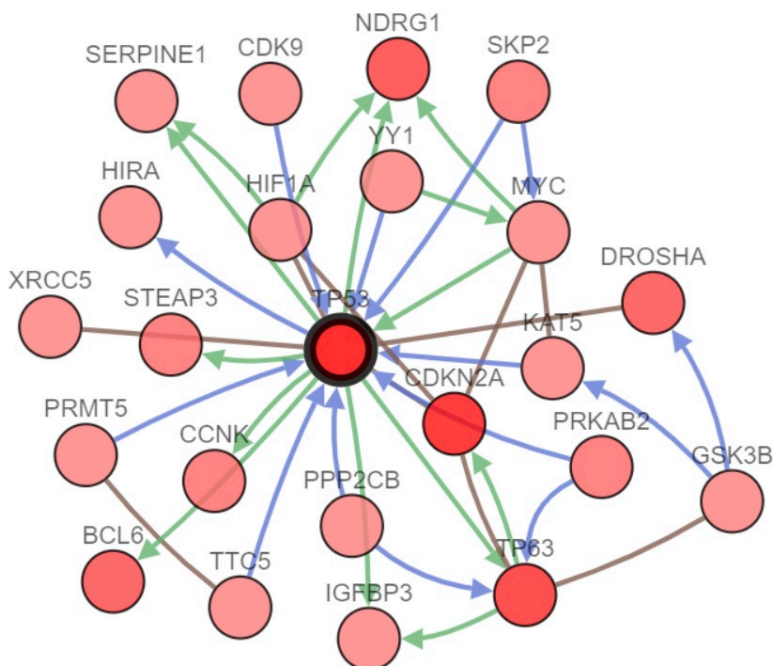
Supplemental material Figure 6: Gene network analysis for WT OSCC from cBioPortal tool. Network legend: Blue line: Controls state change of; Green line: Controls expression of; Brown line: In complex with.



Supplemental material Figure 7: Gene network analysis for MUT OSCC from cBioPortal tool. Network legend: Blue line: Controls state change of; Green line: Controls expression of; Brown line: In complex with.

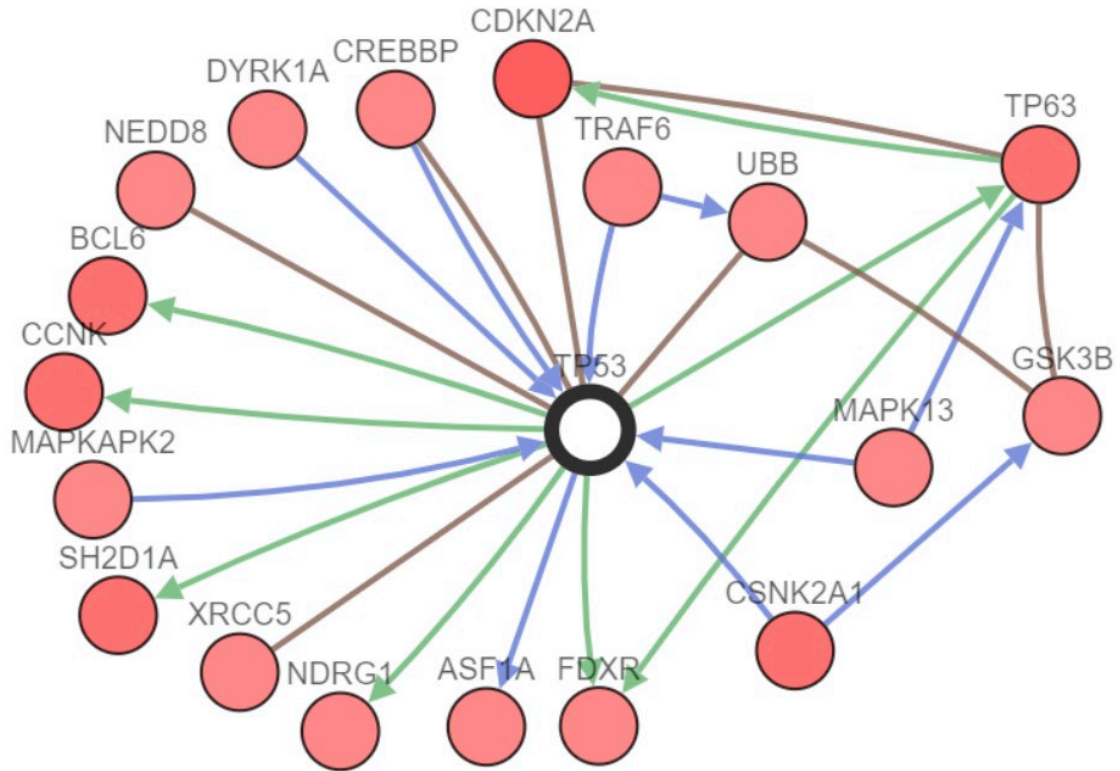


Supplemental material Figure 8: Gene network analysis for WT OP from cBioPortal tool. Network legend: Blue line: Controls state change of; Green line: Controls expression of; Brown line: In complex with.



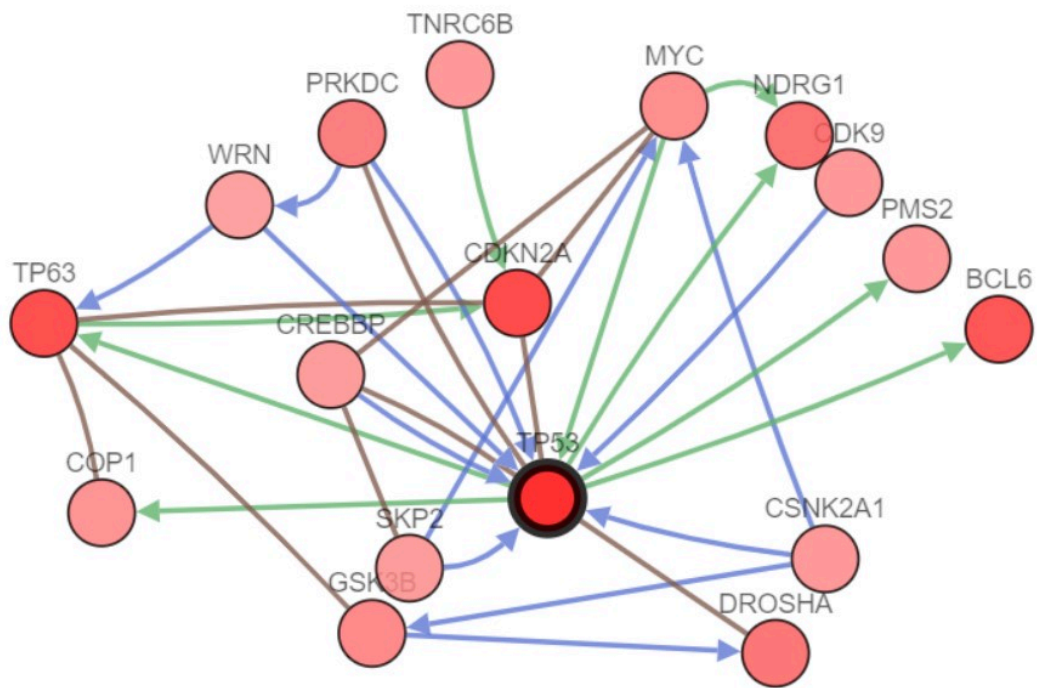
Supplemental material Figure 9: Gene network analysis for MUT OP from cBioPortal tool.

Network legend: Blue line: Controls state change of; Green line: Controls expression of; Brown line: In complex with.



Supplemental material Figure 10: Gene network analysis for WT L from cBioPortal tool.

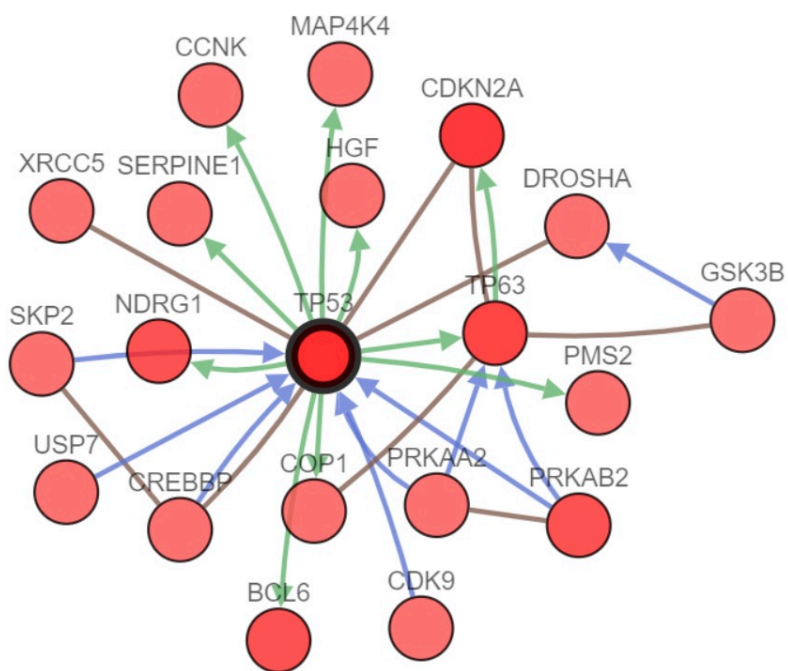
Network legend: Blue line: Controls state change of; Green line: Controls expression of; Brown line: In complex with.



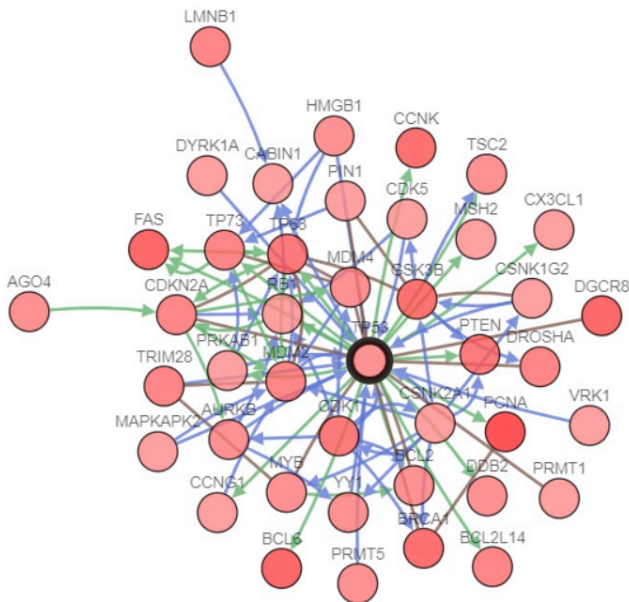
Supplemental material Figure 11: Gene network analysis for MUT L from cBioPortal tool.

Network legend: Blue line: Controls state change of; Green line: Controls expression of;

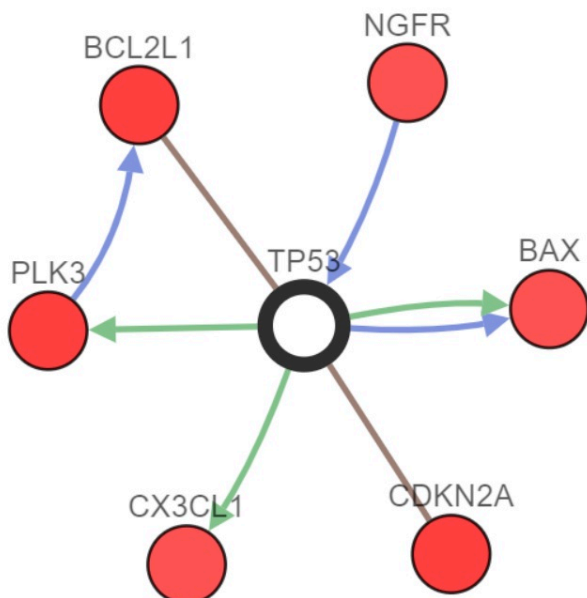
Brown line: In complex with.



Supplemental material Figure 12: Gene network analysis for HPV negative OP from cBioPortal tool. Network legend: Blue line: Controls state change of; Green line: Controls expression of; Brown line: In complex with.



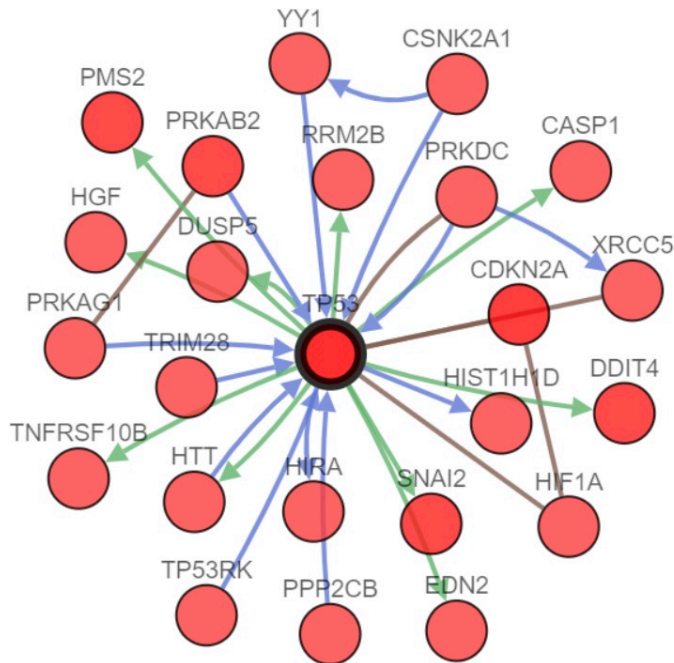
Supplemental material Figure 13: Gene network analysis for HPV positive OP from cBioPortal tool. Network legend: Blue line: Controls state change of; Green line: Controls expression of; Brown line: In complex with.



Supplemental material Figure 14: Gene network analysis for WT HP from cBioPortal tool.

Network legend: Blue line: Controls state change of; Green line: Controls expression of;

Brown line: In complex with.



Supplemental material Figure 15: Gene network analysis for MUT HP from cBioPortal tool.

Network legend: Blue line: Controls state change of; Green line: Controls expression of;

Brown line: In complex with.

In cancer arising from the oral cavity, there were several molecules differentially involved in TP53 network (Supplementary Figs. 6 and 7, Table 3A/B). Both WT and MUT TP53 groups shared common alterations of CDKN2A, TP63 and DROSHA. In WT, the main modification involved the cellular response to DNA-damage stimulus, with changes affecting PMS2, CDK9, DDB2 and EPHA2. In MUT, changes in NDRG1, GSK3B, SNAI2, BCL6, CCNK, PRKDC and RRM2B affected mainly the intrinsic apoptotic process and the transition of the G1/S cell-cycle phase.

In HNSCC of the oropharynx (Supplementary Figs. 8, 9, Table 3C/D), both WT and MUT were associated with alterations in BCL6, TP63, GSK3B, CDKN2A, CCNK and DROSHA.

Surprisingly, CDKN2A in WT resulted altered only in 18.2% of cases (13.6% reported mRNA upregulation, 2.3% homozygous deletion and 2.3% mutation), whereas in MUT, CDKN2A was affected in 78.9% of cases (57.9% reported homozygous deletion and 21.1% mutation).

In particular, WT group resulted affected by deficiencies in both intrinsic and extrinsic apoptotic signals, cell-cycle growth checkpoint at G1/S phase, mismatch repair, positive histone deacetylation, negative regulation of cell–matrix adhesion, fatty acid biosynthetic process, cellular response to starvation, negative regulation of intracellular oestrogen receptor signalling pathway, morphogenesis of embryonic epithelium and negative regulation of phosphatidylinositol 3-kinase signalling. These mechanisms are regulated in particular by PCNA, BCL6, FAS, GSK3B, TP63, TSC2, BRCA1, MDM2, PTEN, TP73, DYRK1A, MSH2, PRKAB1, PRKDC, CDK1, MDM4, RRM2B and E2F2. DGR8, AGO4 and DROSHA regulated primary miRNA processing, involved in gene silencing in the WT OP subgroup. CX3CL1 and MYB showed common alteration in both WT TP53 OP and HPV+ OP subgroups, with positive regulation of transforming growth factor beta production. BCL2, TRIM28 and CCNK emerged to be involved in the regulation of viral genome replication, sharing common alterations in both WT TP53 OP and HPV+ OP group. In MUT, there were different molecules involved in the TP53 network. Noncoding RNA (ncRNA) transcription was linked to alterations in CCNK and CDK9, and in particular, HIF1A and YY1 resulted in a positive regulation of pri-miRNA transcription by RNA polymerase II. CCNK and CDK9 were found also in the HPV– OP subgroup. In terms of pathways, the main alterations involved the apoptotic process, due to alterations in CDKN2A, NDRG1, TP63, BCL6, PRKAB2, PPP2CB, PRMT5, HIF1A, KAT5 and TTC5. Notably, alterations resulted in positive regulation of glycolytic process, beta-catenin-TCF complex assembly, regulation of cellular respiration and positive regulation of epithelial cell proliferation, led by TP63, MYC, KAT5 and HIF1A. The main alterations involved

autophagy mechanisms, due to changes in PRKAB2, HIF1A, KAT5 and GSK3B. At last, changes in SERPINE1, GSK3B and TP63 resulted in modifications in epithelial differentiation. In HNSCC of the larynx (Supplementary Figs. 10, 11, Table 3E/F), CDKN2A, BCL6, TP63, GSK3B and NDRG1 were altered in both WT and MUT; CSNK2A1 and CREBBP were downregulated in WT, whereas the same resulted upregulated in MUT. In terms of pathways, the main alteration in WT affected the signal transduction by p53-class mediators and downstream stressactivated MAPK cascade, due to modifications affecting MAPK13, UBB, TRAF6, MAPKAPK2 and DYRK1A. In MUT, a defect emerged in the crosstalk between regulation of cell growth and cellular response to hypoxia and gamma radiation, as suggested by the alteration of PRKDC, MYC, COP1, CREBBP, NDRG1 and WRN.

Alterations in the hypopharynx subgroups differed between wild-type and mutated TP53 groups (Supplementary Figs. 14, 15, Table 3I/J). CDKN2A showed common alterations in both groups. In the WT group, PLK3, BCL2L1, CX3CL1, BAX and NGFR all resulted in upregulation in their mRNA expression, with some cases of amplification or mutation. These were mainly involved in the negative regulation of apoptotic process, and in the regulation of cell-cycle G1/S-phase transition. Interestingly, CX3CL1 resulted participating in positive regulation of calcium-independent cell-to cell adhesion, regulation of stem cell proliferation and regulation of cell–matrix adhesion. NGFR seems to be related to the positive regulation of pri-miRNA transcription by RNA polymerase II and together with CDKN2A, in RAS protein signal transduction. MUT group showed a higher number of alterations, and CDKN2A was mainly affected. DDIT4 resulted in mRNA upregulation in 60% of cases, affecting the intrinsic apoptotic signaling pathway in response to DNA damage by p53-class mediator and negative regulation of ATP metabolic process. Alterations in metabolic pathways could be of interest in this group of patients because of changes in fatty acid biosynthetic process, vasoconstriction, ATP metabolic process and rhythmic process

involving EDN2, PRKAG1, HTT, CSNK2A1, HGF, HIF1A, PRKAB2 and SNAI2. Of interest in this group are also changes in chromatin assembly and silencing because of mRNA upregulation in 40% of cases of HIST1H1D and downregulation of HIRA. In addition, differences in the TP53 network between HPV<sup>-</sup> and HPV<sup>+</sup> HNSCCs were compared. OP HPV<sup>-</sup> tumours showed common alterations with HPV<sup>+</sup> tumours of the same subsite (Supplementary Figs. 12, 13, Table 3G/H). In particular, TP63, BCL6, GSK3B, DROSHA and CCNK showed similar modifications. CDKN2A mRNA resulted in upregulation in 22.2% of HPV<sup>+</sup> tumours, whereas HPV<sup>-</sup> tumours showed homozygous deletion and mutations in 50% and 33.3%, respectively. In HPV<sup>-</sup>, a wide number of molecules were involved in a negative regulation of cell–matrix adhesion, stem cell differentiation, negative regulation of epithelial cell differentiation and regulation of intracellular oestrogen receptor signalling pathway. Of interest, an alteration in lipid metabolism emerged in alterations in PRKAB2 and PRKAA2, with consequences in lipophagy, carnitine shuttle and fatty acid transmembrane transport. HPV<sup>+</sup> showed modifications of both intrinsic and extrinsic apoptotic processes, due to alterations in histone phosphorylation, peptidyl–threonine phosphorylation, peptidyl–serine phosphorylation and protein autophosphorylation processes, which lead to changes in ubiquitination. Notably, in this cohort, there was an upregulation of PCNA mRNA in 48.1% of samples. The complete list of altered nodes and their function is reported in Supplementary Table 3A–J and Figs. 6–15. Taken together, these data show that distinct TP53 molecular networks are associated with HNSCC in a site- and mutation specific manner. Notwithstanding these differences in molecular pathways, all HNSCC tumours share a common alteration landscape in the crosstalk between cellular stress response, cellcycle progression and apoptotic process.

#### *Survival prediction algorithm results*

By applying the Poeta algorithm (PA)[206] on the TCGA database, we found that disruptive mutations had independent prognostic significance in HNSCC, although with small

difference between disruptive and conservative mutations (disruptive vs conservative mutations, multivariate analysis: HR = 1.077; 95% CI: 0.753–1.541; P = 0.684); (disruptive vs wild-type, multivariate analysis: HR = 1.663; 95% CI: 1.122–2.466; P = 0.011); (conservative vs wild-type, multivariate analysis: HR = 1.545; 95% CI: 1.013–2.357; P = 0.043) (Fig. 5a).

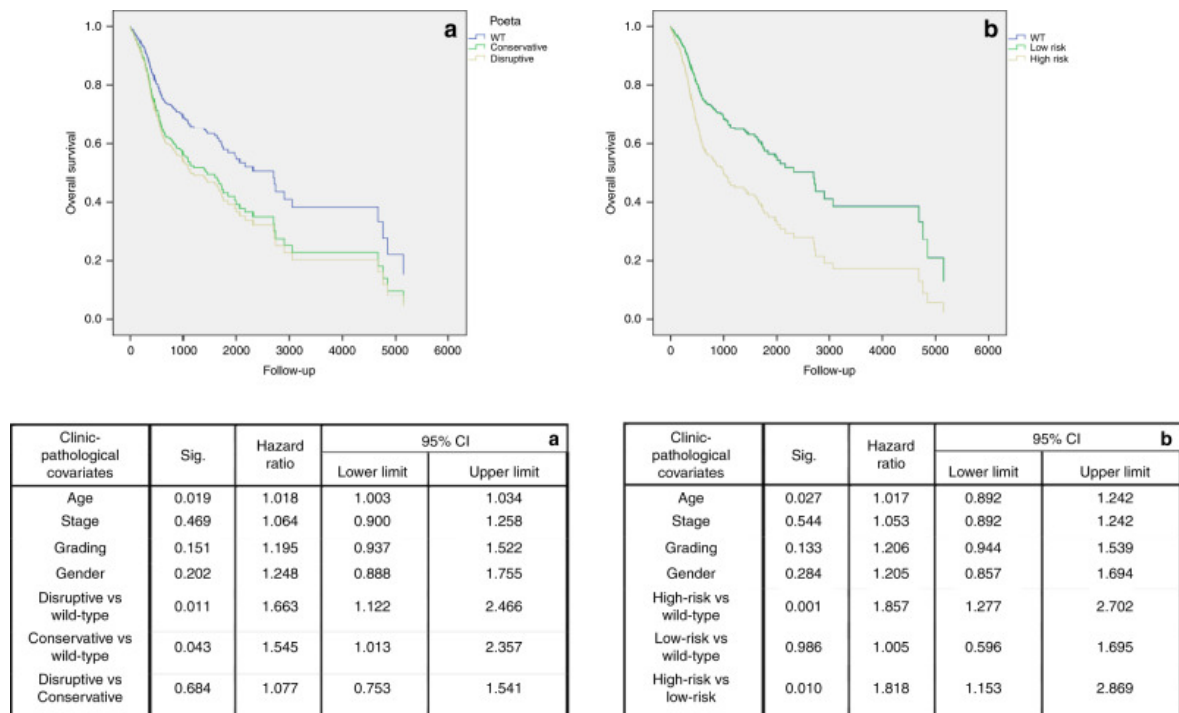


Fig. 5: Overall survival for algorithms of TP53 mutational status. Multivariate survival analysis of patients with head and neck squamous cell carcinoma, showing differences among patients with disruptive (yellow line) and conservative (green line) mutations in TP53 gene according to Poeta's classification (a); and patients with high risk (yellow line) and low risk (green line) death mutations, according to our new classification system (b). Blue lines are, in both of cases, representative of wild-type (WT) patients.

In addition, we integrated the biochemical information from PA to the ones from Martin et al.[200] with the addition of our findings according to the predicted secondary structure and the number of mutated alleles. Patients were classified as carriers of high-risk death mutations, carriers of low-risk death mutations and wild type. Our model successfully identified patients at higher risk of death according to the mutational status, depending on the biochemical alterations, characteristics and predicted secondary structure. High risk of death mutations resulted to be an independent prognostic factor in TCGA head and neck database, with greater difference towards low risk of death mutations (highrisk vs low-risk

mutations, multivariate analysis: HR = 1.818; 95% CI: 1.153–2.869; P = 0.010); (high-risk vs wild-type, multivariate analysis: HR = 1.857; 95% CI: 1.277–2.702; P = 0.001); (low-risk vs wild-type, multivariate analysis: HR = 1.005; 95% CI: 0.596–1.695; P = 0.986) (Fig. 5b). The results of Bonferroni post hoc multiple comparisons for both multivariate survival analyses are reported in Supplementary Table 5A/B. Harrell's C-statistic, Akaike information criterion (AIC) and Bayesian information criterion (BIC) were then used to compare the predictive performance of our model with the PA algorithm. C-statistic, AIC and BIC resulted to be 0.5400, 1829.253 and 1837.29, respectively, using the PA. The results for our model reported a Harrell's C-statistic of 0.5700, AIC of 1819.828 and BIC of 1823.847. These results showed that our model performed better than the one published by Poeta (Very strong improvement  $\Delta$ BIC = 13.443).[207] The newly developed algorithm was applied to each subsite, namely OC, OP and L, as well as lung and oesophagus (HP was excluded because of the small number of samples available). As mentioned above, the dichotomous classification of mutational status was an independent prognostic factor only in OP. PA and our algorithm also performed well in this subgroup (PA: wild-type vs disruptive, multivariate analysis: HR = 0.082; 95% CI: 0.017–0.385; P = 0.002; our algorithm: wild-type vs high-risk, multivariate analysis: HR = 0.082; 95% CI: 0.017–0.402; P = 0.002). In OSCC, PA failed to find any significant prognostic class (wildtype vs disruptive, multivariate analysis: HR = 0.771; 95% CI: 0.483–1.232; P = 0.277 and conservative vs disruptive mutations, multivariate analysis: HR = 0.815; 95% CI: 0.520–1.277; P = 0.372); meanwhile, our algorithm found a class of mutation with a better overall survival (wild-type vs high-risk, multivariate analysis: HR = 0.714; 95% CI: 0.458–1.113; P = 0.137); (low-risk vs high-risk, multivariate analysis: HR = 0.499; 95% CI: 0.283–0.878; P = 0.016). In L and oesophagus, both algorithms failed to find any significant results, while lung tumours showed a unique behaviour. Specifically, wild-type p53 was associated with a worse overall survival compared with the whole group of patients carrying mutations (multivariate analysis: HR =

1.572; 95% CI: 1.080–2.287; P = 0.018). When the PA was applied, it emerged that patients with disruptive mutations had a better overall survival, compared both with wild-type (multivariate analysis: HR = 1.791; 95% CI: 1.186–2.707; P = 0.006) and nondisruptive mutated patients (multivariate analysis: HR = 1.296; 95% CI: 0.939–1.790; P = 0.115). Our algorithm, meanwhile, was able to distinguish a group of high-risk mutations (multivariate analysis: HR = 0.803; 95% CI: 0.537–1.201; P = 0.286), although wild-type patients still reported the worst overall survival compared with low risk of death mutations (multivariate analysis: HR = 1.496; 95% CI: 1.019–2.197; P = 0.040). The results from both algorithms in each subsite are summarised in Fig. 6.

Clinic-pathological covariates	Sig.	Hazard ratio	95% CI	
			Lower limit	Upper limit
PA				
Wild-type vs disruptive	0.277	0.771	0.483	1.232
Conservative vs disruptive	0.372	0.815	0.520	1.277
Our algorithm				
Wild-type vs high-risk	0.137	0.714	0.458	1.113
Low-risk vs high-risk	0.016	0.499	0.283	0.878

Clinic-pathological covariates	Sig.	Hazard ratio	95% CI	
			Lower limit	Upper limit
PA				
Wild-type vs disruptive	0.002	0.082	0.017	0.385
Conservative vs disruptive	0.842	0.848	0.167	4.301
Our algorithm				
Wild-type vs high-risk	0.002	0.082	0.017	0.402
Low-risk vs high-risk	0.885	0.900	0.217	3.735

Clinic-pathological covariates	Sig.	Hazard ratio	95% CI	
			Lower limit	Upper limit
PA				
Wild-type vs disruptive	0.217	0.359	0.070	1.828
Conservative vs disruptive	0.208	1.651	0.757	3.602
Our algorithm				
Wild-type vs high-risk	0.100	0.267	0.055	1.289
Low-risk vs high-risk	0.703	0.818	0.293	1.289

Clinic-pathological covariates	Sig.	Hazard ratio	95% CI	
			Lower limit	Upper limit
PA				
Wild-type vs disruptive	0.006	1.791	1.186	2.707
Conservative vs disruptive	0.115	1.296	0.939	1.790
Our algorithm				
Wild-type vs high-risk	0.040	1.496	0.019	2.197
Low-risk vs high-risk	0.286	0.803	0.537	1.201

Clinic-pathological covariates	Sig.	Hazard ratio	95% CI	
			Lower limit	Upper limit
PA				
Wild-type vs disruptive	0.686	0.706	0.130	3.823
Conservative vs disruptive	0.855	1.092	0.424	2.817
Our algorithm				
Wild-type vs high-risk	0.674	0.699	0.132	3.706
Low-risk vs high-risk	0.681	1.258	0.421	3.761

Fig. 6: Overall survival of Poeta's versus our new proposed classification system. Multivariate survival analysis in patient with squamous cell carcinoma of: oral cavity (a); oropharynx (b); larynx (c); lung (d) and oesophagus (e). Differences in survival are shown according to Poeta's algorithm (PA) and to our new algorithm.

## 6.4 Discussion

Many efforts have been made to classify mutations according to their influence on structural changes, and to investigate if they serve as prognostic factors, but limits have been identified due to the wideness of the mutational landscape of TP53. In this study, we propose a new classification method that identifies patients with mutations at high risk of death in squamous

cell cancers and, in particular, in tumours from the head and neck district. Of the 14 million new cancers diagnosed worldwide every year, 50–60% is characterised by at least one somatic variant of p53.[184] In the HNSCC cohort from TCGA included in this study, 69.9% of patients expressed a mutation in TP53. A web platform has been created to collect and organise the increasing number of researches published about TP53 in cancer (<http://www.p53.fr/>).[186] Due to the increase in detection of single mutations in TP53 gene, several studies have attempted to elucidate the correlation between mutational status and patients' clinicopathological characteristics, with discordant results. Most published studies have employed different classifications and mutation profiles for their analyses. This is a reasonable approach, since a broad range of mutations can affect the TP53 gene and its encoded protein; for example, the 286 HNSCC patients included in our study exhibited 129 different kinds of mutation, of which R273 was the most frequent but occurred in only 13 patients. One of the simplest and most used approach to translate TP53 mutational profile into clinically useful information is to compare wild-type and mutated patients, with the latter subgroup predicting death in different types of cancers. An extensive analysis of 33 TCGA studies showed that the effects of TP53 mutations on patients' prognosis were statistically significant in nine malignancies (lung adenocarcinoma, hepatocellular carcinoma, HNSCC, acute myeloid leukaemia, clear-cell renal cell carcinoma (RCC), papillary RCC, chromophobe RCC, uterine endometrial carcinoma and thymoma).[191] Although this method can be considered “quick and useful”, this approach does not take into account some biochemical and functional characteristics of single TP53 mutations. A previous comprehensive genomic study on the same TCGA cohort provided fundamental insights into the correlation between mutational profile of TP53 and HNSCC; however it did not take into consideration the anatomical sublocalisation of tumours in the HNSCC area, in which HPVpositive oropharynx subgroup frequently exhibits wild-type TP53 and favourable prognosis.[202] After integrating the survival analysis according to the subsite of

HNSCC onset, mutated TP53 resulted to be an independent prognostic factor for overall and diseasefree survival only in OP. These results have salient clinical implications, because, cells with wild-type or higher TP53 expression are more susceptible to radiation therapy, and HPV+ tumours usually display higher radiosensitivity.[208] Therefore, our data suggest that mutations in TP53 gene have a prognostic role in HNSCC, above all, in HPV+ OP tumours where mutational status of this gene should be investigated before considering treatment options.[209] These findings could let us speculate that mutations affecting TP53 in HPV+ tumours make them more similar to HPV- HNSCCs. Although this hypothesis should be analysed in future studies, the results of network analysis showed that MUT OP shared common alterations with other subgroups, in particular homozygous deletions and mutations affecting CDKN2A (78.9% of patients in MUT OP against 13.6% mRNA upregulation in WT OP). Because of the interaction between HPV E7 protein and host cells, CDKN2A mRNA upregulation was also observed in HPV+ tumours arising in the oropharynx. As it is known, HPV E7 protein ubiquitinates the protein of retinoblastoma (pRb) by binding to the cullin 2 ubiquitin ligase complex. Loss of pRb leads to the release of E2F with the transcription of S-phase genes. Hence, HPV+ tumours show an upregulation of CDKN2A as a consequence of negative feedback loop to control cell cycle, from pRb loss.[210] In addition, CX3CL1 and MYB shared common alteration (mRNA upregulation) both in WT OP and HPV+ OP, leading to a positive regulation of transforming growth factor beta production. They could be involved in a cell-response mechanism due to the effect of E7 proteins. It is reported that E7 is able to prevent both Smad transcriptional activity and the ability of TGF- $\beta$  to inhibit DNA synthesis.[211] MYB has been shown to be related to HPV infection, above all in cervical cancer,[212, 213] but its role, together with CX3CL1, has never been elucidated in OP. It is worth noting that BRCA1 was also upregulated in WT OP patients and HPV+ tumours (29.5% and 29.6%, respectively). From our network analysis, BRCA1 was present in both subgroups in complex with the proliferating cell

nuclear antigen (PCNA). PCNA is a protein produced in S phase of the cell cycle, and it acts in replication and repair machinery, favouring the cell-cycle progression.[214] PCNA seems to be an important factor for progression to malignancy in HPV+ tumours, by activation of S phase of the cell cycle.[215] BRCA1 is involved in genome-integrity machinery and cell-cycle checkpoint control.[216] BRCA1 plays a critical role in homologous recombination repair, and cells with deficiency in BRCA1 are more sensible to drugs causing DNA breaks or to ionizing radiation.[217] Tian et al. showed that BRCA1 leads to mono- and polyubiquitination of PCNA by recruiting some effector proteins. It is reported that PCNA monoubiquitylation is necessary for efficient translesion synthesis. Through this mechanism, BRCA1 promotes translesion DNA synthesis and progression of the cell cycle.[218, 219] Taken together, these findings suggest that BRCA1 mRNA upregulation with PCNA could have an important role in HPV + tumours of oropharynx and in chemo-radioresistance of these patients, by promoting translesion DNA synthesis and cell-cycle progression, changing its classical function as tumour suppressor to an oncogene, as already reported in cancer stem cell models of different kinds of tumours.[220] Similar to what was performed in the previously cited genomic analysis,[220] Poeta et al.[206] applied their algorithm only for the whole HNSCC cohort without investigating the results for each subgroup. The reported algorithm was able to prognostically stratify HNSCC patients; in particular, using the wild-type group as reference, only tumours with disruptive mutations showed a worse overall survival, whereas patients with conservative or nondisruptive mutations did not. Similar results were obtained in this study by applying the PA on the TCGA HNSCC cohort (Fig. 5). In addition, conservative mutations were also linked to a worse overall survival, although without differences between disruptive and nondisruptive mutations. Starting from the findings of Poeta et al, we developed our own algorithm reclassifying mutations in high risk of death according to their homozygous alteration, their zinc ligand and H<sup>+</sup>-forming bond alteration. Martin et al. and Baker et al.[200, 201] already stressed the important role of

hydrogen bonding in protein residues. Hence, for example, the mutation Y220C is considered nondisruptive in the PA, since in its tertiary structure, this residue is located far from the functional part. This mutation was reclassified as high risk since tyrosine (Y) is able to create a hydrogen bonding, conversely to what happens when substituted by a cysteine (C). The same can be stated for the residues involved in the zinc ligand, since it is important for the stabilisation of the p53/DNA complex.[200] At last, mutations affecting residues in “unknown” predicted secondary structure were considered as high risk. Comparing the predictive capability of the two algorithms on the TCGA database, our model outperformed the PA. In particular, our classifier was able to better stratify a cohort of patients with higher risk of death, comparing it with both wildtype and nondisruptive mutation groups, while the PA was not able to find a significant difference between nondisruptive and disruptive mutations (Fig. 5). Subsequently, we investigated the predictive performance of both algorithms in each subgroup. Of interest, PA failed to find any significant prognostic class in OSCC, where the new model found a class of mutations with a better overall survival (wild-type vs high-risk, multivariate analysis: HR = 0.714; 95% CI: 0.458–1.113; P = 0.137); (low-risk vs high-risk, multivariate analysis: HR = 0.499; 95% CI: 0.283–0.878; P = 0.016). However, both algorithms failed to find any significant prognostic factor in larynx, with contradictory results in lung and oesophageal cancer. A meta-analysis, published in 2015,[221] reported the same conflicting results in non-small-cell lung carcinoma, since TP53 mutations emerged to be associated with a worse overall survival compared with wild type. Although the meta-analysis included all patients with non-small-cell lung carcinoma, when performing subgroup analysis, only patients with early stages and affected by adenocarcinoma, took advantage of the wild-type status. The same results were reported in other studies.[222, 223] Molina-Vila et al.[224] were the only to apply Poeta et al. classification[206] in a cohort of advanced-stage non-small-cell lung cancer; only nondisruptive mutations were associated with a shorter survival. Our results

cannot be compared, since we included only patients with squamous cell carcinoma, and our cohort consisted of only 80/438 patients with advanced stage (III–IV); because of these promising results, we included all patients in a whole cohort, including patients with head and neck-, oesophageal- and lung squamous cell carcinoma. Patients included in the survival analysis were 914 with complete data about survival status, follow-up time, mutational status, staging, age and gender (grading was removed because it was only available for head and neck patients). Of these, 249 were from oral cavity, 62 from oropharynx, 89 from larynx, 9 from hypopharynx, 72 oesophageal cancers and 433 lung squamous cell cancers. In the multivariate Cox regression model, the dichotomous mutational status (WT/MUT) did not correlate with overall survival (multivariate analysis: HR = 1.174; 95% CI: 0.912–1.511; P = 0.214); we therefore applied both classification systems on the new cohort. PA failed to find any significant association between disruptive and conservative mutations with the overall survival (wild-type vs disruptive mutations, multivariate analysis: HR = 1.125; 95% CI: 0.856–1.478; P = 0.397) (wild-type vs nondisruptive mutations, multivariate analysis: HR = 1.239; 95% CI: 0.937–1.639; P = 0.133). Nondisruptive mutations showed even a worse overall survival compared with disruptive mutations (nondisruptive vs disruptive mutations, multivariate analysis: HR = 1.101; 95% CI: 0.880–1.378; P = 0.399). Conversely, the new proposed algorithm showed a better predictive performance; in particular, patients in the high-risk group showed a worse prognosis, while the low-risk group showed even a better overall survival compared with wild type (wild-type vs high-risk mutations, multivariate analysis: HR = 1.283; 95% CI: 0.991–1.663; P = 0.059); (wild-type vs low-risk mutations, multivariate analysis: HR = 0.881; 95% CI: 0.629–1.236; P = 0.464); (low- vs high-risk mutations, multivariate analysis: HR = 0.687; 95% CI: 0.518–0.911; P = 0.009).

For the first time, our study elucidated the mutational profile of TP53 gene in HNSCC subgroups. To the best of our knowledge, this was the first study to link different molecular aspects of TP53 alterations (mutational profile of TP53, coding gene structure, secondary

structure and well-known hotspot mutations) to the clinical variables of HNSCC patients. Although most tumours arising from the mucosa of the head and neck district are studied together, the results from this study clearly show differences between the OC, OP and L subsites in terms of mutational profile and signalling pathways of TP53. Furthermore, this study suggests that there is a broad range of TP53 residues that could be mutated in HNSCC, which may determine differential effects in terms of mRNA and protein expression, secondary structure, apoptosis activity and DNA-binding affinity. This finding makes it difficult to develop drugs that target selective mutations of TP53 as these would have little implications in the clinical management of HNSCC patients. Finally, whilst this study indicates a prognostic role of TP53 mutations in HNSCC, the influence of TP53 status in cancer prognosis more broadly is still controversial and large, and well-standardised studies are needed.

## **7. CONCLUSIONS**

The use of nutraceuticals is increasingly being investigated for the prevention and therapy of tumors. Fermented Wheat Germ Extract has been tested in vitro on various tumor cell lines. From the experiments conducted and presented in this thesis, FWGE seems to give promising results in the inhibition of cell growth of OSCC cells and in the inhibition of their capacity for migration and invasion. Further research is needed to evaluate its action on normal human cells and to understand the mechanism of action on OSCC cells.

The search for prognostic and therapeutic factors for oral cancer remains a challenge. As emerged from the researches conducted, the OSCC has peculiarities that differentiate it from other types of tumors. For this reason, prognostic factors and/or therapeutic targets that have been identified to be characteristic of some tumors, cannot necessarily be translated into the oral cavity. In particular, summarizing the main results of presented researches, following conclusions can be drawn:

- The role of MSI2 expression in OSCC seems to be not so closely correlated with prognosis, as in other solid and blood tumors. The MSI2 mRNA expression in oral cancer is higher in males and it is correlated with tumor grade. The protein expression of MSI2 in OSCC samples is relatively low, but significantly correlated with Cyclin D1 expression. Further studies are necessary to investigate its role in OSCC genesis, progression, and prognosis.
- High PD-L1 expression did not correlate with poor prognosis of patients suffering for OSCC. The studies published on the topic showed a significant variation in results. Hence, results from the current available literature limit the use of PD-L1 expression by immunohistochemistry as prognostic biomarker in clinical practice. Higher levels of PD-L1 expression are more frequent in females than in males, and such factor should encourage future studies on the sex-related role of this biomarker.
- The mutational profile of TP53 may serve as an independent prognostic factor in HNSCC patients, and is associated with distinctive site-specific biological networks.

## REFERENCES

1. Malvezzi, M., et al., *European cancer mortality predictions for the year 2011*. Ann Oncol, 2011. **22**(4): p. 947-956.
2. Shield, K.D., et al., *The global incidence of lip, oral cavity, and pharyngeal cancers by subsite in 2012*. CA Cancer J Clin, 2017. **67**(1): p. 51-64.
3. Bray, F., et al., *Global cancer statistics 2018: GLOBOCAN estimates of incidence and mortality worldwide for 36 cancers in 185 countries*. CA Cancer J Clin, 2018. **68**(6): p. 394-424.
4. de Martel, C., et al., *Global burden of cancer attributable to infections in 2018: a worldwide incidence analysis*. Lancet Glob Health, 2020. **8**(2): p. e180-e190.
5. Taghavi, N. and I. Yazdi, *Prognostic factors of survival rate in oral squamous cell carcinoma: clinical, histologic, genetic and molecular concepts*. Arch Iran Med, 2015. **18**(5): p. 314-9.
6. Almangush, A., et al., *Prognostic impact of tumour-stroma ratio in early-stage oral tongue cancers*. Histopathology, 2018. **72**(7): p. 1128-1135.
7. Troiano, G., et al., *Prognostic significance of CD68(+) and CD163(+) tumor associated macrophages in head and neck squamous cell carcinoma: A systematic review and meta-analysis*. Oral Oncol, 2019. **93**: p. 66-75.
8. Caponio, V.C.A., et al., *Computational analysis of TP53 mutational landscape unveils key prognostic signatures and distinct pathobiological pathways in head and neck squamous cell cancer*. Br J Cancer, 2020. **123**(8): p. 1302-1314.
9. Troiano, G., et al., *High PD-L1 expression in the tumour cells did not correlate with poor prognosis of patients suffering for oral squamous cells carcinoma: A meta-analysis of the literature*. Cell Prolif, 2019. **52**(2): p. e12537.
10. Le Champion, A., et al., *Low Survival Rates of Oral and Oropharyngeal Squamous Cell Carcinoma*. Int J Dent, 2017. **2017**: p. 5815493.
11. Dirven, R., et al., *Tumor thickness versus depth of invasion - Analysis of the 8th edition American Joint Committee on Cancer Staging for oral cancer*. Oral Oncol, 2017. **74**: p. 30-33.
12. Bitu, C.C., et al., *HOXA1 is overexpressed in oral squamous cell carcinomas and its expression is correlated with poor prognosis*. BMC Cancer, 2012. **12**: p. 146.
13. Lau, A., et al., *Induction chemotherapy for squamous cell carcinomas of the oral cavity: A cumulative meta-analysis*. Oral Oncol, 2016. **61**: p. 104-14.
14. Rogers, S.N., et al., *Survival following primary surgery for oral cancer*. Oral Oncol, 2009. **45**(3): p. 201-11.
15. Lindemann, A., et al., *Targeting the DNA Damage Response in OSCC with TP53 Mutations*. J Dent Res, 2018. **97**(6): p. 635-644.

16. Shapiro, C.L., *Highlights of Recent Findings on Quality-of-Life Management for Patients With Cancer and Their Survivors*. JAMA Oncol, 2016. **2**(11): p. 1401-1402.
17. Wu, X., J. Cheng, and X. Wang, *Dietary Antioxidants: Potential Anticancer Agents*. Nutr Cancer, 2017. **69**(4): p. 521-533.
18. Perrone, D., et al., *Biological and therapeutic activities, and anticancer properties of curcumin*. Exp Ther Med, 2015. **10**(5): p. 1615-1623.
19. Ardito, F., et al., *In vitro study on anti-cancer properties of genistein in tongue cancer*. Onco Targets Ther, 2017. **10**: p. 5405-5415.
20. Ahmad, A., et al., *Molecular targets of naturopathy in cancer research: bridge to modern medicine*. Nutrients, 2015. **7**(1): p. 321-34.
21. Harvie, M., *Nutritional supplements and cancer: potential benefits and proven harms*. Am Soc Clin Oncol Educ Book, 2014: p. e478-86.
22. Telekes, A., et al., *Avemar (wheat germ extract) in cancer prevention and treatment*. Nutr Cancer, 2009. **61**(6): p. 891-9.
23. O'Brien, P.J., *Molecular mechanisms of quinone cytotoxicity*. Chem Biol Interact, 1991. **80**(1): p. 1-41.
24. Piccart-Gebhart, M.J., *Anthracyclines and the tailoring of treatment for early breast cancer*. N Engl J Med, 2006. **354**(20): p. 2177-9.
25. Johannung, G.L. and F. Wang-Johannung, *Efficacy of a medical nutriment in the treatment of cancer*. Altern Ther Health Med, 2007. **13**(2): p. 56-63; quiz 64-5.
26. Iyer, A. and L. Brown, *Fermented wheat germ extract (avemar) in the treatment of cardiac remodeling and metabolic symptoms in rats*. Evid Based Complement Alternat Med, 2011. **2011**: p. 508957.
27. Boros, L.G., M. Nichelatti, and Y. Shoenfeld, *Fermented wheat germ extract (Avemar) in the treatment of cancer and autoimmune diseases*. Ann N Y Acad Sci, 2005. **1051**: p. 529-42.
28. Demidov, L.V., et al., *Adjuvant fermented wheat germ extract (Avemar) nutraceutical improves survival of high-risk skin melanoma patients: a randomized, pilot, phase II clinical study with a 7-year follow-up*. Cancer Biother Radiopharm, 2008. **23**(4): p. 477-82.
29. Jakab, F., et al., *A medical nutriment has supportive value in the treatment of colorectal cancer*. Br J Cancer, 2003. **89**(3): p. 465-9.
30. Yang, M.D., et al., *Inhibitory Effects of AVEMAR on Proliferation and Metastasis of Oral Cancer Cells*. Nutr Cancer, 2016. **68**(3): p. 473-80.
31. Gatenby, R.A. and R.J. Gillies, *Why do cancers have high aerobic glycolysis?* Nat Rev Cancer, 2004. **4**(11): p. 891-9.
32. Illmer, C., et al., *Immunologic and biochemical effects of the fermented wheat germ extract Avemar*. Exp Biol Med (Maywood), 2005. **230**(2): p. 144-9.

33. Hidvegi, M., et al., *Effect of Avemar and Avemar + vitamin C on tumor growth and metastasis in experimental animals*. *Anticancer Res*, 1998. **18**(4A): p. 2353-8.
34. Saiko, P., et al., *Avemar, a nontoxic fermented wheat germ extract, attenuates the growth of sensitive and 5-FdUrd/Ara-C cross-resistant H9 human lymphoma cells through induction of apoptosis*. *Oncol Rep*, 2009. **21**(3): p. 787-91.
35. Comin-Anduix, B., et al., *Fermented wheat germ extract inhibits glycolysis/pentose cycle enzymes and induces apoptosis through poly(ADP-ribose) polymerase activation in Jurkat T-cell leukemia tumor cells*. *J Biol Chem*, 2002. **277**(48): p. 46408-14.
36. Hidvegi, M., et al., *MSC, a new benzoquinone-containing natural product with antimetastatic effect*. *Cancer Biother Radiopharm*, 1999. **14**(4): p. 277-89.
37. Liberati, A., et al., *The PRISMA statement for reporting systematic reviews and meta-analyses of studies that evaluate health care interventions: explanation and elaboration*. *J Clin Epidemiol*, 2009. **62**(10): p. e1-34.
38. Fajka-Boja, R., et al., *Fermented wheat germ extract induces apoptosis and downregulation of major histocompatibility complex class I proteins in tumor T and B cell lines*. *Int J Oncol*, 2002. **20**(3): p. 563-70.
39. Imir, N.G., E. Aydemir, and E. Simsek, *Mechanism of the anti-angiogenic effect of Avemar on tumor cells*. *Oncol Lett*, 2018. **15**(2): p. 2673-2678.
40. Judson, P.L., et al., *Characterizing the efficacy of fermented wheat germ extract against ovarian cancer and defining the genomic basis of its activity*. *Int J Gynecol Cancer*, 2012. **22**(6): p. 960-7.
41. Marcsek, Z., et al., *The efficacy of tamoxifen in estrogen receptor-positive breast cancer cells is enhanced by a medical nutriment*. *Cancer Biother Radiopharm*, 2004. **19**(6): p. 746-53.
42. Mueller, T., K. Jordan, and W. Voigt, *Promising cytotoxic activity profile of fermented wheat germ extract (Avemar(R)) in human cancer cell lines*. *J Exp Clin Cancer Res*, 2011. **30**: p. 42.
43. Otto, C., et al., *Antiproliferative and antimetabolic effects behind the anticancer property of fermented wheat germ extract*. *BMC Complement Altern Med*, 2016. **16**: p. 160.
44. Saiko, P., et al., *Avemar, a nontoxic fermented wheat germ extract, induces apoptosis and inhibits ribonucleotide reductase in human HL-60 promyelocytic leukemia cells*. *Cancer Lett*, 2007. **250**(2): p. 323-8.
45. Tai, C.J., et al., *Fermented wheat germ extract induced cell death and enhanced cytotoxicity of Cisplatin and 5-Fluorouracil on human hepatocellular carcinoma cells*. *Evid Based Complement Alternat Med*, 2013. **2013**: p. 121725.
46. Wang, C.W., et al., *Preclinical evaluation on the tumor suppression efficiency and combination drug effects of fermented wheat germ extract in human ovarian carcinoma cells*. *Evid Based Complement Alternat Med*, 2015. **2015**: p. 570785.

47. Zhang, J.Y., et al., *Effect of fermented wheat germ extract with lactobacillus plantarum dy-1 on HT-29 cell proliferation and apoptosis*. J Agric Food Chem, 2015. **63**(9): p. 2449-57.
48. Barisone, G.A., et al., *A purified, fermented, extract of Triticum aestivum has lymphomacidal activity mediated via natural killer cell activation*. PLoS One, 2018. **13**(1): p. e0190860.
49. Szende, B., et al., *Effect of simultaneous administration of Avemar® and cytostatic drugs on viability of cell cultures, growth of experimental tumors, and survival of tumor-bearing mice*. Cancer Biotherapy and Radiopharmaceuticals, 2004. **19**(3): p. 343-349.
50. Boros, L.G., et al., *Wheat germ extract decreases glucose uptake and RNA ribose formation but increases fatty acid synthesis in MIA pancreatic adenocarcinoma cells*. Pancreas, 2001. **23**(2): p. 141-147.
51. Szende, B., et al., *Effect of simultaneous administration of Avemar and cytostatic drugs on viability of cell cultures, growth of experimental tumors, and survival tumor-bearing mice*. Cancer Biother Radiopharm, 2004. **19**(3): p. 343-9.
52. Heimbach, J.T., et al., *Safety studies regarding a standardized extract of fermented wheat germ*. Int J Toxicol, 2007. **26**(3): p. 253-9.
53. Shibuya, N., et al., *Augmented pentose phosphate pathway plays critical roles in colorectal carcinomas*. Oncology, 2015. **88**(5): p. 309-19.
54. Boros, L.G., et al., *Wheat germ extract decreases glucose uptake and RNA ribose formation but increases fatty acid synthesis in MIA pancreatic adenocarcinoma cells*. Pancreas, 2001. **23**(2): p. 141-7.
55. Kudo, Y., et al., *Establishment of an oral squamous cell carcinoma cell line with high invasive and p27 degradation activities from a lymph node metastasis*. Oral Oncol, 2003. **39**(5): p. 515-20.
56. Lo Muzio, L., et al., *Is expression of p120ctn in oral squamous cell carcinomas a prognostic factor?* Oral Surg Oral Med Oral Pathol Oral Radiol, 2013. **115**(6): p. 789-98.
57. Scoditti, E., et al., *Mediterranean diet polyphenols reduce inflammatory angiogenesis through MMP-9 and COX-2 inhibition in human vascular endothelial cells: a potentially protective mechanism in atherosclerotic vascular disease and cancer*. Arch Biochem Biophys, 2012. **527**(2): p. 81-9.
58. Yeend, T., et al., *The effectiveness of fermented wheat germ extract as an adjunct therapy in the treatment of cancer: A systematic review*. JBI Libr Syst Rev, 2012. **10**(42 Suppl): p. 1-12.
59. Kumar, P., A. Nagarajan, and P.D. Uchil, *Analysis of Cell Viability by the MTT Assay*. Cold Spring Harb Protoc, 2018. **2018**(6).
60. Salo, T., et al., *A novel human leiomyoma tissue derived matrix for cell culture studies*. BMC cancer, 2015. **15**(1): p. 981.

61. Salo, T., et al., *Organotypic three-dimensional assays based on human leiomyoma-derived matrices*. Philosophical Transactions of the Royal Society B: Biological Sciences, 2017. **373**(1737): p. 20160482.
62. Naakka, E., et al., *Fully human tumor-based matrix in three-dimensional spheroid invasion assay*. JoVE (Journal of Visualized Experiments), 2019(147): p. e59567.
63. Schindelin, J., et al., *Fiji: an open-source platform for biological-image analysis*. Nat Methods, 2012. **9**(7): p. 676-82.
64. Xie, M., et al., *Whole Grain Consumption for the Prevention and Treatment of Breast Cancer*. Nutrients, 2019. **11**(8).
65. Vernieri, C., et al., *Diet and supplements in cancer prevention and treatment: Clinical evidences and future perspectives*. Crit Rev Oncol Hematol, 2018. **123**: p. 57-73.
66. Aquino, I.G., et al., *Anticancer properties of the fatty acid synthase inhibitor TVB-3166 on oral squamous cell carcinoma cell lines*. Arch Oral Biol, 2020. **113**: p. 104707.
67. Zhurakivska, K., et al., *The Effects of Adjuvant Fermented Wheat Germ Extract on Cancer Cell Lines: A Systematic Review*. Nutrients, 2018. **10**(10).
68. Teppo, S., et al., *The hypoxic tumor microenvironment regulates invasion of aggressive oral carcinoma cells*. Exp Cell Res, 2013. **319**(4): p. 376-89.
69. Tuomainen, K., et al., *Human Tumor-Derived Matrix Improves the Predictability of Head and Neck Cancer Drug Testing*. Cancers (Basel), 2019. **12**(1).
70. Väyrynen, O., et al., *Effects of ionizing radiation and HPSE1 inhibition on the invasion of oral tongue carcinoma cells on human extracellular matrices in vitro*. Exp Cell Res, 2018. **371**(1): p. 151-161.
71. Vierthaler, M., et al., *Fluctuating role of antimicrobial peptide hCAP18/LL-37 in oral tongue dysplasia and carcinoma*. Oncol Rep, 2020. **44**(1): p. 325-338.
72. Dasari, S. and P.B. Tchounwou, *Cisplatin in cancer therapy: molecular mechanisms of action*. Eur J Pharmacol, 2014. **740**: p. 364-78.
73. Andreadis, C., et al., *5-Fluorouracil and cisplatin in the treatment of advanced oral cancer*. Oral Oncol, 2003. **39**(4): p. 380-5.
74. Galluzzi, L., et al., *Molecular mechanisms of cisplatin resistance*. Oncogene, 2012. **31**(15): p. 1869-83.
75. Feng, X., et al., *The role of NLRP3 inflammasome in 5-fluorouracil resistance of oral squamous cell carcinoma*. J Exp Clin Cancer Res, 2017. **36**(1): p. 81.
76. Pons-Fuster López, E., F. Gómez García, and P. López Jornet, *Combination of 5-Fluorouracil and polyphenol EGCG exerts suppressive effects on oral cancer cells exposed to radiation*. Arch Oral Biol, 2019. **101**: p. 8-12.
77. Kim, E.H., et al., *Targeting Nrf2 with wogonin overcomes cisplatin resistance in head and neck cancer*. Apoptosis, 2016. **21**(11): p. 1265-1278.

78. Fritzell, K., et al., *ADARs and editing: The role of A-to-I RNA modification in cancer progression*. Semin Cell Dev Biol, 2018. **79**: p. 123-130.
79. Soni, S., P. Anand, and Y.S. Padwad, *MAPKAPK2: the master regulator of RNA-binding proteins modulates transcript stability and tumor progression*. J Exp Clin Cancer Res, 2019. **38**(1): p. 121.
80. Kudinov, A.E., et al., *Musashi-2 (MSI2) supports TGF-beta signaling and inhibits claudins to promote non-small cell lung cancer (NSCLC) metastasis*. Proc Natl Acad Sci U S A, 2016. **113**(25): p. 6955-60.
81. Zhan, Y., et al., *Long non-coding RNA DANCR promotes malignant phenotypes of bladder cancer cells by modulating the miR-149/MSI2 axis as a ceRNA*. J Exp Clin Cancer Res, 2018. **37**(1): p. 273.
82. Yang, Z., et al., *Increased musashi 2 expression indicates a poor prognosis and promotes malignant phenotypes in gastric cancer*. Oncol Lett, 2019. **17**(3): p. 2599-2606.
83. Liu, Y., et al., *Musashi-2 is a prognostic marker for the survival of patients with cervical cancer*. Oncol Lett, 2018. **15**(4): p. 5425-5432.
84. Santarius, T., et al., *A census of amplified and overexpressed human cancer genes*. Nat Rev Cancer, 2010. **10**(1): p. 59-64.
85. Ramos-Garcia, P., et al., *An update on the implications of cyclin D1 in oral carcinogenesis*. Oral Dis, 2017. **23**(7): p. 897-912.
86. Casper, J., et al., *The UCSC Genome Browser database: 2018 update*. Nucleic Acids Res, 2018. **46**(D1): p. D762-D769.
87. Gao, J., et al., *Integrative analysis of complex cancer genomics and clinical profiles using the cBioPortal*. Sci Signal, 2013. **6**(269): p. p11.
88. Grossman, R.L., et al., *Toward a Shared Vision for Cancer Genomic Data*. N Engl J Med, 2016. **375**(12): p. 1109-12.
89. McShane, L.M., et al., *REporting recommendations for tumor MARKer prognostic studies (REMARK)*. Breast cancer research and treatment, 2006. **100**(2): p. 229-235.
90. Detre, S., G. Saclani Jotti, and M. Dowsett, *A "quickscore" method for immunohistochemical semiquantitation: validation for oestrogen receptor in breast carcinomas*. J Clin Pathol, 1995. **48**(9): p. 876-8.
91. Ferlay, J., et al., *Cancer incidence and mortality worldwide: sources, methods and major patterns in GLOBOCAN 2012*. Int J Cancer, 2015. **136**(5): p. E359-86.
92. Feller, L.L., et al., *Oral squamous cell carcinoma in relation to field precancerisation: pathobiology*. Cancer Cell Int, 2013. **13**(1): p. 31.
93. Tonella, L., et al., *Gene Expression Signatures for Head and Neck Cancer Patient Stratification: Are Results Ready for Clinical Application?* Curr Treat Options Oncol, 2017. **18**(5): p. 32.

94. Chin, L., J.N. Andersen, and P.A. Futreal, *Cancer genomics: from discovery science to personalized medicine*. Nat Med, 2011. **17**(3): p. 297-303.
95. Kudinov, A.E., et al., *Musashi RNA-Binding Proteins as Cancer Drivers and Novel Therapeutic Targets*. Clin Cancer Res, 2017. **23**(9): p. 2143-2153.
96. Kang, M.H., et al., *Musashi RNA-binding protein 2 regulates estrogen receptor 1 function in breast cancer*. Oncogene, 2017. **36**(12): p. 1745-1752.
97. Ouyang, S.W., et al., *USP10 regulates Musashi-2 stability via deubiquitination and promotes tumour proliferation in colon cancer*. FEBS Lett, 2019. **593**(4): p. 406-413.
98. Zong, Z., et al., *Musashi2 as a novel predictive biomarker for liver metastasis and poor prognosis in colorectal cancer*. Cancer Med, 2016. **5**(4): p. 623-30.
99. Dong, P., et al., *Musashi-2, a novel oncoprotein promoting cervical cancer cell growth and invasion, is negatively regulated by p53-induced miR-143 and miR-107 activation*. J Exp Clin Cancer Res, 2017. **36**(1): p. 150.
100. Li, Z., et al., *Cyclin D1 regulates cellular migration through the inhibition of thrombospondin 1 and ROCK signaling*. Mol Cell Biol, 2006. **26**(11): p. 4240-56.
101. Zhao, Y., et al., *Cyclin D1 overexpression is associated with poor clinicopathological outcome and survival in oral squamous cell carcinoma in Asian populations: insights from a meta-analysis*. PLoS One, 2014. **9**(3): p. e93210.
102. Knudsen, K.E., et al., *Cyclin D1: polymorphism, aberrant splicing and cancer risk*. Oncogene, 2006. **25**(11): p. 1620-8.
103. Zhang, H., et al., *Musashi2 modulates K562 leukemic cell proliferation and apoptosis involving the MAPK pathway*. Exp Cell Res, 2014. **320**(1): p. 119-27.
104. Han, Y., et al., *Musashi-2 Silencing Exerts Potent Activity against Acute Myeloid Leukemia and Enhances Chemosensitivity to Daunorubicin*. PLoS One, 2015. **10**(8): p. e0136484.
105. Hope, K.J., et al., *An RNAi screen identifies Msi2 and Prox1 as having opposite roles in the regulation of hematopoietic stem cell activity*. Cell Stem Cell, 2010. **7**(1): p. 101-13.
106. Anderson, A.C., N. Joller, and V.K. Kuchroo, *Lag-3, Tim-3, and TIGIT: Co-inhibitory Receptors with Specialized Functions in Immune Regulation*. Immunity, 2016. **44**(5): p. 989-1004.
107. Ferris, R.L., et al., *Nivolumab for Recurrent Squamous-Cell Carcinoma of the Head and Neck*. N Engl J Med, 2016. **375**(19): p. 1856-1867.
108. Kobayashi, M., et al., *Enhanced expression of programmed death-1 (PD-1)/PD-L1 in salivary glands of patients with Sjogren's syndrome*. J Rheumatol, 2005. **32**(11): p. 2156-63.
109. Iwai, Y., et al., *Involvement of PD-L1 on tumor cells in the escape from host immune system and tumor immunotherapy by PD-L1 blockade*. Proc Natl Acad Sci U S A, 2002. **99**(19): p. 12293-7.

110. Urbani, S., et al., *PD-1 expression in acute hepatitis C virus (HCV) infection is associated with HCV-specific CD8 exhaustion*. J Virol, 2006. **80**(22): p. 11398-403.
111. James, E.S., et al., *PDCD1: a tissue-specific susceptibility locus for inherited inflammatory disorders*. Genes Immun, 2005. **6**(5): p. 430-7.
112. Dong, H., et al., *B7-H1, a third member of the B7 family, co-stimulates T-cell proliferation and interleukin-10 secretion*. Nat Med, 1999. **5**(12): p. 1365-9.
113. Ohigashi, Y., et al., *Clinical significance of programmed death-1 ligand-1 and programmed death-1 ligand-2 expression in human esophageal cancer*. Clin Cancer Res, 2005. **11**(8): p. 2947-53.
114. Wu, C., et al., *Immunohistochemical localization of programmed death-1 ligand-1 (PD-L1) in gastric carcinoma and its clinical significance*. Acta Histochem, 2006. **108**(1): p. 19-24.
115. Ghebeh, H., et al., *The B7-H1 (PD-L1) T lymphocyte-inhibitory molecule is expressed in breast cancer patients with infiltrating ductal carcinoma: correlation with important high-risk prognostic factors*. Neoplasia (New York, NY), 2006. **8**(3): p. 190.
116. Hamanishi, J., et al., *Programmed cell death 1 ligand 1 and tumor-infiltrating CD8+ T lymphocytes are prognostic factors of human ovarian cancer*. Proc Natl Acad Sci U S A, 2007. **104**(9): p. 3360-5.
117. Cho, Y.A., et al., *Relationship between the expressions of PD-L1 and tumor-infiltrating lymphocytes in oral squamous cell carcinoma*. Oral Oncol, 2011. **47**(12): p. 1148-53.
118. Tsushima, F., et al., *Predominant expression of B7-H1 and its immunoregulatory roles in oral squamous cell carcinoma*. Oral Oncol, 2006. **42**(3): p. 268-74.
119. Higgins, J. and S. Green, *Cochrane handbook for systematic reviews*. The cochrane collaboration, 2008. **5**(0).
120. Mattox, A.K., et al., *PD-1 Expression in Head and Neck Squamous Cell Carcinomas Derives Primarily from Functionally Anergic CD4(+) TILs in the Presence of PD-L1(+) TAMs*. Cancer Res, 2017. **77**(22): p. 6365-6374.
121. Oliveira-Costa, J.P., et al., *Gene expression patterns through oral squamous cell carcinoma development: PD-L1 expression in primary tumor and circulating tumor cells*. Oncotarget, 2015. **6**(25): p. 20902-20.
122. Altman, D.G., et al., *Reporting Recommendations for Tumor Marker Prognostic Studies (REMARK): explanation and elaboration*. PLoS Med, 2012. **9**(5): p. e1001216.
123. Almangush, A., et al., *Prognostic biomarkers for oral tongue squamous cell carcinoma: a systematic review and meta-analysis*. Br J Cancer, 2017. **117**(6): p. 856-866.
124. Ahn, H., et al., *Clinicopathologic implications of the miR-197/PD-L1 axis in oral squamous cell carcinoma*. Oncotarget, 2017. **8**(39): p. 66178-66194.

125. Kogashiwa, Y., et al., *PD-L1 Expression Confers Better Prognosis in Locally Advanced Oral Squamous Cell Carcinoma*. *Anticancer Res*, 2017. **37**(3): p. 1417-1424.
126. Lin, Y.M., et al., *High PD-L1 Expression Correlates with Metastasis and Poor Prognosis in Oral Squamous Cell Carcinoma*. *PLoS One*, 2015. **10**(11): p. e0142656.
127. Satgunaseelan, L., et al., *Programmed cell death-ligand 1 expression in oral squamous cell carcinoma is associated with an inflammatory phenotype*. *Pathology*, 2016. **48**(6): p. 574-80.
128. Straub, M., et al., *CD274/PD-L1 gene amplification and PD-L1 protein expression are common events in squamous cell carcinoma of the oral cavity*. *Oncotarget*, 2016. **7**(11): p. 12024-34.
129. Hirai, M., et al., *Regulation of PD-L1 expression in a high-grade invasive human oral squamous cell carcinoma microenvironment*. *Int J Oncol*, 2017. **50**(1): p. 41-48.
130. Troeltzsch, M., et al., *Is There Evidence for the Presence and Relevance of the PD-1/PD-L1 Pathway in Oral Squamous Cell Carcinoma? Hints From an Immunohistochemical Study*. *J Oral Maxillofac Surg*, 2017. **75**(5): p. 969-977.
131. Chen, T.C., et al., *Associations among pretreatment tumor necrosis and the expression of HIF-1alpha and PD-L1 in advanced oral squamous cell carcinoma and the prognostic impact thereof*. *Oral Oncol*, 2015. **51**(11): p. 1004-1010.
132. Chen, J., et al., *Interferon-gamma-induced PD-L1 surface expression on human oral squamous carcinoma via PKD2 signal pathway*. *Immunobiology*, 2012. **217**(4): p. 385-93.
133. Foy, J.P., et al., *The immune microenvironment of HPV-negative oral squamous cell carcinoma from never-smokers and never-drinkers patients suggests higher clinical benefit of IDO1 and PD1/PD-L1 blockade*. *Ann Oncol*, 2017. **28**(8): p. 1934-1941.
134. Fuse, H., et al., *Enhanced expression of PD-L1 in oral squamous cell carcinoma-derived CD11b(+)Gr-1(+) cells and its contribution to immunosuppressive activity*. *Oral Oncol*, 2016. **59**: p. 20-29.
135. Hanna, G.J., et al., *Tumor PD-L1 expression is associated with improved survival and lower recurrence risk in young women with oral cavity squamous cell carcinoma*. *Int J Oral Maxillofac Surg*, 2018. **47**(5): p. 568-577.
136. Jiang, C., et al., *Oral squamous cell carcinoma suppressed antitumor immunity through induction of PD-L1 expression on tumor-associated macrophages*. *Immunobiology*, 2017. **222**(4): p. 651-657.
137. Katou, F., et al., *Differing phenotypes between intraepithelial and stromal lymphocytes in early-stage tongue cancer*. *Cancer Res*, 2007. **67**(23): p. 11195-201.
138. Kubota, K., et al., *CD163(+)CD204(+) tumor-associated macrophages contribute to T cell regulation via interleukin-10 and PD-L1 production in oral squamous cell carcinoma*. *Sci Rep*, 2017. **7**(1): p. 1755.

139. Lanzel, E.A., et al., *Predicting PD-L1 expression on human cancer cells using next-generation sequencing information in computational simulation models*. *Cancer Immunol Immunother*, 2016. **65**(12): p. 1511-1522.
140. Malaspina, T.S., et al., *Enhanced programmed death 1 (PD-1) and PD-1 ligand (PD-L1) expression in patients with actinic cheilitis and oral squamous cell carcinoma*. *Cancer Immunol Immunother*, 2011. **60**(7): p. 965-74.
141. Poropatich, K., et al., *Comprehensive T-cell immunophenotyping and next-generation sequencing of human papillomavirus (HPV)-positive and HPV-negative head and neck squamous cell carcinomas*. *J Pathol*, 2017. **243**(3): p. 354-365.
142. Ritprajak, P. and M. Azuma, *Intrinsic and extrinsic control of expression of the immunoregulatory molecule PD-L1 in epithelial cells and squamous cell carcinoma*. *Oral Oncol*, 2015. **51**(3): p. 221-8.
143. Stasikowska-Kanicka, O., M. Wagrowska-Danilewicz, and M. Danilewicz, *Immunohistochemical Analysis of Foxp3(+), CD4(+), CD8(+) Cell Infiltrates and PD-L1 in Oral Squamous Cell Carcinoma*. *Pathol Oncol Res*, 2018. **24**(3): p. 497-505.
144. Takahashi, H., et al., *Cancer-associated fibroblasts promote an immunosuppressive microenvironment through the induction and accumulation of protumoral macrophages*. *Oncotarget*, 2017. **8**(5): p. 8633-8647.
145. Weber, M., et al., *PD-L1 expression in tumor tissue and peripheral blood of patients with oral squamous cell carcinoma*. *Oncotarget*, 2017. **8**(68): p. 112584-112597.
146. Wu, L., et al., *Expression of VISTA correlated with immunosuppression and synergized with CD8 to predict survival in human oral squamous cell carcinoma*. *Cancer Immunol Immunother*, 2017. **66**(5): p. 627-636.
147. Maruse, Y., et al., *Significant association of increased PD-L1 and PD-1 expression with nodal metastasis and a poor prognosis in oral squamous cell carcinoma*. *Int J Oral Maxillofac Surg*, 2018. **47**(7): p. 836-845.
148. Riella, L.V., et al., *Role of the PD-1 pathway in the immune response*. *Am J Transplant*, 2012. **12**(10): p. 2575-87.
149. Parry, R.V., et al., *CTLA-4 and PD-1 receptors inhibit T-cell activation by distinct mechanisms*. *Mol Cell Biol*, 2005. **25**(21): p. 9543-53.
150. Chemnitz, J.M., et al., *SHP-1 and SHP-2 associate with immunoreceptor tyrosine-based switch motif of programmed death 1 upon primary human T cell stimulation, but only receptor ligation prevents T cell activation*. *J Immunol*, 2004. **173**(2): p. 945-54.
151. Nicolini, A., A. Carpi, and G. Rossi, *Cytokines in breast cancer*. *Cytokine Growth Factor Rev*, 2006. **17**(5): p. 325-37.
152. Jingjing, W., et al., *Deubiquitination and stabilization of programmed cell death ligand 1 by ubiquitin-specific peptidase 9, X-linked in oral squamous cell carcinoma*. *Cancer Med*, 2018.

153. Casalupe, F., et al., *Emerging drugs targeting PD-1 and PD-L1: reality or hope?* Expert Opin Emerg Drugs, 2014. **19**(4): p. 557-69.
154. Aguiar, P.N., Jr., et al., *A pooled analysis of nivolumab for the treatment of advanced non-small-cell lung cancer and the role of PD-L1 as a predictive biomarker.* Immunotherapy, 2016. **8**(9): p. 1011-9.
155. Teng, F., et al., *Progress and challenges of predictive biomarkers of anti PD-1/PD-L1 immunotherapy: A systematic review.* Cancer Lett, 2018. **414**: p. 166-173.
156. Ma, G., et al., *The prognostic role of programmed cell death-ligand 1 expression in non-small cell lung cancer patients: An updated meta-analysis.* Clin Chim Acta, 2018. **482**: p. 101-107.
157. Wang, Z., et al., *Prognostic and clinicopathological significance of PD-L1 in patients with renal cell carcinoma: a meta-analysis based on 1863 individuals.* Clin Exp Med, 2018. **18**(2): p. 165-175.
158. Zhang, M., et al., *Expression of PD-L1 and prognosis in breast cancer: a meta-analysis.* Oncotarget, 2017. **8**(19): p. 31347-31354.
159. Tsao, M.S., et al., *PD-L1 protein expression assessed by immunohistochemistry is neither prognostic nor predictive of benefit from adjuvant chemotherapy in resected non-small cell lung cancer.* Ann Oncol, 2017. **28**(4): p. 882-889.
160. Qu, H.X., et al., *Clinicopathological and prognostic significance of programmed cell death ligand 1 (PD-L1) expression in patients with esophageal squamous cell carcinoma: a meta-analysis.* J Thorac Dis, 2016. **8**(11): p. 3197-3204.
161. Zhong, A., et al., *Prognostic value of programmed cell death-ligand 1 expression in patients with non-small-cell lung cancer: evidence from an updated meta-analysis.* Onco Targets Ther, 2015. **8**: p. 3595-601.
162. Li, J., P. Wang, and Y. Xu, *Prognostic value of programmed cell death ligand 1 expression in patients with head and neck cancer: A systematic review and meta-analysis.* PLoS One, 2017. **12**(6): p. e0179536.
163. Topalian, S.L., et al., *Mechanism-driven biomarkers to guide immune checkpoint blockade in cancer therapy.* Nat Rev Cancer, 2016. **16**(5): p. 275-87.
164. Taube, J.M., et al., *Colocalization of inflammatory response with B7-h1 expression in human melanocytic lesions supports an adaptive resistance mechanism of immune escape.* Sci Transl Med, 2012. **4**(127): p. 127ra37.
165. Teng, M.W., et al., *Classifying Cancers Based on T-cell Infiltration and PD-L1.* Cancer Res, 2015. **75**(11): p. 2139-45.
166. Lyford-Pike, S., et al., *Evidence for a role of the PD-1:PD-L1 pathway in immune resistance of HPV-associated head and neck squamous cell carcinoma.* Cancer Res, 2013. **73**(6): p. 1733-41.
167. Bigras, G., et al., *Small Biopsies Misclassify up to 35% of PD-L1 Assessments in Advanced Lung Non-Small Cell Lung Carcinomas.* Appl Immunohistochem Mol Morphol, 2018.

168. De Meulenaere, A., et al., *Importance of choice of materials and methods in PD-L1 and TIL assessment in oropharyngeal squamous cell carcinoma*. *Histopathology*, 2018.
169. Scorer, P., et al., *Consistency of tumor and immune cell programmed cell death ligand-1 expression within and between tumor blocks using the VENTANA SP263 assay*. *Diagn Pathol*, 2018. **13**(1): p. 47.
170. Silva, M.A., et al., *PD-L1 immunostaining scoring for non-small cell lung cancer based on immunosurveillance parameters*. *PLoS One*, 2018. **13**(6): p. e0196464.
171. Azuma, K., et al., *Association of PD-L1 overexpression with activating EGFR mutations in surgically resected nonsmall-cell lung cancer*. *Ann Oncol*, 2014. **25**(10): p. 1935-40.
172. D'Incecco, A., et al., *PD-1 and PD-L1 expression in molecularly selected non-small-cell lung cancer patients*. *Br J Cancer*, 2015. **112**(1): p. 95-102.
173. Akbay, E.A., et al., *Activation of the PD-1 pathway contributes to immune escape in EGFR-driven lung tumors*. *Cancer Discov*, 2013. **3**(12): p. 1355-63.
174. Conforti, F., et al., *Cancer immunotherapy efficacy and patients' sex: a systematic review and meta-analysis*. *Lancet Oncol*, 2018. **19**(6): p. 737-746.
175. Leemans, C.R., B.J. Braakhuis, and R.H. Brakenhoff, *The molecular biology of head and neck cancer*. *Nat Rev Cancer*, 2011. **11**(1): p. 9-22.
176. Ali, J., et al., *Genetic etiology of oral cancer*. *Oral Oncol*, 2017. **70**: p. 23-28.
177. Menzies, G.E., et al., *Base damage, local sequence context and TP53 mutation hotspots: a molecular dynamics study of benzo[a]pyrene induced DNA distortion and mutability*. *Nucleic Acids Res*, 2015. **43**(19): p. 9133-46.
178. Tuna, M., C.I. Amos, and G.B. Mills, *Genome-Wide Analysis of Head and Neck Squamous Cell Carcinomas Reveals HPV, TP53, Smoking and Alcohol-Related Allele-Based Acquired Uniparental Disomy Genomic Alterations*. *Neoplasia*, 2019. **21**(2): p. 197-205.
179. Li, X.C., et al., *A mutational signature associated with alcohol consumption and prognostically significantly mutated driver genes in esophageal squamous cell carcinoma*. *Ann Oncol*, 2018. **29**(4): p. 938-944.
180. Mirghani, H., et al., *Does smoking alter the mutation profile of human papillomavirus-driven head and neck cancers?* *Eur J Cancer*, 2018. **94**: p. 61-69.
181. Holloway, E., *From genotype to phenotype: linking bioinformatics and medical informatics ontologies*. *Comp Funct Genomics*, 2002. **3**(5): p. 447-50.
182. Finlay, C.A., P.W. Hinds, and A.J. Levine, *The p53 proto-oncogene can act as a suppressor of transformation*. *Cell*, 1989. **57**(7): p. 1083-93.
183. Kamada, R., et al., *Tetramer formation of tumor suppressor protein p53: Structure, function, and applications*. *Biopolymers*, 2016. **106**(4): p. 598-612.
184. Kandath, C., et al., *Mutational landscape and significance across 12 major cancer types*. *Nature*, 2013. **502**(7471): p. 333-339.

185. Petitjean, A., et al., *Impact of mutant p53 functional properties on TP53 mutation patterns and tumor phenotype: lessons from recent developments in the IARC TP53 database*. Hum Mutat, 2007. **28**(6): p. 622-9.
186. Olivier, M., et al., *The IARC TP53 database: new online mutation analysis and recommendations to users*. Hum Mutat, 2002. **19**(6): p. 607-14.
187. Bernard, X., et al., *Proteasomal degradation of p53 by human papillomavirus E6 oncoprotein relies on the structural integrity of p53 core domain*. PLoS One, 2011. **6**(10): p. e25981.
188. Chen, Y., R. Dey, and L. Chen, *Crystal structure of the p53 core domain bound to a full consensus site as a self-assembled tetramer*. Structure, 2010. **18**(2): p. 246-56.
189. Zenz, T., et al., *TP53 mutation and survival in aggressive B cell lymphoma*. Int J Cancer, 2017. **141**(7): p. 1381-1388.
190. Christopoulos, P., et al., *Detection of TP53 Mutations in Tissue or Liquid Rebiopsies at Progression Identifies ALK+ Lung Cancer Patients with Poor Survival*. Cancers (Basel), 2019. **11**(1).
191. Li, V.D., K.H. Li, and J.T. Li, *TP53 mutations as potential prognostic markers for specific cancers: analysis of data from The Cancer Genome Atlas and the International Agency for Research on Cancer TP53 Database*. J Cancer Res Clin Oncol, 2019. **145**(3): p. 625-636.
192. Wang, Z., M.A. Jensen, and J.C. Zenklusen, *A Practical Guide to The Cancer Genome Atlas (TCGA)*. Methods Mol Biol, 2016. **1418**: p. 111-41.
193. Leroy, B., et al., *Recommended Guidelines for Validation, Quality Control, and Reporting of TP53 Variants in Clinical Practice*. Cancer Res, 2017. **77**(6): p. 1250-1260.
194. Rose, P.W., et al., *The RCSB protein data bank: integrative view of protein, gene and 3D structural information*. Nucleic Acids Res, 2017. **45**(D1): p. D271-D281.
195. Strom, S.P., *Current practices and guidelines for clinical next-generation sequencing oncology testing*. Cancer Biol Med, 2016. **13**(1): p. 3-11.
196. Moon, S., et al., *Systematic Inspection of the Clinical Relevance of TP53 Missense Mutations in Gastric Cancer*. IEEE/ACM Trans Comput Biol Bioinform, 2019. **16**(5): p. 1693-1701.
197. Tahara, T., et al., *Mutation spectrum of TP53 gene predicts clinicopathological features and survival of gastric cancer*. Oncotarget, 2016. **7**(27): p. 42252-60.
198. Ambs, S., et al., *Relationship between p53 mutations and inducible nitric oxide synthase expression in human colorectal cancer*. J Natl Cancer Inst, 1999. **91**(1): p. 86-8.
199. Tretyakova, N., et al., *Formation of benzo[a]pyrene diol epoxide-DNA adducts at specific guanines within K-ras and p53 gene sequences: stable isotope-labeling mass spectrometry approach*. Biochemistry, 2002. **41**(30): p. 9535-44.

200. Martin, A.C., et al., *Integrating mutation data and structural analysis of the TP53 tumor-suppressor protein*. Hum Mutat, 2002. **19**(2): p. 149-64.
201. Baker, E.N. and R.E. Hubbard, *Hydrogen bonding in globular proteins*. Prog Biophys Mol Biol, 1984. **44**(2): p. 97-179.
202. Cancer Genome Atlas, N., *Comprehensive genomic characterization of head and neck squamous cell carcinomas*. Nature, 2015. **517**(7536): p. 576-82.
203. Cirillo, N. and S.S. Prime, *Desmosomal interactome in keratinocytes: a systems biology approach leading to an understanding of the pathogenesis of skin disease*. Cell Mol Life Sci, 2009. **66**(21): p. 3517-33.
204. Mi, H., et al., *PANTHER version 14: more genomes, a new PANTHER GO-slim and improvements in enrichment analysis tools*. Nucleic Acids Res, 2019. **47**(D1): p. D419-D426.
205. Thomas, P.D., et al., *PANTHER: a library of protein families and subfamilies indexed by function*. Genome Res, 2003. **13**(9): p. 2129-41.
206. Poeta, M.L., et al., *TP53 mutations and survival in squamous-cell carcinoma of the head and neck*. N Engl J Med, 2007. **357**(25): p. 2552-61.
207. Raftery, A.E., et al., *Bayesian probabilistic projections of life expectancy for all countries*. Demography, 2013. **50**(3): p. 777-801.
208. Eriksson, D. and T. Stigbrand, *Radiation-induced cell death mechanisms*. Tumour Biol, 2010. **31**(4): p. 363-72.
209. Smith, E.M., et al., *Association between p53 and human papillomavirus in head and neck cancer survival*. Cancer Epidemiol Biomarkers Prev, 2008. **17**(2): p. 421-7.
210. Chung, C.H. and M.L. Gillison, *Human papillomavirus in head and neck cancer: its role in pathogenesis and clinical implications*. Clin Cancer Res, 2009. **15**(22): p. 6758-62.
211. Lee, D.K., et al., *The human papilloma virus E7 oncoprotein inhibits transforming growth factor-beta signaling by blocking binding of the Smad complex to its target sequence*. J Biol Chem, 2002. **277**(41): p. 38557-64.
212. Tian, Y., et al., *CIP2A facilitates the G1/S cell cycle transition via B-Myb in human papillomavirus 16 oncoprotein E6-expressing cells*. J Cell Mol Med, 2018. **22**(9): p. 4150-4160.
213. Martin, C.M., et al., *The use of MYBL2 as a novel candidate biomarker of cervical cancer*. Methods Mol Biol, 2015. **1249**: p. 241-51.
214. Branca, M., et al., *Up-regulation of proliferating cell nuclear antigen (PCNA) is closely associated with high-risk human papillomavirus (HPV) and progression of cervical intraepithelial neoplasia (CIN), but does not predict disease outcome in cervical cancer*. Eur J Obstet Gynecol Reprod Biol, 2007. **130**(2): p. 223-31.
215. Park, J.S., et al., *Presence of oncogenic HPV DNAs in cervical carcinoma tissues and pelvic lymph nodes associating with proliferating cell nuclear antigen expression*. Gynecol Oncol, 1996. **60**(3): p. 418-23.

216. O'Donovan, P.J. and D.M. Livingston, *BRCA1 and BRCA2: breast/ovarian cancer susceptibility gene products and participants in DNA double-strand break repair*. Carcinogenesis, 2010. **31**(6): p. 961-7.
217. Moynahan, M.E., et al., *Brcal controls homology-directed DNA repair*. Mol Cell, 1999. **4**(4): p. 511-8.
218. Tian, F., et al., *BRCA1 promotes the ubiquitination of PCNA and recruitment of translesion polymerases in response to replication blockade*. Proc Natl Acad Sci U S A, 2013. **110**(33): p. 13558-63.
219. Gervai, J.Z., et al., *A genetic study based on PCNA-ubiquitin fusions reveals no requirement for PCNA polyubiquitylation in DNA damage tolerance*. DNA Repair (Amst), 2017. **54**: p. 46-54.
220. Gorodetska, I., I. Kozeretska, and A. Dubrovska, *BRCA Genes: The Role in Genome Stability, Cancer Stemness and Therapy Resistance*. J Cancer, 2019. **10**(9): p. 2109-2127.
221. Gu, J., et al., *TP53 mutation is associated with a poor clinical outcome for non-small cell lung cancer: Evidence from a meta-analysis*. Mol Clin Oncol, 2016. **5**(6): p. 705-713.
222. Fukuyama, Y., et al., *K-ras and p53 mutations are an independent unfavourable prognostic indicator in patients with non-small-cell lung cancer*. Br J Cancer, 1997. **75**(8): p. 1125-30.
223. Kashii, T., et al., *Evaluation of prognostic-significance of p53 gene alterations in patients with surgically resected lung-cancer*. Int J Oncol, 1995. **6**(1): p. 123-8.
224. Molina-Vila, M.A., et al., *Nondisruptive p53 mutations are associated with shorter survival in patients with advanced non-small cell lung cancer*. Clin Cancer Res, 2014. **20**(17): p. 4647-59.

## Appendix 1: Journal publications

- 1) **ZHURAKIVSKA, K.**, TROIANO, G., PANNONE, G., CAPONIO, V.C.A., LO MUZIO, L. An Overview of the Temporal Shedding of SARS-CoV-2 RNA in Clinical Specimens. *Frontiers in Public Health*, 2020, 8, 487
- 2) CAPONIO VCA, TROIANO G, ADIPIETRO I, **ZHURAKIVSKA K**, ARENA C, MANGIERI D, MASCITTI M, CIRILLO N, LO MUZIO L. Computational analysis of TP53 mutational landscape unveils key prognostic signatures and distinct pathobiological pathways in head and neck squamous cell cancer. *Br J Cancer*. 2020 Jul 20. doi: 10.1038/s41416-020-0984-6
- 3) MASCITTI M, **ZHURAKIVSKA K**, TOGNI L, CAPONIO VCA, ALMANGUSH A, BALERCIA P, BALERCIA A, RUBINI C, LO MUZIO L, SANTARELLI A, TROIANO G. Addition of the tumour-stroma ratio to the 8th edition American Joint Committee on Cancer staging system improves survival prediction for patients with oral tongue squamous cell carcinoma. *Histopathology*. 2020 Jul 7. doi: 10.1111/his.14202.
- 4) DIOGUARDI M, SOVERETO D, ILLUZZI G, LANEVE E, RADDATO B, ARENA C, ALBERTO CAPONIO VC, CALORO GA, **ZHURAKIVSKA K**, TROIANO G, LO MUZIO L. Management of Instrument Sterilization Workflow in Endodontics: A Systematic Review and Meta-Analysis. *Int J Dent*. 2020 Feb 8;2020:5824369. doi: 10.1155/2020/5824369
- 5) **ZHURAKIVSKA K**, TROIANO G, MONTELLA M, LO MUZIO L, FIORILLO L, CERVINO G, CICCÌÙ M, D'AMICO C, RULLO R, LAINO G, DI STASIO D, LAINO L. Oral Health and Molecular Aspects of Malignant Fibrous Histiocytoma Patients: A Systematic Review of the Literature. *Int J Environ Res Public Health*. 2020 Feb 23;17(4):1426. doi: 10.3390/ijerph17041426.
- 6) TROIANO G, CAPONIO VCA, BOTTI G, AQUINO G, LOSITO NS, PEDICILLO MC, **ZHURAKIVSKA K**, ARENA C, CIAVARELLA D, MASTRANGELO F, LO RUSSO L, LO MUZIO L, PANNONE G. Immunohistochemical Analysis Revealed a Correlation between Musashi-2 and Cyclin-D1 Expression in Patients with Oral Squamous Cells Carcinoma. *Int J Mol Sci*. 2019 Dec 23;21(1):121. doi: 10.3390/ijms21010121
- 7) ARENA C, TROIANO G, **ZHURAKIVSKA K**, NOCINI R, LO MUZIO L. Stomatitis And Everolimus: A Review Of Current Literature On 8,201 Patients. *Onco Targets Ther*. 2019 Nov 14;12:9669-9683. doi: 10.2147/OTT.S195121
- 8) GUO Z, DU X, WANG L, LI K, JIAO J, GUGLIELMI G, **ZHURAKIVSKA K**, LO MUZIO L, BLAKE GM, CHENG X. Measurements of volumetric bone mineral density in the mandible do not predict spinal osteoporosis. *Dentomaxillofac Radiol*. 2020 Mar;49(3):20190280. doi: 10.1259/dmfr.20190280
- 9) **ZHURAKIVSKA K**, TROIANO G, MONTELLA M, RONCHI A, DI STASIO D, CICCÌÙ M, LAINO L. Surgical Treatment of Oral Cavity Nodular Fasciitis. *J Craniofac Surg*. 2020 Mar/Apr;31(2):e108-e110. doi: 10.1097/SCS.0000000000005877
- 10) CICCÌÙ M, CERVINO G, FIORILLO L, D'AMICO C, OTERI G, TROIANO G, **ZHURAKIVSKA K**, LO MUZIO L, HERFORD AS, CRIMI S, BIANCHI A, DI STASIO D, RULLO R, LAINO G, LAINO L. Early Diagnosis on Oral and Potentially Oral Malignant Lesions: A Systematic Review on the VELscope® Fluorescence Method. *Dent J (Basel)*. 2019 Sep 4;7(3):93. doi: 10.3390/dj7030093
- 11) DIOGUARDI M, CAMPANELLA P, COCCO A, ARENA C, MALAGNINO G, SOVERETO D, AIUTO R, LAINO L, LANEVE E, DIOGUARDI A, **ZHURAKIVSKA K**, MUZIO LL. Possible Uses of Plants of the Genus *Asphodelus* in Oral Medicine. *Biomedicines*. 2019 Sep 2;7(3):67. doi: 10.3390/biomedicines7030067.
- 12) DIOGUARDI M, SOVERETO D, AIUTO R, LAINO L, ILLUZZI G, LANEVE E, RADDATO B, CAPONIO VCA, DIOGUARDI A, **ZHURAKIVSKA K**, TROIANO G, LO MUZIO L. Effects of Hot Sterilization on Torsional Properties of Endodontic Instruments: Systematic Review with Meta-Analysis. *Materials (Basel)*. 2019 Jul 8;12(13):2190. doi: 10.3390/ma12132190
- 13) DIOGUARDI M, GIOIA GD, CALORO GA, CAPOCASALE G, **ZHURAKIVSKA K**, TROIANO G, RUSSO LL, MUZIO LL. The Association between Tooth Loss and Alzheimer's Disease: a Systematic Review with Meta-Analysis of Case Control Studies. *Dent J (Basel)*. 2019 May 1;7(2):49. doi: 10.3390/dj7020049.

- 14) DIOGUARDI M, DI GIOIA G, ILLUZZI G, ARENA C, CAPONIO VCA, CALORO GA, **ZHURAKIVSKA K**, ADIPIETRO I, TROIANO G, LO MUZIO L. Inspection of the Microbiota in Endodontic Lesions. *Dent J (Basel)*. 2019 May 1;7(2):47. doi: 10.3390/dj7020047.
- 15) CAZZOLLA AP, LACAITA MG, LACARBONARA V, **ZHURAKIVSKA K**, DE FRANCO A, GISSI I, TESTA NF, MARZO G, LO MUZIO L. Orthopedic and orthodontic management in a patient with DiGeorge Syndrome and Familial Mediterranean Fever: A case report. *Spec Care Dentist*. 2019 May;39(3):340-347. doi: 10.1111/scd.12381.
- 16) **ZHURAKIVSKA K**, MAIORANO E, NOCINI R et al. Necrotizing sialometaplasia can hide the presence of salivary gland tumors: A case series. *Oral Dis* 2019; 25: 1084-1090.
- 17) **ZHURAKIVSKA K**, TROIANO G, CAPONIO VCA et al. Do Changes in Oral Microbiota Correlate With Plasma Nitrite Response? A Systematic Review. *Frontiers in physiology* 2019; 10: 1029.
- 18) **ZHURAKIVSKA K**, TONI G, LAINO G et al. An unusual case of recurrent gingival hirsutism. *Oral Surg Oral Med Oral Pathol Oral Radiol* 2019.
- 19) TROIANO G, CAPONIO VCA, **ZHURAKIVSKA K** et al. High PD-L1 expression in the tumour cells did not correlate with poor prognosis of patients suffering for oral squamous cells carcinoma: A meta-analysis of the literature. *Cell Prolif* 2019; 52: e12537
- 20) **ZHURAKIVSKA K**, TROIANO G, CAPONIO VCA et al. The Effects of Adjuvant Fermented Wheat Germ Extract on Cancer Cell Lines: A Systematic Review. *Nutrients* 2018; 10
- 21) CAZZOLLA AP, LO MUZIO L, DI FEDE O, LACARBONARA V, COLAPRICO A, TESTA NF, GIUSEPPE T, **ZHURAKIVSKA K**, MARZO G, LACAITA MG Orthopedic-orthodontic treatment of the patient with Turner's syndrome: Review of the literature and case report. *Spec Care Dentist* 2018; 38: 239-248.
- 22) BRAMANTI E, NORCIA A, CICCUI M, MATAACENA G, CERVINO G, TROIANO G, **ZHURAKIVSKA K**, LAINO L Postextraction Dental Implant in the Aesthetic Zone, Socket Shield Technique Versus Conventional Protocol. *J Craniofac Surg* 2018; 29: 1037-1041
- 23) CAZZOLLA AP, TESTA NF, FAVIA G, LACAITA MG, CIAVARELLA D, **ZHURAKIVSKA K**, TROIANO G, LO MUZIO L Multidisciplinary approach in a case of Hand-Schuller-Christian disease with maxillary involvement. *Spec Care Dentist* 2018; 38: 107-111.
- 24) CAZZOLLA AP, TROIANO G, **ZHURAKIVSKA K**, MAIORANO E, FAVIA G, LACAITA MG, MARZO G, DICUONZO F, ANDRESCIANI S, MUZIO LL Langerhans cell histiocytosis of the maxillae in a child treated only with chemotherapy: a case report. *J Med Case Rep* 2017; 11: 130.
- 25) CAZZOLLA AP, **ZHURAKIVSKA K**, CIAVARELLA D, LACAITA MG, FAVIA G, TESTA NF, MARZO G, LA CARBONARA V, TROIANO G, LO MUZIO L Primary hyperoxaluria: Orthodontic management in a pediatric patient: A case report. *Spec Care Dentist* 2018.
- 26) CIAVARELLA D, TEPEDINO M, GALLO C, MONTARULI G, **ZHURAKIVSKA K**, COPPOLA L, TROIANO G, CHIMENTI C, LAURENZIELLO M, LO RUSSO L Post-orthodontic position of lower incisors and gingival recession: A retrospective study. *J Clin Exp Dent* 2017; 9: e1425-e1430
- 27) CICCUI M, CERVINO G, FIORILLO L, D'AMICO C, OTERI G, TROIANO G, **ZHURAKIVSKA K**, LO MUZIO L, HERFORD AS, CRIMI S, BIANCHI A, DI STASIO D, RULLO R, LAINO G, LAINO L Early Diagnosis on Oral and Potentially Oral Malignant Lesions: A Systematic Review on the VELscope((R)) Fluorescence Method. *Dentistry journal* 2019; 7.
- 28) DU X, JIAO J, CHENG X, WANG L, LI K, LIU H, WANG C, ARENA C, **ZHURAKIVSKA K**, GUGLIELMI G Age-related changes of bone mineral density in mandible by quantitative computed tomography. *Journal of biological regulators and homeostatic agents* 2017; 31: 997-1003
- 29) LO RUSSO L, **ZHURAKIVSKA K**, MONTARULI G, SALAMINI A, GALLO C, TROIANO G, CIAVARELLA D Effects of crown movement on periodontal biotype: a digital analysis. *Odontology* 2018.
- 30) TROIANO G, DIOGUARDI M, COCCO A, **ZHURAKIVSKA K**, CIAVARELLA D, MUZIO LL Increase the glyde path diameter improves the centering ability of F6 Skytaper. *Eur J Dent* 2018; 12: 89-93
- 31) TROIANO G, LAINO L, CICCUI M, CERVINO G, FIORILLO L, D'AMICO C, **ZHURAKIVSKA K**, LO MUZIO L Comparison of Two Routes of Administration of Dexamethasone to Reduce the Postoperative Sequelae After Third Molar Surgery: A Systematic Review and Meta-Analysis. *Open Dent J* 2018; 12: 181-188.

- 32) TROIANO G, LAINO L, **ZHURAKIVSKA K**, CICCIO M, LO MUZIO L, LO RUSSO L Addition of enamel matrix derivatives to bone substitutes for the treatment of intrabony defects: A systematic review, meta-analysis and trial sequential analysis. *J Clin Periodontol* 2017; 44: 729-738
- 33) TROIANO G, **ZHURAKIVSKA K**, LO MUZIO L, LAINO L, CICCIO M, LO RUSSO L Combination of Bone Graft and Resorbable Membrane for Alveolar Ridge Preservation: a Systematic Review, Meta-analysis and Trial Sequential Analysis. *J Periodontol* 2017: 1-17.
- 34) DIOGUARDI M, DI GIOIA G, ILLUZZI G, ARENA C, CAPONIO VCA, CALORO GA, **ZHURAKIVSKA K**, ADIPIETRO I, TROIANO G, LO MUZIO L Inspection of the Microbiota in Endodontic Lesions. *Dentistry journal* 2019; 7.
- 35) DIOGUARDI M, GIOIA GD, CALORO GA, CAPOCASALE G, **ZHURAKIVSKA K**, TROIANO G, RUSSO LL, MUZIO LL The Association between Tooth Loss and Alzheimer's Disease: a Systematic Review with Meta-Analysis of Case Control Studies. *Dentistry journal* 2019; 7.
- 36) DIOGUARDI M, SOVERETO D, AIUTO R, LAINO L, ILLUZZI G, LANEVE E, RADDATO B, CAPONIO VCA, DIOGUARDI A, **ZHURAKIVSKA K**, TROIANO G, LO MUZIO L Effects of Hot Sterilization on Torsional Properties of Endodontic Instruments: Systematic Review with Meta-Analysis. *Materials (Basel, Switzerland)* 2019; 12

## Appendix 2: Abstracts and Conference Proceedings

1. Khrystyna Zhurakivska, Giuseppe Troiano, Mario Dioguardi, Marco Mascitti, Andrea Santarelli, Federica Canepa, Olga Di Fede, Lucio Lo Russo “Do the changes in oral microbiota correlate with plasma nitrite response? Congresso SIPMO – XV Nazionale e III Internazionale – Bari, 17-19 Ottobre 2019
2. V. C. A. Caponio, K. Zhurakivska, C. Arena, M. Mascitti, A. Santarelli, R. Mauceri, G. Campisi, L. Lo Muzio “Bioinformatics analysis of TP53 gene in head and neck squamous cell carcinoma patients from the cancer genome atlas” Congresso SIPMO – XV Nazionale e III Internazionale – Bari, 17-19 Ottobre 2019
3. Marco Mascitti, Giuseppe Troiano, Barlattani Alberta, Zhurakivska Khrystyna, Carlo Caponio, Giuseppina Campisi, Andrea Santarelli, Lorenzo Lo Muzio “Immune-phenotype analysis in a large cohort of tongue squamous cell carcinoma patients” Congresso SIPMO – XV Nazionale e III Internazionale – Bari, 17-19 Ottobre 2019
4. Abstract "Stomatitis and EGFR-tyrosine kinase inhibitors: a review of current literature in 4353 patients" Conference " 5th National and 1st International Symposium of Italian Society of Oral Pathology and Medicine."
5. Osteonecrosis of the jaws caused by myelodysplasia: a case report" was accepted for the Conference "5th National and 1st International Symposium of Italian Society of Oral Pathology and Medicine."
6. Zhurakivska K., Guglielmi G., Abate C., Di Fede O., Campisi G., Rubini C., Lo Muzio L. Bisphosphonate related osteonecrosis of the jaws in Italy. An observational report of 24 cases. Collegio dei docenti di odontoiatria, XXV CONGRESSO NAZIONALE, Roma, 12-14 aprile 2018.
7. A. Dedola, K. Zhurakivska, A. Tesei, M. Melillo, F. Mastrangelo  
Mandible eosinophilic lesion regression after endodontic treatment: one year follow-up

8. F. Seidita, G. Capocasale, C. Mangione, K. Zhurakivska, O. Di Fede  
Quality of life in erosive oral lichen planus patients treated with Clobetasol mucoadhesive formulations – a pilot study.  
14° Congresso Nazionale SIPMO (26-28 Ottobre 2017).  
Annali di stomatologia 2017; Suppl 1: 1-81
9. Zhurakivska K., Lucchese A., Serpico R., Santarelli A., Mascitti M., Laino L.  
Oral metastasis of colon cancer. A case report.  
XIV Congresso Nazionale SIPMO, Roma, 26-28 Ottobre 2017  
Annali di stomatologia 2017; Suppl 1: 1-81
10. V. Caponio, G. Troiano, K. Zhurakivska, A. Santarelli, L. Guida, L. Lo Muzio,  
Espressione di LNCRNA, un promettente fattore prognostico nel carcinoma a cellule squamose testa-collo: meta-analisi.  
Collegio dei docenti di odontoiatria, XXIV CONGRESSO NAZIONALE, Milano, 6-8 aprile 2017  
Journal of Osseointegration January-April 2017; 9(1):150
11. G. Troiano, K. Zhurakivska, V. Caponio, L. Boldrup, K. Nylander, A. Santarelli, G. Campisi, L. Lo Muzio.  
I long non-coding RNAs (LNCRNAS) sono espressi in modo anomalo nel carcinoma della lingua e rappresentano promettenti biomarcatori clinici .  
Collegio dei docenti di odontoiatria, XXIV CONGRESSO NAZIONALE, Milano, 6-8 aprile 2017  
Journal of Osseointegration January-April 2017; 9(1):196
12. K. Zhurakivska, L. Laino, G. Montaruli, O. Di Fede, D. Ciavarella, L. Lo Russo.  
Effetti ortodontici e ortopedici dell'espansione rapida del palato chirurgicamente assistita: un'analisi digitale Collegio dei docenti di odontoiatria, XXIV CONGRESSO NAZIONALE, Milano, 6-8 aprile 2017  
Journal of Osseointegration January-April 2017; 9(1):228
13. Mascitti M., Togni L., Rubini C., Lo Muzio L., Zhurakivska K., Arena C., Procaccini M., Santarelli A.

Immunohistochemical expression of CD56 (NCAM) in odontogenic tumors  
Collegio dei docenti di odontoiatria, XXIV CONGRESSO NAZIONALE, Milano,  
6-8 aprile 2017  
Journal of Osseointegration January-April 2017; 9(1):195

14. K. Zhurakivska, G. Troiano, A. Albanese, G. Pizzo, L. Lo Muzio, L. Lo Russo,

Clinical effectiveness of platelet concentrates for periodontal regeneration.

Collegio dei docenti di odontoiatria, XXIII CONGRESSO NAZIONALE, Roma, 6-  
8 Aprile 2016

MINERVA STOMATOLOGICA 2016; 65 (Suppl. 1 to No. 3 ):189

### **Appendix 3: Oral Presentations**

Presentazione del lavoro di ricerca dal titolo “Effetti antitumorali dell’estratto di germe di grano fermentato sulle cellule del carcinoma squamoso orale.” al PhD day del 27° Congresso Nazionale del Collegio dei docenti universitari delle discipline odontostomatologiche.

Presentazione del lavoro di ricerca “Effects of crown movement on periodontal biotype: a digital analysis” nella sessione ricerca del Simposio Scuole Ortodontiche 7---8 aprile 2017, Milano, Centro Congressi San Raffaele.

## Appendix 4: Honors and Awards

Honorable Mention for the presentation of results of the project “Effects of Fermented Wheat Germ Extract on Oral squamous cell carcinoma cells in an in vitro study” at 27° National College of teachers of university odontostomatologic disciplines 2020. **Zhurakivska Khrystyna**, Giuseppe Troiano, Marco Mascitti, Lucrezia Togni, Vera Panzarella, Giuseppina Campisi, Eleonora Lo Muzio, Lorenzo Lo Muzio.

Best poster for “Predict the death of patients with TP53 mutated in Head and Neck squamocellular tumours” Mariele Eleonora Bizzoca, **Khrystyna Zhurakivska**, Marco Mascitti, Andrea Santarelli, Rodolfo Mauceri, Olga Di Fede, Vito Carlo Alberto Caponio, Lorenzo Lo Muzio. College of teachers in dentistry National Congress, 2020.

Honorable Mention for the poster “Expression of a lncRNAs as promising prognostic factors in head and neck squamous cell carcinoma: meta-analysis.” at 24° National College of teachers of university odontostomatologic disciplines 2017

V. Caponio, G. Troiano, **K. Zhurakivska**, A. Santarelli, L. Guida, L. Lo Muzio.

Best poster for “Long non-coding RNAs (lncRNAs) are abnormally expressed in tongue carcinoma and represent promising clinical biomarkers” at at 24° National College of teachers of university odontostomatologic disciplines 2017

G. Troiano, **K. Zhurakivska**, V. Caponio, L. Boldrup, K. Nylander, A. Santarelli, G. Campisi, L. Lo Muzio.